

**Identification and characterization
of light-responsive *cis*-acting elements
in nuclear promoters of *Arabidopsis thaliana***

Inaugural-Dissertation

zur Erlangung des Doktorgrades
der Mathematisch-Naturwissenschaftlichen Fakultät
der Heinrich-Heine-Universität Düsseldorf

vorgelegt von

Marina Mellenthin

aus Otterndorf

Düsseldorf, Mai 2012

aus dem Institut für Botanik
der Heinrich-Heine Universität Düsseldorf

Gedruckt mit der Genehmigung der
Mathematisch-Naturwissenschaftlichen Fakultät der
Heinrich-Heine-Universität Düsseldorf

Referent: Prof. Dr. Margarete Baier
Korreferent: Prof. Dr. Rüdiger Simon

Tag der mündlichen Prüfung: 22. Juni 2012

Gewidmet meiner Familie.

TABLE OF CONTENTS

Summary	i
Zusammenfassung	ii
List of abbreviations	iv
1 INTRODUCTION.....	1
1.1 Light-regulated transcriptional networks in plants	1
1.1.1 Light as environmental factor	1
1.1.2 Gene expression regulation at the level of transcription	1
1.1.3 Light sensitive <i>cis</i> -acting regulatory promoter elements.....	2
1.1.3.1 G-boxes	3
1.1.3.2 Z-boxes	4
1.1.3.3 I-boxes and GATA motifs	4
1.2 Light sensing by photoreceptors.....	5
1.2.1 Phytochromes.....	5
1.2.2 Cryptochromes.....	7
1.2.3 Phototropins	8
1.2.4 Components downstream of photoreceptors	8
1.2.4.1 HY5.....	9
1.2.4.2 PIFs	9
1.2.4.3 COP/DET/FUS	10
1.3 Retrograde plastid signals regulating nuclear gene expression	11
1.3.1 Pigment biosynthesis.....	12
1.3.2 Plastid gene expression	13
1.3.3 Plastid protein import.....	13
1.3.4 ROS.....	13
1.3.5 Redox processes of photosynthesis.....	14
1.3.6 Glutaredoxin and thioredoxin	15
1.3.7 Retrograde responsive <i>cis</i> -elements.....	15
1.4 How carbohydrates influence nuclear gene expression.....	16
1.4.1 Sugars as signaling molecules.....	16
1.4.2 Regulators of sugar signaling.....	16
1.5 Enhancer trapping.....	18
1.5.1 The principle of enhancer trapping	18
1.5.2 The GAL4/UAS system	18
1.5.3 The <i>GAL4-GFP</i> ET construct	19
1.6 Aim of this study.....	19
2 MATERIAL AND METHODS.....	21
2.1 Plant material.....	21
2.2 Growth conditions	22
2.2.1 Sterile culture of <i>Arabidopsis thaliana</i> seedlings.....	22

Table of contents

2.2.2	Growth of mature <i>Arabidopsis thaliana</i> plants on soil.....	22
2.2.3	Monochromatic light treatment	22
2.3	Determination of reporter gene activity.....	22
2.3.1	<i>In vivo</i> GFP fluorescence quantification.....	22
2.3.2	<i>In vitro</i> quantification of GFP fluorescence of ground seedlings	23
2.3.2.1	Determination of GFP fluorescence	23
2.3.2.2	Quantification of protein content.....	23
2.3.2.3	Chlorophyll content determination.....	23
2.3.3	Visualization of GFP reporter gene fluorescence.....	24
2.3.4	Colorimetric quantification of GUS activity	24
2.4	Isolation of DNA from plant material.....	24
2.4.1	Isolation of DNA for PCR.....	24
2.4.2	DNA isolation for Southern blot	25
2.5	Polymerase chain reaction (PCR).....	25
2.5.1	Standard PCR	25
2.5.2	Thermal asymmetric interlaced PCR (TAIL-PCR).....	25
2.5.3	Identification and isolation of homozygous T-DNA insertion lines by PCR	27
2.6	Site-directed mutagenesis of SIG5 promoter.....	28
2.7	Separation of DNA by agarose gel electrophoresis	29
2.8	Purification of PCR products by gel extraction	29
2.9	<i>Escherichia coli</i> manipulations.....	30
2.9.1	Generation of chemically competent <i>E. coli</i>	30
2.9.2	Transformation of <i>E. coli</i>	30
2.9.3	<i>E. coli</i> colony-PCR.....	30
2.9.4	Plasmid isolation from <i>E. coli</i> for sequencing.....	30
2.9.5	Plasmid isolation from <i>E. coli</i> by alkaline lysis	31
2.9.6	cDNA library plasmid isolation.....	31
2.10	Plasmid manipulations.....	31
2.10.1	Ligation with pJET1.2/blunt vector for sequencing	31
2.10.2	Ligation of PCR-amplified DNA into pCR [®] 8/GW/TOPO [®]	31
2.10.3	LR reaction.....	32
2.10.4	Cleaving double-stranded DNA with restriction enzymes	32
2.10.5	Ligation of termini created by restriction enzymes	32
2.11	Sequencing of DNA fragments.....	33
2.12	Analysis of promoter sequences	33
2.13	Southern blot analysis.....	33
2.13.1	Digesting genomic DNA with restriction enzymes for Southern blot analysis.	33
2.13.2	DIG-labeling of hybridization probe	34
2.13.3	Southern transfer	34
2.13.4	Southern blot hybridization	34
2.13.5	Detection	35
2.14	Confocal laser scanning microscopy	35
2.15	Gene expression analyses	36
2.15.1	RNA isolation.....	36
2.15.2	First strand cDNA synthesis.....	36
2.15.3	Quantitative real-time PCR	36
2.15.3.1	Primer design.....	36
2.15.3.2	Fluorometry	36
2.15.3.3	Standardization.....	37
2.15.4	Analysis of mRNA decay profiles.....	37
2.15.4.1	Actinomycin D treatment	37
2.15.4.2	Half-life calculations	37
2.16	Modulation of photosynthetic electron transport chain	38
2.16.1	Inhibitor treatment.....	38

Table of contents

2.16.2 Chlorophyll <i>a</i> fluorescence measurements.....	38
2.17 <i>Agrobacterium tumefaciens</i> manipulations	39
2.17.1 Production of competent <i>A. tumefaciens</i> cells.....	39
2.17.2 Transformation of <i>A. tumefaciens</i>	39
2.18 Transient gene expression in <i>Nicotiana benthamiana</i>	39
2.18.1 Preparation of <i>Agrobacterium</i> suspension for infiltration.....	39
2.18.2 Infiltration of tobacco leaves.....	40
2.19 Generation of stable transformed <i>Arabidopsis thaliana</i>	40
2.19.1 Transformation by floral dip	40
2.19.2 Selection of transformants.....	40
2.20 Crossing <i>Arabidopsis thaliana</i> plants.....	41
2.20.1 Crossing procedure	41
2.20.2 Identification of mutant alleles by phenotype	41
2.20.3 PCR-based identification of mutant alleles	42
2.21 Yeast manipulations	43
2.21.1 Yeast one-hybrid system.....	43
2.21.2 Yeast strain and growth conditions	43
2.21.3 Bait vector construction	43
2.21.4 Transformation of <i>Saccharomyces cerevisiae</i>	44
2.21.5 Yeast colony-PCR.....	44
2.21.6 Plasmid isolation from yeast	44
2.21.7 Setting 3-amino-1,2,4-triazol concentration	45
2.21.8 Library construction.....	45
2.21.8.1 Excision to convert the λ -ACT library into a plasmid library.....	45
2.21.8.2 Analysis of cDNA library quality	46
2.21.9 Yeast one-hybrid screen.....	46
2.21.10 Test for interaction with HY5 transcription factor	46
3 RESULTS	47
3.1 Screening ET lines for light-dependent GFP fluorescence	47
3.2 Enhancer trap line N9249.....	48
3.2.1 Localization of GFP fluorescence	48
3.2.2 Identification of T-DNA insertion site by TAIL-PCR	49
3.2.3 <i>In silico</i> analysis to predict <i>cis</i> -acting elements	51
3.2.4 Southern blot analysis to determine the number of T-DNA insertions	52
3.3 Enhancer trap line N9266.....	53
3.3.1 Localization of GFP fluorescence	53
3.3.2 Identification of T-DNA insertion site by TAIL-PCR	53
3.3.3 <i>In silico</i> analysis to predict <i>cis</i> -acting elements	55
3.3.4 Southern blot analysis to determine the number of T-DNA insertions	55
3.4 Enhancer trap line N9313.....	56
3.4.1 Localization of GFP fluorescence	56
3.4.2 Identification of T-DNA insertion site by TAIL-PCR	57
3.4.3 Southern blot analysis to determine the number of T-DNA insertions	59
3.4.4 <i>SIG5</i> and <i>GFP</i> expression in skotomorphogenic seedlings.....	60
3.4.5 The influence of light quality on transcription	61
3.4.5.1 Modulation of GFP fluorescence by light quality	61
3.4.5.2 Modulation of <i>GFP</i> transcription by monochromatic light.....	62
3.4.5.3 Modulation of <i>SIG5</i> transcription by monochromatic light	63
3.4.5.4 <i>SIG5</i> and <i>GFP</i> mRNA decay profile.....	63
3.4.6 Light responses of seedlings compared with adult plants	65
3.4.6.1 <i>SIG5</i> and <i>GFP</i> transcripts upon 24 h illumination of adult N9313 plants....	65
3.4.6.2 <i>SIG5</i> and <i>GFP</i> transcripts upon 3 h illumination period.....	66

3.4.7	Characterization of blue light sensitive <i>SIG5</i> promoter elements.....	66
3.4.7.1	Blue light response analyses by promoter-reporter gene fusions	67
3.4.7.2	Blue light responsiveness of SALK lines with truncated <i>SIG5</i> promoters ...	68
3.4.7.3	<i>In silico</i> analysis of 196 bp mediating the blue light induction of <i>SIG5</i> transcription.....	70
3.4.8	Characterization of red and far-red light induction of <i>SIG5</i> transcription.....	70
3.4.8.1	Analysis of light sensitivity mediated by the distal 0.8 kb <i>SIG5</i> promoter sequence	70
3.4.8.2	Localization of red light sensitivity in distal and proximal <i>SIG5</i> promoter regions	72
3.4.8.3	Induction of transcription by fragments of the distal <i>SIG5</i> promoter	73
3.4.8.4	Red and far-red light responsiveness of SALK-lines with truncated <i>SIG5</i> promoters.....	74
3.4.8.5	<i>In silico</i> analysis of the distal 0.8 kb <i>SIG5</i> promoter.....	76
3.4.9	The role of photoreceptors in regulating <i>SIG5</i> transcription	76
3.4.9.1	UV-A/ blue light photoreceptors: cryptochromes and phototropins.....	77
3.4.9.2	Red/ far-red light photoreceptors: phytochromes	80
3.4.9.3	The effect of combined phytochrome and cryptochrome knockout	82
3.4.10	The role of HY5 in regulating <i>SIG5</i> transcription	82
3.4.10.1	The role of HY5 in regulating the distal <i>SIG5</i> promoter	83
3.4.10.2	The role of HY5 in regulating <i>SIG5</i> responses to monochromatic light	84
3.4.10.3	Direct interaction of HY5 with the <i>SIG5</i> promoter	85
3.4.11	COPI as regulator of <i>SIG5</i> transcription	89
3.4.12	Screen for transcription factors interacting with the <i>SIG5</i> promoter	90
3.4.12.1	Construction of the bait construct.....	90
3.4.12.2	Setting 3-AT concentration	90
3.4.12.3	Library construction and analysis.....	91
3.4.12.4	Yeast one-hybrid screen	91
3.4.13	Characterization of retrograde signals regulating <i>SIG5</i> transcription.....	93
3.4.13.1	GFP fluorescence of N9313 upon short term treatment with DCMU and DBMIB.....	93
3.4.13.2	GFP fluorescence of N9313 upon long term response	94
3.4.13.3	Effect of DCMU on proximal and distal <i>SIG5</i> promoter.....	97
3.4.13.4	The effect of DCMU on the red light sensitivity of the <i>SIG5</i> promoter	100
3.4.14	Modulation of <i>SIG5</i> transcription by exogenously applied sucrose	101
3.4.14.1	The effect of exogenous sucrose feeding on the distal <i>SIG5</i> promoter	101
3.4.14.2	<i>SIG5</i> promoter-driven transient expression in tobacco upon sucrose feeding.....	101
3.4.14.3	Impact of carbohydrates on <i>GFP</i> and <i>SIG5</i> transcript level	104
3.4.15	Impact of general stress on <i>GFP</i> and <i>SIG5</i> transcription	106
4	DISCUSSION.....	107
4.1	The identification of <i>cis</i> -elements by screening ET lines	107
4.2	Enhancer trap N9249	107
4.2.1	The genome of N9249 contains multiple ET T-DNA insertion sites	107
4.2.2	Connections between GFP fluorescence pattern and the mapped T-DNA insertion site	108
4.2.3	Conclusions on N9249	109
4.3	Enhancer trap N9266	109
4.3.1	Two T-DNAs are inserted in the genome of N9266	109
4.3.2	Connections between the identified T-DNA insertion site and the GFP fluorescence.....	110
4.3.3	Conclusions on N9266	110
4.4	Enhancer trap N9313	111

Table of contents

4.4.1	The chloroplast gene expression system	111
4.4.2	SIG5 function in Arabidopsis.....	112
4.4.3	Blue light regulation of <i>SIG5</i> transcription.....	113
4.4.3.1	196 bp of the proximal <i>SIG5</i> promoter mediate the main blue light sensitivity of <i>SIG5</i>	113
4.4.3.2	<i>cry1</i> and <i>cry2</i> are the UV-A/blue light photoreceptors mediating the main blue light induction of <i>SIG5</i>	114
4.4.3.3	<i>phyB</i> is essential for the blue light induction of <i>SIG5</i>	115
4.4.4	The modulation of <i>SIG5</i> transcription by red and far-red light.....	116
4.4.4.1	The transcription of <i>SIG5</i> is stimulated by red and far-red light.....	116
4.4.4.2	<i>phyA</i> and <i>phyB</i> mediate the red/far-red light induction of <i>SIG5</i>	118
4.4.5	<i>HY5</i> and <i>COP1</i> are part of the network regulating <i>SIG5</i> in the light	119
4.4.5.1	A G-box is a functional light-sensitive <i>cis</i> -acting element of the <i>SIG5</i> promoter	119
4.4.5.2	The interaction of transcription factors with the <i>SIG5</i> promoter.....	121
4.4.6	Photosynthesis is regulating <i>SIG5</i> transcription by retrograde signals	124
4.4.6.1	<i>SIG5</i> regulation by the redox status of the plastoquinone pool.....	124
4.4.6.2	The role of <i>SIG5</i> under oxidative stress	125
4.4.6.3	Redox-regulation of <i>SIG5</i> function by phosphorylation	126
4.4.6.4	Integration of carbohydrate metabolism and redox signals.....	128
4.4.6.5	Regulation of <i>SIG5</i> by photosynthesis – concluding remarks.....	130
4.4.7	Conclusions on N9313	131
5	REFERENCES.....	133
6	APPENDIX	160
6.1	TAIL-PCR settings	160
6.2	PCR primers	161
6.3	Plexiglas transmission spectra and emission spectra of LEDs	164
6.4	Maps of plasmids	165
6.5	List of enhancer trap lines analyzed	167
6.6	List of tables	167
6.7	List of figures	167
	<i>Curriculum vitae</i>	170
	Danksagung	171
	Eidesstattliche Erklärung.....	172

SUMMARY

Enhancer trap lines were used to identify and characterize light-regulated *cis*-acting elements in nuclear promoters of *Arabidopsis thaliana*. The GFP fluorescence of enhancer trap line N9313 correlated in a screen for reporter gene expression with light intensity during growth. N9313 carries a single T-DNA, inserted in the promoter of *SIG5*. *SIG5* controls the expression of the D2 protein of photosystem II (*psbD*). Characterization of the enhancer trap line N9313 demonstrated that *SIG5* expression responds to blue- and red/far-red light via multiple promoter elements. The blue light sensitivity is predominantly located within a 196-bp region of the proximal *SIG5* promoter (-887 to -691 bp). Its overall regulation is slightly affected by the blue light inducibility of the distal *SIG5* promoter (-2000 to -1198 bp). The blue light response of *SIG5* depends on the photoreceptors cryptochrome 1, cryptochrome 2 and phytochrome B. Multiple red/far-red light responsive elements are located between -2000 and -551 bp relative to the *SIG5* CDS. The far-red light response is phytochrome A and phytochrome B dependent, while the red light response is more specifically controlled by phytochrome B. A distal light controlled G-box was identified and proofed by site-directed mutagenesis. The blue and red light signal transduction is controlled by HY5 in a COP1-dependent manner. The presented data show that expression of *psbD* is coordinated with many other blue light and red/far-red light responses via regulation of nuclear *SIG5* transcription.

In addition to the photoreceptor pathways, *SIG5* transcription is shown to be controlled more directly by photosynthesis. The data indicate that *SIG5* transcription is influenced by the redox status of the plastid plastoquinone pool, independently from the applied light quality, with transcription initiation being modulated from the distal as well as the proximal *SIG5* promoter. In addition to retrograde signaling, photosynthesis may modulate *SIG5* transcription via its end-product: Exogenously applied sucrose is regulating the transcription initiation from the distal *SIG5* promoter. Also abiotic stress, like the combination of light and cold, is modulating the transcription initiation from the distal as well as from the proximal *SIG5* promoter. It is hypothesized that *SIG5* expression is coordinated with photosynthetic efficiency and functions as integration point of multiple regulatory signals. The multiple light-responsive regions of the *SIG5* promoter are integrating photoreceptor signaling with retrograde signaling and oxidative stress, to maintain efficient photosynthesis.

ZUSAMMENFASSUNG

Pflanzen passen ihre Entwicklung und ihren Metabolismus kontinuierlich an sich verändernde Lichtbedingungen an. In dieser Arbeit wurden mittels *Arabidopsis thaliana* Enhancer Trap Linien neue, lichtregulierte Elemente in pflanzlichen Promotoren identifiziert und charakterisiert. Es wurden Enhancer Trap Linien bestimmt, in welchen die Reporterogenaktivität mit der Lichtintensität korreliert. Das Enhancer Trap Konstrukt der Linie N9313 ist im Promoter von *SIG5* inseriert. Dieser Sigma-Faktor kontrolliert die lichtabhängige Transkription des plastidären *psbD*, welches das D2 Protein von Photosystem II kodiert. Im Promoter von *SIG5* wurden mehrere Regionen identifiziert, die in Abhängigkeit von Blaulicht und von Rot-/Dunkelrotlicht reguliert werden. Im proximalen Promoter, zwischen der T-DNA Insertion und dem Translationsstart von *SIG5*, befinden sich die primären Blaulicht-sensitiven Elemente in einer 196-bp Sequenz, zwischen Nukleotid -887 und -691, relativ zum Translationsstart von *SIG5*. Die proximale Blaulichtantwort von *SIG5* kann zusätzlich von Elementen im distalen Promoter (-2000 bis -1198 bp) moduliert werden. Die Photorezeptoren cry1, cry2 und phyB vermitteln die Blaulichtinduktion der *SIG5* Transkription. Rot-/Dunkelrotlicht beeinflusst die Transkription über mehrere Bereiche des *SIG5* Promoters, von Nukleotid -2000 bis zu -551. PhyB ist verantwortlich für die Induktion der *SIG5* Transkription im Rotlicht, während die volle Dunkelrotlicht-Sensitivität zusätzlich phyA erfordert. Im distalen *SIG5* Promoter wurde eine G-Box identifiziert, deren Sensitivität gegenüber Licht mittels zielgerichteter Mutagenese gezeigt werden konnte. Die lichtabhängige Expression von *SIG5* wird zudem kontrolliert von HY5 und COP1. Diese Ergebnisse lassen schlussfolgern, dass durch die Regulation der *SIG5* Transkription die *psbD* Expression mit anderen Blaulicht- und Rot-/Dunkelrotlicht-Signalen koordiniert wird.

Die lichtabhängige *SIG5* Transkription wird nicht nur von Photorezeptoren, sondern parallel auch direkt von der Photosynthese reguliert. Die Ergebnisse deuten darauf hin, dass der Redox-Status des plastidären Plastochinon-Pools als Regulator der Initiation der Transkription vom distalen und vom proximalen *SIG5* Promoter aus fungiert. Zudem moduliert die Verfügbarkeit von Saccharose, dem Endprodukt der Photosynthese, die Initiation der Transkription vom distalen *SIG5* Promoter aus. Es konnte gezeigt werden, dass auch abiotischer Stress einen Einfluss auf die *SIG5* Transkriptionsinitiationsrate hat.

Die Ergebnisse der vorliegenden Arbeit zeigen, dass die *SIG5* Transkription als Integrationspunkt mehrerer Signaltransduktionswege fungiert. Die verschiedenen regulatorischen Bereiche des *SIG5* Promoters reflektieren die Komplexität der verschiedenen Signale und integrieren die Lichtwahrnehmung mittels Photorezeptoren mit retrograden Signalen und oxidativem Stress.

LIST OF ABBREVIATIONS

-10	-10 promoter region	Col-0	<i>Arabidopsis thaliana</i>
-35	-35 promoter region		ecotype Columbia-0
3-AT	3-amino-1,2,4-triazole	CPD	disodium 2-chloro-5-(4-methoxyspiro{1,2-dioxetane-3,2'-(5'-chloro)tricyclo-[3.3.1.1 ^{3,7}]decan}-4-yl) phenyl phosphate
A	absorption	cry	cryptochrome
aa	amino acids	C _t	cycle threshold
Ac	acetate	Cyt- <i>b₆/f</i>	cytochrome- <i>b₆/f</i> complex
Act D	Actinomycin D	dATP	deoxyadenosine triphosphate
AD	activation domain	DBMIB	2,5,-dibromo-3-methyl-6-isopropyl- <i>p</i> -benzoquinone
AD primer	arbitrary degenerate primer	DCMU	3'-4'-dichlorophenyl-1,1-dimethyl urea
ANOVA	analysis of variance	dCTP	deoxycytidine triphosphate
<i>A.</i>	<i>Agrobacterium</i>	dGTP	deoxyguanine triphosphate
<i>tumefaciens</i>	<i>tumefaciens</i>	DIG	digoxigenin
bp	base pairs	DNA	deoxyribonucleic acid
BD	DNA-binding domain	dNTPs	deoxyribonucleotid triphosphates
bHLH	basic helix-loop-helix	DO	dropout
BLRP	blue light responsive promoter	DTT	dithiothreitol
BSA	bovine serum albumin	dTTP	deoxythymidine triphosphate
bZIP	basic leucine zipper	dUTP	deoxyuridine triphosphate
C-	carboxyl-	<i>E. coli</i>	<i>Escherichia coli</i>
C24	<i>Arabidopsis thaliana</i> ecotype C24	EDTA	ethylene diamine-N tetra acetic acid
CaMV	cauliflower mosaic virus	EMSA	electrophoretic mobility shift assay
CAPS	cleaved amplified polymorphic sequences	ET	enhancer trap
CCD	charge-coupled device	FAD	flavin adenine dinucleotide
CCE	cryptochrome C-terminal extension		
cDNA	complementary DNA		
CDS	coding sequence		
cGMP	cyclic guanosine monophosphate		
Chl	chlorophyll		
CLSM	confocal laser scanning microscope		

List of abbreviations

FD	ferredoxin	PID	protein import defect
Fig.	figure	PNP	para-nitrophenol
FMN	flavin mononucleotide	PNPG	para-nitrophenyl β -D-glucuronide
FW	fresh weight	PQ	plastoquinone
GBF	G-box binding factor	PSI	photosystem I
GFP	green fluorescent protein	PSII	photosystem II
GRX	glutaredoxin	PTK	plastid transcription kinase
GUS	β -glucuronidase	qP	photochemical quenching
HL	high light	qRT-PCR	quantitative reverse transcriptase PCR
kb	kilo base pairs	r	coefficient of correlation
LB	left border	RB	right border
LB medium	Lysogeny broth medium	RNA	ribonucleic acid
<i>Ler</i>	<i>Arabidopsis thaliana</i> accession Landsberg <i>erecta</i>	ROS	reactive oxygen species
LHCII	light harvesting complex II	RT	room temperature
Lin	lincomycin	SD	synthetic dropout
LL	low light	SDS	sodium dodecyl sulfate
LOV	light, oxygen or voltage	SEM	standard error of the mean
LRE	light responsive element	SIBs	SIG1 binding proteins
LTR	long term response	SNP	single nucleotide polymorphism
M	molar	SSLP	simple sequence length polymorphism
MES	monohydrate 2-(<i>N</i> -morpholino)ethanesulfonic acid	T _A	annealing temperature
mRNA	messenger RNA	Tab.	table
MS	Murashige & Skoog	<i>Taq</i>	<i>Thermus aquaticus</i>
n	number	TATA	TATA box
N-	amino-	TDO	triple dropout
NEP	nuclear encoded polymerase	T _M	melting temperature
NF	norflurazon	TAE	tris acetic acid EDTA
OD	optical density	TAIL-PCR	thermal asymmetric interlaced PCR
ORF	open reading frame	TE	tris EDTA
Φ PSII	effective quantum yield of PSII	TF	transcription factor
PAM	pulse amplitude-modulated	TP	transit peptide
PC	plastocyanin	Tris	tris(hydroxymethyl)-aminomethane
PCR	polymerase chain reaction	TRX	thioredoxin
PEG	polyethylene glycol	U	unit
PEP	plastid encoded polymerase	UAS	upstream activating sequence
PET	photosynthetic electron transport	UCR	unconserved region
PGE	plastid gene expression	UTR	untranslated region
PhANGs	photosynthesis-associated nuclear encoded genes	UV	ultra violet
phot	phototropin	v/v	volume per volume
PHR	photolyase homology region	w/v	weight per volume
phy	phytochrome	Y1H	yeast one hybrid
		YEB	yeas extract and beef

List of abbreviations

YPAD	yeast peptone adenine dextrose		YPD	yeast peptone dextrose
------	-----------------------------------	--	-----	------------------------

Amino acids and nucleic acids were abbreviated according to recommendations given by the IUPAC-IUB Joint Commission on Biochemical Nomenclature (JCBN).

1

INTRODUCTION

1.1 Light regulated transcriptional networks in plants

1.1.1 The environmental factor light

The survival of organisms depends on their ability to accurately sense and respond to their environment. Light is one of the most important environmental factors, as it provides the source of energy for plant life. Changes in light quality, light intensity, direction and duration can occur over broad time scales, from canopy-dependent fluctuations during the course of a day to seasonal differences in day length. Plants have evolved sophisticated mechanisms to sense and respond to their light environments (reviewed in Chen *et al.*, 2004). Plant responses to light occur in the context of multiple developmental processes throughout the plant life cycle, including seed germination (Casal and Sanchez, 1998), seedling photomorphogenesis (Kendrick and Kronenberg, 1994), phototropism (Sakai *et al.*, 2001), gravitropism (Lu and Feldman, 1997), chloroplast development (Stephenson *et al.*, 2009) and chloroplast movement (DeBlasio *et al.*, 2003), shade avoidance (Martínez-García *et al.*, 2010; Keller *et al.*, 2011), circadian rhythms (McClung, 2001; Yanovsky *et al.*, 2001) and flower induction (Evans, 1971; O'Neill, 1992).

1.1.2 Light regulates gene expression at the level of transcription

Transcriptional regulation is a crucial step for function and development of life. Transcription is defined as the interaction between DNA binding transcription factors (TFs) that attach to *cis*-regulatory DNA elements (reviewed in Stower, 2012), and shaped by the influence of additional co-factors and chromatin structure. TFs activate or repress gene transcription in response to changes in the environment as well as during development. The combinations of multiple TFs are essential for diverse gene expression patterns in higher organisms, a fact that places special importance on the number and the interplay of different *cis*-acting elements composing regulatory units that explain the regulatory capacity of a promoter.

Regulation of gene expression in response to the highly variable light environment is an essential process in plant development and function. Regulation of transcription is one of the most important mechanisms by which light regulates plant growth and development (Terzaghi and Cashmore, 1995; Jiao *et al.*, 2007). Microarray analysis showed that a massive change in gene expression occurs during photomorphogenesis: Up to one-third of the genes in *Arabidopsis thaliana* showed changes in expression between light- and dark-grown seedlings (Ma *et al.*, 2001; Tepperman *et al.*, 2001; Casal and Yanowsky, 2005). The effects of light are so profound that many of the major biochemical pathways that are located within the main subcellular organelles are coordinately regulated by light (Ma *et al.*, 2001; Jiao *et al.*, 2005).

The proper adjustment of photosynthesis to the prevalent light environment is of particular importance for plant life and function. Light regulates chloroplast development and function by promoting the expression of nuclear encoded chloroplast genes and photosynthesis-associated genes. The most extensively studied light-responsive genes are *RBCS*, encoding the small subunit of ribulose-1,5-bisphosphate carboxylase/oxygenase, and the *LHC* genes (former *CAB*, encoding light-harvesting chlorophyll *a/b* binding proteins) (reviewed in Argüello-Astorga and Herrera-Estrella, 1998). Both belong to the superfamily of photosynthesis-associated nuclear encoded genes (PhANGs), whose expression is light induced and coordinated with chloroplast development (Gray *et al.*, 2003).

1.1.3 Light-sensitive *cis*-acting regulatory promoter elements

Promoters consist of specific DNA motifs and elements, which act in the recruitment of protein factors. These TFs facilitate transcription of the downstream protein-coding sequence (CDS) of the gene. The conserved DNA elements are called the *cis*-regulatory elements or motifs, and they determine the temporal and spatial expression of the gene (de Boer *et al.*, 1999). The combination, spacing and relative orientation of the TF binding sites influences the assembly of specific multi-protein complexes (Block *et al.*, 1990). Transcriptional regulation of gene expression depends on the regulation of various interactions between these *cis*-elements and their respective TFs.

Cis-acting regulatory elements are specific short DNA sequence motifs of approximately 5-25 bp (Rani, 2007). Several *cis*-acting regulatory elements have been identified as components of light-responsive promoters, named light responsive elements (LREs). Numerous LREs were identified by deletion and mutagenesis analysis of the promoter regions of PhANGs (Giuliano *et al.*, 1988; Menkens *et al.*, 1995). Others were identified by footprinting and gel-retardation assays that screen for binding motifs of known light-responsive TFs (Terzaghi and Cashmore, 1995). Commonly found motifs essential for light-mediated transcriptional activity are the G-box (Giuliano, 1988), the GT1-motif (Chattopadhyay *et al.*, 1998a), the Z-box (Ha and An, 1988; Yadav *et al.*, 2002), the I-box (Donald and Cashmore, 1990) or GATA-motifs (Argüello-Astorga and Herrero-Estrella, 1998).

No single element is found in all light-regulated promoters, suggesting a complex light-regulated network and a lack of a universal switch. This hypothesis is supported by the fact, that none of the known elements has been identified to solely confer light responsiveness to heterologous non-light regulated basal promoters (Park *et al.*, 1996; Chattopadhyay *et al.*, 1998a; López-Ochoa *et al.*, 2007). Thus it was suggested that a combination of different *cis*-acting elements make up the light responsive unit rather than an individual element (Terzaghi and Cashmore, 1995; Puente *et al.*, 1996). Indeed LREs usually act combinatorial; combinations of at least two regulatory elements are required for most light responsiveness (Kuhlemeier *et al.*, 1988; Gilmartin *et al.*, 1990; Terzaghi and Cashmore, 1995; Martínez-Hernández *et al.*, 2002). Additionally it has been shown that artificial sequences composed of paired combinations of tetrameric repeats of G- and GATA-boxes or GT1- and GATA-boxes, but not multimers of a single motif, can function as light responsive elements (Puente *et al.*, 1996; Chattopadhyay *et al.*, 1998a). A known exception is the response of promoters with a single G-box or GATA-motif to continuous high-irradiance light (Puente *et al.*, 1996).

1.1.3.1 G-boxes

The term G-box was first used by Giuliano *et al.* (1988) to describe a DNA sequence present in the 5' flanking region of the light-regulated tomato *RBCS3A* gene. G-box motifs with the core hexamer CACGTG are found in promoters of genes that respond to a variety of different stimuli including light (Schulze-Lefert *et al.*, 1989; Block *et al.*, 1990; Schindler and Cashmore, 1990; López-Ochoa *et al.*, 2007), abscisic acid (ABA) (Mundy *et al.*, 1990; Acevedo-Hernández *et al.*, 2005) or ethylene (Sessa *et al.*, 1995). Several DNA-binding proteins specific for G-box-like motifs, named GBFs (G-box binding factors) (Menkens and Cashmore, 1994), have been identified. Members of the bZIP (basic leucine zipper) family like HY5¹ (LONG HYPOCOTYL 5, also designated as ELONGATED HYPOCOTYL 5) (Oyama *et al.*, 1997) as well as the PIFs (PHYTOCHROME-INTERACTING FACTORS)² have been identified to be GBFs (Menkens and Cashmore, 1994; Menkens *et al.*, 1995; Chattopadhyay *et al.*, 1998b; Martínez-García *et al.*, 2000).

ABI4 (ABSCISIC ACID INSENSITIVE 4) is a negatively acting Apetala2-type TF, binding to G-boxes and therefore blocking the enhancer. ABI4 inhibits the G-box mediated, light-induced expression of PhANGs when chloroplast development is arrested (Koussevitzky *et al.*, 2007).

¹ The HY5 protein is described in more detail in chapter 1.2.4.1

² PIF functions are described in more detail in chapter 1.2.4.2

1.1.3.2 Z-boxes

A Z-DNA-forming sequence (ATACGTGT) is essential for light-dependent developmental expression of *LHCBI.3* (former *CABI*) (Ha and An, 1988). Recent studies have revealed that Z-box containing synthetic and native promoters are responsive to phyA (phytochrome A), phyB, and cry1 (cryptochrome 1) photoreceptors and are under the control of downstream regulatory components such as COP1³ (CONSTITUTIVE PHOTOMORPHOGENIC 1) and HY5 (Puente *et al.*, 1996; Yadav *et al.*, 2002).

Several Z-box binding factors (ZBFs) have been identified and they illustrate the tight connections between different networks that regulate light-dependent transcription. For example, ZBF1/MYC2 is a negative regulator of blue light mediated photomorphogenic growth and acts as a point of cross-talk among light, ABA, and jasmonic acid signaling pathways (Yadav *et al.*, 2002, 2005; Boter *et al.*, 2004; Lorenzo *et al.*, 2004). ZBF1/MYC2 is also binding G-boxes (Yadav *et al.*, 2005), as does bZIP protein ZBF2/GBF1 (Mallappa *et al.*, 2006). ZBF2/GBF1 plays both positive and negative regulatory roles in photomorphogenic growth and PhANG gene expression downstream of cry1 and cry2 (Mallappa *et al.*, 2006).

1.1.3.3 I-boxes and GATA motifs

I-boxes (formerly designated as GA-motif or ARGATGA-motif) are defined as GATAAGR and are involved in light-responses as well as in circadian clock responses (Borello *et al.*, 1993). Martínez-Hernández *et al.*, (2002) identified I-boxes as parts of many light regulated promoters, combined with a G- or GT1-box related element. In most *RBCS* genes a single I-box near a G-box, in about 100-300 bp upstream of the TATA-box, mediates light-responsiveness (Borello *et al.*, 1993; López-Ochoa *et al.*, 2007).

The I-box related GATA motif, GATA, is very common in the promoters of light-regulated genes (Argüello-Astorga and Herrero-Estrella, 1998) and found in light-regulated *LHC* or *RBCS* promoters (Grob and Stuber, 1987). In many *LHCB* promoters two or three GATA elements, separated by a few base pairs, are found close to the TATA box (Castresana *et al.*, 1988; Gidoni *et al.*, 1989; Mitra *et al.*, 1989). In combination with a second LRE, GATA-motifs mediate the transcriptional response to phyA, phyB and cry1 photoreceptors (Anderson *et al.*, 1994; Chattopadhyay *et al.*, 1998a).

I-boxes as well as GATA-motifs were also identified frequently in the promoters of Arabidopsis and rice sucrose transporters, suggesting that these elements may function as a link between light perception and sugar metabolism (Ibraheem *et al.*, 2010).

³ The COP/DET/FUS complex is described in more detail in chapter 1.2.4.3

1.2 Light sensing by photoreceptors

The regulation of plant growth by light signals is mediated mainly by three families of photoreceptors: the UV-A/blue light absorbing cryptochromes (Cashmore *et al.*, 1999) and phototropins (Briggs and Christie, 2002) and the red/far-red light absorbing phytochromes (Wang and Deng, 2004). Additional to the cryptochromes and phototropins, FKF1 (flavin-binding, kelch repeat, F-box) was identified as a UV-A/blue light-specific receptor (Imaizumi *et al.*, 2003; Kim *et al.*, 2007). FKF1 is a member of the ZEITLUPE/ADIAGO putative family of photoreceptors (Schultz, 2005) regulating the circadian clock (Baudry *et al.*, 2010). Additional photoreceptors for sensing UV-B wavelength were postulated (Lorrain *et al.*, 2006; Jiao *et al.*, 2007). Recently Rizzini *et al.* (2011) described a UV-B photoreceptor function for the Arabidopsis UVR8 protein.

Photoreceptors affect gene expression via complex downstream signaling networks. Kinases, phosphatases and degradation pathway proteins were identified as such regulators. Parallel to these signal transduction pathways, photoreceptors modulate gene expression by directly interacting with TFs (Casal and Yanovsky, 2005; Jiao *et al.*, 2007; Liu *et al.*, 2008). Some of these TFs are regulated by only one type of light, whereas many more respond to a wide spectrum of light. Positive and negative transcriptional regulation (Weisshaar *et al.*, 1991), post-translational modification (Klimczak *et al.*, 1992, 1995; Harter *et al.*, 1994; Wellmer *et al.*, 1999) and degradation of these TFs (Hoecker *et al.*, 1999; Sharrock and Clack, 2002; Saijo *et al.*, 2003; Seo *et al.*, 2003, 2004) are important in the light-regulated control of development.

1.2.1 Phytochromes

The red and far-red light-absorbing phytochromes are photochromic biliproteins that convert between inactive and active forms in response to different wavelength of light. Phytochromes are synthesized in the dark in a biologically inactive red light absorbing form (P_r). Red light absorption induces photoconversion to the far-red light absorbing P_{fr} form (Quail, 1997) (fig. 1-1). This photoconversion is reversible upon far-red light absorption and also thermally controlled, a process called dark reversion (Kendrick and Kronenberg, 1994). This results in a dynamic, light-dependent equilibrium of P_r and P_{fr} forms. Phytochromes exist as homodimers (Jones and Quail, 1986; Wagner *et al.*, 1996) or heterodimers (Sharrock and Clack, 2004; Clack *et al.*, 2009) with each monomer comprising an apoprotein covalently attached to a light absorbing linear tetrapyrrole chromophore, phytychromobilin (Lagarias and Rapoport, 1980).

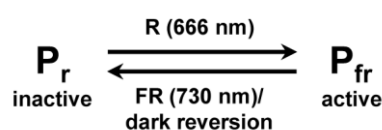


Figure 1-1. Photoconversion and dark reversion between the P_r (inactive) and the P_{fr} (active) form of phytochromes. R: red light, FR: far-red light.

The Arabidopsis genome encodes five genes for phytochromes, *PHYA–E* (Sharrock and Quail, 1989; Clack *et al.*, 1994). Based on their stability in the light, phytochromes have been classified into two types. Type I phytochromes are photo-labile. They accumulate in etiolated seedlings and degrade rapidly upon light exposure. Type II phytochromes are relatively stable in the light (Furuya, 1993). In Arabidopsis, phyA is the only type I phytochrome; phyB-E are type II phytochromes (Quail, 1997; Hirschfeld *et al.*, 1998; Hennig *et al.*, 1999b; Sharrock and Clack, 2002). Consistent with this, phyA displays rapid lability in the P_{fr} form, in contrast to phyB-E, which display relative stability in the P_{fr} form (Franklin and Quail, 2010).

The individual members of the family have distinct, albeit overlapping functions in controlling plant responses (Whitelam and Devlin, 1997; Quail, 1998; Smith, 2000). For all five phytochromes a role in modulating leaf architecture was shown. They are involved in regulation of seedling de-etiolation (reviewed in Franklin and Quail, 2010). PhyA is the predominant phytochrome in etiolated seedlings but is rapidly degraded to much lower levels upon transfer to light (Clough and Vierstra, 1997). PhyA has a significant role in the apical-zone responses of hook opening, cotyledon expansion and chloroplast biogenesis (Tepperman *et al.*, 2004). PhyA regulates transcription of early responding genes under both far-red light and red light (Tepperman *et al.*, 2001, 2006). PhyA is called the main far-red light photoreceptor, and it is the only phytochrome which mediates de-etiolation under far-red light conditions (Dehesh *et al.*, 1993; Nagatani *et al.*, 1993; Parks and Quail, 1993; Whitelam *et al.*, 1993). PhyB is the most abundant phytochrome in light-grown plants (Sharrock and Clack, 2002) and is described as the main red light receptor (Shinomura *et al.*, 1996; Chen *et al.*, 2004). PhyB has a very prominent role in red/far-red light (R/FR) ratio sensing (Somers *et al.*, 1991; Weller *et al.*, 1995; Smith, 2000). In contrast, *phyC*, *phyD*, and *phyE* mutants are only mildly deficient in R/FR sensitivity compared with the wild type (Aukerman *et al.*, 1997; Devlin *et al.*, 1998; Franklin *et al.*, 2003a; Monte *et al.*, 2003; Takano *et al.*, 2005), indicating that these phytochromes mediate more subtle shade/neighbor-induced or R/FR-reversible responses, fine-tuning light development in concert with phyB.

The soluble phytochromes translocate into the nucleus in a light-dependent manner, following a P_r to P_{fr} conformational change (reviewed in Kevei *et al.*, 2007). PhyA translocates to the nucleus in far-red light or white light (Kircher *et al.*, 2002; Nagy and Schäfer, 2002), while phyB to phyE translocate to the nucleus in red or white light (Kircher *et al.*, 2002).

A primary mechanism of phytochrome signalling involves interaction of the P_{fr} form with a subfamily of basic helix-loop-helix (bHLH) TFs, the PIFs⁴, in the nucleus. These phytochrome mediated signals are integrated by the COP/DET/FUS⁵ group of components (Hoecker *et al.*, 1999; Saijo *et al.*, 2003; Seo *et al.*, 2004).

⁴ Functions and regulatory mechanisms of PIFs are described in more detail in chapter 1.2.4.2

⁵ The COP/DET/FUS complex is described in more detail in chapter 1.2.4.3

In addition to regulating gene-expression by direct interaction of phytochromes with target-components in the nucleus, additional, more indirect pathways are discussed. These contain heterotrimeric G-proteins (Okamoto *et al.*, 2001), Ca²⁺/calmodulin (Neuhaus *et al.*, 1993) and cyclic guanosine monophosphate (cGMP) as second messengers (Bowler *et al.*, 1994), and the binding of phytochromes to cytoplasmic proteins (Choi *et al.*, 1999; Fankhauser *et al.*, 1999). Recently, a novel splicing factor was identified as part of the phyB regulated network controlling gene expression in Arabidopsis. The C-terminal RS-domain of the splicing factor RRC1 that is important for the regulation of alternative splicing plays an important role in phyB mediated red light signal transduction (Shikata *et al.*, 2012).

Global gene expression studies have shown that phytochrome responses are associated with massive alterations in gene expression (Ma *et al.*, 2001; Tepperman *et al.*, 2001, 2004; Wang *et al.*, 2002), which suggests a key role for phytochromes in transcriptional control of gene expression.

1.2.2 Cryptochromes

The Arabidopsis genome encodes three members of the cryptochrome family of UV-A/blue light photoreceptors, cry1 (Ahmad and Cashmore, 1993), cry2 (Lin *et al.*, 1995a; Hoffman *et al.*, 1996), and a more divergent family member, cry3 (Kleine *et al.*, 2003).

The cryptochrome apoprotein consists of two domains: an amino-terminal photolyase homology region (PHR), and the carboxy-terminal cryptochrome C-terminal extension (CCE) domain of various length and sequences. PHR is the chromophore-binding domain that binds non-covalently the chromophore FAD (flavin adenine dinucleotide) (Lin *et al.*, 1995b). It has been proposed that the oxidized flavin is the ground-state chromophore, because it absorbs blue light most effectively (Banerjee *et al.*, 2007; Liu *et al.*, 2011b). According to this hypothesis, FAD is reduced upon blue light absorption. The reduction triggers a conformational change of the cryptochrome and the subsequent signal transduction (Banerjee *et al.*, 2007; Bouly *et al.*, 2007; Müller and Ahmad, 2011).

Cry1 and cry2 mediate primarily the regulation of de-etiolation (Lin, 2002; Liscum *et al.*, 2003) and photoperiod-dependent flowering induction (Ahmad and Cashmore, 1993; Guo *et al.*, 1998; Cashmore *et al.*, 1999). Additionally they regulate several other aspects of plant growth and development, including entrainment of the circadian clock (Somers *et al.*, 1998; Yanovsky and Kay, 2003), the high light stress response (Weston *et al.*, 2000; Kleine *et al.*, 2007), osmotic stress response (Xu *et al.*, 2009) and shade avoidance (Keller *et al.*, 2011). Cry1 is a light-stable protein (Shalitin *et al.*, 2003), whereas cry2 is light-labile (Shalitin *et al.*, 2002). In both cry1 and cry2, blue light triggers phosphorylation (Bouly *et al.*, 2003; Burney *et al.*, 2009). In the case of cry2, this is associated with proteolytic degradation of the protein (Shalitin *et al.*, 2002). Consistent with those findings, cry1 is the primary photoreceptor under high blue light fluence rates, whereas cry2 is most important under low blue light fluence rates (Ahmad and Cashmore, 1993; Ahmad *et al.*, 1998b; Lin *et al.*, 1998a). Cryptochromes mediate the blue light control of gene expression via two

mechanisms: (i) light-dependent modulation of transcription by direct interaction with cryptochrome-interacting basic-helix-loop-helix TFs (CIBS) (Liu *et al.*, 2008), and (ii) light-dependent suppression of proteolysis of TFs.

The third *Arabidopsis* cryptochrome, cry3, belongs to the CRY-DASH clade of the photolyase/CRY superfamily, and it is known to act as a single-stranded DNA repairing enzyme (Brudler *et al.*, 2003; Selby and Sancar, 2006; Pokorny *et al.*, 2008). Additional functions for cry3 as a photoreceptor are postulated (Liu *et al.*, 2011), probably in chloroplasts and mitochondria (Kleine *et al.*, 2003).

1.2.3 Phototropins

The phototropins phot1 and phot2 are UV-A/blue light receptors that mediate phototropism (reviewed in Christie and Briggs, 2005), chloroplast movement (Wada *et al.*, 2003), stomatal opening (Kinoshita *et al.*, 2001), rapid growth inhibition of etiolated seedlings (Folta and Spalding, 2001), and leaf expansion in *Arabidopsis* (Ohgishi *et al.*, 2004). Phot1 functions as the primary phototropic receptor under low to moderate fluence intensities, whereas in high fluence rates phot1 and phot2 function as redundant receptors (reviewed in Briggs and Christie, 2002).

The photosensitive amino-terminal region of phototropins is composed of two flavin mononucleotide (FMN)-binding domains (Christie *et al.*, 1999) designated as light, oxygen, or voltage (LOV). The carboxy-terminal region includes a Ser/Thr protein kinase domain (Briggs and Christie, 2002). In darkness, LOV domains bind FMN non-covalently. Blue light irradiation causes the formation of a covalent adduct between a conserved cysteine within the LOV domain and the FMN (Salomon *et al.*, 2000; Crosson and Moffat, 2001, 2002). Under these conditions the kinase domain catalyzes autophosphorylation (Christie *et al.*, 1998; Liscum *et al.*, 2003). The autophosphorylation is the initial event in the transmission of the light signal.

The phototropins play a modest role in the blue light-induced remodeling of the transcriptional program; for example, phot1 is essential for the high blue light-induced destabilization of the *LHCB* and *RBCL* transcripts (Folta and Kaufmann, 2003; Ohgishi *et al.*, 2004).

1.2.4 Components downstream of photoreceptors

For each developmental response on the level of transcription, more than one photoreceptor can contribute to the perception of light signals, indicating that signal integration points for different light signals exist (Jiao *et al.*, 2007; Liu *et al.*, 2011). Functional interdependence between phytochrome and cryptochrome photoreception systems takes place directly by physical interaction of the photoreceptors (Ahmad *et al.*, 1998a; Hennig *et al.*, 1999a; Más *et al.*, 2000). Cryptochromes are discussed to be substrates for the kinase activity of

phytochromes in the P_{fr} form (Ahmad *et al.*, 1998a; Más *et al.*, 2000). Additionally, they act on common TF(s) (reviewed in Jiao *et al.*, 2007).

Various regulators of light-dependent gene expression are identified that act downstream of the light sensing photoreceptors. A large fraction of the genes whose transcription responds to light encodes TFs, in addition to kinases, phosphatases and degradation-pathway proteins. Due to the high number of TFs involved, transcriptional cascades are predicted to control the expression of multiple downstream target genes (reviewed in Jiao *et al.*, 2007; Lee *et al.*, 2007a).

1.2.4.1 HY5

The bZIP protein HY5 is a key TF mediating the blue light and red light responses of photoregulated promoters in a phytochrome and cryptochrome-dependent manner (Whitelam and Devlin, 1998; Osterlund *et al.*, 2000; Sellaro *et al.*, 2011). HY5 is a pivotal positive regulator of photomorphogenic seedling development (Oyama *et al.*, 1997; Lau and Deng, 2010). In addition, HY5 mediates plant responses to UV-B (Oravec *et al.*, 2006) and to different hormones, such as ABA, gibberellins, cytokinin, and auxin (reviewed in Lau and Deng, 2010). Recently, a ChIP-chip approach has revealed that HY5 binds > 9.000 genes, affecting the expression of > 1.000 target genes (Zhang *et al.*, 2011). Furthermore, HY5 indirectly regulates many other genes (Zhang *et al.*, 2011). Therefore, HY5 is one of the central modulators of gene expression for the coordination of light signals and plant development.

At the transcriptional level, HY5 expression is positively regulated by light via a phytochrome-dependent pathway (Oyama *et al.*, 1997; Tepperman *et al.*, 2001). HY5 protein stability is regulated by the COP/DET/FUS protein degradation machinery (Ang *et al.*, 1998; Holm *et al.*, 2002; Saijo *et al.*, 2003). HY5 binds to promoters of light-inducible genes; G-box (Chattopadhyay *et al.*, 1998b; Gao *et al.*, 2004; Zhang *et al.*, 2011), Z-box (Yadav *et al.*, 2002), C-box (nGACGTCn), GC-hybrid (GACGTG) and CA-hybrid (GACGTA) (Song *et al.*, 2008) motifs are HY5 binding consensus sequences.

1.2.4.2 PIFs

The PIFs are a group of nuclear localized, G-box binding bHLH TFs (Martínez-García *et al.*, 2000; Huq and Quail, 2002; Huq *et al.*, 2004). Genetic and biochemical data show that they act directly downstream of phytochromes and mediate their signaling (reviewed in Chen and Chory, 2011). They can directly interact with phytochromes, with stronger preference for phyB than to phyA (Zhu *et al.*, 2000). In the light, activated phytochromes in the P_{fr} form interact with PIFs and result in the phosphorylation (reviewed in Fankhauser, 2000), subsequent ubiquitination and degradation via the 26S proteasome (Bauer *et al.*, 2004; Park *et al.*, 2004; Al-Sady *et al.*, 2006). This results, for example, in the initiation of transcription of genes inducing photomorphogenesis (fig. 1-2; reviewed in Leivar and Quail, 2011). PIFs

compose one of the two main light signaling branches downstream of photoreceptors which are the PIFs pathway and the COP1-HY5 pathway (Lau and Deng, 2010).

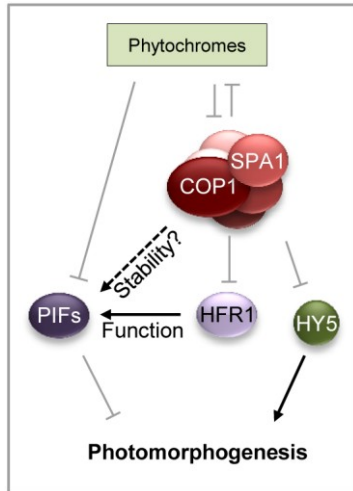


Figure 1-2. Phytochrome signaling pathways to turn on photomorphogenesis. Phytochromes trigger the degradation of the mainly negatively acting PIFs. The activity of the PIFs could be enhanced by the 26S proteasome through HFR1 (LONG HYPOCOTYL IN FAR-RED 1) repression; the protein stability of at least PIF3 is promoted by three different protein complexes, a SPA1-COP1 complex (Saijo *et al.*, 2003), a DET1-COP10 complex (Yanagawa *et al.*, 2004) and the COP9 signalosome (Wei and Deng, 2003). Alternatively, phytochromes derepress the positively acting transcriptional regulators, including HY5 and HFR1, by inhibiting the proteasome. Modified according to Chen and Chory (2011).

PIFs have been shown to positively or negatively regulate gene expression: PIFs are essential for the repression of photomorphogenesis in darkness (reviewed in Leivar and Quail, 2011); on the contrary, PIF4 and PIF5 promote shade avoidance syndrome (Lorrain *et al.*, 2008), and PIF3 acts positively in light-induced chloroplast development (Monte *et al.*, 2004).

1.2.4.3 COP/DET/FUS

Proteins of the CONSTITUTIVE PHOTOMORPHOGENIC/DEETIOLATED/FUSCA (COP/DET/FUS) group are components of an ubiquitin-proteasome pathway (reviewed in Casal and Yanovsky, 2005). They act downstream of both, the phytochrome and cryptochrome pathways (Osterlund *et al.*, 1999, 2000; Wang *et al.*, 2001; Yang *et al.*, 2001) and act as negative regulators by suppressing photomorphogenesis in darkness (Sullivan *et al.*, 2003).

One of these components, COP1, a RING-finger type E3 ubiquitin-protein ligase, is called the master regulator of photomorphogenic development (Osterlund *et al.*, 2000). In the dark COP1 is localized in the nucleus, targeting specific proteins for degradation by assisting their ubiquitinylation (Hardtke and Deng, 2000; Seo *et al.*, 2003). The E3 ubiquitin ligase activity of COP1 is modulated by interaction with SUPPRESSOR OF PHYTOCHROME A 1 (SPA1) (Saijo *et al.*, 2003), a negative regulator of far-red light phyA signaling (Hoecker *et al.*, 1999; Saijo *et al.*, 2003). The SPA1/COP1 complex regulates the proteolysis of several TFs like HY5 (Ang *et al.*, 1998; Osterlund *et al.*, 2000), HYH (Holm *et al.*, 2002) and HFR1 (Duek *et al.*, 2004; Yang *et al.*, 2005) (fig. 1-3). In the light, COP1 moved from the nucleus into the cytosol, a process that allows HY5 to accumulate and to interact with DNA (von Arnim and Deng, 1994). COP1 is also associated with the light-induced degradation of cry1

(Yang *et al.*, 2001; Lian *et al.*, 2011; Liu *et al.*, 2011) and cry2 (Wang *et al.*, 2001; Zuo *et al.*, 2011).

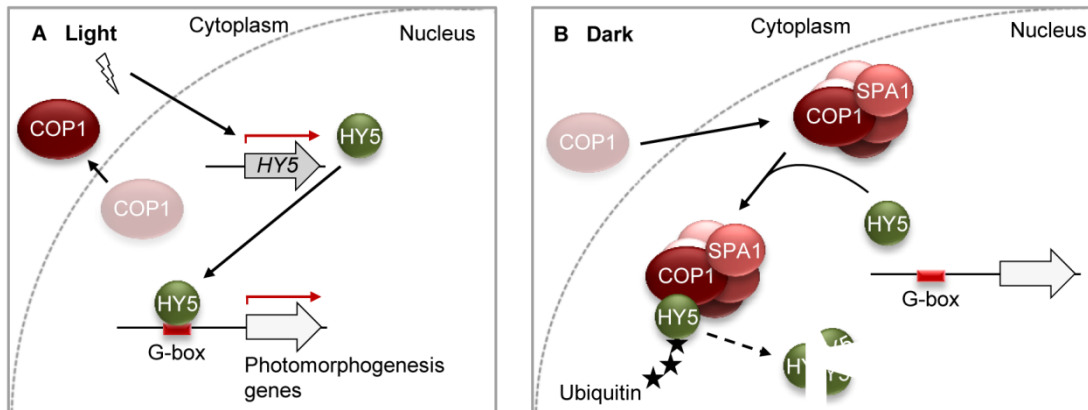


Figure 1-3. Mechanism of HY5 regulation by light. A: *HY5* transcription is stimulated in the light. *HY5* binds to G-box containing promoters of photomorphogenesis genes and initiates transcription. B: In the dark, COP1 is translocated into the nucleus. The SPA1/COP1 complex regulates *HY5* activity by targeted ubiquitin-mediated proteolysis through the 26S proteasome.

1.3 Retrograde plastid signals regulating nuclear gene expression

During the process of evolution most of the genes encoded by the cyanobacterial ancestor of plastids were transferred into the host nuclear genome which reduced the plastid genome in land plants to about 120 genes (Martin and Herrmann, 1998). Plastid biogenesis relies on the import of about 3,000 nuclear encoded plastid proteins (reviewed in Jarvis, 2008). Several genes encoding photosynthetic proteins are regulated in parallel at the levels of transcription and at the translational level (Kuhlemeier, 1992). Changes in functional or metabolic states of plastids affect the expression of nuclear genes encoding plastid proteins, a regulation important for maintaining plastid function (reviewed in Woodson and Chory, 2008). Signals originating from plastids and mitochondria are called retrograde signals.

Retrograde plastid signals have two main functions: First, the expression of subunits of multi-protein complexes that are encoded by both nuclear and plastid genomes must be coordinated to ensure proper function; second, adjusting nuclear gene expression and protein flow to the external environment as the environment affects metabolic activities and the functional state of the plastids. Consequently, retrograde plastid-to-nucleus signaling is a critical component of plant responses to abiotic stresses, such as high light and drought stress (reviewed in Pogson *et al.*, 2008). The generation of reduction equivalents during photosynthesis is a light-driven process; therefore light intensity and light quality are prominent modulators of retrograde signaling.

Retrograde plastid signals are currently classified into five major groups: (i) pigment biosynthesis, i.e. intermediates of carotenoid and tetrapyrrole biosynthesis; (ii) plastid gene expression (PGE); (iii) plastid protein import; (iv) generation of reactive oxygen species (ROS) and ROS-related processes and (v) redox processes in photosynthesis. In addition,

multiple interactions of these pathways with sugar and hormone signalling occur (reviewed in Pesaresi *et al.*, 2007).

Recently Estavillo *et al.*, (2011) identified a novel retrograde signaling pathway regulating the expression of various stress-regulated genes. The phosphonucleotide 3'-phosphoadenosine 5'-phosphate (PAP) accumulates in response to stress and moves from the chloroplast to the nucleus, where its activity leads to the activation of stress-responsive genes. They further show that the phosphatase SAL1 functions as negative regulator of PAP accumulation in plastids and mitochondria (Estavillo *et al.*, 2011).

A few proteins have been identified that act as general or pleiotropic regulators coordinating the modulation of nuclear transcription upon retrograde plastid signals, for instance ABI4 (Koussevitzky *et al.*, 2007), PRL1 (PLEIOTROPIC RESPONSE LOCUS 1) (Baruah *et al.*, 2009) or GLK (GOLDEN2-LIKE) (Waters *et al.*, 2009). However, components acting downstream of these regulators are still unknown (Pfannschmidt, 2010).

The redox-sensitive TF Rap2.4 is a regulator of the chloroplast antioxidant enzyme 2-Cys peroxiredoxin A (2CPA) (Shaikhali *et al.*, 2008). Rap2.4a functions as redox sensor, as its activity is regulated by dithiol/disulfide transition of regulatory cysteinyl residues, and transducer of redox information (Shaikhali *et al.*, 2008). RCD1 is another protein involved in retrograde signaling in young Arabidopsis leaves. Analysis of the *redox imbalanced (rimb)* mutants, which are impaired in 2CPA promoter regulation in the seedling stage (Heiber *et al.*, 2007), identified *rimb1* being allelic with RCD1/CLONE EIGHTY ONE (CEO1) (Hiltscher *et al.*, in preparation). RCD1 interacts with Rap2.4a, in a way that is slightly redox-dependent (Hiltscher *et al.*, in preparation).

1.3.1 Pigment biosynthesis

In albino mutants or when chloroplasts are photo-bleached after treatment with the herbicide norflurazon (NF), which inhibits carotenoid biosynthesis (Bartels and Watson, 1978), the expression of PhANGs is shut off in response to the dysfunctional state of the chloroplasts (Oelmüller *et al.*, 1986; Gray *et al.*, 2003). Studying the *genomes uncoupled (gun)* mutants, which exhibit NF-insensitive *LHCB* expression (Susek *et al.*, 1993), led to the identification of proteins that alter the expression of certain photosynthesis associated genes. Some of the *GUN* genes encode components of tetrapyrrole biosynthesis, and the tetrapyrrole magnesium protoporphyrin IX was considered as good candidate signaling molecule for a number of years (Mochizuki *et al.*, 2001; Larkin *et al.*, 2003). However, recent evidence has cast doubt on this hypothesis (Mochizuki *et al.*, 2008, 2010; Moulin *et al.*, 2008).

1.3.2 Plastid gene expression

Treatment of plants with plastid-specific translation inhibitors such as chloramphenicol or lincomycin (LIN) resulted in the discovery of the PGE pathway that is only active early in seedling development (Oelmüller *et al.*, 1986). This pathway of retrograde signaling is light-independent, as was discovered using *lip1* and *cop1-4* mutants. These mutants accumulate significant levels of the light-induced *LHCB1.2* transcript when grown in the dark, but its levels are reduced when seedlings are exposed to LIN (Sullivan and Gray, 1999). Up to now, no experimental evidence for protein or RNA export from the plastid has been obtained (Beck, 2005).

1.3.3 Plastid protein import

Expression of nuclear encoded photosynthetic genes is compromised in a mutant lacking the major protein import receptor of the TOC machinery, Toc159 (Bauer *et al.*, 2000; Kakizaki *et al.*, 2009). The signaling pathway appears to be mediated by GUN1 and GLK1 (Kakizaki *et al.*, 2009), but is still controversially discussed (Pfannschmidt, 2010).

1.3.4 ROS

Several ROS are continuously produced in plants as byproducts of aerobic metabolism (Halliwell and Gutteridge, 1999). Organellar electron transport chains are major sites for the generation of ROS, such as $^1\text{O}_2$ (singlet oxygen), H_2O_2 (hydrogen peroxide) and O_2^- (superoxide anion). Under low light ROS are seldom generated and most of them are detoxified by antioxidant systems (reviewed in Apel and Hirt, 2004). Under abiotic stress conditions, like excess light or low temperature, much more ROS are generated than the antioxidant systems can deal with (Karpinski, 1997, 1999; Li *et al.*, 2009b), a situation called oxidative stress (Foyer *et al.*, 1994).

Parallel to damaging cellular compounds (Halliwell, 1987; reviewed in Møller *et al.*, 2007) the oxidized products can be important secondary signaling molecules (reviewed in Mittler *et al.*, 2004). The ROS generation in chloroplasts results in changes of the nuclear transcriptome, indicating that they act as a retrograde signal (Desikan *et al.*, 2000, 2001a; Moseyko *et al.*, 2002). However, ROS, with exception of H_2O_2 , are very short lived (Møller *et al.*, 2007), and therefore dissociate before they can cross the envelope and serve as a direct signal outside of the chloroplast. Furthermore, ROS are rather unspecific signaling molecules as many other stress-related processes such as pathogen defense, programmed cell death or wounding responses also involve ROS (Doke, 1985; Bolwell *et al.*, 1998, 2002; Schopfer *et al.*, 2001; Mahalingham and Fedoroff, 2003). Therefore ROS are postulated to initiate signaling cascades within the chloroplast, which then pass the envelope by unknown means (reviewed in Apel and Hirt, 2004; Pfannschmidt, 2010).

1.3.5 Redox processes of photosynthesis

Photosynthetic electron transport (PET) is performed by a chain of redox components that are electrochemically connected in series. As photosynthesis is a light-driven process, the reduction/oxidation (redox) state of PET components conveys information about environmental light conditions. In higher plants, redox states of PET components have been proposed as chloroplast signals influencing nuclear gene expression, mostly at the level of transcription (e.g. Escoubas *et al.*, 1995; Pfannschmidt, 2003; Fey *et al.*, 2005).

Plastoquinone (PQ) is a mobile membrane-intrinsic electron carrier that connects photosystem II (PSII) with the cytochrome *b₆/f* complex and is involved in both linear and cyclic electron transport (Allen, 2003). The redox state of the PQ pool is one of the major determinants of PET-derived retrograde signaling (fig. 1-4) (Escoubas *et al.*, 1995; Karpinski *et al.*, 1999; Pfannschmidt *et al.*, 2001). Under low light intensities the rate of PET is low and most PET components like the PQ pool are in oxidized states. In high-light conditions, due to higher excitation pressure, PET components are generally in reduced states.

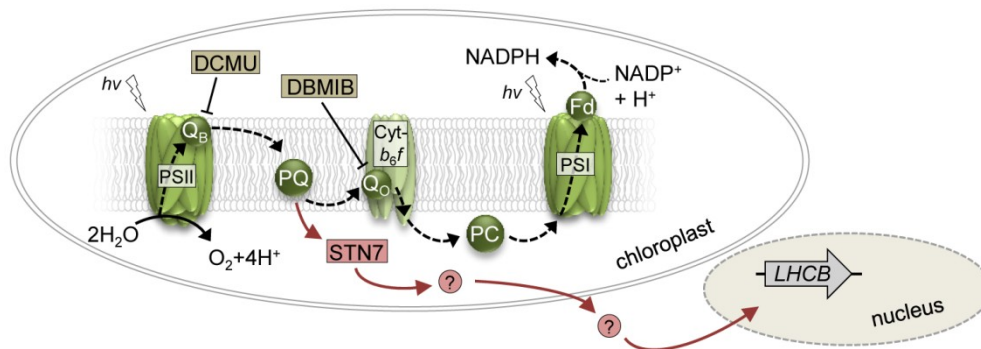


Figure 1-4. Possible signal transduction pathway of photosynthetic redox signals. The PQ pool is the origin of redox signals that are sensed by the redox-sensitive kinase STN7 (Bellafiore *et al.*, 2005). So far unidentified components transport the redox signal to the nucleus where it modulates transcription of photosynthesis-associated target genes like *LHCB*. Dashed arrows represent electron transport from water to NADPH. Inhibitors of the photosynthetic electron transport chain modulate the redox status of the PQ pool: DCMU and DBMIB oxidize or reduce the PQ pool, respectively. Their binding sites are depicted. Q_B: Plastochinon Q_B, Q_O: PQ binding site of the cytochrome *b₆/f* complex, PC: plastocyanin, Fd: ferredoxin. The components are not scaled in size.

Herbicides like 3-(3,4-dichlorophenyl)-1,1-dimethylurea (DCMU) and 2,5,-dibromo-3-methyl-6-isopropyl-*p*-benzoquinone (DBMIB) have been applied to manipulate the redox status of the PQ pool (Farineau *et al.*, 1984; Pfannschmidt *et al.*, 2001). These herbicides specifically block electron transport before (DCMU) or after (DBMIB) the PQ pool (Trebst, 1980), mimicking the effect of low- or high-light intensities, respectively. Genes that are induced by high light are also induced by DBMIB treatment in the absence of high light; in contrast, DCMU treatment inhibits high-light induced gene expression (Maxwell *et al.*, 1995; Durnford and Falkowski, 1997; Karpinski *et al.*, 1999). These results point towards a regulatory role of the redox state of the PQ pool.

In chloroplast-to-nucleus signal transduction, photosynthetic redox signals from the PQ pool are converted into a protein phosphorylation cascade (Chandok *et al.*, 2001; Steiner *et*

et al., 2009). The thylakoid membrane kinase STN7 is involved in regulating short term adaptations (state transitions) as well as long term adaptations of the photosynthetic apparatus, including alteration of expression of nuclear encoded plastid proteins (Bellafiore *et al.*, 2005; Bonardi *et al.*, 2005). STN7 is a redox-sensitive kinase and activated by reduction of the PQ pool (Bellafiore *et al.*, 2005). The redox state of the thioredoxin (TRX) pool also controls the activity of STN7 (Rintamaki *et al.*, 2000; Hou *et al.*, 2002).

1.3.6 Glutaredoxin and thioredoxin

Important regulators of redox signaling pathways are the NADPH-dependent glutathione/glutaredoxin (GRX) system and the NADPH-dependent TRX system, which together determine protein thiol/disulfide status depending on signals generated in the PET chain. TRXs and GRXs are ubiquitous proteins catalyzing disulfide reduction *in vivo* through a redox-active dithiol. They play key roles in the maintenance of cellular redox homeostasis through the sensing and transfer of reducing equivalents to target proteins, such as peroxidases, reductases, enzymes of photosynthesis or through structural modifications of target proteins (Arnér and Holmgren, 2000; Baier *et al.*, 2004b; Buchanan and Balmer, 2005; Rouhier *et al.*, 2008; Montrichard *et al.*, 2009). Oxidized TRXs as well as GRXs are reduced by thioredoxin reductases or glutathione, respectively (Holmgren, 1989).

GRX and TRX function as sensor of the plastid redox state and as transmitters to other proteins and finally to the nucleus (Bräutigam *et al.*, 2009). Their function depends on the reduction of their dithiol, which is connected with the redox state of the PET chain. TRX is photosynthetically reduced by ferredoxin (Schurmann, 2003), whereas glutathione is oxidized by ROS (Ghezzi and Bonetto, 2003; Mullineaux and Rausch, 2005). TRXs partially control the generation of ROS by competing with the electron transfer to molecular oxygen (Karpinska *et al.*, 2000). The synthesis of oxidized glutathione may be a pathway by which redox signals can directly leave the plastid (Mullineaux and Rausch, 2005).

1.3.7 Retrograde responsive *cis*-elements

Cis-acting elements required for retrograde regulation are either identical to or largely overlapping with light-responsive elements (Vorst *et al.*, 1993; Bolle *et al.*, 1996; Kusnetsov *et al.*, 1996). A minimal promoter region from Arabidopsis *LHCB* is sufficient for both light- and plastid-responsive expression (McCormac *et al.*, 2001). Another example is a 52-bp promoter element containing an I- and a G-box that was identified in the promoter of *RBCS8B* in *Nicotiana plumbaginifolia*, which was able to confer phytochrome-, cryptochrome- and retrograde-controlled reporter gene expression in Arabidopsis (Martínez-Hernández *et al.*, 2002). ABI4 is a negatively acting TF that competitively binds a G-box *cis*-element in response to plastid signals and inhibits the induction of *LHCB* expression (Koussevitzky *et al.*, 2007). Transcription of *2CPA* is also regulated by photosynthetic redox signals. The redox-regulation, controlled by the acceptor availability at photosystem I (PSI), takes place on a 216-bp redox box of the *2CPA* promoter (Baier *et al.*, 2004a).

1.4 How carbohydrates influence nuclear gene expression

In addition to retrograde signals, photosynthesis can modulate the nuclear gene expression via carbohydrates. Sugars not only fuel cellular carbon and energy metabolism but also play pivotal roles as signaling molecules (reviewed in Rolland *et al.*, 2006). In photosynthetic cells, photosynthates generated in the Calvin cycle are exported, mainly as triose-phosphates, from the chloroplast to the cytosol, where they are used in glycolysis or converted to sucrose for local use or export to sink tissues (reviewed in Hill, 1998). Excess photosynthates are transiently stored as starch in the chloroplast during the day. Transitory starch breakdown is performed during the night, mainly via maltose and glucose export. Plant sugar metabolism is a very dynamic process, and metabolic fluxes and sugar concentrations change dramatically both during development and in response to environmental signals such as diurnal changes and biotic and abiotic stress (Roitsch, 1999; Bläsing *et al.*, 2005; Smith *et al.*, 2005).

1.4.1 Sugars as signaling molecules

Sugars regulate cellular activity at multiple levels, from transcription and translation to protein stability and activity (reviewed in Rolland *et al.*, 2006). Genes that encode proteins involved in photosynthesis and carbon metabolism are a prime target of sugar signaling and subject to transcriptional feedback regulation. In general, source activities like photosynthesis are upregulated under low sugar conditions, and down regulated when carbon sources are abundantly available (Krapp *et al.*, 1993; Sheen, 1994). In addition to the feedback inhibition of sugars, genes encoding storage proteins and enzymes for starch synthesis in the sink tissues are induced by high levels of sucrose or other metabolizable sugars (Smeekens, 2000).

Most information on regulatory *cis*-acting elements involved in sugar signaling comes from a few selected genes, encoding sweet potato tuber and cereal seed proteins, and proteins involved in maize photosynthesis. Sucrose-responsive *cis*-acting elements are the sucrose-responsive element (SURE), A- and B-boxes, the TGGACGG element, and an SP8 motif (Geisler *et al.*, 2006; reviewed in Rolland *et al.*, 2006).

1.4.2 Regulators of sugar signaling

The sensors and the signaling pathways mediating sugar-dependent regulation of nuclear gene expression are largely unknown, but Arabidopsis HEXOKINASE 1 (HXK1) plays a central role in sensing and responding to glucose signals (Jang *et al.*, 1997; Harrington and Bush, 2003; Cho *et al.*, 2006). The HXK1-mediated signaling function is correlated with the repression of photosynthetic genes (Xiao *et al.*, 2000; Moore *et al.*, 2003). HXK-independent signaling pathways sense glucose as well as fructose or sucrose (reviewed in Rolland *et al.*, 2006). Plants contain several fructokinases, some of which might be involved in sugar sensing (Pego and Smeekens, 2000). A disaccharide sensing system may exist at the plasma

membrane (Loreti *et al.*, 2000; Atanassova *et al.*, 2003; Tiessen *et al.*, 2003). Protein phosphorylation could play a role in mediating sucrose regulation (Ransom-Hodkins *et al.*, 2003). SnRK1 is a protein kinase that plays an important role in plant sugar and starvation signaling, mediated by sucrose (Zhang *et al.*, 2001; Halford *et al.*, 2003). Ca^{2+} as a second messenger is also involved in sugar signaling (Ohto and Nakamura, 1995; Martínez-Noël *et al.*, 2006).

The phytohormone ABA is a central element of sugar signaling (reviewed in Rolland *et al.*, 2006). Especially during germination and early seedling development, interaction between ABA and carbohydrate signaling can be observed (Leon and Sheen, 2003; Gibson 2005). As ABA plays an important role in redox signaling (Rossel *et al.*, 2006), this phytohormone functions as integrator of sugar and redox signaling. As an example, the redox box of the *2CPA* promoter mediates ABA responsiveness (Baier *et al.*, 2004a) and also the redox-sensitive *2CPA* regulator ABI4 is controlled by ABA (fig. 1-5) (Arenas-Huertero *et al.*, 2000; Söderman *et al.*, 2000).

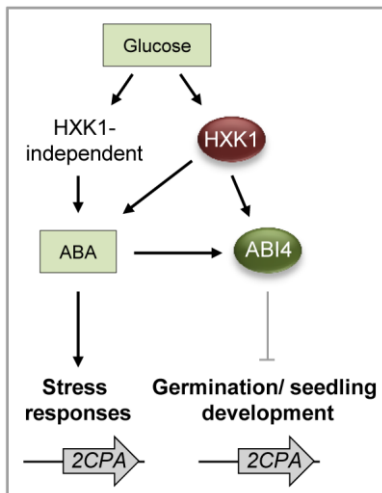


Figure 1-5. Simplified model of interactions between sugar and ABA signaling. HXK1-mediated glucose signaling that controls seedling development involves an increase in ABA and induces both ABA synthesis and ABA signaling gene expression. ABI4 activity is controlled by ABA. The ABA-regulated *2CPA* promoter is stress inducible and target of ABI4 during seedling development (Hiltscher *et al.*, in preparation).

Plant carbohydrate signaling as well as redox-signaling are directly connected with the prevalent light conditions. Even though multiple light-sensitive *cis*-acting promoter elements have been identified in the past, in many cases the elements that mediate light-dependent regulation of nuclear transcription are yet unknown. Novel approaches are needed, and hold the potential to further elucidate the light-regulated nuclear gene expression and subsequently the respective signal transduction networks in plants.

1.5 Enhancer trapping

1.5.1 The principle of enhancer trapping

Enhancer trap (ET) lines contain a reporter gene with an unregulated weak or minimal promoter (O'Kane and Gehring, 1987) that has been inserted via *Agrobacterium*-mediated transformation semi-randomly into the wild-type genome. When insertion occurs in the proximity of a transcriptional enhancer region, the reporter gene is expressed under the control of the neighboring enhancers. In contrast, in gene/promoter traps the reporter gene construct is lacking a promoter and is expressed under the control of a native promoter (Friedrich and Soriano 1991). Thus, patterns of reporter gene expression represent the expression of an endogenous gene. Large collections of gene/promoter trap and ET lines have been generated in *Arabidopsis* (e.g. Bechtold *et al.*, 1993; Topping *et al.*, 1994; Sundaresan *et al.*, 1995; Campisi *et al.*, 1999; Springer, 2000).

Enhancer elements are autonomous modules, with each module performing a specific function, such as activation of its target gene at a specific developmental stage or in a specific cell type, in a distance and orientation independent manner (Blackwood and Kadonaga, 1998; Struhl, 2001). Since reporter gene expression marks the activity of such enhancer modules, ET lines have been used to identify regulatory sequences responsible for specific expression patterns. Using ET lines, genes involved in processes such as senescence (He *et al.*, 2001), responses to oxygen deprivation (Baxter-Burrell *et al.*, 2003) and shoot induction (Cary *et al.*, 2002) as well as genes regulated by the circadian clock (Michael and McClung, 2003) were identified. ET lines were also used for analysis of root cap function (Tsugeki and Fedoroff, 1999), cyclin function (Swaminathan *et al.*, 2000), stem cell development (Sabatini *et al.*, 2003; Gallois *et al.*, 2004), seed development (Weijers *et al.*, 2003), stomatal guard cell development (Laplaze *et al.*, 2005) and lateral root development (Gardner *et al.*, 2009).

1.5.2 The GAL4/UAS system

The GAL4/UAS two-component system was developed in *Drosophila* with the aim to change gene expression (Brand and Perrimon, 1993). Transgenic *Drosophila* were generated, expressing different patterns of a yeast transcription activator, GAL4. A chosen target gene can be placed under the control of a GAL4-activated promoter (UAS, upstream activation sequences), transformed into *Drosophila* and maintained silently in the absence of GAL4. Genetic crosses between this single line and an ET line specifically activate the target gene in a chosen tissue or cell type, to study phenotypic consequences of the induced misexpression. GAL4-mediated transactivation is a widely used system to elucidate the cell-specific functions of known genes, for targeted cell ablation and as the basis of enhancer or suppressor screens (e.g. Brand and Perrimon, 1993; Gustafson and Boulianne, 1996; Haseloff, 1999; Wysocka-Diller *et al.*, 2000; Sabatini *et al.*, 2003; Weijers *et al.*, 2003; Gallois *et al.*, 2004; Scott *et al.*, 2007).

1.5.3 The *GAL4-GFP* ET construct

The *GAL4/UAS* system developed in *Drosophila* was adapted for *Arabidopsis* (Haseloff, 1999). A *GAL4* ET T-DNA vector was designed comprising a *GAL4*-responsive modified green fluorescent protein (*GFP*) gene under the control of UAS (fig. 1-6) (Haseloff, 1999; Laplaze *et al.*, 2005). The codon usage of *GAL4* was altered to allow efficient expression in plants, resulting in a gene designated as *GAL4-VP16*. The *GFP* sequence was modified for proper expression in *Arabidopsis*. The resulting *mGFP5-ER* lacks a cryptic intron, has improved fluorescence properties and is targeted to the endoplasmatic reticulum (Haseloff *et al.*, 1997; Haseloff, 1999). Therefore patterns of *GAL4-VP16* gene expression are immediately detectable, with each *GAL4*-expressing cell marked by green fluorescence.

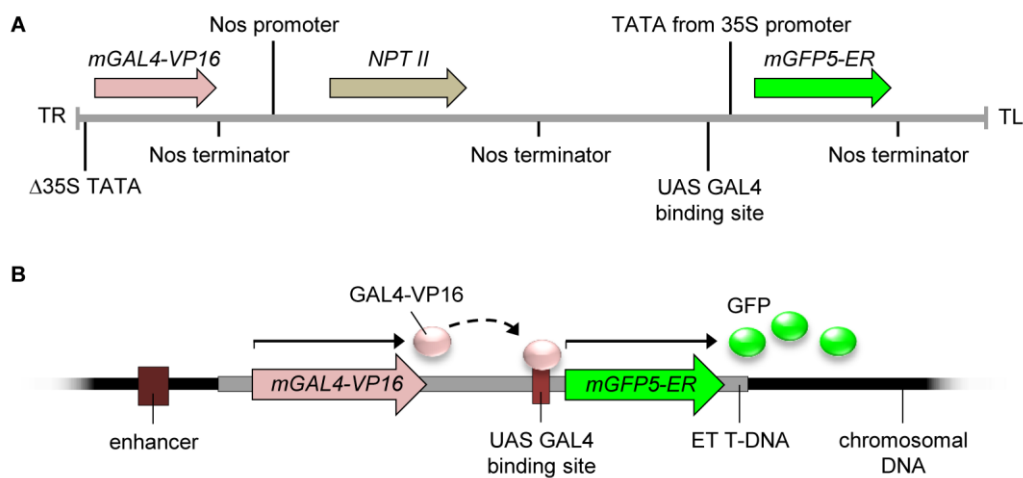


Figure 1-6. Arabidopsis *GAL4-GFP* ET lines. **A:** Assembly of the engineered ET T-DNA. The vector contains a *GAL4-VP16* gene adjacent to a minimal promoter ($\Delta 35S$ TATA) at the right border (TR) of the transferred DNA, a kanamycin resistance selection marker (*NPTII*) and a *GAL4*-responsive *mGFP5-ER* gene, under the control of UAS. **B:** Scheme of the ET mechanism. *Agrobacterium tumefaciens* mediated plant transformation was used to randomly integrate the T-DNA vector into the nuclear *Arabidopsis* genome (Haseloff, 1999; Laplaze *et al.*, 2005). Activation of the *mGAL4-VP16* gene by a cellular enhancer results in the expression of the *GFP* reporter gene, allowing the characterization of expression patterns by fluorescence microscopy.

1.6 Aim of this study

The present work aims at understanding the regulation of nuclear gene expression in response to changing light conditions. ET lines are used to detect light-sensitive *cis*-acting elements in the nuclear genome. ET lines identify light-responsive DNA motifs outside of the known light-sensitive promoter elements. So far, most analyses searching for *cis*-acting elements were restricted to proximal promoter regions. In this study ET lines are used to search for novel light-regulated DNA sequences without this limitation.

To elucidate the signaling network underlying nuclear gene expression regulation, the identified light responsive *cis*-acting elements are further characterized for their connection to chloroplast function. Photosynthates and chloroplast redox signals as well as different

photoreceptors are investigated to unravel their influences in regulating the identified *cis*-acting elements. The analyses permit new insights into the signal transduction of retrograde chloroplast-to-nucleus signaling and the integration with photoreceptor mediated sensing of light.

2

MATERIAL AND METHODS

2.1 Plant material

Seeds of *Arabidopsis thaliana* var. C24, Col-0 and *Ler*, *GAL4-GFP* ET population with a *GFP* reporter gene under control of a truncated 35S promoter (Haseloff, 1999; Laplaze *et al.*, 2005) and T-DNA insertion lines of the SALK population were obtained from the Nottingham Arabidopsis Stock Centre (NASC, Loughborough, UK). Photoreceptor mutants, *hy1*, *cop1* and *hy5* mutants (tab. 2-1) were obtained from NASC or kindly provided by Prof. A. Batschauer (Marburg, Germany).

Table 2-1. Mutants and SALK T-DNA insertion lines used for analysis of the influence of their gene products on light-dependent *SIG5* and *GFP* transcription.

Gene	Gene code	Allele / SALK line	Mutant	Ecotype	Reference
<i>CRY1</i>	At4g08920	SALK_042397C	<i>cry1</i>	Col-0	-
<i>HY1</i>	At2g26670	<i>hy1-1</i>	<i>hy1</i>	<i>Ler</i>	Koornneef <i>et al.</i> , 1980, Muramoto <i>et al.</i> , 1999
<i>HY1</i> <i>CRY1</i>	At2g26670, At4g08920,	<i>hy1-1</i> , <i>cry1-1</i> (former <i>hy4-1</i> , <i>hy4-2.23N</i>),	<i>hy1 cry1 cry2</i>	<i>Ler</i>	López-Juez <i>et al.</i> , 2008
<i>CRY2</i>	At1g04400	<i>fha-1</i>			
<i>PHYA</i>	At1g09570	<i>phyA-201</i> (former <i>fre-1</i>)	<i>phyA</i>	<i>Ler</i>	Reed <i>et al.</i> , 1993
<i>PHYB</i>	At2g18790	<i>phyB-5</i> (former <i>phyB-8-36</i> , <i>hy3-8-36</i>)	<i>phyB</i>	<i>Ler</i>	Reed <i>et al.</i> , 1993
<i>PHYA</i> <i>PHYB</i>	At1g09570, At2g18790	<i>phyA-201 phyB-5</i>	<i>phyA phyB</i>	<i>Ler</i>	Reed <i>et al.</i> , 1994
<i>PHOT1</i>	At3g45788	<i>phot1-5</i> (<i>nph1-5</i>)	<i>phot1</i>	Col-0	Huala <i>et al.</i> , 1997
<i>PHOT1</i> <i>PHOT2</i>	At3g45788, At5g58140	<i>phot1-5 phot2-1</i> (<i>npl1-1</i>)	<i>phot1 phot2</i>	Col-0	Kagawa <i>et al.</i> , 2004
<i>HY5</i>	At5g11260	<i>hy5-1</i>	<i>hy5</i>	Col-0	Oyama <i>et al.</i> , 1997
<i>HY5</i>	At5g11260	SALK_056405C	<i>hy5</i>	<i>Ler</i>	-
<i>COP1</i>	At2g32950	<i>cop1-6</i>	<i>cop1</i>	Col-0	McNellis <i>et al.</i> , 1994

2.2 Growth conditions

2.2.1 Sterile culture of *Arabidopsis thaliana* seedlings

Seeds of *Arabidopsis* were surface sterilized for 1 min in 80 % (v/v) ethanol, and then for 8 min in 20 % (v/v) household bleach (Glorix, Lever Farbergé, The Netherlands) and washed five times with sterile water. Seeds were sown on sterile Murashige and Skoog (MS; Duchefa, Haarlam, The Netherlands) medium, pH 5.7, supplemented with 2.5 g l⁻¹ Phytigel (Sigma, Steinheim, Germany) with or without 0.5 % to 2 % (w/v) sucrose or 2 % to 4 % (w/v) sorbitol, as indicated. Unless otherwise indicated, experiments were performed with seedlings grown on MS medium supplemented with 0.5 % (w/v) sucrose under short day conditions (10 h light, 22 °C/ 14 h dark, 18 °C) at 120 μmol photons m⁻² s⁻¹ white light (Philips F17TS/TL741, 17 watt). Seeds were cold-treated for 2 days in the dark before they were transferred to the appropriate experimental light conditions.

2.2.2 Growth of mature *Arabidopsis thaliana* plants on soil

After 2 d cold-treatment seeds were sown on soil (B400 with Cocopor, Toresa, Floraton I, supplemented with 1.5 g l⁻¹ Osmocote Extract, 1 g l⁻¹ Dolomit chalk and 0.1 g l⁻¹ Radigen; mixture was mixed with 10 % (v/v) sand) and plants were grown in the greenhouse.

2.2.3 Monochromatic light treatment

Sterilized *Arabidopsis* seeds were cold-treated for 2 days in the dark before they were transferred to 100 μmol photons m⁻² s⁻¹ white light (Philips F17TS/TL741, 17 watt) with short day conditions (10 hours light, 22 °C/ 14 hours dark, 18 °C) for 10 d. Seedlings were dark-adapted for 24 h and subsequently irradiated with 80-100 μmol photons m⁻² s⁻¹ continuous blue light (LED, centroid at 471 nm; CLF PlantClimatics, Emersacker, Germany), continuous red light (LED, centroid at 673 nm) or continuous far red light (LED, centroid at 745 nm) at 22 °C for 24 h before harvested for RNA analysis. Emission spectra of LEDs are given in appendix 6.3.

2.3 Determination of reporter gene activity

2.3.1 *In vivo* GFP fluorescence quantification

GAL4-GFP ET lines were screened for light-dependent reporter gene expression pattern using a fast *in vivo* approach that allowed quantification of GFP fluorescence of intact seedlings. Plants were grown in 96-well microtiter plates on 100 μl MS medium (for recipe see 2.2.1) per well supplemented with 0.5 % (w/v) sucrose under short day conditions at 10, 100 or 200 μmol photons m⁻² s⁻¹ white light. Reporter gene expression of 10 d old seedlings was measured in the Fluoroskan Ascent FL fluorometer (Thermo Fisher Scientific, Dreieich, Germany) with 500 ms integration time, excitation at 485 nm and emission at 527 nm.

Results were given as means of nine measurement points covering a single well. For calculation of GFP fluorescence of the ET lines mean fluorescence of wild-type C24, the genetic background of the *GAL4-GFP* lines, grown on the same 96-well plate, was subtracted.

2.3.2 *In vitro* quantification of GFP fluorescence of ground seedlings

2.3.2.1 Determination of GFP fluorescence

Seedlings were pooled and 10-20 mg material was homogenized in 500 μ l sodium phosphate, pH 7.0. Samples were centrifuged at 20.000 x *g* for 2 min. 100 μ l of the supernatant was transferred to a black 96-well plate in triplicate. GFP fluorescence was quantified in a Mithras LB 940 top reader fluorometer (Berthold Technologies GmbH & Co. KG, Bad Wildbad, Germany) with 100 ms counting time; excitation filter 460/10 and emission filter F510 with 3 repeats per read.

2.3.2.2 Quantification of protein content

Total protein content of ground seedlings was determined using the Bio-Rad Protein Assay (Bio-Rad Laboratories GmbH, München, Germany), according to the manufacturer's instructions. The Bio-Rad Protein Assay bases on a method of Bradford and allows determination of soluble protein concentration. An acidic solution containing Coomassie[®] Brilliant Blue G-250 dye was added to the protein solution produced as described in chapter 2.3.2.1 and subsequent absorption at 595 nm was determined using a spectrophotometer (UVmini-1240, Shimadzu, Duisburg, Germany) in a total volume of 500 μ l. Comparison to a standard curve performed with bovine serum albumin (BSA) provided a relative measurement of protein concentration.

2.3.2.3 Chlorophyll content determination

Total chlorophyll (Chl) was determined spectroscopically after grinding the seedlings in liquid nitrogen and extracting Chl with 1 ml 80 % (v/v) buffered acetone. After 1 h incubation in the dark at -20 °C samples were centrifuged for 5 min at 20.000 x *g*. Concentrations of Chl *a* and Chl *b* were calculated from the absorbance of the supernatants at 663.6 nm and 646.6 nm (UVmini-1240, Shimadzu, Duisburg, Germany) according to Porra *et al.* (2002) by the following equations:

$$\text{Chl } a = 12.25 \times A_{663.6} - 2.55 \times A_{646.6} \text{ [}\mu\text{g ml}^{-1}\text{]}$$

$$\text{Chl } b = 20.31 \times A_{646.6} - 4.91 \times A_{663.6} \text{ [}\mu\text{g ml}^{-1}\text{]}$$

$$\text{Chl } a + b = 17.76 \times A_{646.6} + 7.34 \times A_{663.6} \text{ [}\mu\text{g ml}^{-1}\text{]}$$

2.3.3 Visualization of GFP reporter gene fluorescence

GFP fluorescence was visualized using the FluorCam 800 MF (Photon System Instruments, Brno, Czech Republic) with a GG495 + LP660 + BS505-560 filter set, 21 % Act2 light intensity and the shutter of the camera set to 10 ms. The excitation peak was centered at about 488 nm using a short-pass 480 nm filter and the emission peak was at 507-509 nm using a 530/25 filter.

2.3.4 Colorimetric quantification of GUS activity

GUS expression was quantified colorimetrically, according to Aich *et al.* (2001). The substrate used for this assay was para-nitrophenyl β -D-glucuronide (PNPG), which generated para-nitrophenol (PNP) when cleaved by the enzyme β -glucuronidase (GUS). PNP is a chromogenic product and was quantified spectrophotometrically at PNP maximal absorbance at 405 nm. 15-30 mg plant material was ground in 300 μ l 50 mM sodium phosphate, pH 7.0, 10 mM DTT, 0.1 % (v/v) Triton X-100 and 10 mM EDTA. After centrifugation at 20.000 x g for 5 min, the supernatant was used for quantification of GUS activity and total protein content in parallel. The protein contents were determined as described in chapter 2.3.2.2. For determination of the GUS content 20 μ l supernatant (from tobacco) or 200 μ l supernatant (from Arabidopsis seedlings) was added to 500 μ l 1 mg ml⁻¹ PNPG in 50 mM sodium phosphate, pH 7.0, 10 mM DTT, 0.1 % (v/v) Triton X-100 and 10 mM EDTA. Zero value at A₄₀₅ was determined and served as initial value for subsequent calculation of ΔA_{405} . After incubation at 37 °C for 1 h the reaction was determined by adding 500 μ l 400 mM Na₂CO₃ leading to a drift in pH that inhibits GUS activity. A₄₀₅ was determined and ΔA_{405} was used for calculation of PNP values as μ M PNP min⁻¹ with molar extinction coefficient of PNP at pH 7.0 of 9000 according to Aich *et al.* (2001).

2.4 Isolation of DNA from plant material

2.4.1 Isolation of DNA for PCR

One cotyledon per Arabidopsis seedling was homogenized in 200 μ l 50 mM Tris/HCl pH 8.0, 25 mM EDTA, 250 mM NaCl and 0.5 % (w/v) SDS. After extraction with 200 μ l phenol-chloroform-isoamyl alcohol (25:24:1) samples were centrifuged at 20.000 x g for 5 min at room temperature. The upper phase was transferred to 200 μ l isopropanol. Deoxyribonucleic acids were precipitated for 1 h at -20 °C and sedimented by centrifugation at 20.000 x g for 15 min. Precipitates were resuspended in 100 μ l sterile water and stored at -20 °C.

2.4.2 DNA isolation for Southern blot

Genomic DNA of ET lines and C24 wild-type plants was extracted using the DNeasy Plant Mini Kit (Qiagen, Hilden, Germany), as recommended by the supplier. DNA was stored at -20 °C.

2.5 Polymerase chain reaction (PCR)

2.5.1 Standard PCR

PCR reactions were performed in 20 mM Tris/HCl pH 8.4, 50 mM KCl, 1.5 mM MgSO₄ and 0.5 mM MgCl₂ using the heat-stable *Taq* polymerase to catalyze the reaction. 2 µl DNA (2.4.1) were used in a 20 µl sample containing 2 mM dNTPs and 0.5 mM of each primer (forward and reverse). General PCR reaction protocol is shown in table 2-2. Annealing temperatures were adjusted depending on the melting temperature (T_m) of the gene specific primers used (all primers used in this work are either described in the text or listed with corresponding annealing temperatures in appendix 6.2).

Table 2-2. General PCR reaction protocol.

Reaction step	Cycles	Temperature [°C]	Time [s]
Initial denaturation	1	94	180
Denaturation	40	94	15-30
Primer annealing		$T_m - 5$ °C	15-30
Elongation		72	60 kb ⁻¹
Final elongation	1	72	180

The High Fidelity PCR Enzyme Mix (Fermentas, St. Leon-Rot, Germany) was used for amplification of PCR products that should be amplified with high accuracy. This mix is a blend of a *Taq* DNA polymerase and a second DNA polymerase with proofreading activity.

2.5.2 Thermal asymmetric interlaced PCR (TAIL-PCR)

Thermal asymmetric interlaced PCR (TAIL-PCR) was performed as described by Liu *et al.*, (1995) with modifications in annealing-temperatures, cycle numbers and template dilutions. TAIL-PCR is a technique for isolation of target sequences adjacent to known sequences. In the present work TAIL-PCR was used for amplification of insertion-specific PCR products to map genomic sequences flanking T-DNA insertions in *Arabidopsis thaliana* ET lines. TAIL-PCR uses a set of three nested T-DNA specific right border primers in successive reactions together with a shorter arbitrary degenerate (AD) primer with lower melting temperature (tab. 2-3). The specific right border primers and their annealing positions within the T-DNA region are shown in figure 2-1.

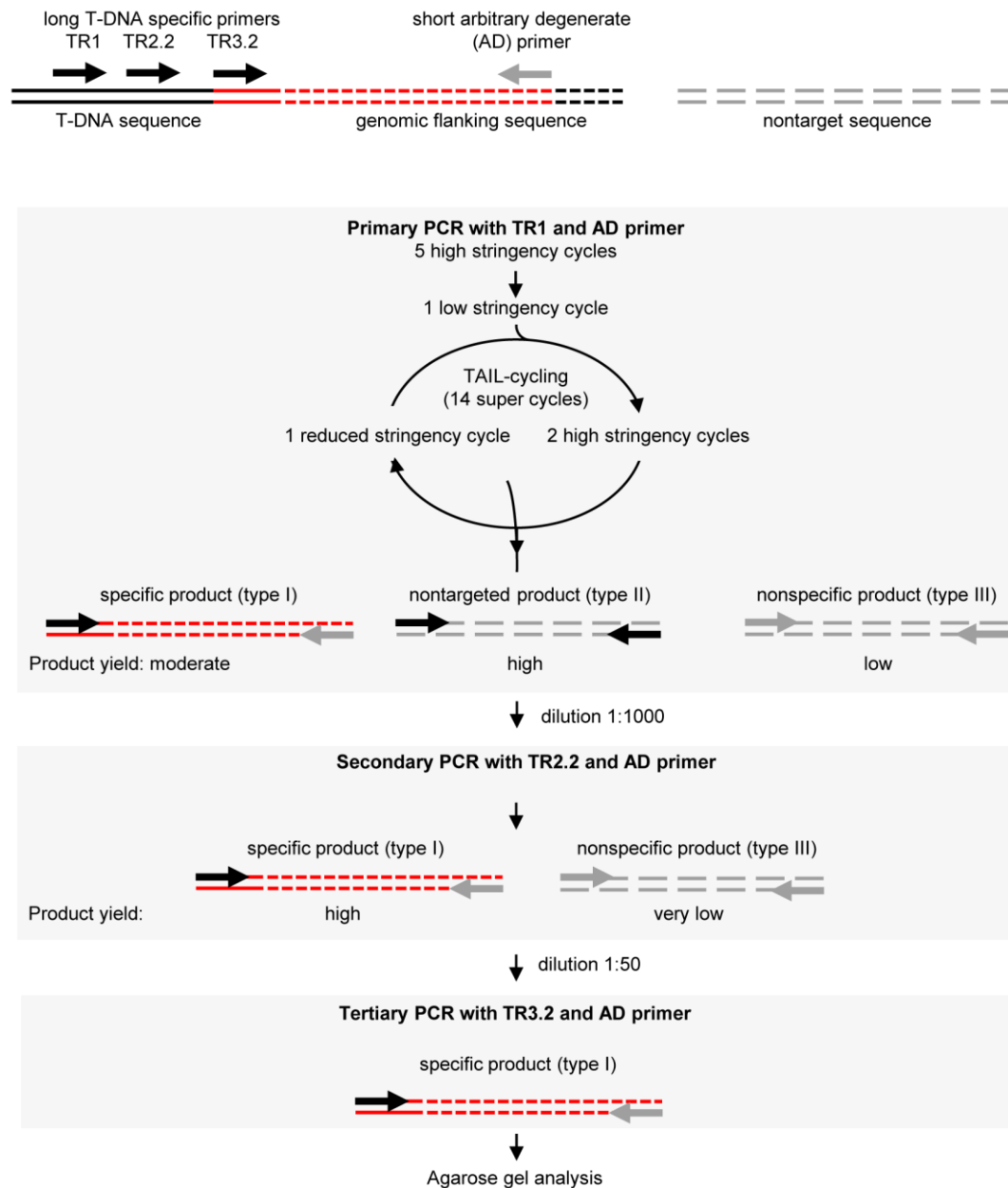


Figure 2-2. TAIL-PCR procedure for specific amplification or genomic sequence flanking a T-DNA insertion. Three PCR reactions amplify sequences using nested T-DNA specific primers (black arrows) on one side and one AD primer (grey arrow) on the other side. One or more sides within the flanking sequence are adapted for annealing to the AD primer through a special low stringency cycle. High-stringency annealing favours the specific primer, resulting in a linear amplification of target molecules. By interspersing low-stringency cycles to allow AD primer binding with, double-stranded molecules can be amplified, and the linear amplification of target molecules (type I, highlighted in red) becomes logarithmic. In the secondary and tertiary reactions nonspecific product II fails to be reamplified and thus is not shown (modified from Liu *et al.*, 1995).

2.5.3 Identification and isolation of homozygous T-DNA insertion lines by PCR

Seeds of the segregating lines were germinated on soil (2.2.2). At the end of the vegetation period, seeds were harvested from individual plants. Homozygous plants were established from plants whose progeny segregated with 3:1 ratio and identified by a PCR-based approach. The T-DNA insertion sites in ET lines and in SALK lines were detected with primers TR3.2 (2.5.2) or Lb1.3 (ATTTTGCCGATTCGGAAC) that bind specific to the

ET T-DNA and the SALK T-DNA sequences, respectively. Both primers were combined with primers designed to anneal the genomic DNA flanking the insertion sites (listed in appendix 6.2, tables A2 and A3). A second PCR was performed that amplified the wild-type sequences if T-DNAs were not homozygously inserted. In contrast to wild-type, plants with homozygous T-DNA insertions failed in amplification of these products due to the large T-DNA insertion. Progeny of these plants was again tested by PCR to verify the absence of the wild-type allele.

2.6 Site-directed mutagenesis

Three predicted light responsive *cis*-acting elements in the distal *SIG5* promoter were mutated to prevent *cis*-element functionalities. Introduced mutations are listed in table 2-4. Site-directed mutagenesis was PCR-mediated according to Montemartini *et al.* (1999). The following general procedure, as shown in figure 2-3, was applied to generate the different variants: two PCR products that overlap in the sequence containing the same mutation were synthesized in two separate PCRs. The oligonucleotides used to create the mutants are listed in appendix 6.2 in table A4. The two reaction products were separated on an agarose gel and the DNA bands were excised and purified as described in chapters 2.7 and 2.8. This purified DNA served as template for a second PCR performed with both outer primers.

Table 2-4. *cis*-acting elements, modified by site-directed mutagenesis.

<i>cis</i> -element	Introduced mutation ^a	Reference
GATA-motif	AAAGATAAGAGT → AAAG <u>TATTC</u> AGT	Donald and Cashmore, 1990
G-box	ATACACGTGGAT → ATACA <u>ATT</u> GGAT	McKendree and Ferl, 1992
GC-box	GACGACGTGGCC → GTCGA <u>ATT</u> CGCC	McKendree and Ferl, 1992

^a *cis*-acting element is underlined, mutated nucleotides are highlighted in black

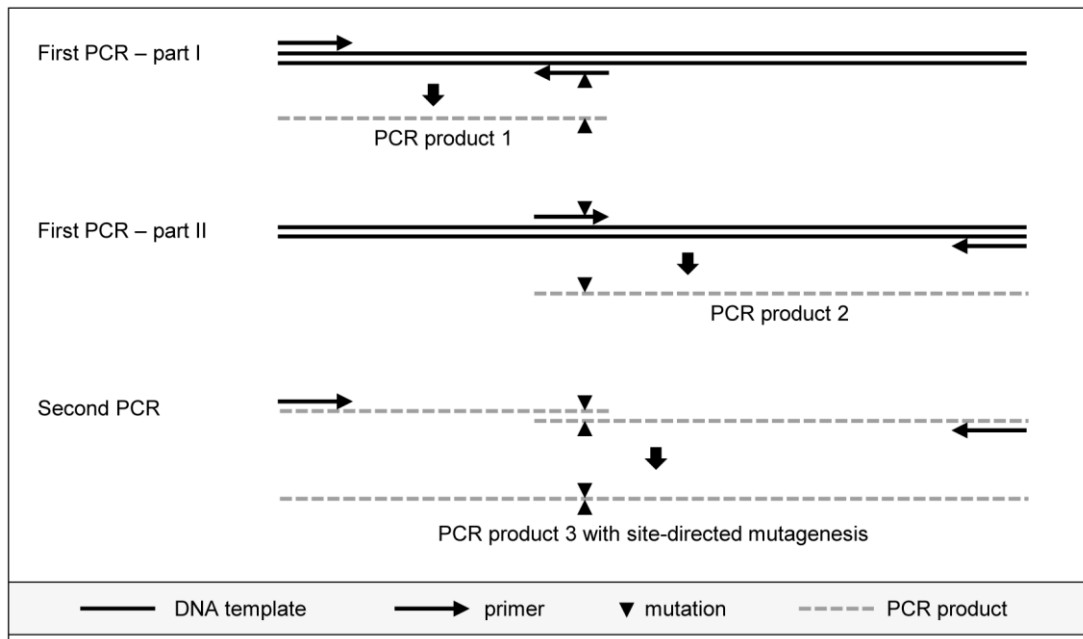


Figure 2-3. Schematic view of PCR-based site-directed mutagenesis. In two consecutive PCR reactions a mutation is introduced into a DNA sequence by primers carrying the mutation. The second PCR results in a mixture of PCR products 1 to 3. For purification of PCR product 3, extraction out of agarose gel after electrophoresis can be performed. Method according to Montemartini *et al.* (1999).

2.7 Separation of DNA by agarose gel electrophoresis

Amplified PCR products were separated electrophoretically on 1-4 % (w/v) TAE agarose gels, depending on the DNA fragment size. Agarose was melted in 1 x TAE buffer (0.8 mM Tris-acetate pH 7.5, 0.02 mM EDTA) and supplemented with 0.5 $\mu\text{g ml}^{-1}$ ethidiumbromide. Samples were mixed with 25 % (v/v) DNA-loading-buffer (0.05 % (w/v) bromphenol blue, 0.05 % (w/v) xylene cyanol, 6 % (v/v) glycerol) prior to separation at constant 120 V in 1 x TAE buffer. DNA was visualized in a UV-light box with a CCD-camera at 312 nm (INTAS, Göttingen, Germany).

2.8 Purification of PCR products by gel extraction

Gel slices containing PCR products were cut out of the agarose gel under UV light (312 nm). Extraction was done using the GeneJETTM Gel Extraction Kit (Fermentas, St. Leon-Rot, Germany) as recommended by the supplier. In principle the DNA was solubilized by melting the agarose gel in a high salt buffer, bound to a silica membrane, washed and eluted by low salt buffer or water.

2.9 *Escherichia coli* manipulations

2.9.1 Generation of chemically competent *E. coli*

Escherichia coli (*E. coli*) DH5 α were inoculated in 5 ml Lysogeny broth (LB) liquid medium (1 % (w/v) tryptone, 0.5 % (w/v) yeast extract, 1 % (w/v) NaCl) and grown overnight at 37 °C and 200 rpm. With this pre-culture 100 ml LB were inoculated till OD₆₀₀ had reached an optical density of 0.4 to 0.6. The culture was chilled on ice for 10 min before harvesting the cells by centrifugation at 1.600 x g and room temperature (RT) for 7 min. The cell pellet was resuspended in 5 ml ice-cold CaCl₂ medium (60 mM CaCl₂, 15 % (v/v) glycerol, 10 mM Pipes, pH 7.0 adjusted with KOH). Subsequently the cells were sedimented again by 7 min centrifugation at 1.600 x g and RT. The resulting pellet was resuspended in 2 ml ice-cold CaCl₂ medium. The resulting competent cells were aliquoted into 100 μ l each and immediately frozen in liquid nitrogen and stored at -70 °C. For a single transformation 25-50 μ l of the cell suspension was used.

2.9.2 Transformation of *E. coli*

Recombinant vectors were transformed into chemically competent *E. coli* DH5 α by heat shock. After on ice thawing of the bacterial cells the plasmid was added to the cells. The samples were incubated on ice for 30 min. The cells were heated to 42 °C for 60 s and immediately cooled on ice additional 2 min. To recover the cells after the heat-shock 200 μ l LB liquid media (for recipe see 2.9.1) were added and the cells were incubated at 37 °C for 1 h. Positive transformants harboring recombinant vector were selected on nutrient agar plates (1 % (w/v) peptone, 0.5 % (w/v) yeast extract, 1 % (w/v) NaCl, 1.5 % (w/v) agar, pH 7.5) containing the appropriate antibiotics.

2.9.3 *E. coli* colony-PCR

A single colony of transformed *E. coli* was transferred into 20 μ l of PCR solution (as described in chapter 2.5.1). The general PCR protocol described in table 2.2 was modified as initial denaturation was increased to 10 min for cell lysis.

2.9.4 Plasmid isolation from *E. coli* for sequencing

Isolation of plasmid DNA from *E. coli* was performed using the Wizard[®] Plus SV Minipreps DNA Purification System (Promega, Madison, USA) according to the manufacturer's instructions. This principle of plasmid isolation based on binding of plasmid DNA to a silica membrane under high salt conditions, and subsequent washing steps to remove RNA, cell debris and proteins. Plasmid DNA was eluted in TE buffer (10 mM Tris/HCl pH 8.0, 1 mM EDTA) and stored at -20 °C.

2.9.5 Plasmid isolation from *E. coli* by alkaline lysis

Isolation of plasmid DNA from *E. coli* for restriction digests was performed by alkaline lysis. Single colony of transformants was used to inoculate 5 ml LB liquid media containing the appropriate antibiotic and incubated overnight at 37 °C and 200 rpm. Cells were collected by centrifugation at 20.000 x g for 1 min. The pellet was resuspended in 100 µl 50 mM Tris/HCl pH 8.0, 10 mM EDTA and 100 µg ml⁻¹ ribonuclease A (Roche, Penzberg, Germany). 200 µl 200 mM NaOH, 1 % (w/v) SDS were added and solutions were mixed by inverting the samples 4 times. 150 µl 3.1 M potassium acetate pH 5.5 were added and mixed by inverting the tube several times. To pellet the cell debris, the samples were centrifuged at 20.000 x g for 10 min. The supernatant was mixed with 40 µl 3 M sodium acetate and 1 ml ethanol to precipitate plasmid DNA. The DNA was harvested by centrifugation at 20.000 x g for 10 min. The pellet was washed with 70 % (v/v) ethanol and resuspended in 50 µl sterile TE buffer (for recipe see 2.9.4.). The plasmids were stored at -20 °C.

2.9.6 cDNA library plasmid isolation

For large-scale plasmid isolation of cDNA library in pACT the PureYield™ Plasmid Maxiprep System was used (Promega, Madison, USA) according to the manufacturer's instructions using a vacuum pump and a vacuum manifold (Vac-Man® Laboratory Vacuum Manifold, Promega, Madison, USA). One column was utilized for purification of plasmid DNA from 1 l of saturated *E. coli* culture.

2.10 Plasmid manipulations

2.10.1 Ligation with pJET1.2/blunt vector for sequencing

PCR products were cloned into pJET1.2/blunt cloning vector (appendix 6.4, fig. A3) for sequencing or for amplification using the CloneJET™ PCR Cloning Kit (Fermentas, St. Leon-Rot, Germany) as recommended by the supplier. pJET1.2/blunt contains a lethal restriction enzyme that is disrupted by ligation of a blunt DNA insert into the cloning site. Recircularized vector molecules lacking an insert express the lethal gene which kills the host *E. coli* after transformation. As PCR products are generated using *Taq* polymerase, products were blunted prior to ligation with a DNA blunting enzyme, provided with the CloneJET™ PCR Cloning Kit.

2.10.2 Ligation of PCR-amplified DNA into pCR®8/GW/TOPO®

PCR products were cloned into the Gateway compatible pCR®8/GW/TOPO® vector (appendix 6.4, fig. A4) according to the manufacturer's instructions (Invitrogen, Carlsbad, USA). Primers used for amplification of the PCR products are listed in appendix 6.2 in tables A5 and A6. Chemically competent DH5α *E. coli* were transformed with the resulting constructs as previously described (2.9.2). The orientation of the inserted sequences in

pCR[®]8/GW/TOPO[®] was determined by restriction digestion with one enzyme cutting the insert and another enzyme cutting the pCR[®]8/GW/TOPO[®] backbone.

2.10.3 LR reaction

The binary vector chosen for Gateway[®] recombination cloning reaction was pHGWFS7.0 (Karimi *et al.*, 2002; fig. 2-6) that allows both GFP and GUS to be expressed under the control of the inserted promoter sequence. As entry and destination vectors both have resistance to the same antibiotic, it was necessary to prevent colonies containing the entry vector pCR8[®]/GW/TOPO[®] from growing after the LR recombination reaction. Therefore the pCR8[®]/GW/TOPO[®] vector was double digested with *Psp1406I* and *EcoRV* leading to a fragment containing the inserted promoter sequence flanked by the *attL1* and *attL2* recombination sites. As the full 35S promoter contains an *EcoRV* restriction site, pCR8[®]/GW/TOPO[®] containing full 35S promoter was single digested with *Psp1406I*.

Following gel purification (2.8) 75 ng digested entry vector was added to 75 ng pHGWFS7.0 plasmid and 0.5 µl LR Clonase II enzyme mix (Invitrogen, Carlsbad, USA) in a total volume of 5 µl filled up with TE buffer (for recipe see 2.9.4). After incubation at 25 °C for 1 h, 1 µl proteinase K solution (Invitrogen, Carlsbad, USA) was added and samples were incubated at 37 °C for 10 min to terminate the reaction.

2.10.4 Cleaving double-stranded DNA with restriction enzymes

For standard restriction digestions of plasmid DNA 1 µg plasmid DNA isolated by alkaline lysis was digested in 20 µl total volume at 37 °C (or adapted to optimal temperature of the enzyme used) for 1 h. The fragment pattern was visualized by agarose gel electrophoresis (2.7).

2.10.5 Ligation of termini created by restriction enzymes

Ligations were performed using the LigaFast[™] Rapid DNA Ligation System (Promega, Madison, USA) according to the manufacturer's instructions. Ligation was performed with a 1:2 molar ratio of vector:insert DNA with 100 ng vector DNA. Molar ratio of vector:insert was calculated using the following equation:

$$\frac{\text{ng of vector} \times \text{kb size of insert}}{\text{kb size of vector}} \times \text{molar ratio} \frac{\text{insert}}{\text{vector}} = \text{ng of insert}$$

Ligation was performed at RT for 5 min with subsequent inactivation of the T4 DNA ligase by heating to 70 °C for 10 min. Ligation reaction was directly used for transformation of *E. coli* as described in 2.8.2.

2.11 Sequencing of DNA fragments

All cloned DNA was analyzed by sequencing following plasmid purification (2.9.4). Sequencing of 1-2 µg purified plasmid DNA was performed at GATC (GATC Biotech AG, Konstanz, Germany) with an ABI 3730xl system by chain terminator sequencing (Sanger sequencing). All sequencing results were analyzed by comparison with database entries using BLASTN (<http://www.ncbi.nlm.nih.gov>). A BLAST algorithm for highly similar sequences (megablast) and a database containing the *Arabidopsis thaliana* (L.) Heynh. accession Col-0 whole genome sequence (taxid: 3702) were used for comparison.

2.12 Analysis of promoter sequences

A promoter motif search was performed by *in silico* analysis by PLACE (<http://dna.affrc.go.jp/PLACE/signal-scan.html>; Higo *et al.*, 1999) and PlantCARE (<http://bioinformatics.psb.ugent.be/web-tools/plantcare/html>; Rombauts *et al.*, 1999). PLACE and PlantCARE are databases of plant *cis*-acting regulatory elements, enhancer and repressors. They allow the identification and localization of known plant regulatory promoter motifs in query sequences.

2.13 Southern blot analysis

2.13.1 Digesting genomic DNA with restriction enzymes for Southern blot analysis

3 µg of genomic DNA was restricted with 30 U *ApoI* and *BgIII*, respectively (Fermentas, St. Leon-Rot, Germany) in a total volume of 300-400 µl. *ApoI* has a six bp recognition site with two variable nt (5'-RAATY-3') whereas the second enzyme, *BgIII*, has a six bp recognition sequence (5'-AGATCT-3'). The length and variability of the recognition sequence indicates how frequently the enzyme will cut, on average, in a random sequence of DNA. *BgIII* digestion was performed in 50 mM Tris/HCl pH 7.5, 10 mM MgCl₂, 100 mM NaCl and 0.1 mg ml⁻¹ BSA at 37 °C overnight. *ApoI* digestion was done in 33 mM Tris-acetate pH 7.9, 10 mM magnesium acetate, 66 mM potassium acetate and 0.1 mg ml⁻¹ BSA. Digestion was performed at 37 °C for 2 h due to star-activity of the restriction enzyme. The restricted DNA was purified by sodium acetate precipitation. For this samples were mixed with 1/10 volume 3 M sodium acetate pH 5.2 and 3 volumes ethanol and incubated at -20 °C for 3 d. After centrifugation at 20.000 x g for 15 min the pellet was washed with 1.4 ml ice-cold 70 % (v/v) ethanol and resuspended in 20 µl sterile water. DNA was stored at -20 °C.

2.13.2 DIG-labeling of hybridization probe

A 504 bp *GAL4* probe was synthesized using primers mPPR1-5 (5'-CGGCAAGCTT-GGATCCAACAATG-3') and mPPR1-3 (5'-CCCGGAGCTCGTCCCCCAGGCTG-3') and digoxigenin (DIG) labeled with the DIG Probe Synthesis Kit (Roche, Penzberg, Germany). Genomic DNA of ET line N9313 was used as template in a PCR reaction, in which the PCR product is DIG labeled due to DIG-dUTP incorporation according to the random primed labeling technique. PCR reaction was performed with 200 μ M dATP, dCTP and dGTP, 130 μ M dTTP and 70 μ M DIG-dUTP, 1 μ M of each primer and 50 ng genomic DNA as recommended by the supplier. The PCR reaction protocol is shown in table 2-5.

Table 2-5. PCR protocol for DIG labeling of *GAL4* probe.

Reaction step	Cycles	Temperature [°C]	Time [s]
Initial denaturation	1	94	120
Denaturation	35	94	30
Primer annealing		55	30
Elongation		72	40
Final elongation	1	72	420

2.13.3 Southern transfer

DNA cleaved with *ApoI* or *BglII* (2.13.1.) was separated on a 1 % (w/v) TAE agarose gel (2.7) during a 4 h run at 80 V and blotted onto a Amersham HybondTM-N membrane (GE Healthcare, Buckinghamshire, UK) by capillary transfer. The gel was incubated 2 times for 15 min in 0.5 M NaOH and 0.5 M NaCl to denature the double-stranded DNA, washed with distilled water, followed by incubation in 0.5 M Tris/HCl and 3 M NaCl 2 times for 15 min for neutralization. To prepare the membrane it was incubated in distilled water for 10 min followed by incubation in 3 M NaCl and 0.3 M sodium citrate for 20 min. For blotting, the prepared blotting membrane was placed on the prepared gel sitting upside down on 6 layers of Whatman 3MM (GE Healthcare, Buckinghamshire, UK) soaked with 3 M NaCl and 0.3 M sodium citrate. On the membrane two layers of soaked Whatman 3MM were placed, followed by about 15 cm of paper towels, a glass plate and a weight of about 1 kg. The transfer was done overnight by capillary soaking at RT. After transfer the DNA was fixed on the membrane by UV crosslinking using 30.000 μ J cm⁻².

2.13.4 Southern blot hybridization

The hybridization solution was prepared by dissolving DIG Easy Hyb Granules (Roche, Penzberg, Germany) in 64 ml sterile double distilled water for 5 min at 37 °C. The DIG labeled *GAL4* probe was denatured by boiling for 5 min and immediately cooled on ice-water and then added to 20 ml of hybridization solution pre-heated to hybridization temperature. The optimal hybridization temperature was calculated according to GC content and the homology of probe to target according to the following equation:

$$T_{\text{opt}} [^{\circ}\text{C}] = 49.82 + 0.41 (\% \text{ G+C}) - (600 / l) - 20 \text{ } ^{\circ}\text{C}$$

l means length of the hybrid in bp. The membrane was pre-hybridized 30 min in 25 ml DIG Easy Hyb at 4 °C below T_{opt} . The pre-hybridization solution was poured off and the hybridization solution containing the labeled probe was added to the membrane. Hybridization was performed overnight at T_{opt} . After hybridization the membrane was washed two times at 68 °C for 15 min in preheated 75 mM NaCl, 7.5 mM sodium citrate pH 7.0 with 0.1 % (w/v) SDS and two times at 68 °C for 15 min in preheated 15 mM NaCl, 1.5 mM sodium citrate pH 7.0 with 0.1 % (w/v) SDS to remove unbound probes.

2.13.5 Detection

Southern blot detection was done using the CDP-Star, ready to use Kit (Roche, Penzberg, Germany) containing a chemiluminescent substrate for alkaline phosphatase. After hybridization and stringency washes the membrane was rinsed with DIG Wash buffer (100 mM malic acid, 150 mM NaCl pH 7.5 and 0.3 % (v/v) Tween 20) at RT for 5 min. Blocking solution was added to the membrane followed by 2 h incubation at RT with gentle agitation. The blocking solution was prepared by diluting 1 % (w/v) Blocking reagent (Roche, Penzberg, Germany) in 100 mM malic acid and 150 mM NaCl pH 7.5 at 65 °C. The membrane was then incubated in antibody solution (anti-digoxigenin-AP 37.5 mU ml⁻¹ in blocking solution) for 30 min at RT, followed by two washing steps, 15 min with DIG Wash buffer, and equilibration for 5 min in 0.1 M Tris/HCl, 0.1 M NaCl pH 9.5. Visualization was done with the chemiluminescence substrate disodium 2-chloro-5-(4-methoxyspiro{1,2-dioxetane-3,2'-(5'-chloro)tricyclo-[3.3.1.1^{3,7}]decan}-4-yl) phenyl phosphate (CDP). Enzymatic dephosphorylation of CDP by alkaline phosphatase leads to a light emission at a maximum wavelength of 466 nm. For this the equilibrated membrane was put on a hybridization bag and covered with 20 drops CDP-Star, ready-to-use solution. The membrane was incubated at 37 °C for 10 min followed by 30 min incubation at RT. Detection was done using the Luminescent Image analyzer LAS-4000 (GE-Healthcare, München, Germany), with 3 min detection time.

2.14 Confocal laser scanning microscopy

For fluorescence microscopic investigations to study GFP expression in different tissues of the ET seedlings a confocal laser scanning microscope type Zeiss LSM 510 Meta with multiline argon ion laser was used (Carl Zeiss Inc., Thornwood, USA). Cells were examined with a 40X 1.3 numerical aperture Zeiss oil-immersion objective. GFP was excited at 488 nm and the emission was recorded through the meta-channel at 497 to 550 nm. Fluorescence images were analyzed with LSM Image Browser software (Carl Zeiss Inc., Thornwood, USA).

2.15 Gene expression analyses

2.15.1 RNA isolation

For RNA isolation 10-15 seedlings were pooled and immediately harvested in liquid nitrogen. Tissues were thoroughly ground using the Precellys[®] 24 (Peqlab, Erlangen, Germany) with 2 times 20 s homogenization at 5.500 rpm. RNA isolation was done using the RNeasy Plant Mini Kit (Qiagen, Hilden, Germany) or the GeneMATRIX Universal RNA Purification KIT (EURx, Gdansk, Poland) according to the manufacturer's instructions. The purity of the RNA was assessed spectrophotometrically by measuring A_{260}/A_{280} ratio (BioPhotometer Plus, Eppendorf, Hamburg, Germany). RNA was stored at -70 °C.

2.15.2 First strand cDNA synthesis

cDNA synthesis was performed with the High-Capacity cDNA Reverse Transcription Kit (Applied Biosystems, Carlsbad, USA). 1 µg total RNA was used for cDNA synthesis in 10 µl total volume with 1 x RT Buffer, 4 mM dNTP mix, 1 x RT Random Primers and 50 U MultiScribe[™] reverse transcriptase. At 25 °C for 10 min the random primers were extended prior to increase of the reaction temperature to 37 °C for cDNA synthesis for 120 min. The reverse transcriptase is inactivated by incubation at 85 °C for 5 min after the cDNA synthesis was complete. cDNA was diluted 1:10 in RNase-free sterile water prior to use for quantitative real-time PCR.

2.15.3 Quantitative real-time PCR

2.15.3.1 Primer design

Real-time PCR primer pairs were designed using QuantPrime software (Arvidsson *et al.*, 2008; <http://www.quantprime.mpimp-golm.mpg.de>) and span intron-exon borders, with exception of the primers annealing to the intron-lacking *GFP* sequence. Real-time PCR primers are listed in appendix 6.2, table A7. Routinely the primer specificity was checked by analyzing melting curves that displayed a single peak for each PCR product of interest, and by gel electrophoresis, which has to result in a single PCR product with desired length.

2.15.3.2 Fluorometry

For quantification of transcript abundances the amount of double-stranded PCR products was determined fluorometrically after each polymerization step using SYBR Green. The fluorescent dye intercalates into double-stranded DNA and gives a characteristic fluorescence signal at 585 nm after excitation with 470 nm. Real-time amplification was performed using the Brilliant II SYBR[®] Green Master Mix (Agilent Technologies, Santa Clara, USA) according to the manufacturer's instructions in a Stratagene MX3005P Cycler (Agilent Technologies, Santa Clara, USA). Each 10 µl PCR reaction contained 2 µl cDNA sample, 600 nM of the respective forward and reverse primer and 1 x Brilliant II SYBR

Green Master Mix. PCR was performed using a two-step cycling protocol (tab. 2-6). After 40 cycles, the PCR products were denatured at 95 °C for 1 min, followed by ramping down to 55 °C with up to 2 °C s⁻¹. Then the temperature was slowly increased from 55 °C to 95 °C at a ramp speed of 0.2 °C s⁻¹ and fluorescence data were continuously collected to monitor the melting kinetics of the PCR product. The generated dissociation curves allow controlling the specificity of the PCR reaction from the melting kinetics of the fluorescence emission. All reactions took place at least in duplicates, representing technical replicates. No template controls for each gene were performed. Reactions were performed for at least two biological replicates, each representing an independent RNA isolation.

Table 2-6. General real-time PCR reaction protocol.

Reaction step	Cycles	Temperature [°C]	Time
Activation of DNA polymerase	1	95	15 min
Denaturation	40	95	10 s
Primer annealing and elongation		60	30 s
Dissociation curve	1	72	0.2 °C s ⁻¹

2.15.3.3 Standardization

Levels of each transcript relative to the *ACT2* (At3g18780) control gene, that has been described to be expressed constitutively (An *et al.*, 1996), were quantified as described by Pfaffl (2004) by relative quantification. To calculate the expression of the target genes in relation to *ACT2* the following equation was used: $R = 2^{-[\Delta C_t \text{ sample} - \Delta C_t \text{ ACT2}]}$, meaning $R = 2^{-\Delta \Delta C_t}$ based on a statistic real-time PCR efficiency of 2 and with the threshold value (C_t) differences (Δ) of samples and *ACT2* reference gene.

2.15.4 Analysis of mRNA decay profiles

2.15.4.1 Actinomycin D treatment

For inhibition of transcription seedlings were treated with Actinomycin D (Act D). Arabidopsis ET line N9313 was grown as previously described in chapter 2.2.1. 10 d old seedlings were transferred to 200 µM Act D (Sigma-Aldrich Chemie GmbH, Steinheim, Germany) in liquid MS medium for up to 20 h. Plants were kept at 120 µmol photons m⁻² s⁻¹ continuous light during incubation. Plants incubated with liquid MS medium served as a control.

2.15.4.2 Half-life calculations

The half-life of each mRNA of interest was quantified from the C_t values of RNA samples isolated after 1, 2, 4, 8 and 20 h of Act D treatment. Transcript levels were determined relative to the internal standard transcript of the housekeeping gene *ACT2*. However, as a result of inhibition of transcription and subsequent mRNA decay, the yield of the internal

control *ACT2* cDNA decreased over time after Act D treatment. Therefore C_t values of *ACT2* amplicates of Act D treated samples were adjusted considering the mRNA half-life of *ACT2* ($t^{1/2}_{ACT2} = 12$ h) as determined by Narsai *et al.* (2007). The adjusted C_t values were used for calculation of ΔC_t and $\Delta\Delta C_t$ values to determine mRNA level relative to *ACT2*. mRNA decay has generally been found to obey first-order kinetics (Ross, 1995; Gutierrez *et al.*, 2002); therefore an exponential regression model ($A = 1e^{-kt}$) was applied, allowing a k_{decay} to be calculated for each transcript. The mRNA half-life was then calculated using the following equation: $t^{1/2} = \ln(2) / k_{decay}$.

2.16 Modulation of photosynthetic electron transport chain

2.16.1 Inhibitor treatment

Linear photosynthetic electron transport was blocked with 3-(3',4'-dichlorophenyl)-1,1'-dimethyl urea (DCMU; Sigma, Steinheim, Germany) that irreversibly binds to the Q_B binding niche of the D1 protein of PSII and therefore inhibits the reduction of the PQ pool. Arabidopsis seedlings were sprayed with 10 μ M DCMU, tobacco leaves were sprayed with 1 mM DCMU, both directly before the plants were transferred to the appropriate light conditions, as indicated. DCMU stock solution was 10 mM in 50 % (v/v) ethanol, and the applied concentration was prepared by dilution in water directly prior to use.

Alternatively Arabidopsis seedlings were sprayed with 20 μ M 2,5-dibromo-3-methyl-6-isopropyl-p-benzoquinone (DBMIB; Sigma, Steinheim, Germany) that binds to the PQ oxidation site of the cytochrome *b₆/f* complex (Trebst, 1980) thus reducing the PQ pool. As DBMIB is a light-labile component and unstable in tissues (Alfonso *et al.*, 2000; Pfannschmidt *et al.*, 2001), the incubation time was restricted to 4 h. DBMIB stock solution was 100 mM in 10 % (v/v) Me₂SO in ethanol. The applied concentration was prepared by dilution in water directly prior to use.

2.16.2 Chlorophyll a fluorescence measurements

In vivo Chl *a* parameters were determined at room temperature with a pulse amplitude-modulated (PAM) fluorometer (Dual-PAM-100, Heinz Walz GmbH, Effeltrich, Germany). After dark-acclimation (20 min) the measuring beam was turned on, and minimal fluorescence (F_0) was determined. Then leaves were exposed to a 500-ms flash of saturating white light (6.000 μ mol photons $m^{-2} s^{-1}$) to determine maximal fluorescence (F_m) and the optimum quantum yield F_v/F_m value was determined as $F_m - F_0 / F_m$ (van Kooten and Snel, 1990). Subsequently, leaves were illuminated with 100 μ mol photons $m^{-2} s^{-1}$ of actinic red light of 600 nm. Fluorescence was recorded in the saturation pulse mode by application of saturating flashes every 30 s to determine maximal fluorescence of illuminated leaves (F_m') until a stable fluorescence level (F_t) was reached. Actinic light was switched off, and far-red light was turned on to oxidize the electron transport chain and to determine minimal fluorescence (F_0') in the light-acclimated state. The steady-state fluorescence F_s was

calculated as $F_t - F_0'$. The fluorescence quenching parameter qP (photochemical quenching) was determined as $qP = (F_m' - F_s) / (F_m' - F_0)$ (Schreiber *et al.*, 1986). The effective quantum yield of PSII (Φ PSII) was determined as Φ PSII = $(F_m' - F_s) / F_m'$ (Pfannschmidt *et al.* 2001).

2.17 *Agrobacterium tumefaciens* manipulations

2.17.1 Production of competent *A. tumefaciens* cells

10 ml YEB (5 g l⁻¹ Bacto Peptone, 1 g l⁻¹ yeast extract, 5 g l⁻¹ beef extract, 5 g l⁻¹ sucrose, 0.5 g l⁻¹ MgSO₄ x 7 H₂O) containing rifampicin (150 µg ml⁻¹) and gentamycin (25 µg ml⁻¹) were inoculated with *Agrobacterium tumefaciens* strain GV3101(pMP90) (Koncz and Schell, 1996) and incubated overnight at 28 °C and 180 rpm. With 2 ml of this culture 50 ml YEB containing the appropriate antibiotics were inoculated and incubated till OD₆₀₀ reached values of 0.5 to 1. The culture was cooled to 4 °C and the cells were pelleted by centrifugation at 5.000 x g and 4 °C for 5 min. The pellet was resuspended in 1 ml 20 mM CaCl₂ and divided into 0.2 ml aliquots for transformation.

2.17.2 Transformation of *A. tumefaciens*

Agrobacterium tumefaciens strain GV3101(pMP90) (Koncz and Schell, 1996) was transformed using the freeze-thaw method (Weigel and Glazebrook, 2002). 0.2 ml freshly prepared competent cells and 1 µg plasmid DNA (2.9.5) were mixed and incubated for 15 min on ice. The cells were frozen in liquid N₂ for 5 min and then transferred to a 37 °C water bath for additional 5 min. 1 ml YEB was added and the cells were incubated for 2-4 h at 28 °C. The cells were plated on YEB plates containing 1.5 % (w/v) agar, rifampicin (150 µg ml⁻¹), gentamycin (25 µg ml⁻¹) and spectinomycin (50 µg ml⁻¹), and incubated at 28 °C for 2 d. Colonies were plated on fresh YEB plates and incubated at 28 °C for 24 h before transformed *Agrobacteria* were used for plant transformation.

2.18 Transient gene expression in *Nicotiana benthamiana*

2.18.1 Preparation of *Agrobacteria* suspension for infiltration

Transient expression in tobacco was done based on the p19 co-expression system described by Voinnet *et al.* (2003). *Nicotiana benthamiana* plants were grown in the greenhouse for four to five weeks before infiltration. *Agrobacterium tumefaciens* strain GV3101(pMP90) carrying individual pSIG5-Δ35S:GFP::GUS, Δ35S:GFP::GUS or 35S:GFP::GUS constructs, respectively, and strain GV3101(pMP90) carrying the 35S CaMV driven p19 protein of tomato bushy stunt virus were inoculated in 10 ml YEB medium containing the appropriate antibiotics (GV3101(pMP90): rifampicin 150 µg ml⁻¹, gentamycin 25 µg ml⁻¹; p19 protein: kanamycin 100 µg ml⁻¹; pHGWFS7.0: spectinomycin 100 µg ml⁻¹) and grown at 28 °C and 180 rpm until OD₆₀₀ reaches at least 0.5. For co-infiltrations, both *Agrobacteria* cultures were

mixed (40 % p19 and 60 % pHGWFS7.0, respectively). Cells were collected by centrifugation for 8 min at 3.000 x g at room temperature and resuspended in 100 mM MES pH 5.6 plus 10 mM CaCl₂. After supplemented with 150 µM acetosyringone, bacterial suspension was incubated in this medium for 2 h and then infiltrated into tobacco leaves.

2.18.2 Infiltration of tobacco leaves

Infiltration of tobacco leaves was performed according to English *et al.* (1997). A small hole was made on the lower surface of the leaf using a razor blade. A 1 ml syringe (without needle) was used to inject defined volumes of *Agrobacterium* culture into intercellular spaces of the leaves.

2.19 Generation of stable transformed *Arabidopsis thaliana*

2.19.1 Transformation by floral dip

Transformation of *Arabidopsis thaliana* was performed by floral dip method as previously described by Clough and Bent (1998). Plants of ecotype C24 were grown to flowering stage in the greenhouse. 5 plants were planted per 81 cm² pot. To prevent the soil from falling into inoculation medium, soil was wetted before inoculation. Plants were dipped when most inflorescences were about 5-10 cm tall. For this 10 ml YEB was inoculated with transformed *Agrobacteria* and grown overnight at 28 °C and 180 rpm containing the appropriate antibiotics. With this suspension 400 ml YEB supplemented with the appropriate antibiotics was inoculated. The suspension was incubated overnight at 28 °C and 180 rpm. The cells were pelleted at 4.000 x g for 20 min. The pellet was resuspended in 200 ml YEB supplemented with 0.01 % (v/v) Tween 20. Inflorescences of *Arabidopsis* plants without siliques were dipped for 10 min. The plants were covered with plastic foil overnight and then transferred to the green house.

2.19.2 Selection of transformants

Transformed *Arabidopsis* seeds were identified according to Harrison *et al.* (2006). Seeds were surface sterilized and sown on MS medium supplemented with 0.5 % (w/v) sucrose and hygromycin B at a concentration of 20 µg ml⁻¹. Plates were cold treated for 2 d and then transferred to growth chamber for 6 h, with 100-120 µmol photons m⁻² s⁻¹ white light at 22 °C in order to stimulate germination. The plates were then transferred to darkness for 2 d. Seedlings were then treated with white light again for additional 24-48 h. Positive transformants with hygromycin B resistance were identified by elongated hypocotyls and transferred to MS medium supplemented with 0.5 % (w/v) sucrose for 3-6 d before being planted on soil. The plants stayed in the growth chamber until the end of the growth period where the seeds were collected. Plants of segregating T₂ population were analyzed by PCR for existence of the sequence of the recombinant plasmid (primers are listed in appendix 6.2, table A8).

2.20 Crossing *Arabidopsis thaliana* plants

2.20.1 Crossing procedure

All crossing steps were performed under magnification using a pair of fine tweezers. Any siliques, open flowers, or open buds were removed from the inflorescence of the maternal mutant plant as they were self-fertilized. Buds that start to open were chosen for crossing procedure. Sepals, petals and anthers were removed without touching or damaging the pistil. An anther from a mature flower of the crossing partner was rubbed onto the stigma of the emasculated plant. After performing as many crosses as possible on each inflorescence, the meristem and all smaller buds were removed. The seeds of developed siliques were harvested before pod shatter causes loss of the seeds. The F₁ progeny was allowed to self-fertilize and the segregating F₂ progeny was analyzed using a combination of typical phenotypic responses of photoreceptor mutants and PCR based identification of mutated alleles.

2.20.2 Identification of mutant alleles by phenotype

Seedlings with homozygous *cry1*, *phyA* or *phyB* mutations were identified by selecting long hypocotyls in blue, red or white light, respectively, according to Neff and Chory (1995). Seeds were surface sterilized and grown on solidified MS medium supplemented with 0.5 % (w/v) sucrose as previously described. After 2 d cold treatment at 4 °C in darkness, the plates were transferred to 50 μmol photons m⁻² s⁻¹ red light (LED, centroid at 673 nm; CLF PlantClimatics, Emersacker, Germany) and 20 °C for 2 h to induce germination. To screen for homozygous photoreceptor mutations, seedlings were then transferred to 50 μmol photons m⁻² s⁻¹ continuous light of distinct wavelength for 5 d. Homozygous *cry1* mutants were identified by long hypocotyl after treatment with blue light (2.2.3), *phyA* mutants were identified by long hypocotyl after treatment with red light (2.2.3), and *phyB* mutants were identified by long hypocotyl phenotype after treatment with white light centroid at 455 nm and 557 nm (LED, CLF PlantClimatics, Emersacker, Germany). Emission spectra of the LEDs are given in appendix 6.3.

Plants carrying the homozygous *phot1* allele were identified by measurements of phototropic response (fig. 2-4). The measurements of phototropic curvature were performed as described in Lascève *et al.* (1999). The sterilized seeds were placed in rows on MS medium in square Petri plates. After cold treatment and the 2 h illumination with red light the plates were kept upright, wrapped in foil and seedlings were grown in complete darkness for 3 d at 20 °C. To induce hypocotyl curvature, the etiolated seedlings were irradiated for 16 h with unilateral blue light at a fluence rate of about 1 μmol photons m⁻² s⁻¹. After illumination, the seedlings without curvatures were selected being homozygous *phot1* mutants. The genotypes of the mutants were reconfirmed by PCR-based identification of the mutant allele.

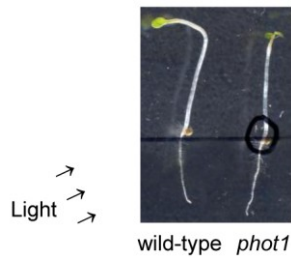


Figure 2-4. Hypocotyl phototropism in etiolated wild-type and *phot1* mutant seedlings of *Arabidopsis thaliana*. Hypocotyl curvatures of 3.5 d old seedlings were determined after a 16 h exposure to unilateral blue light ($1 \mu\text{mol photons m}^{-2}\text{s}^{-1}$). *phot1* mutants fail in performing hypocotyl curvature.

2.20.3 PCR-based identification of mutant alleles

The genotypes of each of the mutant combinations (with exception of the *cry1-1* mutant) were confirmed by PCR. Primers used for the identification are listed in appendix 6.2 in table A9. All crossings were analyzed for the presence of homozygous ET T-DNA with primers listed in table A2. Some mutations create cleaving amplified polymorphic sequence (CAPS) marker or simple sequence length polymorphism (SSLP) (table 2.7).

Table 2.7. Identification of mutant alleles by CAPS or SSLP markers

Mutation	Marker for identification
<i>cry2-1</i>	CAPS marker, cleavage with <i>Bsl</i> I
<i>hy1-1</i>	SSLP marker, 13-bp deletion
<i>phyA-201</i>	CAPS marker, cleavage with <i>Mse</i> I
<i>phyB-5</i>	CAPS marker, cleavage with <i>Bsa</i> BI
<i>phot2-1</i>	CAPS marker, cleavage with <i>Mfe</i> I

The *phot1-5* mutation, a large-scale rearrangement that disrupts the gene within intron 12, was detected using primers amplifying a 244-bp product in wild-type but not in the mutant. Homozygous wild-type *PHOT1* plants of the F_2 progeny were identified by analyzing the F_3 progeny for the absence of the mutant *phot1* sequence. The SALK_056405C line carries a T-DNA insertion in the second intron of *HY5*. The insertion was identified using the Primer LBB1.3 and a second primer annealing with the genomic *HY5* sequence. In a second PCR the wild-type *HY5* sequence was amplified in plants that do not carry homozygous T-DNA insertion. The *cry1-1* mutation (former *hy4-1* or *hy4-2.23N*) was annotated as result of a chromosomal rearrangement (Neff and Chory, 1998). Primers published to amplify 130-bp and 180-bp fragments for the wild-type and 180-bp fragments for the mutants failed in amplification of the 180-bp fragment. Ahmad and Cashmore (1993) published the *hy4-1* mutation as single nucleotide polymorphism leading to an amino acid exchange in *CRY1*. However, sequencing the *CRY1* gene sequence in *cry1-1* background identified the allele not to contain any of the published *hy4-1*, *hy4-2*, *hy4-3* or *hy4-4* mutations. Interestingly the mutants showed the blue light inducible long hypocotyl phenotype described in Neff and Chory (1998). Therefore *cry1-1* mutants were only screened for the homozygous mutation by phenotype (2.20.2).

2.21 Yeast manipulations

2.21.1 Yeast one-hybrid system

Yeast one-hybrid (Y1H) assays developed from the yeast two-hybrid systems that identify protein-protein interactions (Vidal and Legrain, 1999). The concept of the Y1H uses the yeast transcription factor GAL4. GAL4 increase the rate of transcription of its target gene by binding to upstream activating DNA sequences (UAS) and thus targeting RNA polymerase II to the corresponding promoters. The DNA binding domain and the activating functions are located in physically separable domains (Keegan *et al.*, 1986) and are referred to as the DNA-binding domain (BD) and the activation domain (AD), respectively. In this study the target DNA sequences, or bait sequences were cloned into pHIS2 (appendix 6.4, fig. A6) and tested for interaction with a library of candidate cDNAs encoding potential DNA-binding proteins, the prey, expressed as fusions to the GAL4 AD in the pACT plasmid (appendix 6.4, fig. A7). Interaction between a DNA-binding protein and the target bait sequence stimulates transcription of *HIS3* reporter gene (fig. 2-5), enabling the histidine auxotroph yeast host strain Y187 to grow on minimal medium lacking histidine.

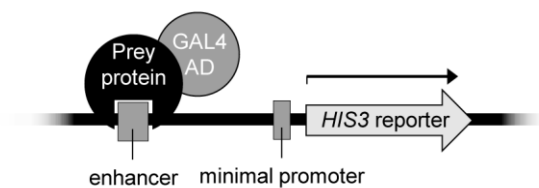


Figure 2-5. Schematic diagram of the yeast one-hybrid system. A *cis*-regulatory element of interest is fused upstream of *HIS3* reporter gene. Prey protein encoded by cDNA library and fused to GAL4 AD binds the *cis*-element resulting in activating the transcription of the reporter gene.

2.21.2 Yeast strain and growth conditions

The *Saccharomyces cerevisiae* strain Y187 (*MAT α* , *ura3-52*, *his3-200*, *ade2-101*, *trp1-901*, *leu2-3*, *112*, *gal4 Δ* , *met-*, *gal80 Δ* , *URA3::GAL1_{UAS}GAL1_{TATA}-lacZ*, *MEL1*, with reporter genes *HIS3* and *lacZ*) was grown on rich yeast extract-peptone-dextrose (YPD) medium (2 % (w/v) peptone, 2 % (w/v) glucose and 1 % (w/v) yeast extract) at 30 °C and 250 rpm or on solidified medium supplemented with 2 % (w/v) agar. For selection of transformants yeast cells were grown on minimal synthetic dropout (SD) medium (2.67 % (w/v) Minimal SD Base (Clontech Laboratories, Inc., Montain View, USA) and 0.062 % (w/v) DO Supplement (Clontech Laboratories, Inc., Montain View, USA)) lacking specific amino acids, depending on the plasmids that were used for transformation.

2.21.3 Bait vector construction

Promoter fragments were generated by PCR using genomic DNA of the ecotype C24 as template. For cloning purposes, restriction sites were added to the 5' border and the 3' border of each fragment by PCR amplification with an appropriately designed oligonucleotide (*SacI* and *SmaI* or *SacI* and *EcoRI*, respectively; primers are listed in appendix 6.2, table A10). The PCR products containing the two restriction sites were ligated with pJET1.2/blunt vector

as described previously. For ligation with pHIS2, pJET1.2/blunt containing the different PCR fragments and the pHIS2 vector were double digested with *SacI* and *SmaI* or with *SacI* and *EcoRI*, respectively. The restricted DNA fragments were ligated as described previously.

2.21.4 Transformation of *Saccharomyces cerevisiae*

For yeast transformation, the lithium acetate (LiAc) method was used according to Gietz and Schiestl (2007). 5 ml YPAD liquid medium (YPD medium supplemented with 80 mg l⁻¹ adenine hemisulfate) was inoculated with a single colony of Y187 and grown overnight. 50 ml pre-warmed 2 x YPAD (2 x YPD medium supplemented with 80 mg l⁻¹ adenine hemisulfate) liquid medium were inoculated with 2.5 x 10⁸ cells of the saturated culture and grown for about 4 h till OD₆₀₀ reached a value of 2 indicating 2 x 10⁷ cells ml⁻¹ (a suspension containing 1 x 10⁶ cells ml⁻¹ will give an OD₆₀₀ of 0.1). Cells were sedimented by centrifugation at 3.000 x g for 5 min, washed two times with 25 ml sterile water and resuspended in 1 ml sterile water. Cells were sedimented again at 13.000 x g for 30 s and resuspended in 1 ml sterile water. For each transformation 100 µl samples containing 10⁸ cells were used. The cells were pelleted again and resuspended in a mixture of 66.6 % (w/v) PEG 3350, 100 mM LiAc, 0.1 mg denatured single-stranded carrier DNA (denatured by boiling for 5 min in a water bath followed by immediately chilling in an ice/water bath), and 100 ng plasmid DNA for single transformations or 500 ng plasmid DNA for double transformations, respectively, in a total transformation volume of 360 µl. The tubes were incubated in a water bath at 42 °C for 30 min. The cells were harvested by centrifugation at 13.000 x g for 30 s and resuspended in 1 ml sterile water. 20 µl and 200 µl of the cell suspension were plated onto the appropriate SD selection medium. The cells were grown for 2-3 d at 30 °C.

2.21.5 Yeast colony-PCR

A single colony was resuspended in 50 µl water supplemented with 60 U ml⁻¹ lyticase and incubated at 30 °C for 30 min. Cell lysis was performed by heating the suspension to 95 °C for 10 min. The supernatant was collected after sedimentation of the cell debris at 20.000 x g for 2 min, and 2 µl of the supernatant was used for PCR in 20 µl total reaction volume, as described in chapter 2.5.1.

2.21.6 Plasmid isolation from yeast

A fresh colony was used to inoculate 5 ml of the appropriate SD medium. After overnight incubation cells were pelleted at 20.000 x g for 5 min and the pellet was resuspended in about 100 µl residual volume. 20 µl lyticase (5 U µl⁻¹ in TE) was added and suspension was incubated at 37 °C for 60 min. Reaction was determined by addition of 20 µl 20 % (w/v) SDS and thoroughly mixing. Samples were put through one freeze/thaw cycle at -20 °C and thoroughly mixed to ensure complete lysis of the cells. Volume was brought up to 200 µl

with TE, pH 7.0. After extraction with 200 μ l phenol-chloroform-isoamyl alcohol (25:24:1) the samples were centrifuged at 20.000 x g for 10 min at room temperature. The upper phase was transferred to 8 μ l 10 M ammonium acetate and 500 μ l of ethanol. The plasmid DNA was precipitated for 1 h at -70 °C and sedimented by centrifugation at 20.000 x g for 10 min. Precipitates were resuspended in 50 μ l TE and stored at -20 °C.

2.21.7 Setting 3-amino1,2,4-triazol concentration

HIS3 reporter gene in pHIS2 is driven by a minimal promoter $P_{minHIS3}$. This minimal promoter causes an autoactivation of the *HIS3* gene even without promoter sequence inserted in the MCS (Fields, 1993; Durfee *et al.*, 1993). In addition to this also the inserted promoter sequence of interest maybe is able to induce or stimulate the autoactivation of *HIS3* transcription as it is possible that an endogenous expressed yeast protein binds to the site or a neighboring sequence and activates the reporter gene. To suppress the yeast growth on selection medium due to this leaky *HIS3* expression the competitive inhibitor 3-amino1,2,4-triazol (3-AT) was added to the minimal SD medium. 5 ml liquid SD/-Trp medium was inoculated with yeast strain Y187 transformed with p*SIG5* fragments in pHIS2 and grown overnight. OD₆₀₀ of the cultures was adjusted to 0.01 with sterile water. 5 μ l of the adjusted cultures were dropped onto solid SD/-His/-Trp plates supplemented with 10-100 μ M 3-AT. Plates were incubated 2-3 d at 30 °C. 3-AT concentrations were chosen for individual constructs that allow growth of no or only very small yeast colonies, indicating a sufficient suppression of *HIS3* function in the absence of the prey.

2.21.8 Library construction

A LAMBDA ACT cDNA library generated from mRNA isolated from 3 d old etiolated *Arabidopsis thaliana* Col-0 seedlings (Kim *et al.*, 1997) was used for yeast one-hybrid screen. The library uses pACT (pSE1107) as the vector backbone (appendix 6.4, fig. A7; Durfee *et al.*, 1993).

2.21.8.1 Excision to convert the λ -ACT cDNA library into a plasmid library

To convert the λ -ACT cDNA library into a plasmid library an *in vivo* plasmid excision was performed. 5 ml liquid LB supplemented with 50 μ g ml⁻¹ kanamycin was inoculated with *E. coli* strain BNN132 and incubated overnight at 37 °C and 150 rpm. 50 μ l of this culture were used to inoculate 5 ml liquid LB medium supplemented with 50 μ g ml⁻¹ kanamycin. The culture was incubated at 37 °C and 250 rpm for 2 h until cells reached a density of about 3 x 10⁸ cells ml⁻¹. 2 ml of the culture were harvested by centrifugation at 20.000 x g for 2 min and resuspended in 2 ml 10 mM MgCl₂. 10⁸ phage of the amplified library were added and the suspension was incubated at 30 °C without shaking for 30 min. 2 ml liquid LB was added and the suspension was incubated in a roller drum at 30 °C for 1 h. The cells were spread on 10 solid LB medium plates (\varnothing 150 mm) supplemented with 50 μ g ml⁻¹ ampicillin and 0.2 %

(w/v) glucose and incubated overnight at 37 °C. Dilutions of the original infection were plated to determine efficiency. The cells were resuspended by addition of 10 ml liquid LB to each plate. Bacteria from 3-4 plates were pooled and used to inoculate 3 l of LB supplemented with 50 µg ml⁻¹ ampicillin. The cultures were grown to stationary phase overnight.

2.21.8.2 Analysis of cDNA library quality

After excision 14 colonies were picked to analyze the quality of the cDNA library by analyzing sizes of cDNA inserts in pACT. The isolated plasmids were cleaved by restriction endonuclease *XhoI* as cDNAs were ligated in the *XhoI/XhoI* site of pACT. The resulting fragment sizes were determined by gel electrophoresis in a 1.2 % (w/v) agarose gel by comparison with a DNA standard.

2.21.9 Yeast one-hybrid screen

The transformation with cDNA library in pACT was performed as described in chapter 2.21.4 with few modifications. Y187 cells were first transformed with bait vector. 10 ml SD medium lacking tryptophan were inoculated with a single colony of these transformants and grown overnight at 30 °C and 250 rpm. The transformation procedure was scaled up 14-fold with 10 µg cDNA in pACT used for every transformation reaction. 200 µl of cell suspension was plated per petri dish (Ø 145 mm), with 100 plates in total, containing SD/TDO supplemented with 20 mM 3-AT. 1:10, 1:100, 1:1000 and 1:10000 dilutions of the cell suspension were plated onto SD/-L/-T medium to determine the transformation efficiency.

2.21.10 Test for interaction with HY5 transcription factor

The CDS of the transcription factor HY5 was cloned without initial start codon in frame into the *BamHI/XhoI* site of pACT2 (appendix 6.4, fig. A8). A 196-bp fragment of the *Arabidopsis RBCS1A* promoter was cloned into the *SacI/EcoRI* site of pHIS2 and used as a control for interaction, as this fragment was shown to interact with HY5 in an electrophoretic mobility shift assay (EMSA) (Chattopadhyay *et al.*, 1998b). Primers used for amplification of the CDS of HY5 and of the *RBCS1A* promoter fragment are listed in appendix 6.2, table A11. With both bait and prey transformed yeast cells were tested for interaction as described in 2.21.7. The comparison of the size of the resulting colonies with colonies of single transformed cells not containing the prey onto SD/-H/-T medium with the same 3-AT concentrations indicated the strength of interaction.

3

RESULTS

3.1 Screening ET lines for light-dependent GFP fluorescence

A collection of *GAL4-GFP* ET lines (Haseloff, 1999; Laplaze *et al.*, 2005) was screened for light-dependent reporter gene expression pattern. The names of all analyzed lines are given in appendix 6.5. The seedlings were grown in 96-well plates on solidified MS medium supplemented with 0.5 % (w/v) sucrose. The seedlings were illuminated during growth with light intensities ranging from 10 to 200 $\mu\text{mol photons m}^{-2} \text{s}^{-1}$ white light. The GFP fluorescence of 10-11 d old seedlings was quantified using a top reader fluorometer.

62 different ET lines were analyzed. The GFP fluorescence of different ET lines was of different intensity (fig. 3-1) and in some lines undetectable. In seven lines the GFP fluorescence intensities correlated with the applied light intensity (fig. 3-1), representing 11 % of the screened population. From the ET lines with light-dependent GFP fluorescence, three lines with high absolute GFP fluorescence values were analyzed in more detail: N9249, N9266 and N9313.

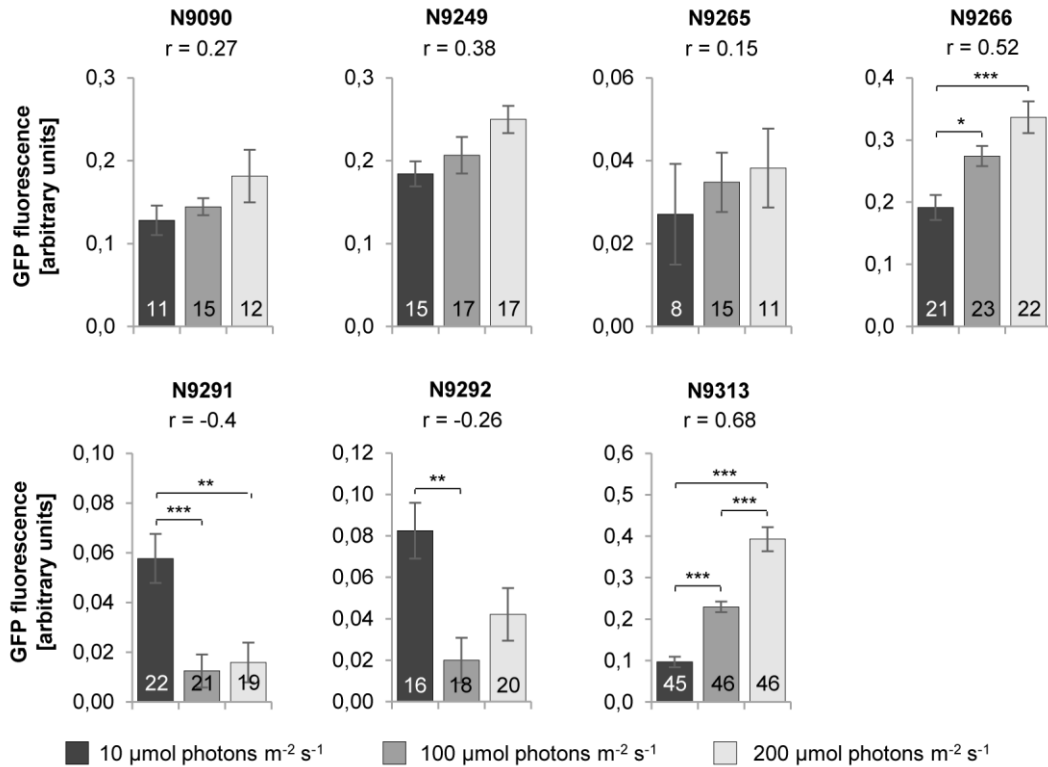


Figure 3-1. GFP fluorescence of *GAL4-GFP* ET lines, modulated by light intensity. Seedlings were grown on MS medium supplemented with 0.5 % (w/v) sucrose for 10-11 d under short day conditions and illuminated with 10, 100 or 200 $\mu\text{mol photons m}^{-2} \text{s}^{-1}$ white light. Fluorescence of wild-type C24 seedlings was subtracted. Bars represent mean values (\pm SEM). The numbers at the bottom of each bar indicate the sample sizes (n). r = coefficient of correlation. One-way ANOVA was performed comparing all groups with Bonferroni's post-test. Statistical significance of difference is indicated as asterisks above bars (* $p < 0.05$, ** $p < 0.01$, *** $p < 0.001$).

3.2 Enhancer trap line N9249

The GFP fluorescence values of ET line N9249 correlated with light intensity during growth, indicating that the reporter gene was under the control of a light-responsive enhancer element. To test this hypothesis, N9249 was characterized by fluorescence microscopy, mapping the T-DNA insertion site by TAIL-PCR and Southern blot analysis.

3.2.1 Localization of GFP fluorescence

Confocal microscopic studies were performed to determine the tissues in which the GFP was expressed. The GFP in the ET collections analyzed localizes to the endoplasmic reticulum (Haseloff, 1999).

The seedlings were analyzed 10-11 d after germination. The GFP fluorescence of ET N9249 was mainly localized in epidermis cells of the cotyledons, including the guard cells of the stomata (fig. 3-2 A). A weaker fluorescence signal was observed in the root stele (fig. 3-2 B).

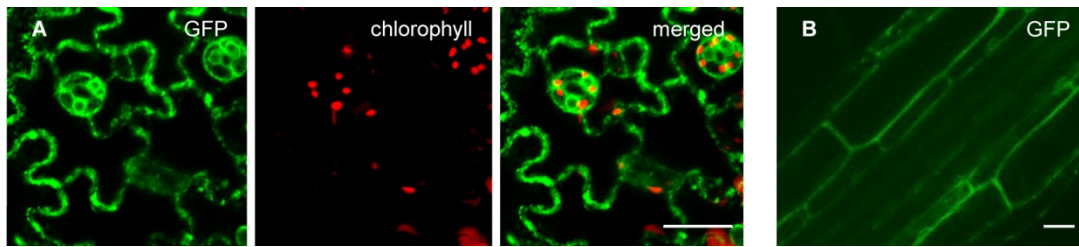


Figure 3-2. Spatial GFP expression in ET N9249 seedlings, analyzed by CLSM. **A:** Cotyledon, transverse confocal section of the adaxial epidermis. GFP was expressed in epidermis cells including stomata **B:** Longitudinal confocal section of the primary root. GFP was expressed in the root stele (bar = 20 μ m).

3.2.2 Identification of T-DNA insertion site by TAIL-PCR

To identify the *cis*-acting elements mediating the GFP fluorescence, the ET T-DNA insertion site in the genome of N9249 was localized. A TAIL-PCR amplified the right border of the ET T-DNA and the flanking genomic DNA. The principle of the TAIL-PCR is described in more detail in 2.5.2.

The tertiary TAIL-PCR with DNA isolated from N9249 as template resulted in a 323-bp amplicon, specific for the primer TR3.2, annealing to the T-DNA, and AD1, annealing to genomic DNA (fig. 3-3). This amplicon did not appear in the control reactions performed with one primer, demonstrating that it is a specific type I TAIL-PCR product.

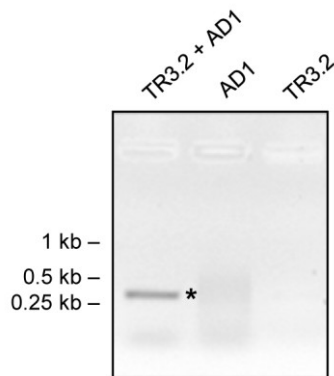


Figure 3-3. TAE agarose gel electrophoresis of tertiary TAIL-PCR products of N9249. The combination of both primers TR3.2 and AD1 amplified a 323-bp fragment (marked by asterisk), which was absent in the control reactions performed with only one of the primers. TAE gel, 1.2 % (w/v) agarose.

The amplicon was purified and cloned into pJET1.2/blunt. The resulting recombinant plasmids were tested by PCR for the presence of the target with the primers TR3.2 and AD1. A plasmid that included the type I target was sequenced to determine the TAIL-PCR product identity.

Identification of the T-DNA insertion site was done by aligning the sequencing result with database entries by BLASTN. BLAST stands for Basic Local Alignment Search Tool and is an algorithm that is used to separately search databases (Altschul *et al.*, 1990, 1997). BLASTN compares a nucleotide query sequence against a nucleotide sequence database. A database containing *Arabidopsis thaliana* (L.) Heynh. accession Col-0 whole genome

sequence (taxid: 3702) was used for comparison with the TAIL-PCR product sequence. The identification of the different components of the sequenced TAIL-PCR fragment is depicted in figure 3-4. The cloning site of the vector, the right border of the ET T-DNA and both PCR primers were assigned to the sequence. The TAIL-PCR product amplified a nucleotide sequence of chromosome 5.

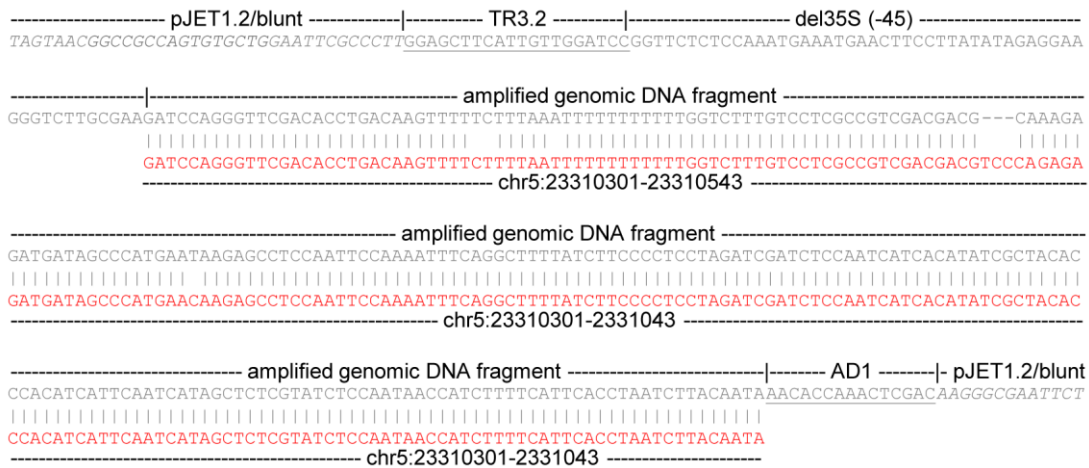


Figure 3-4. Attribution of components of tertiary TAIL-PCR product of N9249. The amplified genomic DNA fragment included a 242-bp sequence that corresponded to the nucleotide sequence of chromosome 5 of *Arabidopsis thaliana* (highlighted in red). The pJET1.2/blunt vector backbone is depicted in italic, the primer sequences are underlined.

The BLAST analysis of the TAIL-PCR product sequence revealed that the ET T-DNA of N9249 was inserted 2063 bp upstream of At5g57560 and 573 bp upstream of At5g57565 translational start sites (fig. 3-5).

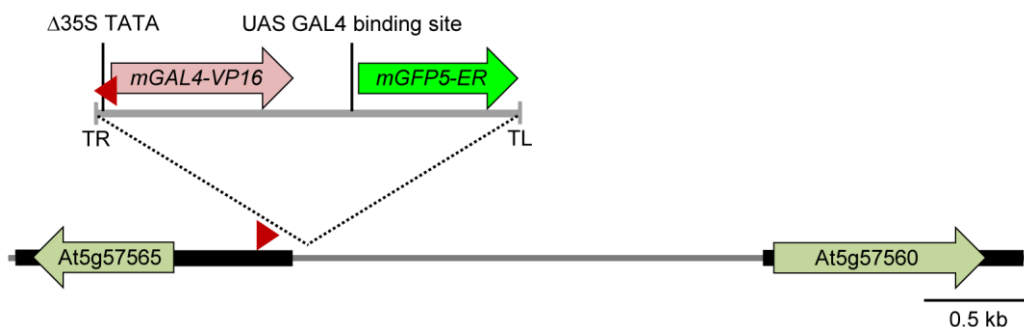


Figure 3-5. Diagram of the identified ET T-DNA insertion site in N9249. The ET T-DNA was inserted between ORFs of At5g57565 and At5g57560. Arrows indicate CDSs, black bars indicate 5' and 3' UTRs. TR and TL label the borders of the ET T-DNA. TAIL-PCR primer binding sites are depicted as red triangles.

The identified T-DNA insertion site was controlled by PCR. Primer TR3.2 was combined with a primer designed to anneal the genomic DNA flanking the T-DNA insertion site. The expected 1648-bp PCR product was amplified with DNA isolated from N9249 but

not in the control reaction with DNA from wild-type C24 (fig. 3-6). This confirmed the mapped T-DNA insertion site of N9249 between At5g57560 and At5g57565.

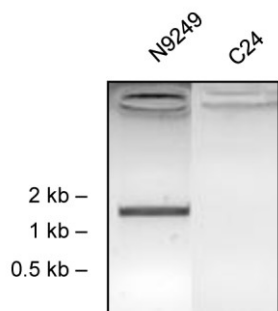


Figure 3-6. TAE agarose gel electrophoresis of PCR amplicon, confirming the T-DNA insertion site of N9249. The PCR product was amplified with DNA from N9249. A control reaction was performed with DNA of C24. TAE gel, 1.2 % (w/v) agarose.

3.2.3 *In silico* analysis to predict *cis*-acting elements

The localization of the ET T-DNA insertion site allowed the prediction of light-responsive *cis*-acting elements mediating the light-response of the GFP in N9249. Two online tools were used to predict light responsive *cis*-acting elements: the PlantCARE database of plant *cis*-acting regulatory elements, enhancer and repressors (Rombauts *et al.*, 1999), and the PLACE database of motifs found in plant *cis*-acting regulatory DNA elements (Higo *et al.*, 1999). The sequence upstream of the mapped T-DNA insertion site, up to the translational start site of At5g57565, was analyzed, in total 526 bp. The analysis resulted in the prediction of four different motifs involved in light responsiveness in plants in the 5' UTR of At5g57565 (tab. 3-1).

Table 3-1. Light responsive motifs identified in the 5' UTR of At5g57565 as predicted by PlantCARE and PLACE database.

Motif	Sequence ^a	Position ^b	Description
TCT	TCTTAC (+)	-54 to -48	part of a light responsive element
Box 4	ATTAAT (+)	-166 to -161	part of a conserved DNA module involved in light responsiveness in <i>Petroselinum crispum</i>
ATC	TGCTATCCG (+)	-226 to -218	part of a conserved DNA module involved in light responsiveness in <i>Zea mays</i>
GAG	ACTCTCT (-)	-339 to -334	part of a light responsive element in <i>Arabidopsis thaliana</i>

^a (+) and (-) indicates the sense and complementary strand, respectively

^b positions are relative to the translation start site of At5g57565

3.2.4 Southern blot analysis to determine the number of T-DNA insertions

Southern blot analysis was performed to determine the number of T-DNA insertion sites per ET line. If a single T-DNA was inserted in the genome, cleavage of genomic DNA of the respective ET line with a restriction endonuclease, which does not cleave within the sequence of the particular probe, would lead to a single fragment on the blot after hybridization.

Genomic DNA of N9249 and of C24 was cleaved with the two restriction endonucleases *ApoI* and *BglII* in parallel. After blotting, the DNA was hybridized with a DIG-labeled *GAL4* probe, annealing to the *GAL4* gene of the ET T-DNA. As a result, the DNA isolated from ET N9249 showed several fragments on the blot after hybridization (fig. 3-7).

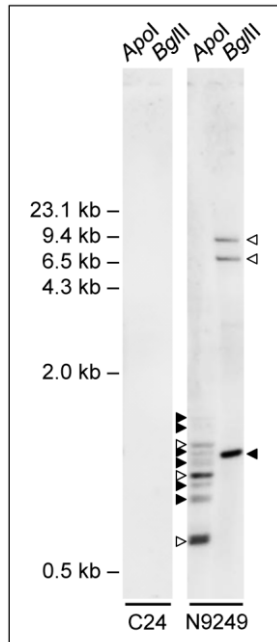


Figure 3-7. Molecular characterization of ET N9249 by Southern blot. Some DNA fragments could be explained due to the identified T-DNA localization on chromosome 5 (black triangles). Cleavage with both restriction enzymes led to additional fragments that could not be explained by the localized T-DNA insertion site (white triangles).

An *in silico* restriction analysis of the mapped T-DNA insertion site of N9249 was performed to assign the DNA fragments on the blot. The restriction analysis was performed with the online tool NEBcutter V2.0 (<http://tools.neb.com/NEBcutter2/index.php>) (Vincze *et al.*, 2003). The analysis resulted in the identification of some fragments on the blot, which were explained by the identified T-DNA insertion site (fig. 3-7, black triangles). Some additional fragments could not be explained by this (fig. 3-7, white triangles).

The Southern blot analysis demonstrated that several ET T-DNA constructs were inserted in the genome of N9249. It was not possible to identify additional insertion sites by TAIL-PCR. Consequently, the ET N9249 was excluded from further analyses.

3.3 Enhancer trap line N9266

3.3.1 Localization of GFP fluorescence

In 10-11 d old N9266 seedlings GFP fluorescence was localized in mesophyll cells of cotyledons and primary leaves and in leaf and hypocotyl epidermal cells including the guard cells of the stomata (fig. 3-8). GFP fluorescence was not detectable in the root, demonstrating tissue specificity of reporter gene expression in N9266.

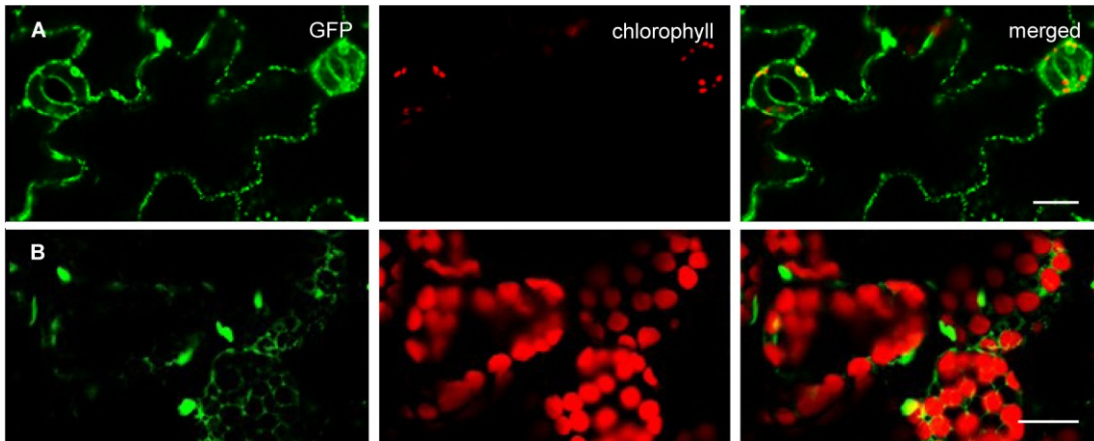


Figure 3-8. Spatial GFP expression in ET N9266 seedlings, analyzed by CLSM. A: Cotyledon, transverse confocal section of the adaxial epidermis **B:** Transverse confocal section of spongy mesophyll of cotyledon (bar = 20 μ m).

3.3.2 Identification of T-DNA insertion site by TAIL-PCR

To identify the ET T-DNA insertion sites, TAIL-PCRs were performed. A 126-bp fragment specific for the used TR3.2 and AD2 primers in tertiary TAIL-PCR was amplified, which did not appear in the control reactions with only one primer (fig. 3-9).

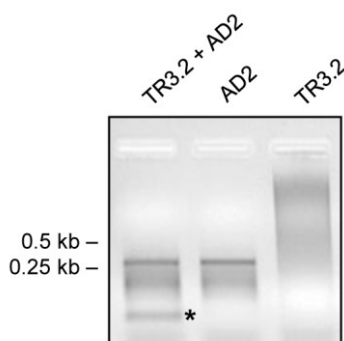


Figure 3-9. TAE agarose gel electrophoresis of tertiary TAIL-PCR products of N9266. The combination of both primers TR3.2 and AD2 amplified a 126-bp fragment (marked by asterisk), which was absent in the control reactions performed with only one of the primers. TAE gel, 1.2 % (w/v) agarose.

The TR3.2-AD2 product of interest was separated from the unspecific AD2-AD2 products by excision out of the gel and ligation with pJET1.2/blunt. The resulting recombinant plasmids were tested by PCR for the presence of the target with the primers TR3.2 and AD2, and sequenced. The T-DNA insertion site was identified by aligning the

sequencing result with database entries (Arabidopsis accession Col-0 whole genome sequence) by BLASTN. The identification of the different components of the sequenced TAIL-PCR product is depicted in figure 3-10.

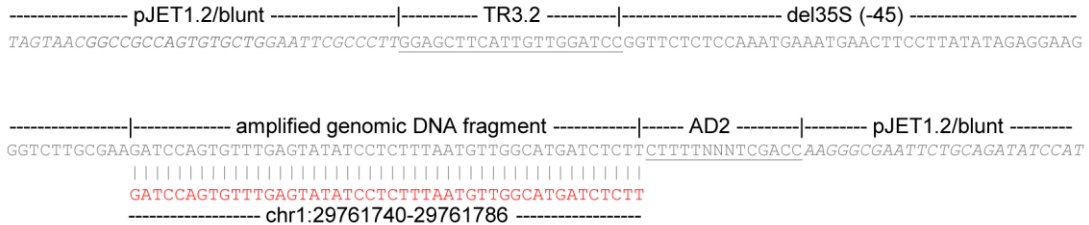


Figure 3-10. Attribution of components of tertiary TAIL-PCR product of N9266. The amplified genomic DNA fragment contained a 46-bp sequence that corresponded to a sequence of chromosome 1 of *Arabidopsis thaliana* (highlighted in red). The pJET1.2/blunt vector backbone is depicted in italic, the primer sequences are underlined.

The pJET1.2/blunt sequence adjacent to the cloning site, both TAIL-PCR primers and the truncated 35S promoter of the ET T-DNA were identified. A 46-bp fragment of the TAIL-PCR product was aligned to a sequence of chromosome 1. The T-DNA of N9266 was inserted in an intergenic region between At1g79110 and At1g79120, 1187 bp downstream of At1g79110 and 5540 bp downstream of At1g79120 translation start sites (fig. 3-11).

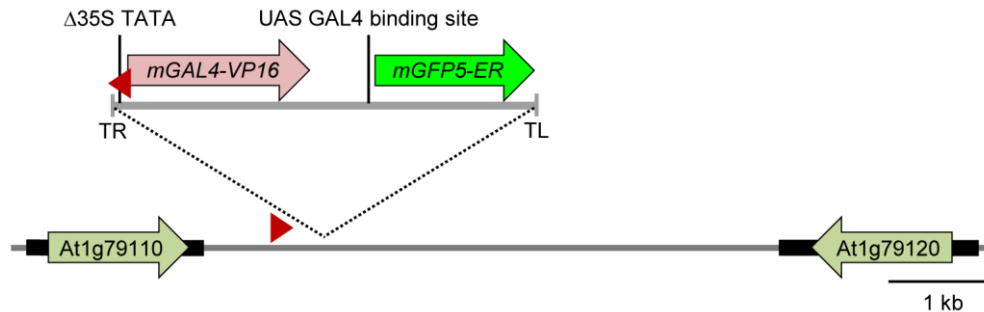


Figure 3-11. Diagram of the identified ET T-DNA insertion site in N9266. The ET T-DNA was inserted in an intergenic region between ORFs of At1g79110 and At1g79120. Arrows indicate CDSs, black bars indicate 5' and 3' UTRs. TR and TL label the borders of the ET T-DNA. TAIL-PCR primer binding sites are depicted as red triangles.

The identified T-DNA insertion site was checked by PCR using the primer TR3.2 in combination with a primer designed to anneal to the genomic DNA flanking the T-DNA insertion site. The expected 1566-bp PCR product was amplified with DNA isolated from N9266, but not in the control reaction (fig. 3-12). This result confirmed the mapped T-DNA insertion site of N9266 between the two genes At1g79110 and At1g79120.

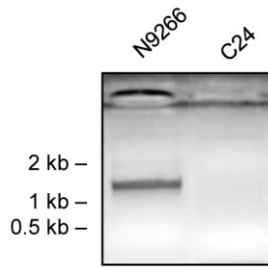


Figure 3-12. TAE gel electrophoresis of PCR amplicon, confirming the T-DNA insertion site of N9266. The 1566-bp product was amplified with DNA from N9266 but not in a control reaction with DNA of C24. TAE gel, 1.2 % (w/v) agarose.

3.3.3 *In silico* analysis to predict *cis*-acting elements

The PlantCARE database (Rombauts *et al.*, 1999) and the PLACE database (Higo *et al.*, 1999) of plant *cis*-acting regulatory DNA elements were used to investigate the genomic region upstream of the mapped T-DNA insertion site in N9266 and downstream of At1g79110 CDS. A region of about 1.1 kb was analyzed to identify putative *cis*-regulatory elements. Several motifs involved in light responsiveness were predicted, even though the analyzed sequence was not part of a promoter (tab. 3-2).

Table 3-2. Light responsive motifs identified in about 1.1 kb upstream of the mapped T-DNA insertion site of ET N9266 as predicted by PlantCARE and PLACE databases.

Motif	Sequence ^a	Position ^b	Description
I-Box	CTCTTATGCT (-)	-1014 to -1005	Part of a light responsive element of <i>Nicotiana glauca</i>
I-Box	GATAAGATA (-)	-806 to -798	Part of a light responsive element of <i>Glycine max</i>
G-Box	CACGTC (+)	-633 to -628	<i>cis</i> -acting regulatory element involved in light responsiveness of <i>Zea mays</i>
Box 4	ATTAAT (+)	-501 to -496 -495 to -490 -493 to -488 -414 to -409 -121 to -116	Part of conserved DNA module involved in light responsiveness in <i>Petroselinum crispum</i>
TCT	TCTTAC (+)	-381 to -376	Part of a light responsive element of <i>Arabidopsis thaliana</i>
I-Box	ATGATATGA (+)	-213 to -205	Part of a light responsive element of <i>Pisum sativum</i>
Box I	TTTCAAA (+)	-156 to -150	Light responsive element
3-AF1 binding site	AATAGATATTT (+)	-89 to -79	Light responsive element of <i>Solanum tuberosum</i>
GA	AAGGAAGA (+)	-28 to -21	Part of a light responsive element of <i>Glycine max</i>

^a (+) and (-) indicates the sense and complementary strand, respectively

^b positions are relative to the T-DNA insertion site in N9266

3.3.4 Southern blot analysis to determine the number of T-DNA insertions

Southern blot analysis was performed to determine the number of T-DNA insertion sites in N9266. Similar to ET N9249, also in the case of N9266 several DNA fragments were detected on the blot after hybridization with a *GAL4* probe (fig. 3-13).

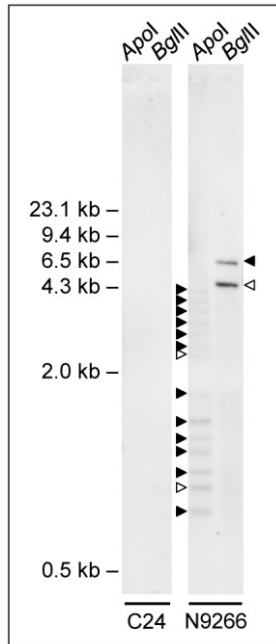


Figure 3-13. Molecular characterization of ET N9266 by Southern blot. Most of the DNA fragments could be explained due to the identified T-DNA localization on chromosome 1 (black triangles). Additional fragments (white triangles) were due to additional T-DNA insertion sites.

An *in silico* restriction analysis of the mapped T-DNA insertion site of N9266 was performed to assign the DNA fragments on the blot. Some fragments on the blot were explained by the identified T-DNA insertion site on chromosome 1 (fig. 3-13, black triangles), whereas additional fragments could not be assigned (white triangles).

The Southern blot analysis showed that two T-DNAs were inserted in the genome of N9266. As the localization of the second T-DNA insertion site by TAIL-PCR was impossible, ET N9266 was not further analyzed.

3.4 Enhancer trap line N9313

The ET line N9313 showed the most distinct connection between GFP fluorescence values and light intensity (fig. 3-1). The relative GFP fluorescence reached values of ≥ 0.4 , which were the highest detected in all ET lines analyzed. This indicated that the *GFP* of N9313 was under the control of a strong *cis*-acting enhancer element.

3.4.1 Localization of GFP fluorescence

Confocal microscopic studies were performed to analyze the spatial GFP expression pattern. The GFP in 10 d old phototrophically grown N9313 seedlings was ubiquitously expressed. It was located in epidermis and mesophyll cells of cotyledons and primary leaves (fig. 3-14 A and B, respectively) and also detectable in root cells. In the roots it accumulated in the tips of primary and secondary roots (fig. 3-14 C and D).

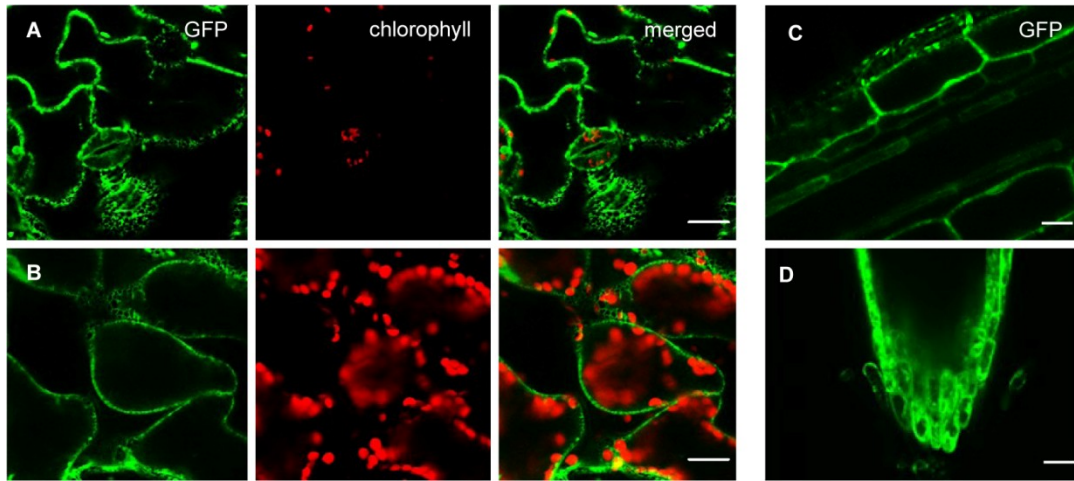


Figure 3-14. Spatial GFP expression in N9313 seedlings, analyzed by CLSM. A: Cotyledon, transverse confocal section of the adaxial epidermis B: Transverse confocal section of spongy mesophyll C: Longitudinal confocal section of primary root D: Longitudinal confocal section of root tip (bar = 20 μ m).

3.4.2 Identification of T-DNA insertion site by TAIL-PCR

To identify the ET T-DNA insertion site of N9313, TAIL-PCRs were performed. A 190-bp fragment specific for the used TR3.2 and AD2 primers in tertiary TAIL-PCR was amplified, which did not appear in the control reactions with only one primer (fig. 3-15).

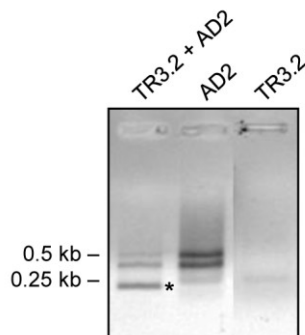


Figure 3-15. TAE agarose gel electrophoresis of tertiary TAIL-PCR products of N9313. The combination of both primers TR3.2 and AD2 amplified a 190-bp fragment (marked by asterisk), which was absent in the control reactions performed with only one of the primers. TAE gel, 1.2 % (w/v) agarose.

The TR3.2-AD2 product of interest, which did not appear in the control reactions performed with only one of the primers, was separated from the unspecific products by excision out of the gel and ligation with pJET1.2/blunt. The resulting recombinant plasmids were tested by PCR for the presence of the type I target with the TR3.2 and AD2 primers, and sequenced. The identification of the ET T-DNA insertion site was done by aligning the sequencing results with database entries (Arabidopsis accession Col-0 whole genome sequence) by BLASTN. The identification of the different components of the recombinant plasmid is depicted in figure 3-16.

```

----- pJET1.2/blunt -----|----- TR3.2 -----|-----
GGTGCTGTACGAGCTCGGATCCACTAGTAACGGCCGCCAGTGTGCTGGAATTCGCCCTTTCATTGTTGGATCCGGTTCTCTCCAAATGAAATGAAC

----- del35S (-45) -----|----- amplified genomic DNA fragment -----
TTCCTTATATAGAGGAAGGGTCTTGCGAAGATCCAGTGTGCTTGAGAGATTATATTATTAGATTCANNNNNNNAGTTTAAGTTATTAACATA
|||||
GCTTGAGAGATTACATTATTAATTCATTTTTTTGAGTTTAAGTTATTAACATA
----- chr5:8160945-8161040 -----

----- amplified genomic DNA fragment -----|----- AD2 -----|----- pJET1.2/blunt -----
TAAGTTTTACCCTACTGCTTGAATACTTTTGGGAAACATGTTTCATCTCACTCGACC AAGGGCGAATTCCTGCAGATATCCATCACACTGGCGGGCCG
|||||
TAGGTTTTACCCTACTGCTTGAATACTTTTGGGAAACATG
----- chr5:8160945-8161040 -----

```

Figure 3-16. Attribution of components of the type I tertiary TAIL-PCR product of N9313. The amplified genomic DNA fragment included a 95-bp sequence that corresponded to a sequence of chromosome 5 of *Arabidopsis thaliana* Col-0 (highlighted in red). The pJET1.2/blunt vector backbone is depicted in italic, the primer sequences are underlined.

The pJET1.2/blunt sequence adjacent to the cloning site, both TAIL-PCR primers and the truncated 35S promoter of the ET T-DNA were identified. A 95-bp fragment of genomic DNA was amplified in TAIL-PCR with N9313 and matched a region on chromosome 5. The T-DNA of N9313 was inserted between the two genes At5g24130 and At5g24120, respectively (fig. 3-17), between nucleotide positions 8160944 and 8160945. The T-DNA was inserted in the same orientation than At5g24120, which encodes sigma factor 5 (*SIG5*). *SIG5* is a subunit of plastid RNA polymerases whose transcription has previously shown to be light inducible (Tsunoyama *et al.*, 2002; Mochizuki *et al.*, 2004; Onda *et al.*, 2008).

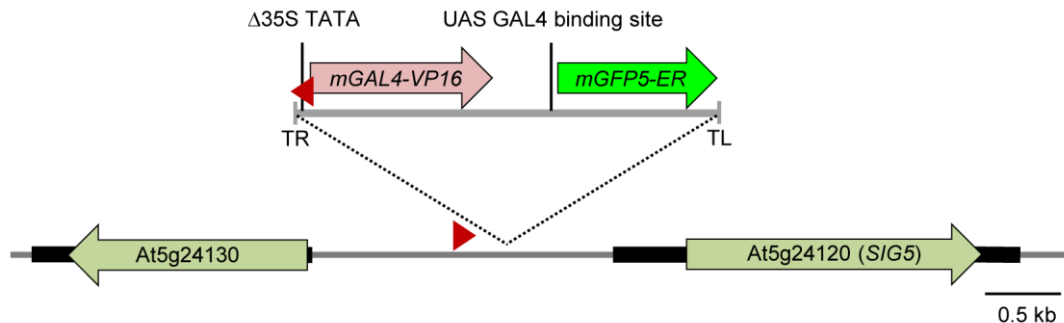


Figure 3-17. Diagram of the identified ET T-DNA insertion site in N9313. The ET T-DNA was inserted in an intergenic region between ORFs of At5g24130 and *SIG5*. Arrows indicate CDSs, black bars indicate 5' and 3' UTRs. TR and TL label the borders of the ET T-DNA. TAIL-PCR primer binding sites are depicted as red triangles.

The identified T-DNA insertion site was confirmed by PCR using the primer TR3.2 in combination with a primer designed to anneal to the genomic DNA flanking the T-DNA insertion site (primer sequences: appendix 6.2, table A2). The expected 879-bp PCR product was amplified with DNA isolated from N9313, but not in the control reaction (fig. 3-18). This result confirmed the mapped T-DNA insertion site of N9313 between the two genes At5g24130 and *SIG5*.

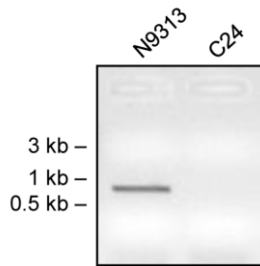


Figure 3-18. TAE gel electrophoresis of PCR amplicon, confirming the T-DNA insertion site of N9313. The 879-bp product was amplified with DNA from N9313 but not in a control reaction with DNA of C24. TAE gel, 1.2 % (w/v) agarose.

3.4.3 Southern blot analysis to determine the number of T-DNA insertions

For further analysis of N9313 plants with homozygous T-DNA insertion were used. These plants were identified by PCR using primers that anneal to both sides of the T-DNA insertion. In contrast to wild-type plants, ET plants with homozygous T-DNA insertions failed in amplification of the 2-kb PCR products due to the 5.5-kb ET T-DNA insertion. Seeds of these plants were used in all further experiments described.

Southern blot analysis was performed to determine the number of T-DNA insertion sites in N9313. After cleavage of DNA from N9313 with *Bgl*III, a single 1.7-kb DNA fragment was hybridized with the DIG-labeled *GAL4* probe, whereas cleavage with *Apo*I produced five different fragments (fig. 3-19 A).

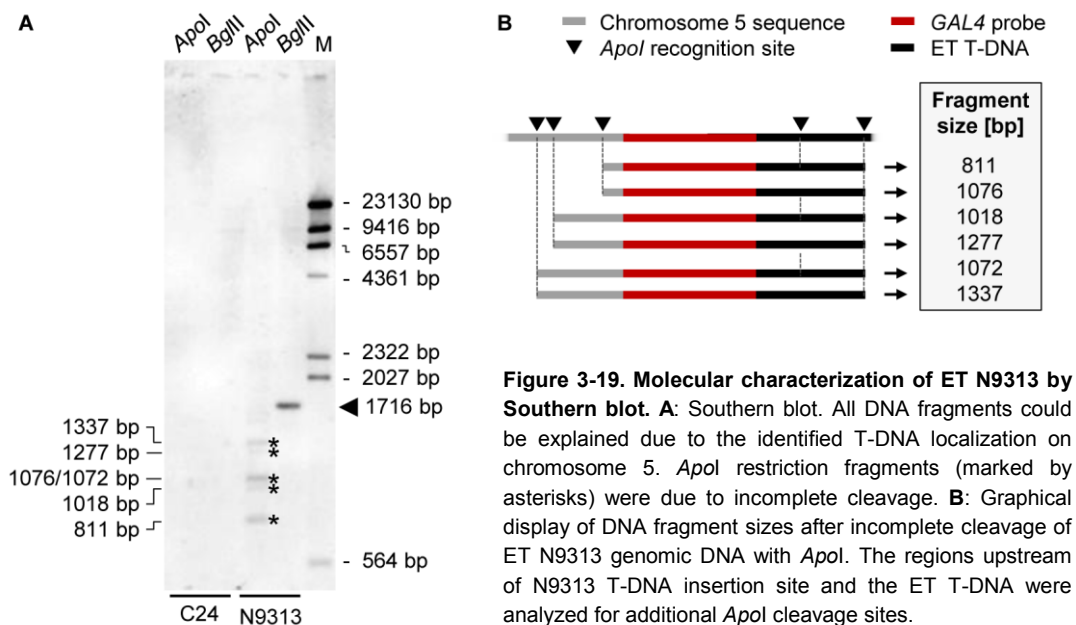


Figure 3-19. Molecular characterization of ET N9313 by Southern blot. A: Southern blot. All DNA fragments could be explained due to the identified T-DNA localization on chromosome 5. *Apo*I restriction fragments (marked by asterisks) were due to incomplete cleavage. **B:** Graphical display of DNA fragment sizes after incomplete cleavage of ET N9313 genomic DNA with *Apo*I. The regions upstream of N9313 T-DNA insertion site and the ET T-DNA were analyzed for additional *Apo*I cleavage sites.

An *in silico* restriction analysis of the region adjacent to the ET T-DNA insertion on chromosome 5 was performed. The online tool NEBcutter V2.0 (<http://tools.neb.com/NEBcutter2/index.php>; Vincze *et al.*, 2003) was used to analyze the cleavage fragments on the Southern blot. The analysis showed that all fragments on the blot were explained by the

identified T-DNA insertion site. With regard to the T-DNA insertion site, the five fragments of the *ApoI* restriction can be explained by incomplete restriction due to the limited restriction time (fig. 3-19 B). A single ET T-DNA insertion was responsible for the GFP expression in N9313, being located in the promoter of *SIG5*. ET line N9313 was analyzed in more detail. The single T-DNA insertion site permitted the localization of the *cis*-acting DNA motifs in the *SIG5* promoter region that mediated the observed light-sensitive GFP expression in N9313 seedlings (fig. 3-1).

3.4.4 *SIG5* and *GFP* expression in skotomorphogenic seedlings

The *SIG5* transcript abundances in rosette leaves of 4 weeks old Arabidopsis plants correlate with light intensity during growth (Tsunoyama *et al.*, 2002). In the present study, N9313 seedlings showed a correlation between the intensity of GFP fluorescence and the intensity of light during growth (fig. 3-1). It was analyzed whether the transcription of *GFP* and *SIG5* in Arabidopsis seedlings did solely depend on illumination, or if there was a basal light-independent expression. Therefore the mRNA abundances of 10 d old, dark grown etiolated seedlings were determined by qRT-PCR. The transcript level of seedlings illuminated with $120 \mu\text{mol photons m}^{-2} \text{s}^{-1}$ continuous white light served as reference. *SIG5* transcripts of etiolated wild-type seedlings were only detectable in trace amounts (fig. 3-20 A). *SIG5* as well as *GFP* transcript levels of N9313 were below the limit of determination (fig. 3-20 B and C, respectively).

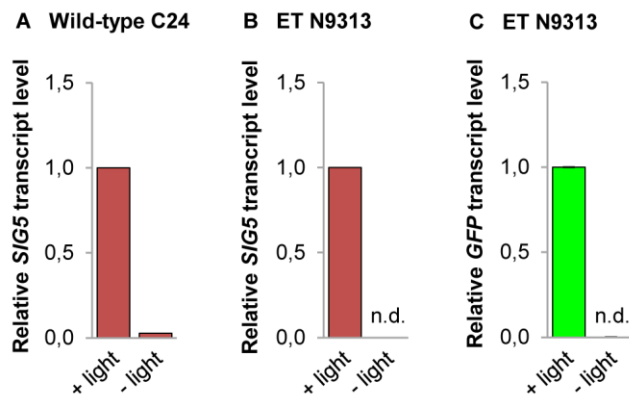


Figure 3-20. Relative *SIG5* transcript level in etiolated C24 wild-type (A) and *SIG5* and *GFP* transcript levels in N9313 (B and C). The seedlings were grown on MS medium supplemented with 0.5 % (w/v) sucrose at 22 °C either illuminated with $120 \mu\text{mol photons m}^{-2} \text{s}^{-1}$ continuous white light or in darkness. Relative transcript levels were determined by qRT-PCR relative to *ACT2* transcript level. The transcript levels of illuminated seedlings were set to 1.0.

The *GFP* reporter gene, inserted in the promoter of *SIG5*, was not transcribed in dark-grown seedlings. These results, in addition to the positive correlation of GFP fluorescence and light intensity during seedling development, demonstrated that the *GFP* expression in N9313 is light induced. Moreover, these results indicated that the light-responsive GFP fluorescence was regulated at the level of transcription.

Similarly to *GFP*, *SIG5* transcript accumulation in N9313 depended on illumination. It was assumed, that light-sensitive *cis*-acting elements are located upstream of both genes in N9313. The *GFP* was inserted about 1.2 kb upstream of the *SIG5* translational start site (fig. 3-17). Therefore multiple light-sensitive promoter elements regulated *SIG5* transcription,

some of which were located in distal promoter regions of more than 1.2 kb distance and some of which were located in more proximal regions.

3.4.5 The influence of light quality on transcription

It was shown that *GFP* of N9313, inserted in the promoter of *SIG5*, as well as *SIG5* were transcribed in a light-dependent manner (fig. 3-20). *SIG5* transcripts have previously been shown to accumulate with increasing white light intensity (Tsunoyama *et al.*, 2002). In more detail, monochromatic blue light extensively induces the *SIG5* transcript abundance in rosette leaves of 4 weeks old *Arabidopsis* plants. In contrast, red light not induces *SIG5* transcription (Tsunoyama *et al.*, 2002; Mochizuki *et al.*, 2004; Onda *et al.*, 2008). As the *GFP* of N9313 was regulated in a light-dependent manner (fig. 3-1, fig. 3-20), it was analyzed whether the specific blue light induction of transcription was mediated by distal *SIG5* promoter regions, upstream of the T-DNA insertion site of N9313. In the following the terms “distal and proximal *SIG5* promoter” designate the nucleotides upstream and downstream of position -1198 relative to the *SIG5* CDS, which determined the N9313 T-DNA insertion site.

3.4.5.1 Modulation of GFP fluorescence by light quality

To modulate the light quality, white light was filtered with light-transmissive plexiglass. N9313 seedlings were germinated and grown under blue light illumination (peaks at 470 nm; appendix 6.3, fig. A1 A) or red/far-red light illumination ($\lambda > 600$ nm; appendix 6.3, fig. A1 B) at an intensity of $10 \mu\text{mol photons m}^{-2} \text{s}^{-1}$. $10 \mu\text{mol photons m}^{-2} \text{s}^{-1}$ white light served as reference. The GFP fluorescence of 10 d old seedlings was quantified using a top reader fluorometer. The GFP fluorescence of N9313 reached significantly higher levels upon red/far-red light illumination than upon blue light illumination (fig. 3-21).

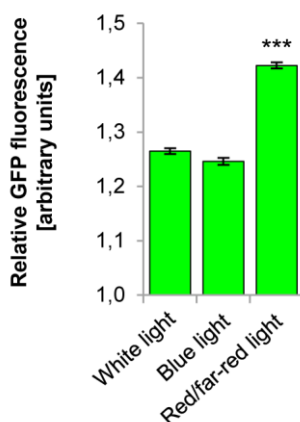


Figure 3-21. GFP fluorescence in N9313 upon monochromatic light treatment. Red/far-red light increased GFP fluorescence level compared to white or blue light. The seedlings were grown on MS medium supplemented with 0.5 % (w/v) sucrose for 10 d under short day conditions. They were illuminated with $10 \mu\text{mol photons m}^{-2} \text{s}^{-1}$ white light or blue light or red/far-red light. The GFP fluorescence was detected using a top reader fluorometer. Bars represent means (\pm SEM). $n = 69-92$ seedlings. *** indicates significant differences from the white light reference samples (Student *t*-test, $p < 0.001$).

These results indicated that the well-known blue light induction of *SIG5* transcription (Tsunoyama *et al.*, 2002; Mochizuki *et al.*, 2004; Onda *et al.*, 2008) was mediated by promoter elements located downstream of the T-DNA insertion site of N9313. However, the

red/far-red light illumination induced a significant increase of GFP fluorescence intensities compared with white light grown seedlings. Previously, the group of Yoshinori Toyoshima analyzed *SIG5* transcript levels of rosette leaves and did not find an accumulation of *SIG5* transcripts upon red light illumination (Tsunoyama *et al.*, 2002, Mochizuki *et al.*, 2004; Onda *et al.*, 2008). Consequently the red/far-red light mediated induction of GFP fluorescence of N9313 was extensively investigated to elucidate the reasons for these unexpected results.

3.4.5.2 Modulation of *GFP* transcription by monochromatic light

It was analyzed whether the observed red/far-red light induction of GFP fluorescence did reflect the *GFP* transcript level. The seedlings were grown for 10 d on MS plates supplemented with 0.5 % (w/v) sucrose under short day conditions at $120 \mu\text{mol photons m}^{-2} \text{s}^{-1}$ white light. Consistent with the experimental design by Tsunoyama *et al.* (2002) and Mochizuki *et al.* (2004), the white light grown seedlings were dark-adapted for 24 h to decrease the start expression level of *SIG5*. The dark adapted seedlings were treated with monochromatic blue light (471 nm), monochromatic red light (673 nm) or monochromatic far-red light (745 nm) for 24 h. The subsequent quantification of transcript abundances by qRT-PCR demonstrated that *GFP* transcript levels of N9313 were induced by blue light, by red light and by far-red light (fig. 3-22). In contrast to previously published data that did not find red light sensitivity of *SIG5* transcription (Tsunoyama *et al.*, 2002; Mochizuki *et al.*, 2004; Onda *et al.*, 2008), 14-fold accumulation of *GFP* mRNA was observed after red light illumination. Blue light and far-red light induced *GFP* mRNA levels less than 5-fold.

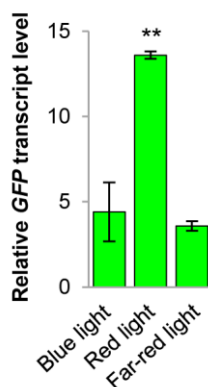


Figure 3-22. Relative *GFP* transcript level in ET N9313 in response to monochromatic light. 10 d old seedlings of N9313 grown under short day conditions on MS medium supplemented with 0.5 % (w/v) sucrose at $120 \mu\text{mol photons m}^{-2} \text{s}^{-1}$ white light were dark adapted for 24 h and then exposed to $100\text{-}120 \mu\text{mol photons m}^{-2} \text{s}^{-1}$ monochromatic blue, red or far-red light for 24 h. Relative *GFP* transcript levels were determined by qRT-PCR relative to *ACT2* transcript level. Relative *GFP* transcript level of dark adapted seedlings prior to the transfer to monochromatic light was set to 1.0. The data were means of 2 biological replicates (\pm SEM). ** indicates significant differences from the dark adapted samples (Student *t*-test, $p < 0.01$).

The observed red light induced accumulation of *GFP* transcript level indicated a novel mechanism of *SIG5* regulation in Arabidopsis: red light-sensitive *cis*-acting elements, located in distal promoter regions, regulated *SIG5* transcription during seedling development.

3.4.5.3 Modulation of *SIG5* transcription by monochromatic light

To investigate whether the *GFP* transcript levels of N9313 (fig. 3-22) reflected *SIG5* transcript levels upon monochromatic light treatment, *SIG5* transcript abundances in N9313 and in wild-type C24 were determined. The treatment with monochromatic light was done in parallel to the preliminarily described experimental conditions (3.4.5.2). In accordance with previously published results (Tsunoyama *et al.*, 2002; Mochizuki *et al.*, 2004; Onda *et al.*, 2008), *SIG5* transcripts in both, C24 and N9313, accumulated upon blue light illumination, 70-fold and 260-fold, respectively (fig. 3-23). Additionally the *SIG5* transcripts accumulated 25-fold/ 90-fold upon red light treatment and 6-fold/15-fold upon far-red light treatment.

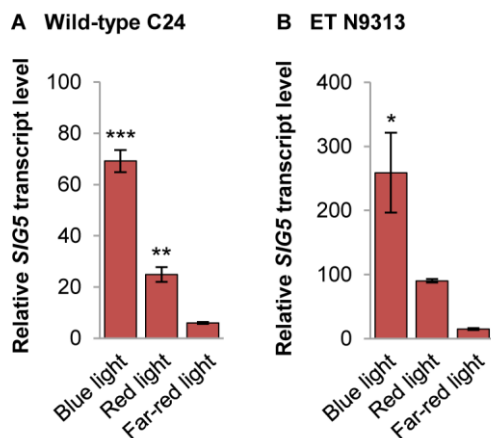


Figure 3-23. Relative *SIG5* transcript level in C24 wild-type and ET N9313 in response to monochromatic light. 10 d old seedlings grown under short day conditions on MS medium supplemented with 0.5 % (w/v) sucrose at 120 $\mu\text{mol photons m}^{-2} \text{s}^{-1}$ white light were dark adapted for 24 h and then exposed to 100-120 $\mu\text{mol photons m}^{-2} \text{s}^{-1}$ monochromatic blue, red or far-red light for 24 h. Relative *SIG5* transcript levels were determined by qRT-PCR relative to *ACT2* transcript level. *SIG5* transcript level of dark adapted seedlings prior to the transfer to monochromatic light was set to 1.0. The data are means of 2 biological replicates (\pm SEM). * indicates significant differences from the dark adapted samples. (Student *t*-test, * $p < 0.05$, ** $p < 0.01$, *** $p < 0.001$)

SIG5 transcripts of both C24 and N9313 accumulated upon blue light illumination and to a minor extent upon red light and far-red light illumination. In contrast to this, strong accumulation of *GFP* mRNA of N9313 was observed after monochromatic red light illumination (fig. 3-22). Therefore the blue light-sensitive promoter elements seemed to be located downstream of the T-DNA insertion site of N9313 in the proximal *SIG5* promoter.

The red light-induced accumulation of *SIG5* transcripts in the wild-type confirmed the hypothesis of red light-sensitive *cis*-acting elements, located in the distal *SIG5* promoter. *SIG5* transcription of N9313 was regulated by a truncated 1.2 kb promoter and also stimulated by red light illumination. It was concluded that multiple red light sensitive *cis*-acting elements were located in the proximal as well as in the distal *SIG5* promoter.

3.4.5.4 *SIG5* and *GFP* mRNA decay profile

For subsequent quantitative comparison of *SIG5* transcript level with *GFP* transcript level, the mRNA decay rates were determined. Arabidopsis seedlings were grown on solidified MS medium supplemented with 0.5 % (w/v) sucrose at 22 °C and 100 $\mu\text{mol photons m}^{-2} \text{s}^{-1}$ continuous white light for 10 d. The seedlings were harvested and incubated with the transcriptional inhibitor Actinomycin D (Act D) in liquid MS medium and with MS medium lacking Act D as control. Act D binds DNA at the transcription initiation complex and

prevents elongation by RNA polymerase (Sobell, 1985). *SIG5* and *GFP* transcript levels were determined over time relative to *ACT2* transcript level.

mRNA generally obeys first-order kinetics (Ross, 1995; Gutierrez *et al.*, 2002); therefore an exponential regression model ($A = 1 e^{-kt}$) was applied, allowing k_{decay} to be calculated for each transcript. The mRNA half-life was then calculated using the following equation:

$$t_{1/2} = \ln(2) / k_{\text{decay}}$$

The relative stability of *SIG5* mRNA in Act D treated plants was reduced compared to MS treated control plants that showed stable *SIG5* transcript level over the 20 h analyzed (fig. 3-24 A). In contrast to *SIG5*, the *GFP* transcripts remain more stable after Act D treatment (fig. 3-24 B). The calculated relative half-life of *GFP* transcripts was about 5-times the *SIG5* mRNA half-life.

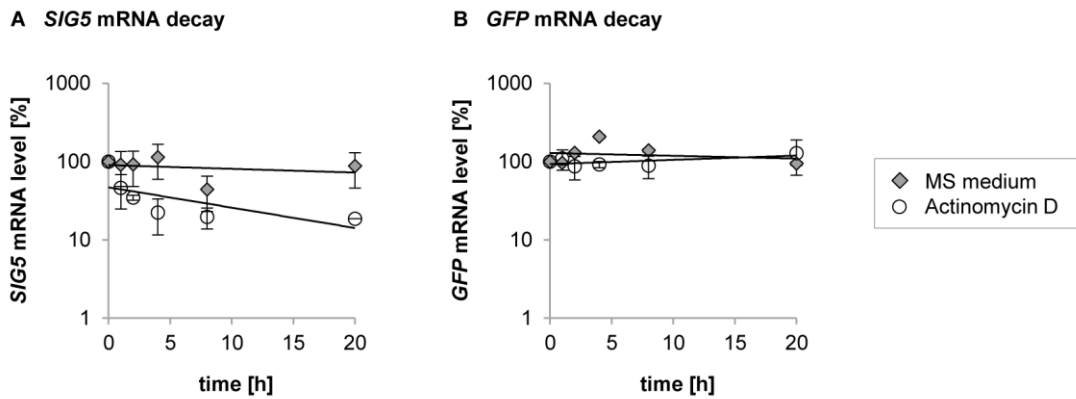


Figure 3-24. Stability of *SIG5* and *GFP* transcripts in N9313. 10 d old seedlings were treated with 200 μM Act D in liquid MS medium or with MS medium as a control. Seedlings were grown in continuous light ($100 \mu\text{mol photons m}^{-2} \text{s}^{-1}$). Samples were taken 0, 1, 2, 4, 8 and 20 h after the start of the treatment. The amounts of *SIG5* (A) and *GFP* (B) transcripts were detected by qRT-PCR with *ACT2* as internal control. Normalization of transcript level values of Act D treated samples were modified as outlined in the methods. Data are means of two replicates (\pm SEM).

The enhanced stability of *GFP* mRNA led to considerable elevated transcript levels upon induction of transcription, compared to *SIG5* transcript levels. In addition, reductions of transcription initiation rates appeared as delayed when comparing *GFP* transcript levels with *SIG5* transcript levels.

3.4.6 Light responses of seedlings compared with adult plants

Within the framework of this thesis it has been shown that *SIG5* transcripts as well as *GFP* transcripts of N9313 seedlings accumulated during a 24 h illumination period with monochromatic red light (fig. 3-22, 3-23). Previously the group of Yoshinori Toyoshima analyzed *SIG5* transcript levels of rosette leaves of 4 weeks old Arabidopsis plants (accession Col-0). The authors were not able to detect an accumulation of transcripts upon red light illumination (Tsunoyama *et al.*, 2002, Mochizuki *et al.*, 2004; Onda *et al.*, 2008).

To further characterize the red light induction of *SIG5* transcription observed in the framework of this thesis, the experimental procedures were modified and adapted to the conditions analyzed by Yoshinori Toyoshima.

3.4.6.1 *SIG5* and *GFP* transcripts upon 24 h illumination of adult N9313 plants

According to Tsunoyama *et al.* (2002), Mochizuki *et al.* (2004) and Onda *et al.* (2008) seedlings were germinated and grown on soil for 4 weeks at 22 °C under continuous white light ($20 \mu\text{mol photons m}^{-2} \text{s}^{-1}$). The plants were dark adapted for 24 h (according to Mochizuki *et al.* (2004) and Onda *et al.* (2008); Tsunoyama *et al.* (2002) applied 16 h darkness) and transferred to $50 \mu\text{mol photons m}^{-2} \text{s}^{-1}$ monochromatic red light or monochromatic blue light. As the seedlings accumulated transcripts upon 24 h illumination, the adult plants were also treated with red light for 24 h. The seedlings were harvested and mRNA levels of rosette leaves were determined by qRT-PCR. Accumulation of *SIG5* transcripts upon blue light illumination (about 60-fold) as well as upon red light illumination (about 40-fold) were detected (fig. 3-25 A). In parallel, *GFP* transcript levels were quantified and they were significantly induced upon both light treatments, 12-fold and 19-fold, respectively (fig. 3-25 B).

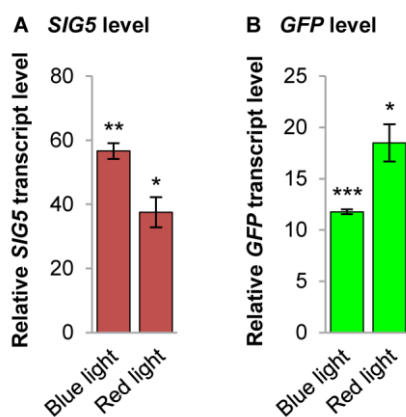


Figure 3-25. Relative transcript levels in 4 weeks old N9313 plants. N9313 was grown on soil under continuous white light ($20 \mu\text{mol photons m}^{-2} \text{s}^{-1}$) for 4 weeks at 22 °C. The plants were dark adapted for 24 h and subsequently exposed to $50 \mu\text{mol photons m}^{-2} \text{s}^{-1}$ monochromatic blue light or monochromatic red light at 22 °C for 24 h. Rosette leaves harvested from two or three independent plants were used per RNA isolation. Relative *SIG5* (A) and *GFP* (B) transcript levels were determined by qRT-PCR relative to *ACT2* transcript level. Relative transcript level of dark adapted seedlings prior to the transfer to monochromatic light was set to 1.0. The data are means of 2 biological replicates (\pm SEM). * indicates significant inductions compared to the dark adapted samples. (Student *t*-test, * $p < 0.05$, ** $p < 0.01$, *** $p < 0.001$)

These result demonstrated that the red light induction of *SIG5* transcription was not limited to cotyledons or seedlings. According to the previous results obtained with 10 d old seedlings (fig. 3-22, 3-23) also in rosette leaves the *SIG5* transcription was more blue light sensitive than red light sensitive, whereas the *GFP* transcription was more red light sensitive

than blue light sensitive. In this study, the *SIG5* promoter analyzed in both 10 d old seedlings and 4 weeks old plants, induced transcription upon 24 h treatment with monochromatic red light.

3.4.6.2 *SIG5* and *GFP* transcripts upon 3 h illumination period

Tsunoyama *et al.* (2002), Mochizuki *et al.* (2004) and Onda *et al.* (2008) analyzed the *SIG5* transcript levels after 1.5 h to 5 h red light illumination. Possibly the observed accumulation of transcripts upon 24 h illumination (fig. 3-25) happened so slow or initiated so late, that transcript amounts were undetectable after a red light illumination period limited to a few hours. To test this hypothesis, the prior experiment was repeated with harvesting the leaves for mRNA isolation after 3 h of red light illumination. As a result, the transcript levels of both, *SIG5* and *GFP*, were significantly induced after this 3 h treatment, 26-fold and 6-fold, respectively (fig. 3-26).

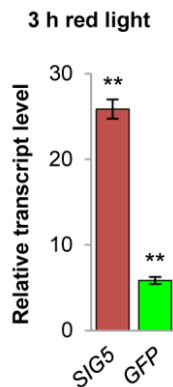


Figure 3-26. Relative transcript levels in 4 weeks old N9313 plants upon 3 h red light illumination. N9313 was grown on soil for 4 weeks at 22 °C, illuminated with continuous white light of 20 $\mu\text{mol photons m}^{-2} \text{s}^{-1}$. The plants were dark adapted for 36 h and subsequently exposed to 50 $\mu\text{mol photons m}^{-2} \text{s}^{-1}$ monochromatic red light at 22 °C for 3 h. Rosette leaves harvested from two or three independent plants were used per RNA isolation. Relative transcript levels were determined by qRT-PCR relative to *ACT2* transcript level. Relative transcript level of dark adapted seedlings prior to the transfer to monochromatic light was set to 1.0. The data are means of 2 biological replicates (\pm SEM). ** indicates significant inductions compared to the dark adapted samples. (Student *t*-test, $p < 0.01$)

These results demonstrated that the red light induction of *SIG5* transcription in adult *Arabidopsis* plants was a relatively rapid response, detectable by qRT-PCR after a 3 h time period of illumination. It was not possible to fathom the reason for the differences in the red light response of *Arabidopsis* between the analyses made in the framework of this thesis and the data previously published by Yoshinori Toyoshima.

3.4.7 Characterization of blue light sensitive *SIG5* promoter elements

The observed blue light mediated induction of *SIG5* transcript abundance (fig. 3-23) confirmed previously published data (Tsunoyama *et al.*, 2002; Mochizuki *et al.*, 2004; Onda *et al.*, 2008). The regulation of *SIG5* transcription was further analyzed, to characterize the blue light sensitive *cis*-acting elements in the *SIG5* promoter.

3.4.7.1 Blue light response analyses by promoter-reporter gene fusions

Promoter-reporter gene fusions were used to confirm the previous assumption, that blue light sensitive promoter elements were located in the proximal *SIG5* promoter that mediated blue light specific induction of transcription (3.4.5.3). Three different *SIG5* promoter fragments from Arabidopsis accession C24 were analyzed for light sensitive *cis*-acting elements: (i) 2 kb upstream of the translation start of *SIG5*, including the 483-bp 5' UTR, designated as p*SIG5*_{2kb}. This 2 kb fragment was divided into two parts: (ii) the region upstream of the ET T-DNA insertion in N9313, about 0.8 kb, designated as p*SIG5*_{distal}, and (iii) the region downstream of the T-DNA insertion site, about 1.2 kb, designated as p*SIG5*_{proximal} (fig. 3-27). The p*SIG5*_{proximal} sequence has previously been shown to induce *SIG5* transcript accumulation upon blue light illumination in N9313 (fig. 3-23 B) in a wild-type like manner (fig. 3-23 A), indicating the localization of blue light-sensitive *cis*-acting elements in this 1.2 kb promoter region.

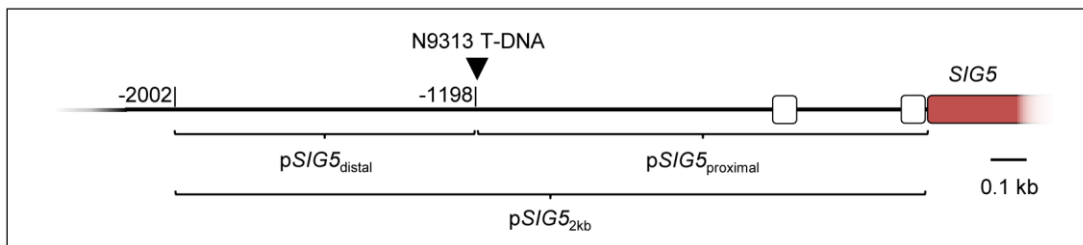


Figure 3-27. Diagram of three different *SIG5* promoter fragments, used for promoter-reporter gene analyses. The different fragments were fused to Δ 35S promoter and *GFP-GUS* reporter genes. The T-DNA insertion site in ET N9313 at position -1198 relative to translation start (marked by arrowhead) depicts the division of the larger 2 kb fragment into a distal (-2002 to -1198) and a proximal (-1197 to -1) one (the UTR is depicted as white boxes, *SIG5* CDS as grey box).

The promoter fragments were fused to the truncated (-48) 35S promoter from cauliflower mosaic virus (CAMV) that drives *GAL4-GFP* expression in the ET lines, and to the *GFP-GUS* reporter genes. The reporter genes were transiently expressed in *Nicotiana benthamiana* leaves. As a control for transfection and reporter gene expression, the reporter gene fused to the full 35S promoter was used. In parallel the truncated (-48) 35S CAMV promoter was tested to monitor autoactivation of the reporter gene.

Blue light sensitivity mediated by the proximal or the distal *SIG5* promoter

It was tested whether the 2 kb *SIG5* promoter mediated reporter gene expression in a light-dependent manner. Therefore the p*SIG5*_{2kb} construct of interest and the control constructs were introduced into the same leaf to exclude variations of expression due to developmental differences or position effects during incubation of the infiltrated leaves. The same volumes of *Agrobacterium* solutions with the same titer were introduced into the leaf lamina. Half of the leaf surface was darkened with aluminum foil immediately after infiltration. As a result, the 2 kb *SIG5* promoter induced GFP fluorescence in a light-dependent manner (fig. 3-28 A).

The 35S control constructs stimulated GFP expression on both sides of the leaf, whereas the p*SIG5*_{2kb} fragment was not able to induce GFP expression to detectable levels in darkness. The truncated 35S promoter served as control and demonstrated that the observed light-sensitive initiation of transcription was not mediated by the Δ 35S promoter.

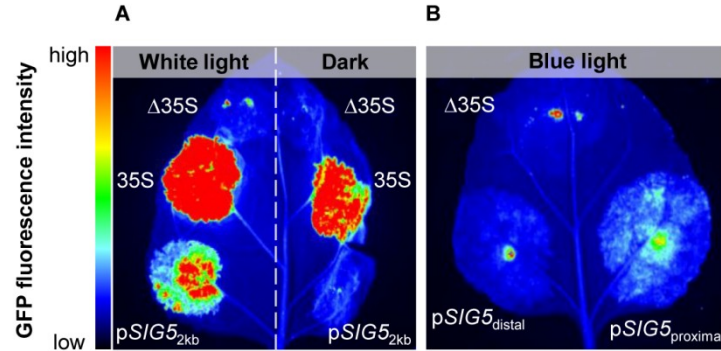


Figure 3-28. 2 kb *SIG5* promoter mediated light response in tobacco and the proximal *SIG5* promoter was blue light sensitive. Arabidopsis *SIG5* promoter fragments were fused to Δ 35S promoter and GFP. The GFP was transiently expressed in tobacco leaves. Δ 35S and full 35S promoters fused to GFP served as controls. The GFP fluorescence was observed under UV illumination. False color code depicts fluorescence intensity. **A:** The leaves were incubated 4 d at 100-120 $\mu\text{mol photons m}^{-2} \text{s}^{-1}$ with continuous white light. Half of the leaf surface was darkened. The experiment was repeated once, the picture is representative. **B:** After infiltration the leaves were incubated 4 d at 100-120 $\mu\text{mol photons m}^{-2} \text{s}^{-1}$ with continuous monochromatic blue light.

It was further analyzed which part of the 2 kb *SIG5* promoter mediated the blue light induction of transcription (fig. 3-23). Therefore the 2 kb promoter fragment was divided into two parts, a proximal one and a distal one (for definition see fig. 3-27). These two fragments were analyzed for their ability to induce reporter gene expression upon blue light illumination in tobacco. The proximal 1.2 kb fragment of the *SIG5* promoter induced GFP expression, in contrast to the distal 0.8 kb promoter fragment (fig. 3-28 B). The p*SIG5*_{proximal} sequence has previously been shown to induce *SIG5* transcript accumulation upon blue light illumination in N9313 seedlings (fig. 3-23 B). It was assumed that blue light-sensitive *cis*-acting elements are located within the proximal 1.2 kb *SIG5* promoter region.

3.4.7.2 Blue light responsiveness of SALK lines with truncated *SIG5* promoters

The 1.2 kb sequence upstream of the *SIG5* translation start site included promoter motifs that mediated a blue light induction of transcription in tobacco (fig. 3-28 B). To narrow down the localization of the blue light sensitive elements of the *SIG5* promoter, as a first approach *Arabidopsis thaliana* T-DNA insertion lines were analyzed. Five different T-DNA insertion lines of the SALK-collection (Alonso *et al.*, 2003) were selected. Their T-DNA was disrupting the *SIG5* promoter, but not the *SIG5* CDS. SALK_015625 carried a T-DNA insertion at position -1618 relative to the translation start site, SALK_077048 at position -1032, SALK_072457 at position -887, SALK_019261 at position -691 and SALK_133729 at position -515 (fig. 3-29).

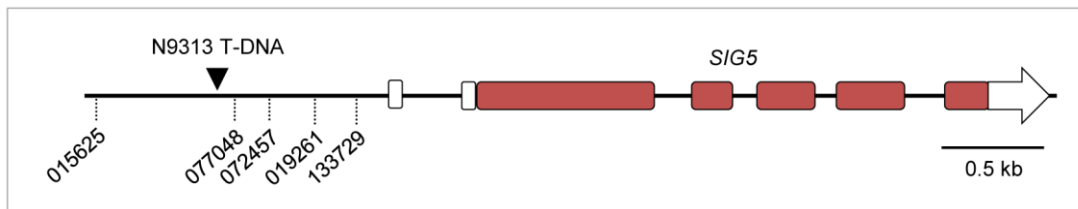


Figure 3-29. Diagram of the localization of T-DNA insertions in the promoter of *SIG5*. The numbers indicate the names of the respective SALK line. The ET T-DNA insertion site of N9313 is marked by arrowhead. *SIG5* exons are depicted as grey boxes, the UTRs as white boxes.

Prior to analyses, the T-DNA insertion genotype of the plants was analyzed by PCR. Genomic DNA was tested with primers binding upstream and downstream of the respective T-DNA insertion site. Subsequently, one of these primers was combined with the primer LBB1.3, annealing with the left border of the SALK T-DNA. For all five lines analyzed, the T-DNA insertion sites in the *SIG5* promoter were confirmed in the PCR with the LBB1.3 primer. Homozygous plants were identified by the absence of the PCR product obtained with the two gene specific primers that comprise the T-DNA insertion site. Seeds originating from plants with homozygous T-DNA insertions were used for further analyses.

10 d old white light grown seedlings of the SALK-lines were dark-adapted for 24 h to decrease the start expression level of *SIG5* and subsequently treated with monochromatic blue light for 24 h. Transcript levels were determined by qRT-PCR (fig. 3-30). In the SALK population the T-DNA construct has been introduced into Arabidopsis accession Columbia, so Col-0 plants were used as wild-type reference. The *SIG5* transcript abundances corresponded to wild-type level in the three lines with T-DNA insertions at positions -1618, -1032 and -887 relative to translation start of *SIG5*, resulting in an about 40-fold induction of *SIG5* mRNA levels. In contrast, seedlings with T-DNA insertions at positions -691 and -515 were impaired in their blue light response of *SIG5* transcription.

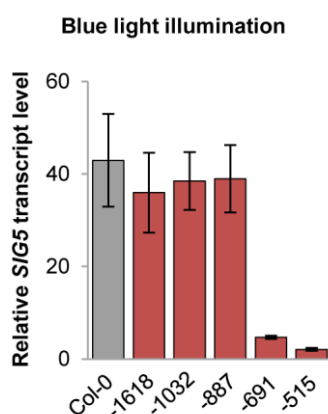


Figure 3-30. Relative *SIG5* transcript level in Col-0 wild-type and SALK T-DNA insertion lines in response to monochromatic blue light. The numbers give the distances of the T-DNA insertions relative to the *SIG5* translation start site. 10 d old seedlings grown under short day conditions on MS medium supplemented with 0.5 % (w/v) sucrose at $120 \mu\text{mol photons m}^{-2} \text{s}^{-1}$ white light were dark adapted for 24 h and then exposed to monochromatic blue light for 24 h. Relative *SIG5* transcript levels were determined by qRT-PCR relative to *ACT2* transcript level. Values were normalized to *SIG5* transcript level of 24 h dark-adapted seedlings. The data are means of 2-3 biological replicates (\pm SEM). * indicates significant differences (Student *t*-test, $p < 0.05$).

These results demonstrated that blue light sensitive *cis*-acting elements were located in a 196-bp region of the *SIG5* promoter: the blue light sensitivity was located between the positions -887 and -691 relative to the translation start site of *SIG5*.

3.4.7.3 *In silico* analysis of 196 bp mediating the blue light induction of *SIG5* transcription

The blue light sensitivity of the *Arabidopsis* *SIG5* promoter was narrowed down to a 196-bp region (fig. 3-30). The PlantCARE (Rombauts *et al.*, 1999) and the PLACE (Higo *et al.*, 1999) databases of plant *cis*-acting regulatory DNA elements were used to analyze this 196-bp region for the presence of common light-responsive *cis*-acting elements. Two GATA motifs, an ACE motif, a GA motif and an I-box were identified as light sensitive elements in this region (tab. 3-3).

Table 3-3. Light responsive motifs identified in the 196-bp blue light sensitive promoter region of *SIG5* as predicted by PlantCARE and PLACE databases.

Motif	Sequence ^a	Position ^b	Description
GATA motifs	GATA (-)	-871 to -868	Light regulated element
	GATA (+)	-841 to -838	
ACE motif	AAAACGTTTA (+)	-733 to -764	<i>cis</i> -acting element involved in light responsiveness
GA motif	AAGGAAGA (+)	-715 to -708	Part of a light responsive element
I-box	CACTTATGCT (+)	-742 to -733	Part of a light responsive element

^a (+) and (-) indicates the sense and complementary strand, respectively

^b positions are relative to the translation start site of *SIG5*

The identification of different light-responsive motifs in the 196-bp blue light sensitive *SIG5* promoter region indicated, that one or more of these elements mediated the observed blue light sensitivity of the *Arabidopsis thaliana* *SIG5* promoter.

3.4.8 Characterization of red and far-red light induction of *SIG5* transcription

GFP transcripts of ET N9313 have been shown to accumulate upon illumination with monochromatic red light (fig. 3-22). The same was observed for the *SIG5* promoter downstream of the T-DNA insertion site. The 1.2 kb sequence, controlling the *SIG5* transcription in N9313, mediated a red light specific accumulation of *SIG5* transcripts (fig. 3-23 B). It was assumed that multiple red light responsive *cis*-acting elements were located in the proximal as well as in the distal *SIG5* promoter. The red light response of *SIG5* transcription was analyzed in more detail.

3.4.8.1 Analyses of light sensitivity mediated by the distal 0.8 kb *SIG5* promoter sequence

The red light-mediated induction of *GFP* transcription in N9313 (fig. 3-22) demonstrated that light sensitive motifs are located upstream of the T-DNA insertion site. The 0.8 kb region upstream of the T-DNA insertion site failed in mediating blue light-induced transcription in tobacco (fig. 3-28 B). It was analyzed, whether the distal 0.8 kb region in general included light sensitive *cis*-acting motifs. As previously described, the promoter fragment was fused to a Δ 35S promoter and a *GFP-GUS* reporter gene.

Transient expression analysis in tobacco

The pSIG5_{distal} construct was transiently expressed in *Nicotiana benthamiana*. After infiltration the leaves were incubated for 6 d under illumination with continuous white light. When comparing different infiltrated leaves in this study, all GFP analyses were done with the shutter set to 10 ms and the same intensity of the detector, as indicated. The distal SIG5 promoter region was able to induce GFP expression (fig. 3-31). This demonstrated that light-sensitive *cis*-acting elements were located within the distal 0.8 kb SIG5 promoter sequence.

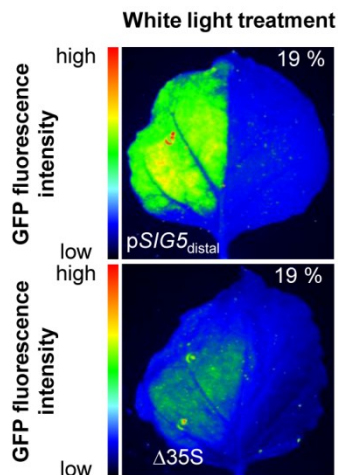


Figure 3-31. White light induced GFP expression, mediated by distal 0.8 kb SIG5 promoter region in tobacco. Distal 0.8 kb of Arabidopsis SIG5 promoter was fused to Δ 35S minimal promoter and GFP. The GFP was transiently expressed in tobacco leaves. Only the left side of the leaves was infiltrated. Δ 35S promoter fused to GFP served as control. The leaves were incubated 6 d at 100-120 $\mu\text{mol photons m}^{-2} \text{s}^{-1}$ continuous white light. The GFP fluorescence was observed under UV illumination with percentage representing the sensitivity of the detector. False color code depicts fluorescence intensity.

Analysis in Arabidopsis

It was analyzed whether the induction of transcription, mediated by the distal 0.8 kb SIG5 promoter fragment (fig. 3-31) correlated with the light intensity. *Arabidopsis thaliana* accession C24 was transformed with the pSIG5_{distal} construct. The transformation was done by *Agrobacterium tumefaciens* mediated floral dip method according to Clough and Bent (1998). Seedlings of the segregating T₂ generation of six independent lines were illuminated with light intensities of 10 or 200 $\mu\text{mol photons m}^{-2} \text{s}^{-1}$ white light for 10 d. As the reporter used in this study was a GFP::GUS fusion protein, GUS expression was analyzed to quantify the reporter gene activity. The GUS expression was quantified spectrophotometrically using PNPG as substrate, which was converted to the chromogenic PNP when cleaved by GUS. The GUS expression was determined from Δ A₄₀₅ as nmol PNP min⁻¹. Since Chl and protein contents of the seedlings were affected by light, the GUS expression was normalized as nmol PNP min⁻¹ per g fresh weight of the seedlings. In the six independent lines analyzed, the PNP amount per fresh weight was 2.3-fold higher in seedlings grown at 200 $\mu\text{mol photons m}^{-2} \text{s}^{-1}$ compared to the PNP values from seedlings grown at 10 $\mu\text{mol photons m}^{-2} \text{s}^{-1}$ (fig. 3-32).

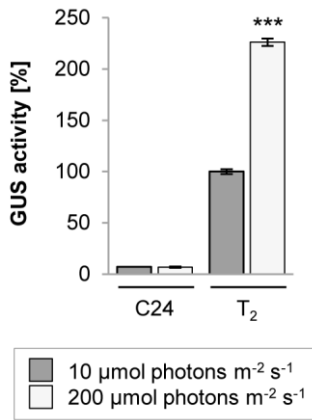


Figure 3-32. Light-dependent reporter gene expression, mediated by distal 0.8 kb *SIG5* promoter in transgenic *Arabidopsis* seedlings. *Arabidopsis* plants of the C24 accession were transformed with distal 0.8 kb *SIG5* promoter fragment fused to $\Delta 35\text{S}$ promoter and GUS. Seedlings of segregating T₂ generation of six independent lines were grown on MS medium supplemented with 0.5 % (w/v) sucrose for 10 d at 10 or 200 $\mu\text{mol photons m}^{-2} \text{s}^{-1}$ white light. 20-25 seedlings per line were pooled for colorimetric GUS quantification. GUS activity was determined as $\text{nmol PNP min}^{-1} \text{g}^{-1} \text{FW}$. 2-5 measurements were done per line. Results are mean values of the six lines (\pm SEM). Value of T₂ plants grown at 10 $\mu\text{mol photons m}^{-2} \text{s}^{-1}$ were defined as 100 % GUS activity. *** indicates significant differences from the respective value obtained at 10 $\mu\text{mol photons m}^{-2} \text{s}^{-1}$ light intensity (Student *t*-test, $p < 0.001$).

The distal 0.8 kb *SIG5* promoter region regulated transcription in a light sensitive manner. This result confirmed the results of the promoter-reporter gene analyses performed in tobacco (fig. 3-31). It demonstrated that light sensitive *cis*-acting elements were located in this distal *SIG5* promoter sequence.

3.4.8.2 Localization of red light sensitivity in distal and proximal *SIG5* promoter regions

It was assumed that multiple red light responsive *cis*-acting elements were located in the proximal as well as in the distal *SIG5* promoter (for definition see fig. 3-29). To analyze, in which region of the 2 kb promoter the red light sensitive elements were located, the distal 0.8 kb promoter region, which has previously been shown to include light sensitive elements (fig. 3-32), and the proximal 1.2 kb promoter region were analyzed for their ability to induce transcription upon red light illumination. After infiltration, the tobacco leaf was exposed to monochromatic red light for 4 d. Both, the distal as well as the proximal *SIG5* promoter fragments, induced GFP expression (fig. 3-33). This confirmed the previous hypothesis, that red light sensitive *cis*-acting promoter motifs were located in the proximal 1.2 kb region as well as in the distal 0.8 kb region of the *SIG5* promoter.

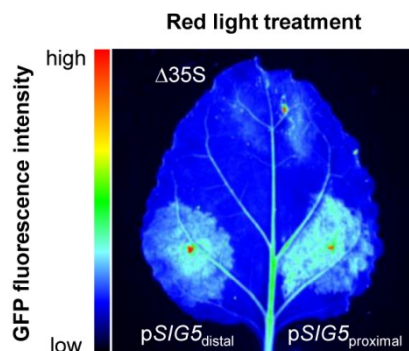


Figure 3-33. Red light induced GFP expression mediated by proximal and distal *SIG5* promoter regions in tobacco. Both *Arabidopsis SIG5* promoter fragments were fused to $\Delta 35\text{S}$ promoter and GFP. The GFP was transiently expressed in tobacco leaves. $\Delta 35\text{S}$ promoter fused to GFP served as control. The leaves were incubated 4 d at 100-120 $\mu\text{mol photons m}^{-2} \text{s}^{-1}$ with continuous monochromatic red light. The GFP fluorescence was observed under UV illumination. False color code depicts fluorescence intensity. The experiment was repeated once, the picture is representative.

3.4.8.3 Induction of transcription by fragments of the distal *SIG5* promoter

To further characterize the distal *SIG5* promoter, the 0.8 kb fragment was divided into smaller fragments that were analyzed separately (fig. 3-34).

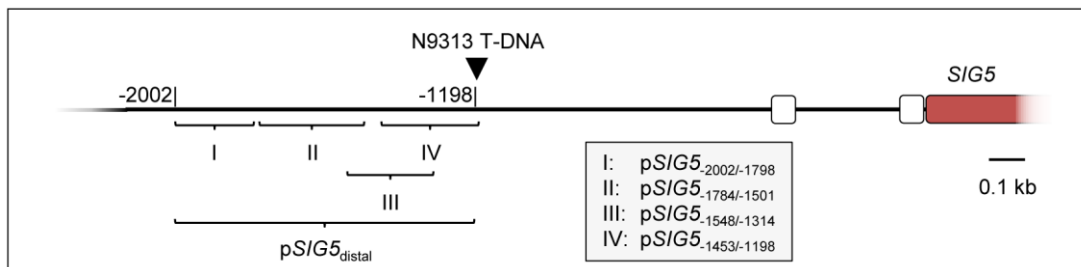


Figure 3-34. Map of different distal *SIG5* promoter fragments used in promoter reporter gene analysis. The T-DNA insertion site in ET N9313 at position -1198 relative to translation start of *SIG5* (marked by arrowhead) depicted the border of the distal promoter fragment (*pSIG5_{distal}*), which ranges up to -2002 relative to translation start. This 0.8 kb fragment was further divided into four smaller overlapping fragments. The different fragments were analyzed in promoter reporter gene studies. The 5' UTR is depicted as white boxes, the *SIG5* CDS as grey box.

The different promoter fragments were fused to a (-48) Δ 35S promoter and a *GFP-GUS* reporter gene. The fragments were tested for their ability to induce transient reporter gene expression upon monochromatic red light treatment in tobacco. As it was shown that blue light has only little effect on the distal *SIG5* promoter (fig. 3-28 B), the experiment was done in parallel with blue light illumination as a control. All tested distal *SIG5* promoter fragments induced reporter gene expression upon red light treatment (fig. 3-35 A). This experiment demonstrated that multiple red light sensitive *cis*-acting elements were located within the distal 0.8 kb *SIG5* promoter.

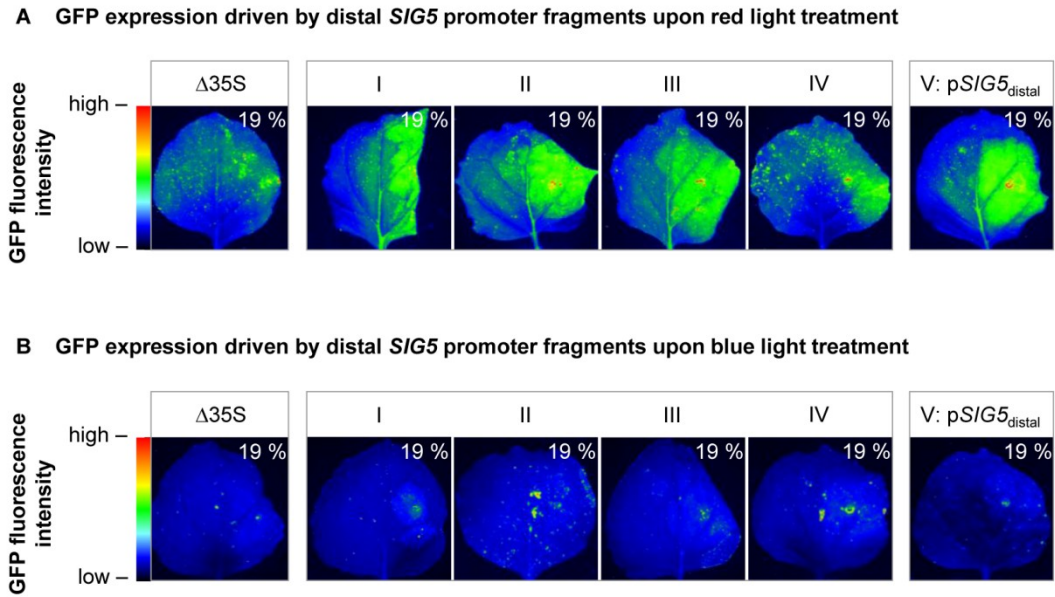


Figure 3-35. Red and blue light induced GFP expression mediated by distal *SIG5* promoter fragments in tobacco. The *SIG5* promoter fragments were fused to $\Delta 35S$ promoter and GFP. The GFP was transiently expressed in tobacco leaves. Only the right side of the leaves was infiltrated. $\Delta 35S$ promoter fused to GFP served as control. The leaves were incubated 2 d at $100\text{-}120 \mu\text{mol photons m}^{-2} \text{s}^{-1}$ under continuous white light, 24 h dark adapted and then treated with $100\text{-}120 \mu\text{mol photons m}^{-2} \text{s}^{-1}$ continuous red light (**A**) or blue light (**B**) for 48 h. The GFP fluorescence was observed under UV illumination with percentage representing the sensitivity of the detector. False color code depicts fluorescence intensity. The experiment was repeated once, the pictures are representative.

3.4.8.4 Red and far-red light responsiveness of SALK lines with truncated *SIG5* promoters

To further characterize the red light responsive *SIG5* transcription, *Arabidopsis thaliana* T-DNA lines were used. As previously described, in these lines SALK T-DNAs were inserted at different positions in the *SIG5* promoter (fig. 3-29). It was analyzed whether the different truncations of the *SIG5* promoter, due to the different SALK T-DNA insertions, affected the red light induction of *SIG5* transcription. Monochromatic far-red light has also been shown to induce an accumulation of *SIG5* transcripts (fig. 3-23). It was analyzed whether this far-red light response was affected by the different SALK T-DNA insertions.

The seedlings were grown at $120 \mu\text{mol photons m}^{-2} \text{s}^{-1}$ white light for 10 d. Subsequently the seedlings were dark-adapted for 24 h to decrease the start expression level of *SIG5*. The dark adapted seedlings were treated with monochromatic red light or monochromatic far-red for 24 h and the transcript levels were determined by qRT-PCR. As a result, the red light- and the far-red light-mediated accumulations of *SIG5* transcript levels were influenced by the reduction of the *SIG5* promoter length (fig. 3-36).

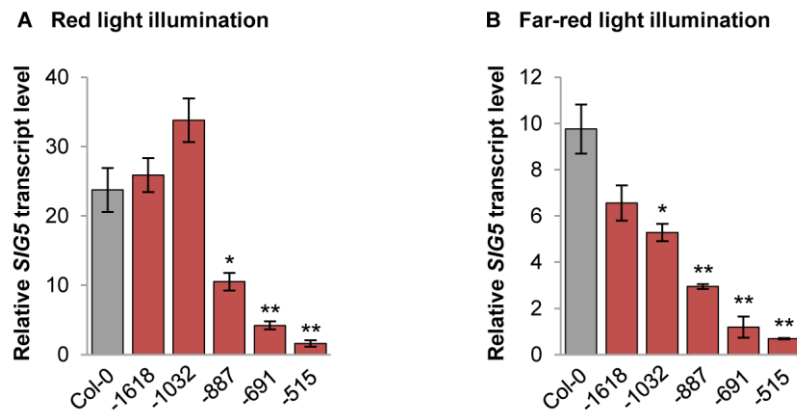


Figure 3-36. Relative *SIG5* transcript levels in Col-0 wild-type and SALK T-DNA insertion lines in response to monochromatic red (A) and far-red (B) light. The numbers give the distances of the T-DNA insertions relative to the *SIG5* translation start site. 10 d old seedlings grown under short day conditions on MS medium supplemented with 0.5 % (w/v) sucrose at $120 \mu\text{mol photons m}^{-2} \text{s}^{-1}$ white light were dark adapted for 24 h and then exposed to monochromatic light for 24 h. Relative *SIG5* transcript levels were determined by qRT-PCR relative to *ACT2* transcript level. The values were normalized to *SIG5* transcript level of 24 h dark-adapted seedlings. The data are means of 2 (-515 data), 3 or 4 (Col-0 in far-red) biological replicates (\pm SEM). * indicates significant differences from the respective Col-0 reference value. (Student *t*-test, * $p < 0.05$, ** $p < 0.01$)

The truncation at position -1618 did not alter red light responsive *SIG5* transcript level, whereas the mRNA level increased due to the T-DNA insertion at position -1032 (fig. 3-36 A). Further reduction of the *SIG5* promoter length resulted in gradually reduced transcript amounts. This data demonstrated that a region up to position -1618 relative to the translation start of *SIG5* included the promoter elements necessary for the red light-induction of *SIG5* transcription. Additionally, regulatory promoter elements that repress transcription upon red light illumination are located between position -1618 and position -1032. The gradually diminished transcript level of *SIG5* with gradual reduction of the promoter length demonstrated, that the red light sensitivity of *SIG5* transcription was mediated by multiple *cis*-acting elements with additive function. Additional red light responsive elements have been shown to be located in distal regions of the *SIG5* promoter, ranging from -2002 to -1198 (fig. 3-33, fig. 3-35 A). In summary these results demonstrated that the observed red light-induction of *SIG5* transcription was mediated by multiple *cis*-acting promoter elements, which were located in the proximal as well as in the distal *SIG5* promoter.

In contrast to the red light response, the far-red light mediated accumulation of *SIG5* transcription was diminished by T-DNA insertion at position -1618 (fig. 3-36 B). This indicated that some regulatory DNA elements were located upstream of this position. The step-by-step truncation of the *SIG5* promoters due to the different T-DNA insertions gradually reduced the far-red light mediated induction of transcription. These results showed that the far-red light sensitivity of the *SIG5* promoter was mediated by multiple *cis*-acting elements with additive function.

3.4.8.5 *In silico* analysis of the distal 0.8 kb *SIG5* promoter

Multiple regions of the distal 0.8 kb *SIG5* promoter fragment have been shown to regulate red light responsive transcription (fig. 3-35 A). These results indicated the localization of multiple light responsive *cis*-acting elements in this fragment. The PlantCARE (Rombauts *et al.*, 1999) and the PLACE (Higo *et al.*, 1999) databases of plant *cis*-acting regulatory DNA elements were used to analyze the 0.8 kb sequence for the presence of common light-responsive *cis*-acting elements. In total 15 different light sensitive motifs were identified in this region (tab. 3-4). The identification of different light-responsive motifs in the 0.8 kb promoter sequence indicated, that some of these elements mediated the red light sensitivity of the distal *SIG5* promoter.

Table 3-4. Light responsive motifs identified in 0.8 kb upstream of the mapped T-DNA insertion site of N9313 as predicted by PlantCARE and PLACE databases.

Motif	Sequence ^a	Position ^b	Description
ACE	ACGTGGA (-)	-1802 to -1796	<i>cis</i> -acting element involved in light responsiveness in <i>Petroselinum hortense</i>
ACE	CTAACGTATT (-)	-1452 to -1443	<i>cis</i> -acting element involved in light responsiveness in <i>Petroselinum crispum</i>
AT1	ATTAATTTTAAA (+)	-1434 to -1423	Part of a light responsive module in <i>Solanum tuberosum</i>
ATCT	AATGTAATCT (+)	-1470 to -1461 -1215 to -1206	Part of conserved DNA module involved in light responsiveness in <i>Arabidopsis thaliana</i>
Box 4	ATTAAT (+)	-1434 to -1429	Part of conserved DNA module involved in light responsiveness in <i>Petroselinum crispum</i>
Box I	TTTCAAA (+) TTTCAAA (-)	-1908 to -1902 -1758 to -1752	Light responsive element in <i>Pisum sativum</i>
CATT	GCATTTC (+)	-1693 to -1688	Part of a light responsive element in <i>Zea mays</i>
GC-Box	CACGTC (+)	-1725 to -1720	<i>cis</i> -acting regulatory element involved in light responsiveness in <i>Pisum sativum</i> and <i>Zea mays</i>
G-Box	CACGTGG (-)	-1800 to -1795	<i>cis</i> -acting regulatory element involved in light responsiveness in <i>Brassica napus</i>
GAG	GGAGATG (-)	-1706 to -1700	Part of a light responsive element in <i>Hordeum vulgare</i>
GATA	AAGATAAGATT (-)	-1598 to -1588	Part of a light responsive element in <i>Arabidopsis thaliana</i>
L-Box	AAATTAACCAAC (-)	-1438 to -1429	Part of a light responsive element in <i>Lycopersicon esculentum</i>
TCT	TCTTAC (+)	-1547 to -1452	Part of a light responsive element in <i>Arabidopsis thaliana</i>

^a(+) and (-) indicates the sense and complementary strand, respectively

^b positions are relative to the translation start site of *SIG5*

3.4.9 The role of photoreceptors regulating *SIG5* transcription

Previous studies have analyzed the role of blue light sensing photoreceptors in mediating the blue light induction of *SIG5* transcription. The blue light induction of *SIG5* is mediated by cryptochromes rather than by phototropins (Onda *et al.*, 2008). Both cry1 and cry2 function as photoreceptor for *SIG5* (Mochizuki *et al.*, 2004; Nagashima *et al.*, 2004b). Mutational analysis revealed that the blue light induction of *SIG5* transcripts is mediated by cry1 and cry2 at lower fluences (about 5 $\mu\text{mol photons m}^{-2} \text{s}^{-1}$), and predominantly by cry1 at higher fluence rates (50 $\mu\text{mol photons m}^{-2} \text{s}^{-1}$) (Onda *et al.*, 2008). These studies have been performed with rosette leaves of 4 weeks old adult *Arabidopsis* plants. Blue light sensing photoreceptors were analyzed for their role in regulating *SIG5* transcription in *Arabidopsis* seedlings.

The present study revealed that monochromatic red and far-red light regulated *SIG5* transcription as well. Therefore, in addition to blue light photoreceptors, different red and far-red light photoreceptors were investigated, too.

Single, double, and triple null combinations of *Arabidopsis* mutants lacking the photoreceptors *cry1*, *cry2*, *phyA*, *phyB*, *phot1* and *phot2*, and the heme oxygenase *HY1* were analyzed. ET line N9313 was crossed with the respective mutants to analyze their role in regulating the light-dependent transcription of *GFP* in N9313. Plants with homozygous mutations of the respective photoreceptors were identified by phenotype as outlined in the methods. The results from the phenotypic screens were confirmed by PCR. Plants with homozygous mutations as well as homozygous ET T-DNA insertions were used for the subsequent analyses. In parallel to the analyses of the crossings with N9313, the *SIG5* transcript levels upon monochromatic light treatment of the different photoreceptor mutants were determined.

3.4.9.1 UV-A/blue light photoreceptors: cryptochromes and phototropins

GFP fluorescence of N9313 in cryptochrome or phototropin mutant background

The *GFP* transcripts in N9313 accumulated upon monochromatic blue light illumination (fig. 3-22). It was analyzed, whether this blue light induction of gene expression was impaired in mutants lacking the UV-A/blue light photoreceptors *cry1*, *cry2*, *phot1* and *phot2*.

The *cry1* single mutant and the *cry1cry2* and *phot1phot2* double mutants were crossed with N9313. The GFP fluorescence of 10 d old white light grown seedlings with the respective mutant background was quantified and compared with GFP fluorescence levels of N9313 seedlings. The GFP fluorescence was determined relative to Chl *a* content of the seedlings. The GFP fluorescence of *phot1phot2* mutant plants corresponded to N9313 levels (fig. 3-37). *cry1* mutant plants showed GFP fluorescence values reduced to 79 %, compared with N9313. The GFP fluorescence of *cry1cry2* double mutant plants was significantly diminished to 7 % compared with N9313.

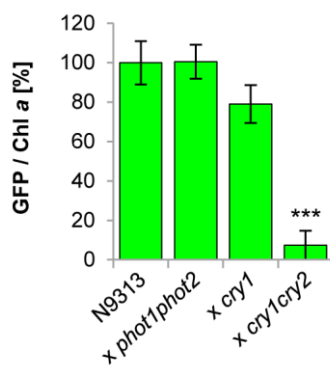


Figure 3-37. GFP fluorescence of N9313 and N9313 crossed with cryptochrome and phototropin mutants. Seedlings were grown on solidified MS medium supplemented with 0.5 % (w/v) sucrose for 10 d at $120 \mu\text{mol photons m}^{-2} \text{s}^{-1}$ under short day conditions. About 10 seedlings were pooled for each GFP extraction. The GFP fluorescence was determined relative to Chl *a* content. The GFP fluorescence was detected using a fluorometer; the fluorescence of wild-type C24 seedlings was subtracted. The chlorophylls were quantified spectrophotometrically. Relative GFP fluorescence of N9313 was set as 100 %. Results are mean values of 4 (N9313 x *phot1phot2*), 5 (N9313 x *cry1*) or 8 measurements (\pm SEM). *** indicates significant differences from the N9313 value (Student *t*-test, $p < 0.001$).

These results demonstrated that *phot1* and *phot2* were not involved in regulating GFP expression of N9313, according to the *SIG5* transcription of rosette leaves, which has been

shown to be not regulated by phototropins (Onda *et al.*, 2008). In contrast, both *cry1* and *cry2* seemed to be required for a GFP expression level corresponding to N9313. These data indicated a major role for *cry2* in regulating GFP fluorescence in N9313. Previously *cry2* has been shown to mediate the blue light induction of *SIG5* transcription together with *cry1* in rosette leaves only at low fluence rates (about 5 $\mu\text{mol photons m}^{-2} \text{s}^{-1}$) (Onda *et al.*, 2008). This indicated an altered effect of *cry2* on *SIG5* transcription in adult Arabidopsis plants compared to seedlings.

Role of phototropins and cryptochromes on *SIG5* regulation

The blue light induction of *SIG5* transcription was predominantly mediated by a region located downstream of the T-DNA insertion site of N9313 (fig. 3-30). Therefore, in addition to the GFP fluorescence of N9313, the *SIG5* transcript levels of photoreceptor mutants were analyzed. *phot1*, *phot1phot2*, *cry1* and *cry2* mutants had a Col-0 background; the *cry1cry2* double mutant was in *Ler* background. Therefore transcript levels were compared with the levels resulting from the respective mutant background. It was shown, that the induction of *SIG5* transcripts upon blue light illumination was not impaired in both phototropin mutants (fig. 3-38 A). The *cry2* mutation had also no effect on *SIG5* transcript levels, whereas the *SIG5* transcription of *cry1* and *cry1cry2* mutants was reduced in the blue light-response of transcription to 7-fold and 4-fold induction of mRNA levels, respectively, compared with an about 40-fold induction of the respective wild-types (fig. 3-38 B).

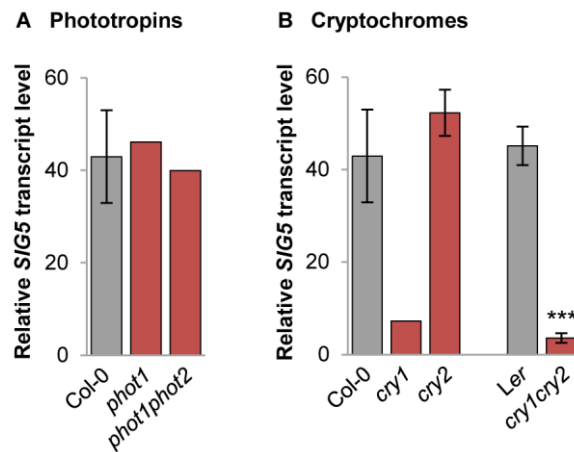


Figure 3-38. Relative *SIG5* transcript level in phototropin mutants (A) and cryptochrome mutants (B) in response to monochromatic blue light. 10 d old seedlings grown under short day conditions on MS medium supplemented with 0.5 % (w/v) sucrose at 120 $\mu\text{mol photons m}^{-2} \text{s}^{-1}$ white light were dark adapted for 24 h and then exposed to 100-120 $\mu\text{mol photons m}^{-2} \text{s}^{-1}$ monochromatic blue light for 24 h. *SIG5* transcript levels were determined by qRT-PCR relative to *ACT2* transcript level. Relative *SIG5* transcript level of dark adapted seedlings prior to transfer to monochromatic light was set to 1.0. The data are means of 1 (*phot1*, *phot1phot2*, *cry1*), 2 (Col-0, *cry2*), or 3 biological replicates (\pm SEM). *** indicates significant differences of the *cry1cry2* value from the *Ler* value (Student *t*-test, $p < 0.001$).

These data demonstrated that *cry1* was the major cryptochrome mediating the blue light induction of *SIG5* transcription in seedlings, when illuminated with high blue light fluences of about 100-120 $\mu\text{mol photons m}^{-2} \text{s}^{-1}$. This result was consistent with data resulted from the analysis of adult Arabidopsis plants (Onda *et al.*, 2008). Additionally, the GFP fluorescence of N9313 seemed to be predominantly regulated by *cry2* and not *cry1* (fig. 3-37). This indicated an effect of *cry2* on distal *SIG5* promoter regions, whereas the

major blue light photoreceptor of *SIG5* signaling, *cry1*, was regulating the proximal *SIG5* promoter and was only rarely influencing the distal promoter.

In contrast to cryptochromes, phototropins did not regulate the transcription of *SIG5* in *Arabidopsis thaliana* seedlings, confirming the results obtained from the analyses of rosette leaves (Onda *et al.*, 2008).

The role of cryptochromes in regulating the proximal and the distal *SIG5* promoter

To test the hypothesis that *cry1* was regulating the proximal *SIG5* promoter, relative *SIG5* transcript levels of N9313 x *cry1cry2* seedlings were determined upon blue light illumination, and compared with data obtained from *cry1cry2* mutants. The relative *GFP* transcript levels were determined to confirm the data obtained from GFP fluorescence analyses (fig. 3-37) which indicated that the distal *SIG5* promoter of *cry1cry2* double mutants was nearly blue light insensitive. The blue light accumulation of *SIG5* transcripts of N9313 x *cry1cry2* was severely impaired (23-fold induction compared with a 260-fold induction of N9313; fig. 3-39 B). The *GFP* transcript level of N9313 x *cry1cry2* was only slightly decreased to about 50 % compared with N9313 (fig. 3-39 A).

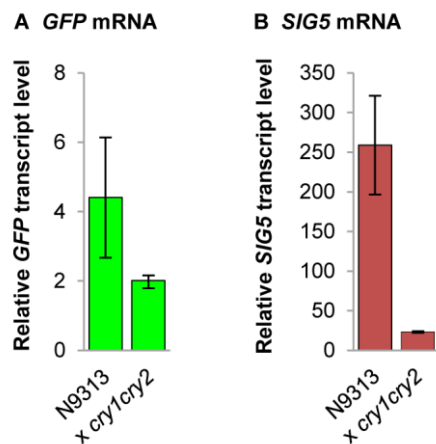


Figure 3-39. Relative transcript level in ET N9313 and N9313 x *cry1cry2* in response to blue light. 10 d old seedlings grown under short day conditions on MS medium supplemented with 0.5 % (w/v) sucrose at $120 \mu\text{mol photons m}^{-2} \text{s}^{-1}$ white light were dark adapted for 24 h and then exposed to $100\text{-}120 \mu\text{mol photons m}^{-2} \text{s}^{-1}$ monochromatic blue light for 24 h. Relative transcript levels were determined by qRT-PCR relative to *ACT2* transcript level. Relative transcript levels of dark adapted seedlings prior to transfer to monochromatic light were set to 1.0. The data are means of 2 biological replicates (\pm SEM). * indicates significant differences from the N9313 values (Student *t*-test, $p < 0.05$).

The *cry1cry2* mutation diminished the blue light induced accumulation of *SIG5* transcripts. The reduction of transcript amounts was similar in N9313 x *cry1cry2* (8 % compared to N9313) and in *cry1cry2* mutants (9 % compared to *Ler*, fig. 3-38 B). This demonstrated that the proximal 1.2 kb *SIG5* promoter, as present in N9313 x *cry1cry2*, responded in a *cry1/cry2*-dependent manner like the full-length promoter present in *cry1cry2* mutant seedlings. These data confirmed the hypothesis, that the proximal *SIG5* promoter included the *cry1*-regulated *cis*-acting elements that were predominantly mediating *SIG5* transcription upon illumination with high blue light intensities.

The *GFP* transcripts of N9313 in *cry1cry2* mutant background were still induced 2-fold upon blue light illumination. This indicated that *GFP* transcription in N9313 upon blue light illumination did not solely depend on *cry1* and *cry2*. However, the remaining blue light-induced accumulation of *GFP* transcripts had less physiological relevance, when the 5-

times slower decay rate of the *GFP* transcripts compared with the *SIG5* transcripts (3.4.5.4) was taken into account.

3.4.9.2 Red/far-red light photoreceptors: phytochromes

In contrast to previous studies, which did not show a red light sensitivity of the *SIG5* promoter (Tsunoyama *et al.*, 2002; Mochizuki *et al.*, 2004; Onda *et al.*, 2008), this study has demonstrated the existence of a red light-mediated induction of *SIG5* transcription in *Arabidopsis* (fig. 3-23, 3-36 A). Monochromatic far-red light has also been shown to induce *SIG5* transcription (fig. 3-23, 3-36 B). To further investigate the observed red and far-red light inductions of *SIG5* transcription, mutants of the red and far-red light sensitive phytochromes were analyzed.

The role of *phyA* and *phyB* on the distal *SIG5* promoter

To analyze the role of *phyA* and *phyB* in regulating the distal *SIG5* promoter, the *phyA* and *phyB* single mutants and the *phyAphyB* double mutant were crossed with N9313. In addition to the phytochrome mutants, the *hy1* mutant was analyzed. The *hy1* mutant was deficient in phytochrome chromophore biosynthesis (Muramoto *et al.*, 1999) and therefore lacked functional phytochromes. The GFP fluorescence of 10 d old white light grown seedlings with mutant background was quantified and compared with the GFP fluorescence levels of N9313.

The *phyB* mutation reduced the Chl content (Reed *et al.*, 1993). Similar to the Chl content, the total protein content in *phyB* mutants was reduced. Consequently, the GFP fluorescence was determined relative to the fresh weight of the seedlings. The relative GFP fluorescence in all mutants analyzed was reduced, ranging from 67 % and 66 % for the *phyA* and the *phyB* mutants, respectively, over 52 % for the *phyAphyB* double mutant, to 43 % for the *hy1* mutant, compared with N9313 (fig. 3-40).

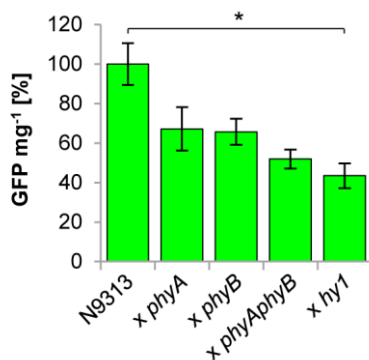


Figure 3-40. GFP fluorescence of N9313 and N9313 crossed with phytochrome and *hy1* mutants. Seedlings were grown on solidified MS medium supplemented with 0.5 % (w/v) sucrose for 10 d at $120 \mu\text{mol photons m}^{-2} \text{s}^{-1}$ under short day conditions. About 10 seedlings were pooled for each GFP extraction. The GFP fluorescence was determined relative to fresh weight of the seedlings. The GFP fluorescence was detected using a fluorometer; the fluorescence of wild-type C24 seedlings was subtracted. Relative GFP fluorescence of N9313 was set as 100 %. Results are mean values of 3 (N9313 x *phyAphyB* and x *hy1*), 5 (N9313) or 8 measurements (\pm SEM). One-way ANOVA was performed comparing all groups with Bonferroni's post-test. Statistical significance of difference is indicated as asterisks above bars (* $p < 0.05$).

The GFP fluorescence in *phyA* and *phyB* mutant background was impaired to similar levels of about 65 % relative to N9313. The double mutant showed further reduced GFP fluorescence values, similar to the *hy1* mutant. These results demonstrated that both *phyA* and *phyB* influenced the GFP expression in N9313. The data also indicated that other phytochromes than *phyA* and *phyB* were hardly involved.

The role of *phyA* and *phyB* upon monochromatic light treatment

To further investigate the light-dependent induction of *SIG5* transcription, phytochrome single and double mutants were analyzed with respect to their ability to induce *SIG5* transcription upon monochromatic light treatment. *phyA*, *phyB* and *phyAphyB* mutants, in parallel with their genetic background, the Arabidopsis accession *Ler*, were illuminated with monochromatic blue light, red light or far-red light. The relative *SIG5* transcript levels of the seedlings were determined by qRT-PCR. The blue light induction of *SIG5* transcription was impaired in *phyB* and *phyAphyB* mutants to an 11-fold and a 5-fold induction, respectively, compared with the 45-fold induction of the wild-type (fig. 3-41). Both mutants were also impaired in their responses to red light (3-fold and 5-fold, with 17-fold induction of the wild-type) as well as to far-red light (1.4-fold and 3.8-fold, with 11-fold induction of the wild-type). *phyA* mutant plants failed in accumulation of *SIG5* transcripts upon far-red light illumination (2-fold induction, with 11-fold induction in the wild-type).

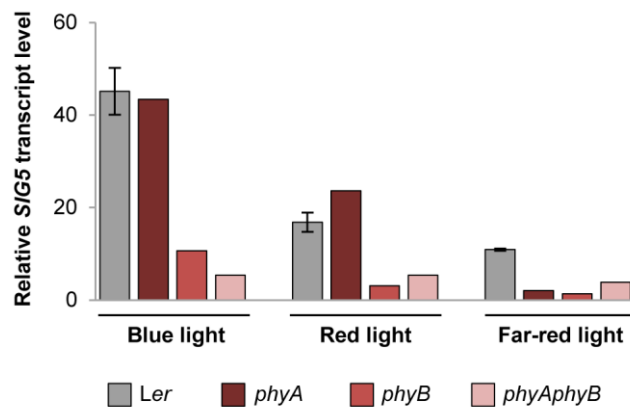


Figure 3-41. Relative *SIG5* transcript level in phytochrome mutants in response to monochromatic light. 10 d old seedlings grown under short day conditions on MS medium supplemented with 0.5 % (w/v) sucrose at 120 $\mu\text{mol photons m}^{-2} \text{s}^{-1}$ white light were dark adapted for 24 h and then exposed to 100-120 $\mu\text{mol photons m}^{-2} \text{s}^{-1}$ monochromatic blue light, red light or far-red light for 24 h. *SIG5* transcript levels were determined by qRT-PCR relative to *ACT2* transcript level. Relative *SIG5* transcript level of dark adapted seedlings prior to transfer to monochromatic light was set to 1.0. The *Ler* data are means of 3 biological replicates (\pm SEM).

These results demonstrated that the photoreceptor *phyA* was involved in the far-red light induction of *SIG5* transcription, whereas it did not mediate the blue light or red light induction of transcription. *phyB* mutants showed reduced *SIG5* transcript levels under all three light conditions analyzed, demonstrating a generally impaired *SIG5* transcription in *phyB* deficient seedlings.

3.4.9.3 The effect of combined phytochrome and cryptochrome knockout

In white light grown seedlings with *hy1* mutant background the GFP fluorescence was reduced to about 40 % of the level of N9313 (fig. 3-41). To test, whether this residual fluorescence level was due to the blue light sensing cryptochromes, N9313 was crossed with the triple knockout mutant *hy1cry1cry2*, which lacked all functional phytochromes as well as *cry1* and *cry2*. The GFP fluorescence of 10 d old white light grown seedlings was quantified and determined relative to the fresh weight of the seedlings as the Chl *a* content and the total protein content in the plants with mutant background were reduced (tab. 3-5).

Table 3-5. Chl *a* content and total protein content of N9313 and N9313 crossed with *hy1cry1cry2* mutant. About 10 seedlings were pooled for each measurement. Quantifications were done spectrophotometrically. Data are mean values (\pm SEM).

Sample	Chl <i>a</i> (mg g ⁻¹ FW)	n	Total protein content (mg g ⁻¹ FW)	n
N9313	0.39 \pm 0.02	4	0.63 \pm 0.04	8
N9313 x <i>hy1cry1cry2</i>	0.05 \pm 0.01	3	0.23 \pm 0.02	5

The relative GFP fluorescence values of the crossings were compared with the GFP fluorescence levels of N9313. As a result, the GFP fluorescence in *hy1cry1cry2* background was reduced to 33 % (fig. 3-42).

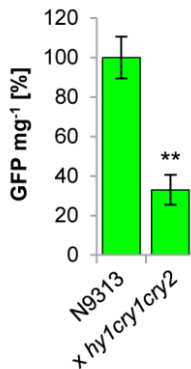


Figure 3-42. GFP fluorescence of N9313 and N9313 crossed with *hy1cry1cry2* mutant. Seedlings were grown on solidified MS medium supplemented with 0.5 % (w/v) sucrose for 10 d at 120 μ mol photons m⁻² s⁻¹ under short day conditions. About 10 seedlings were pooled for each GFP extraction. The GFP fluorescence was determined relative to fresh weight of the seedlings. The GFP fluorescence was detected using a fluorometer; the fluorescence of wild-type C24 seedlings was subtracted. Relative GFP fluorescence of N9313 was set as 100 %. Results are mean values of 3 (N9313) or 5 measurements (\pm SEM). ** indicates significant differences from the N9313 value (Student *t*-test, $p < 0.01$).

The residual GFP fluorescence in *hy1* mutant background of about 43 %, relative to N9313 (fig. 3-40), was reduced to 33 % in *hy1cry1cry2* mutant background. This indicated the involvement of additional regulatory pathways parallel to the photoreceptor mediated regulation of *SIG5* transcription in *Arabidopsis thaliana* seedlings.

3.4.10 The role of HY5 in regulating *SIG5* transcription

HY5 is a transcription factor that positively regulates photomorphogenic seedling development (Koornneef *et al.*, 1980; Oyama *et al.*, 1997). HY5 acts downstream of cryptochromes as well as downstream of phytochromes (Whitelam and Devlin, 1998; Osterlund *et al.*, 2000).

The light-dependent induction of *SIG5* transcription was regulated by cryptochromes as well as by phytochromes. It was analyzed whether HY5 was involved in mediating the light-dependent transcription of Arabidopsis *SIG5*. Two different HY5 deficient lines were analyzed in this study. In the mutant *hy5-1* the fourth codon (CAA = Q) was substituted for a stop codon (TAA) (fig. 3-43) (Oyama *et al.*, 1997). The second line analyzed was a SALK insertion mutant, with T-DNA insertion in the second intron of *HY5*.

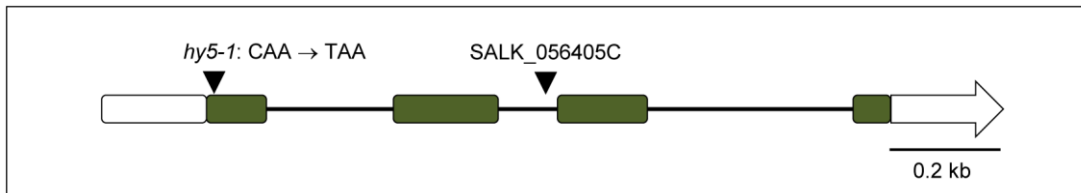


Figure 3-43. Diagram illustrating the localization of mutations and T-DNA insertions in the *HY5* gene. Exons are depicted as grey boxes, UTRs as white boxes. *hy5-1* mutation and SALK insertion site are depicted as arrowheads.

The available SALK_056405C seed stock was annotated as homozygous population (NASC, www.arabidopsis.info). To verify the homozygosity of the T-DNA insertion, *HY5* transcript level of SALK_056405C seedlings were compared with *HY5* transcript level of *hy5-1* seedlings by qRT-PCR analysis. 15 seedlings were pooled per RNA isolation. Δ Ct values were determined relative to *ACT2*. The homozygosity of the SALK T-DNA insertion was confirmed, as the resulting relative *HY5* transcript level of SALK_056405C seedlings was reduced to 0.02 % compared with *hy5-1* (tab. 3-6).

Table 3-6. Relative *HY5* transcript abundances in two different *hy5* mutants. Δ Ct values were determined by qRT-PCR relative to *ACT2* values. Seedlings were grown on MS medium supplemented with 0.5 % (w/v) sucrose at 120 μ mol photons $m^{-2} s^{-1}$ white light for 10 d.

Sample	Δ Ct value	Relative transcript values [%]
<i>hy5-1</i>	3.7	100
SALK_056405C	15.8	0.02

3.4.10.1 The role of HY5 in regulating the distal *SIG5* promoter

The HY5 deficient line SALK_056405C was crossed with N9313 to analyze the role of HY5 in regulating the light-dependent GFP expression driven by the distal *SIG5* promoter. Plants with homozygous ET T-DNA insertion and homozygous SALK T-DNA insertion were identified by PCR. For subsequent analysis, the GFP fluorescence intensity of 10 d old light grown seedlings was compared with the GFP fluorescence intensity of N9313 seedlings. The GFP fluorescence of N9313 in *hy5* background was not detectable any more (fig. 3-44).

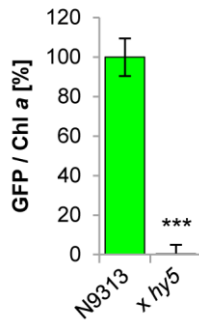


Figure 3-44. GFP fluorescence of N9313 in *hy5* background. Seedlings were grown on solidified MS medium supplemented with 0.5 % (w/v) sucrose for 10 d at 120 $\mu\text{mol photons m}^{-2} \text{s}^{-1}$ under short day conditions. About 10 seedlings were pooled for each GFP extraction. The GFP fluorescence was determined relative to Chl *a* content. The GFP fluorescence was detected using a fluorometer; the fluorescence of wild-type C24 seedlings was subtracted. The chlorophylls were quantified spectrophotometrically. Relative GFP fluorescence of N9313 was set as 100 %. The results are mean values of 4 (N9313 x *hy5*) or 8 measurements (\pm SEM). *** indicates significant differences from the N9313 value (Student *t*-test, $p < 0.001$).

The observed absence of GFP fluorescence demonstrated that unlike the photoreceptors HY5 is essential for the induction of transcription mediated by the distal *SIG5* promoter region.

3.4.10.2 The role of HY5 in regulating *SIG5* responses to monochromatic light

It was analyzed whether HY5 regulated the observed accumulation of *SIG5* transcripts upon illumination with monochromatic blue light or red light (fig. 3-23 A). The transcript levels of the two HY5 deficient lines, *hy5-1* and SALK_056405C, were quantified after illumination with blue light or red light. The data were compared with the *SIG5* transcript levels of the respective genetic background; accession Col-0 for *hy5-1* and *Ler* in case of SALK_056405C. *SIG5* transcript levels were reduced in both lines, after blue light treatment (43-fold induction to 4-fold induction, and 45-fold induction to 8-fold induction, respectively) as well as after red light treatment (21-fold induction to 0.6-fold induction, and 17-fold induction to 0.4-fold induction, respectively) (fig. 3-45).

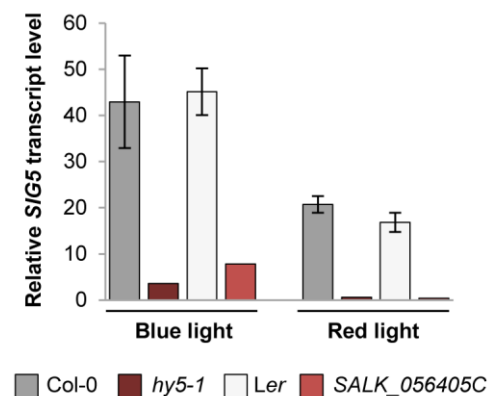


Figure 3-45. Relative *SIG5* transcript level in *hy5* mutants in response to monochromatic light. *hy5-1* was compared with its genetic background Col-0, SALK_056405C was compared with *Ler* background. 10 d old seedlings grown under short day conditions on MS medium supplemented with 0.5 % (w/v) sucrose at 120 $\mu\text{mol photons m}^{-2} \text{s}^{-1}$ white light were dark adapted for 24 h and then exposed to 100-120 $\mu\text{mol photons m}^{-2} \text{s}^{-1}$ monochromatic blue light or red light for 24 h. *SIG5* transcript levels were determined by qRT-PCR relative to *ACT2* transcript level. Relative *SIG5* transcript levels of dark adapted seedlings prior to the transfer to monochromatic light were set to 1.0. The wild-type data are means of 2 (Col-0) or 3 biological replicates (\pm SEM).

The observed diminishment of *SIG5* transcript levels compared to the respective wild-types showed that HY5 acted downstream of the blue light sensors as well as the red light sensors in regulating *SIG5* transcription in Arabidopsis seedlings.

3.4.10.3 Direct interaction of HY5 with the *SIG5* promoter

It was analyzed whether the transcription factor HY5 was able to interact directly with the *SIG5* promoter.

Influence of mutations in predicted HY5 binding sites on light-dependent transcription

The HY5 protein interacts with promoters of light-inducible genes via G-boxes (Chattopadhyay *et al.*, 1998b; Gao *et al.*, 2004; Zhang *et al.*, 2011), Z-boxes (Yadav *et al.*, 2002), C-boxes, GC-hybrids and CA-hybrids (Song *et al.*, 2008). The 2 kb *SIG5* promoter sequence, which mediated light-responsive *SIG5* transcription (fig. 3-29 A), was analyzed for the existence of these HY5 binding sites by PlantCARE (Rombauts *et al.*, 1999) and PLACE (Higo *et al.*, 1999) databases of plant *cis*-acting regulatory DNA elements. Three predicted HY5 binding sites of the *SIG5* promoter were identified in the distal *SIG5* promoter and analyzed: a G-box, a GC-box and a GATA-motif (fig. 3-46).

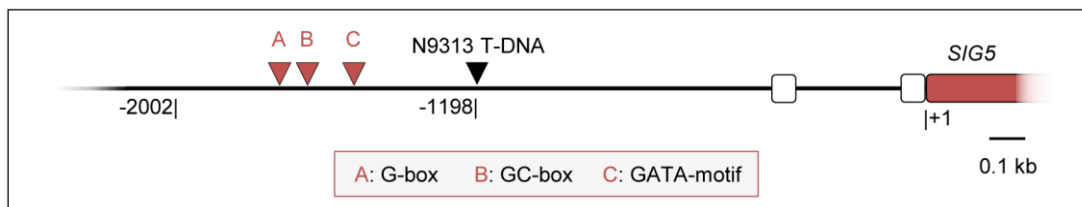


Figure 3-46. Diagram of the localization of predicted HY5 binding sites in the promoter of *SIG5*. The HY5 binding sites G-box, GC-box and GATA-motif are depicted as red arrowheads. A black arrowhead gives the T-DNA insertion site of N9313 at position -1198 relative to the translation start site of *SIG5*. The 2 kb promoter region analyzed for HY5 binding sites is highlighted in red. *SIG5* exons are depicted as grey boxes, the 5' UTR as white boxes. Numbers give the distances relative to the translation start site of *SIG5*.

The three predicted HY5 binding sites were mutated to investigate their functionalities. The mutations were introduced independently, as mutations of single *cis*-acting elements have previously been shown to almost abolish the activity of *RBCS* promoters (Donald and Cashmore, 1990; Lübberstedt *et al.*, 1994; Argüello-Astorga and Herrera-Estrella, 1998). Site-directed mutagenesis was PCR-mediated according to Montemartini *et al.* (1999). The general procedure of this method is described in chapter 2.6. The mutations were introduced according to McKendree and Ferl (1992) and Donald and Cashmore (1990) (tab. 3-7).

Table 3-7. HY5 binding sites of the 2 kb *SIG5* promoter and introduced mutations.

<i>cis</i> -element	Sequence ^a	Position ^b	Introduced mutation ^c	Reference
G-box	CACGTG (+)	-1800 to -1795	CA AT TG	McKendree and Ferl, 1992
GC-box	GACGTG (+)	-1725 to -1720	GA AT TC	McKendree and Ferl, 1992
GATA-motif	GATAAG (+)	-1595 to -1590	GA TA TC	Donald and Cashmore, 1990

^a (+) and (-) indicates the sense and complementary strand, respectively

^b positions are relative to the translation start site of *SIG5*

^c mutated nucleotides are highlighted in black

The three predicted HY5 binding sites were located upstream of the T-DNA insertion site of N9313, within the 0.8 kb distal *SIG5* region, which was previously shown to mediate light-dependent reporter gene expression (fig. 3-31, 3-32). Therefore the effects of the mutations were analyzed within this 0.8 kb distal fragment of the *SIG5* promoter, ranging from -2002 to -1197 relative to the translation start side of the *SIG5* gene. As previously described, the promoter fragments were fused to a $\Delta 35S$ promoter and a GFP::*GUS* reporter gene (3.4.7.1). The resulting constructs were transiently expressed in tobacco leaves with the wild-type 0.8 kb sequence of accession C24 as reference, and the $\Delta 35S$ promoter as control. The mutated construct of interest and both control constructs were introduced into the same leaf to exclude variations of expression due to developmental differences or position effects during incubation of the infiltrated leaves. The same volumes of *Agrobacterium* solutions with the same titer were introduced into the leaf lamina. After infiltration the leaves were incubated in white light for 5 d. The *GUS* expression was quantified spectrophotometrically using PNP_G as substrate. The total protein content of the analyzed leaf extracts was used for normalization. The mutation of the G-box significantly lowered the *GUS* activity to 71 % (fig. 3-47 A). The mutations of the GC-box as well as of the GATA-motif did not reduce the *GUS* activities (fig. 3-47 B and C).

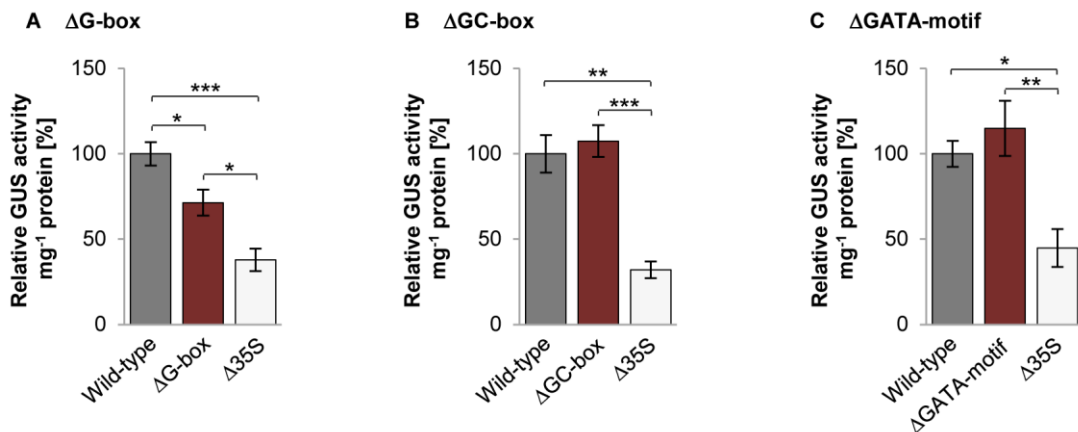


Figure 3-47. Transient *GUS* expression regulated by distal 0.8 kb *SIG5* promoter fragments with different mutated *cis*-elements. The tobacco leaves were infiltrated with $pSIG5_{\text{distal}}$ (-2002 to -1197 relative to translation start) with wild-type C24 sequence or with different mutations of predicted *cis*-acting elements, a G-box (A), a GC-box (B) and a GATA-motif (C), fused to $\Delta 35S$ promoter and *GUS*. After infiltration the leaves were illuminated with $100\text{-}120 \mu\text{mol photons m}^{-2} \text{s}^{-1}$ white light for 5 d. $\Delta 35S$ was used as control. Each leaf was infiltrated in parallel with $pSIG5_{\text{distal}}$, $pSIG5_{\text{mutated}}$ and $\Delta 35S$. Values are given as %, with $pSIG5_{\text{distal}}$ of each leaf set to 100 %. *GUS* activity was determined as $\mu\text{mol PNP min}^{-1} \text{mg}^{-1} \text{protein}$. The total protein content and the PNP content were determined spectrophotometrically. The *GUS* activity shown is the mean value of two independent infiltrations with two measurements per infiltration, \pm SEM. One-way ANOVA was performed comparing all groups with Bonferroni's post-test. Statistical significance of difference is indicated as asterisks above bars. (* $p < 0.05$, ** $p < 0.01$, *** $p < 0.001$)

The significant reduction of *GUS* activity upon mutation of the G-box showed that this G-box was a functional active *cis*-acting element in the promoter of *SIG5*, in contrast to the GC-box and the GATA-motif.

The distal G-box mediating the red light response of transcription

The G-box was located in the distal 0.8 kb *SIG5* promoter fragment that has previously been shown to mediate transcription upon red light illumination (fig. 3-33). To analyze whether the G-box was involved in mediating transcription upon illumination with red light, tobacco leaves were treated with monochromatic red light after infiltration with *SIG5* promoter reporter gene constructs. The subsequent quantification of relative GUS activity showed, that the mutation of the G-box reduced the GUS activity to 81 % compared with the wild-type sequence upon illumination with red light (fig. 3-48).

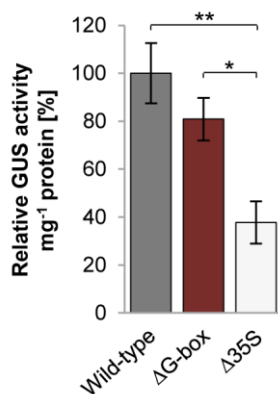


Figure 3-48. GUS expression regulated by distal 0.8 kb *SIG5* promoter fragment with mutated G-box upon red light illumination. The tobacco leaves were infiltrated with p*SIG5*_{distal} (-2002 to -1197 relative to translation start) with wild-type C24 sequence or including a mutated G-box, fused to Δ 35S promoter and GUS. After infiltration the leaves were illuminated with 100-120 $\mu\text{mol photons m}^{-2} \text{s}^{-1}$ monochromatic red light for 5 d. Δ 35S was used as control. Each leaf was infiltrated in parallel with p*SIG5*_{distal}, p*SIG5* _{Δ G-box} and Δ 35S. Values are given as %, with p*SIG5*_{distal} of each leaf set to 100 %. GUS activity was determined as $\mu\text{mol PNP min}^{-1} \text{mg}^{-1}$ protein. The total protein content and the PNP content were determined spectrophotometrically. The GUS activity shown is the mean value of two independent infiltrations with two measurements per infiltration (\pm SEM). One-way ANOVA was performed comparing all groups with Bonferroni's post-test. Statistical significance of difference is indicated as asterisks above bars. (* $p < 0.05$, ** $p < 0.01$)

These results supported the assumption that the G-box in the distal promoter of *SIG5*, a potential HY5 binding site, was a functional active *cis*-acting element. Furthermore this G-box seemed to play a role in the red light induction of gene expression.

However, the Δ G-box mutation did not reduce the GUS activity to the Δ 35S driven control level. It was concluded that additional light-responsive *cis*-acting elements of the distal 0.8 kb *SIG5* promoter fragment, in addition to the functional G-box, regulated *SIG5* transcription.

Interaction of HY5 with distal *SIG5* promoter fragments in yeast

It was analyzed if the HY5 transcription factor was directly interacting with the *SIG5* promoter. The interaction was tested by a targeted yeast one-hybrid approach. The CDS of HY5 was cloned into the pACT2 vector. Primers were designed to amplify the CDS without initial start codon but with *Bam*HI and *Xho*I sites at the 5' and 3' end, respectively, and two additional nucleotides between the *Bam*HI site and the CDS to clone HY5 in frame with GAL4 AD.

A 196-bp fragment of the Arabidopsis *RBCS1A* promoter has been shown by electrophoretic mobility shift assay (EMSA) to contain a binding site for HY5 (Chattopadhyay *et al.*, 1998b). This 196-bp fragment was cloned into pHIS2 vector to serve

as a positive control for interaction with HY5 transcription factor in yeast (primers used for amplification: appendix 6.2, tab. A2-11).

The previously characterized proximal 1.2 kb and the distal 0.8 kb *SIG5* promoter fragments from *Arabidopsis thaliana* accession C24 were cloned upstream of the *HIS3* gene in the pHIS2 vector. Additionally four smaller overlapping fragments of the distal 0.8 kb sequence were analyzed (fig. 3-49).

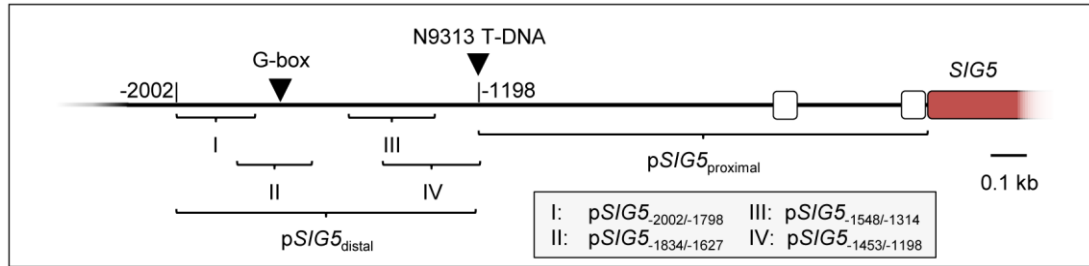


Figure 3-49. Map of different *SIG5* promoter fragments tested for interaction with HY5 in yeast. The T-DNA insertion site in ET N9313 at position -1198 relative to translation start of *SIG5* (marked by arrowhead) depicts the border of the distal promoter fragment (*pSIG5_{distal}*), which ranges up to -2002 relative to translation start. This 0.8 kb fragment was further divided into four smaller overlapping fragments. The 5' UTR is depicted as white boxes, the *SIG5* CDS as grey box.

The resulting bait constructs were transformed into the *Saccharomyces cerevisiae* strain Y187. The cells were selected on SD/-T medium, a nutritional selective medium for the pHIS2 bait vector. The growth of colonies on SD/-T medium indicated the uptake of the plasmid into the cells. The uptake of the plasmid was confirmed by PCR using the primers that were previously used to amplify the *pSIG5* fragments. The transformed yeast cells were tested for their ability to grow on selective SD/-H/-T medium. The *HIS3* reporter gene in pHIS2 was driven by a minimal promoter, $P_{minHIS3}$, which caused an autoactivation of the *HIS3* even in the absence of a prey construct (Durfée *et al.*, 1993; Fields, 1993). To suppress this unspecific yeast growth on selection medium, the competitive inhibitor 3-AT was added to the selective minimal SD medium.

The single transformed yeast cells were transformed with the prey construct, HY5 in pACT2. Double-transformed yeast cells were tested for interaction by dropping defined cell density onto solidified SD/TDO medium supplemented with different 3-AT concentrations. Comparison of colony size with colonies of single transformed cells not containing HY5 in pACT2 onto SD/-H/-T medium with the same 3-AT concentrations indicated the strength of HY5 interaction. The control *RBCS1A* promoter showed interaction with HY5 as the double transformed cells showed increased growth pattern compared with the single transformed cells containing only the bait construct (fig. 3-50 A). The co-transformation with the prey plasmid did not increase the growth behavior on selective medium, indicating that HY5 did not interact with the distal (fig. 3-50 B) or the proximal *SIG5* promoter fragments (fig. 3-50 C), nor with the smaller distal fragments (fig. 3-50 D to G). These results indicated that the transcription factor HY5 was not directly interacting with the *SIG5* promoter.

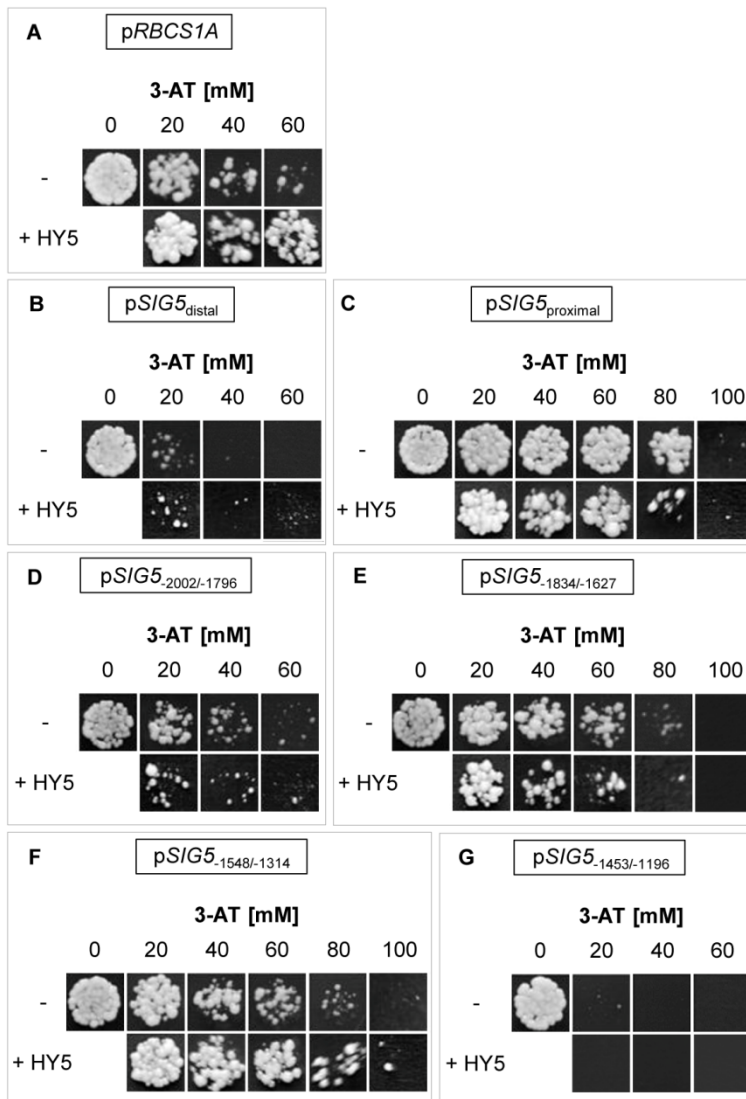


Figure 3-50. HY5 CDS was interacting with *RBCS1A* promoter fragment but not with *SIG5* promoter fragments. Y187 was transformed with *pRBCS1A*, *pSIG5_{distal}*, *pSIG5_{proximal}* or four smaller fragments of the distal *SIG5* sequence in *pHIS2*, or cotransformed together with HY5 CDS in *pACT2*, respectively. 5 μ l of liquid culture with an optical density at 600 nm adjusted to 0.01 were dropped onto solidified SD/-H/-T (upper row) or SD/-H/-L/-T (lower row) supplemented with different 3-AT concentrations. 0 mM indicated cells dropped onto SD/-T as control.

3.4.11 COP1 as regulator of *SIG5* transcription

HY5 protein stability is regulated by the COP/DET/FUS protein degradation machinery (Ang *et al.*, 1998; Osterlund *et al.*, 2000). As HY5 has been shown to be an essential element for the light-dependent induction of *SIG5* transcription (fig. 3-45), it was postulated that COP1 was also involved in the regulation of *SIG5*. To test this hypothesis, the *SIG5* transcript levels of *cop1* mutants were determined and compared with transcript levels of the corresponding wild-type. 10 d old seedlings were dark-adapted for 24 h and harvested for RNA isolation. Δ Ct values were determined relative to *ACT2*. In the dark COP1 was mediating the degradation of HY5 in the wild-type (Osterlund *et al.*, 2000). Relative *SIG5* transcript levels of the *cop1* mutant were expected to be elevated when COP1 did not degrade HY5 in the dark. The *cop1* mutation resulted in 17-fold increased *SIG5* transcript levels compared with the *SIG5* transcript levels of Col-0 (tab. 3-8). It was concluded that COP1 was a regulator of light-dependent *SIG5* transcription via HY5.

Table 3-8. Relative SIG5 transcript abundances in Col-0 wild-type and in cop1 mutants. Δ Ct values were determined by qRT-PCR relative to ACT2 values. Seedlings were grown on MS medium supplemented with 0.5 % (w/v) sucrose at 120 μ mol photons $m^{-2} s^{-1}$ white light for 10 d and dark-adapted for 24 h prior to RNA isolation.

Sample	Δ Ct value	Relative transcript values [%]
Col-0	9,67	100
cop1	5,58	1700

3.4.12 Screen for transcription factors interacting with the SIG5 promoter

Within the red light sensitive distal 0.8 kb *SIG5* promoter a *cis*-acting G-box was identified, which was involved in the red light induction of gene expression. Mutation analysis of this motif revealed that additional red light sensitive *cis*-acting elements were located in the distal *SIG5* promoter (fig. 3-48). *In silico* analysis of the 0.8 kb has previously predicted 15 different light-responsive *cis*-acting elements being located in this region (tab. 3-4). To identify TFs that interact with the red light sensitive distal *SIG5* promoter, a one-hybrid screen was performed in yeast.

3.4.12.1 Construction of the bait construct

The previously characterized distal 0.8 kb *SIG5* promoter fragment from *Arabidopsis thaliana* accession C24 was cloned upstream of the *HIS3* gene in the pHIS2 vector. The resulting bait construct, designated pHIS2-p*SIG5*, was transformed into the yeast strain Y187. The cells were selected on SD/-T medium, a nutritional selective medium for the pHIS2 bait vector. The growth of colonies on SD/-T medium indicated the uptake of the plasmid into the cells. The uptake of the plasmid was confirmed by PCR using the primers that were previously used to amplify the p*SIG5*_{distal} amplicon.

3.4.12.2 Setting 3-AT concentration

The *HIS3* reporter gene in pHIS2 was driven by a minimal promoter $P_{minHIS3}$, which causes an autoactivation of the *HIS3* gene even without a promoter sequence inserted in the MCS (Fields, 1993; Durfee *et al.*, 1993). Therefore the obtained yeast reporter strain (designated Y187-pHIS2-p*SIG5*) expressed the *HIS3* reporter gene at basal level even in the absence of a prey construct. To suppress this unspecific yeast growth on selection medium, the competitive inhibitor 3-AT was added to the selective minimal SD medium.

5 μ l of liquid yeast culture with an optical density at 600 nm adjusted to 0.01 were dropped onto solidified SD/-H/-T plates supplemented with different 3-AT concentrations. The plates were incubated at 30 °C for 2 d. The Y187-pHIS2-p*SIG5* growth was impaired at concentrations of 20 mM 3-AT; 40 mM 3-AT completely inhibited the growth of the cells (fig. 3-51). Consequently the Y1H screen was performed on selective media supplemented with 40 mM 3-AT.

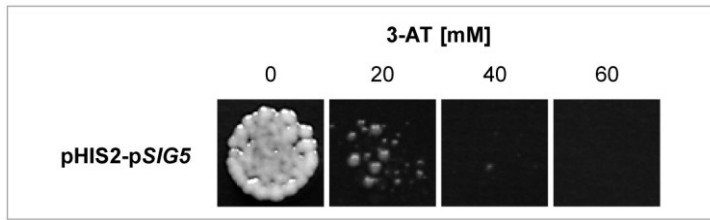


Figure 3-51. Setting 3-AT concentration for Y187-pHIS2-pSIG5. 5 μ l liquid yeast culture was dropped onto SD/-H/-T plates supplemented with 0-60 mM 3-AT. The plates were incubated 3 d at 30 °C.

3.4.12.3 Library construction and analysis

A LAMBDA ACT cDNA library generated with mRNA isolated from 3 d old etiolated *Arabidopsis thaliana* Col-0 seedlings (Kim *et al.*, 1997) was used for the Y1H screen. As early light-responsive genes include a large proportion of TFs (Casal and Yanovsky, 2005; Jiao *et al.*, 2007) it was assumed, that TFs were already overrepresented in the mRNA pool of etiolated seedlings. The λ -ACT cDNA library was converted into a plasmid library by *in vitro* plasmid excision. A total of 140.000 single *E. coli* colonies were transformed and the isolated plasmids were pooled.

The quality of the library was analyzed via restriction analysis. 14 colonies were analyzed to determine the sizes of cDNA inserts in pACT. As the cDNA library was ligated in the *XhoI/XhoI* site of pACT, the plasmids were cleaved by restriction endonuclease *XhoI*. The resulting cDNA fragment sizes were determined by gel electrophoresis and comparison with a DNA size standard. cDNA fragments of about 0.6-1.3 kb were determined (tab. 3-9). An average size of the cDNA inserts in pACT of 0.9 kb was estimated, demonstrating a suitable quality of the cDNA fragments composing the library.

Table 3-9. cDNA insert sizes in λ -ACT library.

cDNA insert size [kb]	Percentage of colonies [%]
≤ 0.5	0
0.6 / 0.7	50
0.8 / 0.9	14
1.0 / 1.1	14
1.2 / 1.3	22

3.4.12.4 Yeast one-hybrid screen

The prepared cDNA library was introduced into the Y187 cells carrying the pHIS2-pSIG5 bait construct. The transformants were screened on selective medium lacking histidine, leucine and tryptophan, supplemented with 40 mM 3-AT. The transformation efficiency of cDNA library transformation was calculated: in total 1.5×10^6 transformants were obtained.

From these transformants about 100 cDNA clones were obtained that were able to grow on the selective medium. Thirty of these clones were tested for their ability to grow on selective media supplemented with up to 100 mM 3-AT. All of them were able to grow under such conditions on SD/-H/-L/-T media. As example, growth pattern of five different clones are depicted in fig. 3-52. The Y187-pHIS2-pSIG5 single transformant was used as

control and failed to grow under the tested conditions on SD/-H/-T medium (fig. 3-52, upper row). This demonstrated activation of the *HIS3* gene above background levels. It indicated specific interaction of the distal *SIG5* promoter with the polypeptides that were encoded by the cDNAs in yeast.

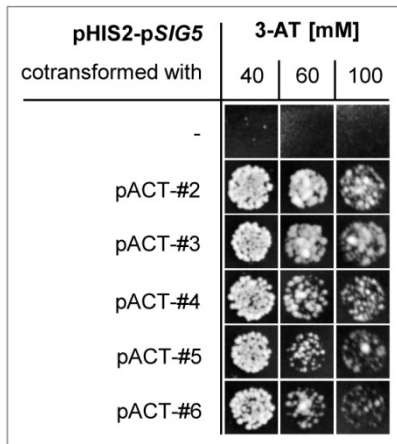


Figure 3-52. Growth of cDNA clones on media with different 3-AT concentrations. Y187-pHIS2-pSIG5 was transformed with cDNA clone no. 2 to 6 in pACT. 5 µl of liquid yeast culture with an optical density at 600 nm adjusted to 0.01 were dropped onto solidified SD/-H/-L/-T plates supplemented with 40, 60 or 100 mM 3-AT. Y187-pHIS2-pSIG5 without prey plasmid served as control and was dropped onto SD/-H/-T medium.

The plasmids of eleven of the thirty tested cDNA clones were isolated from yeast and introduced into *E. coli* for amplification and further characterization. After isolation from bacteria, the plasmids were sequenced. The identification of the cDNA sequences was done by aligning the sequencing results with database entries by BLASTN. The cDNAs of nine different clones matched annotated Arabidopsis cDNA sequences. The gene identities, the homologies of the sequencing results and the corresponding annotated cDNA sequences, and short descriptions of the respective genes are summarized in tab. 3-10.

Table 3-10. Characterization of bait cDNAs, identified by Y1H screen.

cDNA clone	Gene identity	Homology	Description of the respective gene
2	At2g27385	666 bp (100 %)	Pollen Ole e 1 allergen and extensin family protein; unknown function
3	At5g03240	723 bp (100 %)	Polyubiquitin 3; function: protein degradation
7	At2g45180	627 bp (100 %)	Bifunctional inhibitor/lipid-transfer protein/seed storage 2S albumin superfamily protein 3; function: lipid binding
8	At4g16260	788 bp (100 %)	Glycosyl hydrolase superfamily protein; function: hydrolyzing O-glycosyl compounds
10	At1g10840	523 bp (100 %)	Eukaryotic initiation factor 3H1 subunit (TIF3H1); function: translation initiation
14	At1g76700	846 bp (100 %)	DNAJ heat shock N-terminal domain-containing protein; function: unfolding protein binding
16	At3g15110	631 bp / 642 bp (98 %)	Unknown protein; function: unknown
22	At4g28360	559 bp (100 %)	Ribosomal protein L22p/L17e family protein; function: structural constituent of ribosome
29	At1g05190	825 bp / 833 bp (99 %)	Embryo defective 2394 (emb2394); function: structural constituent of ribosome

The sequencing results matched with high homologies proteins involved in protein degradation (#3), lipid binding (#7), unfolding protein binding (#14) or ribosome structure (#22, #29). None of the cDNAs identified in the Y1H screen encoded for a DNA-binding

protein. These results indicated unspecific interaction between the prey DNA sequence and the bait oligopeptides. Therefore the analysis of the Y1H results was terminated at this point without sequencing further bait plasmids. The performed Y1H approach did not lead to the identification of a TF interacting with the distal 0.8 kb *SIG5* promoter.

3.4.13 Characterization of retrograde signals regulating *SIG5* transcription

The Arabidopsis *SIG5* promoter included several red light and far-red light sensitive elements, which were located at both proximal and distal regions. However, the GFP fluorescence in seedlings with *hylcry1cry2* mutant background was only reduced to 33 % (fig. 3-42). These results indicated that additional signals, in parallel to the photoreceptors, were involved in mediating the light-dependent induction of *SIG5* transcription.

The best analyzed function of *SIG5* is controlling transcription of *psbD* (encoding D2, a PSII core protein). *SIG5* specifically recognized the *psbD* blue light-responsive promoter (BLRP) (Nagashima *et al.*, 2004b; Tsunoyama *et al.*, 2002, 2004). This correlation between *SIG5* function and photosynthesis indicated that the expression of the nuclear encoded *SIG5* could be regulated by retrograde signals, coupling *SIG5* transcription with the physiological state of the chloroplasts. It was subsequently analyzed whether the *SIG5* promoter was regulated in correlation with the redox state of chloroplasts.

Monochromatic red light was predominantly absorbed by the antenna of PSII (Duysens and Ames, 1962; Myers, 1971) and therefore led to a reduction of the components of the PET chain. To analyze the influence of retrograde signals on *SIG5* expression, the redox status of the plastid PQ pool was modulated independently from the light conditions by application of two inhibitors of photosynthetic electron transport. The two inhibitors had opposite effects on the net redox state of the PQ pool. DCMU inhibited the photosynthetic electron flow by irreversible binding to the Q_B binding niche of the PSII reaction center protein D1, thus resulting in the oxidation of the PQ pool (Trebst, 1980; Sandmann and Bölgner, 1986). In contrast, DBMIB inhibited the oxidation of the PQ pool by binding to the PQ oxidation site of the cytochrome *b₆/f* complex (Trebst, 1980).

3.4.13.1 GFP fluorescence of N9313 upon short term treatment with DCMU and DBMIB

10 d old white light grown N9313 seedlings were sprayed with 10 µM DCMU or 20 µM DBMIB. As DBMIB was a light-labile component and unstable in tissues (Alfonso *et al.*, 2000; Pfannschmidt *et al.*, 2001), the incubation time was restricted to 4 h. In contrast, DCMU was a very stable compound that easily penetrated tissues and closed the reaction centers completely for several days (Pfannschmidt *et al.*, 2001). After 4 h the GFP fluorescence of the seedlings was determined using a top reader fluorometer. The treatment with DCMU resulted in a reduction of GFP fluorescence levels of N9313 from 4.2 to 3.6, whereas the DBMIB treatment had no effect (fig. 3-53 A).

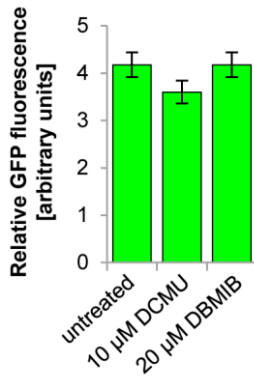


Figure 3-53. GFP fluorescence in N9313 upon 4 h treatment with DCMU or DBMIB. The seedlings were grown on MS medium supplemented with 0.5 % (w/v) sucrose for 10 d under short day conditions at $120 \mu\text{mol photons m}^{-2} \text{s}^{-1}$ white light. $10 \mu\text{M}$ DCMU or $20 \mu\text{M}$ DBMIB were sprayed onto the seedlings and incubated for 4 h. The GFP fluorescence was detected using a top reader fluorometer. The data are mean values of 24-36 seedlings (\pm SEM). * indicates significant differences from the untreated value. (Student *t*-test, $p < 0.05$)

The effect of DCMU on the photosynthetic electron transport chain was verified by determination of the effective quantum yield of PSII (ΦPSII). The limited electron transfer from the first stable electron acceptor, Q_A to Q_B by DCMU resulted in a decline in ΦPSII (Haynes *et al.*, 2000). The effect of DBMIB could not be monitored by the ΦPSII values (Pfannschmidt *et al.*, 2001). ΦPSII of the DCMU treated seedlings and the untreated controls were determined with a pulse amplitude-modulated fluorometer (PAM). The ΦPSII values of inhibitor treated plants were significantly reduced from 0.76 to 0.3 (fig. 3- 54).

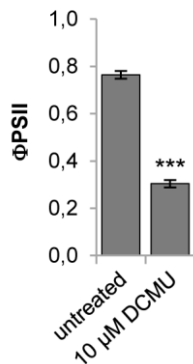


Figure 3-54. ΦPSII of N9313 seedlings with or without DCMU treatment. The seedlings were grown on MS medium supplemented with 0.5 % (w/v) sucrose for 10 d under short day conditions at $120 \mu\text{mol photons m}^{-2} \text{s}^{-1}$ white light. $10 \mu\text{M}$ DCMU was sprayed onto the seedlings and incubated for 4 h. The data are mean values of 24-36 seedlings (\pm SEM). *** indicates significant differences from the untreated value. (Student *t*-test, $p < 0.001$)

The reduction of the ΦPSII values upon DCMU treatment demonstrated the effective modulation of the photosynthetic electron transport chain and therefore the redox state of the PQ pool. This suggested the possibility that the observed slight reduction of GFP fluorescence of N9313 upon DCMU treatment (fig. 3-53) was due to an oxidation of the PQ pool. This would mean that the redox state of the PQ pool could modulate the *SIG5* transcription.

3.4.13.2 GFP fluorescence of N9313 upon long term response

With GFP as reporter gene the reduction of transcription initiation, as in the previously described short term experiment, was hardly detectable. The GFP protein half-life was previously determined as 26 h (Corish and Tyler-Smith, 1999), or as 54 h (Sacchetti *et al.*, 2001). Due to this high protein stability, the influence of DCMU on GFP fluorescence was observed in a long term experiment.

The treatment with monochromatic red light as well as with DCMU or DBMIB generated an imbalance in excitation energy distribution between the two photosystems. To counteract such imbalances, plants redistributed light energy in a long term by re-adjustment of the photosystem stoichiometry. Plastid redox signals have been shown to modulate the expression of nuclear encoded photosynthetic genes (reviewed in Woodson and Chory, 2008), a process called long-term response (LTR).

According to Pfannschmidt *et al.*, (2001) a LTR was induced. N9313 seedlings were first grown under white light until the four-leaf stage before they were subjected to red light or far-red light for 96 h. Responses of these plants were compared with responses of plants that stayed under the white light or that were pre-treated with DCMU prior to the light shift. DCMU was used as antagonist to the respective light-induced redox signal by applying DCMU directly before the plants were transferred to red light.

Determination of Chl fluorescence parameters

To test whether the applied treatments were inducing LTR, Chl fluorescence parameters were determined by standard PAM fluorescence measurements. The F_s/F_m ratio was determined. The steady state fluorescence F_s was typically increasing after acclimation to far-red light and decreased after acclimation to red light (Pfannschmidt *et al.*, 2001), and therefore could be used as an indicator for a LTR. The seedlings showed F_s/F_m values increasing after acclimation to far-red light as well as after acclimation to red light when pretreated with DCMU (fig. 3-55 A).

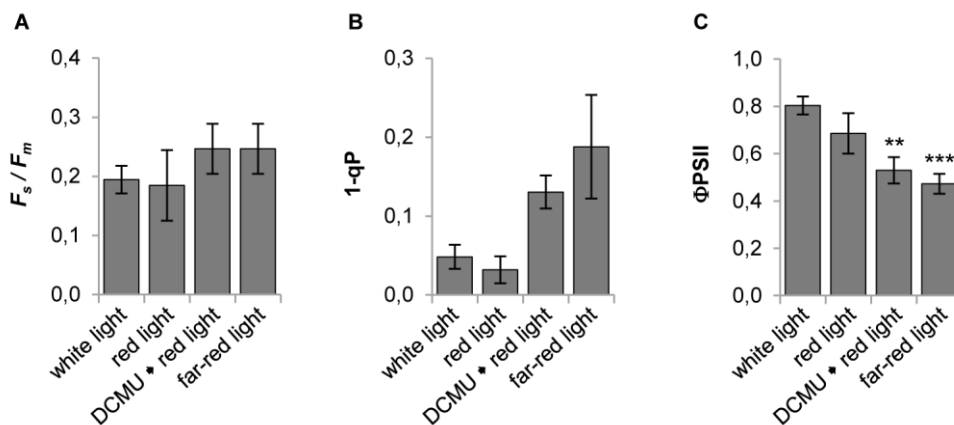


Figure 3-55. Chl fluorescence parameter after light shift with or without DCMU pre-treatment. 8 d old seedlings grown under constant white light illumination on MS medium without sucrose were acclimated to 100-120 $\mu\text{mol photons m}^{-2} \text{s}^{-1}$ red light or far-red light with or without treatment with 10 μM DCMU prior to the light shift. The seedlings were acclimated to the different light conditions for 4 d. F_s/F_m (A), 1-qP (B) and Φ_{PSII} values (C) were determined using a PAM fluorometer. As a reference, plants were grown for 12 d under white light. All values were determined by 3-8 independent measurements (\pm SEM). * indicates significant differences from the white light reference plant values (Student *t*-test, ** $p < 0.01$, *** $p < 0.001$).

Changes in the redox state of the PET chain were also reflected in alterations of the excitation pressure of PSII. The excitation pressure was defined as the reduction state of Q_A , expressed as 1-qP (Dietz *et al.*, 1985; Huner *et al.*, 1998). Far-red light treated plants showed increased 1-qP values, as did the DCMU treated red light illuminated plants (fig. 3-55 B). In contrast, the Φ PSII (effective quantum yield) values were higher in red light illuminated plants than in DCMU pretreated and far-red light illuminated plants (fig. 3-55 C).

Taken together the Chl fluorescence parameters showed that the plants acclimated to the respective light quality, with a limited electron transport capacity in far-red light acclimated plants compared to the red light acclimated plants. The Φ PSII values of the DCMU treated plants (Φ PSII = 0.53 ± 0.06) indicated a limited but not blocked photosynthetic electron transport.

Determination of Chl a/b ratio

The LTR induced changes in the antenna that were indicated by characteristic changes in the Chl *a/b* ratio. Chl *b* was mainly associated with the PSII antenna (Melis, 1989), and therefore accumulated during acclimation to far-red light (Fey *et al.*, 2005).

Chl *a* to Chl *b* ratios were determined to verify the Chl fluorescence data obtained from the PAM measurements. The seedlings acclimated to far-red light and the red light illuminated seedlings pretreated with DCMU showed a significantly lower Chl *a/b* ratio than the white light grown reference plants (fig. 3-56).

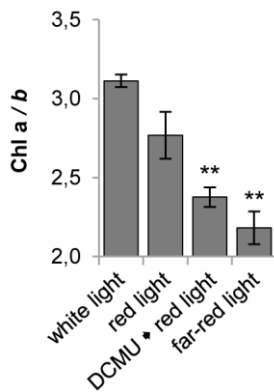


Figure 3-56. Chl *a/b* ratio after LTR. N9313 seedlings were grown on MS medium without sucrose at $100 \mu\text{mol photons m}^{-2} \text{s}^{-1}$ constant white light. 8 d after germination the seedlings were transferred to red or far-red light with or without treatment with $10 \mu\text{M}$ DCMU, and acclimated to the different light conditions for 4 d. The chlorophylls were quantified spectrophotometrically. As a reference, plants were grown for 12 d under white light. The data are means of 2-3 replicates (\pm SEM) with 5-6 seedlings pooled for each extraction. ** indicates significant differences from the white light reference plant value. (Student *t*-test, ** $p < 0.01$)

The Chl *a/b* ratios demonstrated rearrangements of the antennae and their Chl binding proteins during long term acclimation. The values of DCMU treated plants did not reach the values of the far-red light acclimated plants. These data confirmed the Chl fluorescence data that showed a partial inhibition of the LTR to red light by the DCMU treatment.

GFP fluorescence values

The GFP fluorescence of ground seedlings was determined relative to the fresh weight, as chlorophylls were modulated by the different light conditions (Adams and Demmig-Adams, 1992; Ilag *et al.*, 1994; Reinbothe *et al.*, 1996) as well as the total protein content of the seedlings (Rai and Laloraya, 1967; Raghavan and DeMaggio, 1971).

The seedlings acclimated to monochromatic red light showed significantly higher GFP fluorescence values of 203 mg⁻¹ FW compared with 51 mg⁻¹ FW for seedlings acclimated to far-red light (fig. 3-57). The treatment with DCMU prior to the light shift to red light diminished the red light induced accumulation of GFP fluorescence to 82 mg⁻¹ FW, similar to the levels of far-red light acclimated plants.

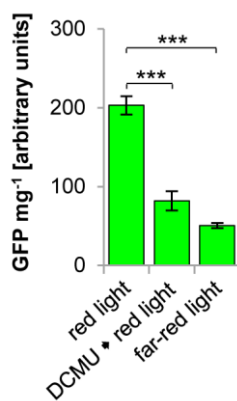


Figure 3-57. GFP fluorescence after LTR. N9313 seedlings were grown on MS medium without sucrose at 100 $\mu\text{mol photons m}^{-2} \text{s}^{-1}$ constant white light. 8 d after germination the seedlings were transferred to red or far-red light with or without treatment with 10 μM DCMU, and acclimated to the different light conditions for 4 d. About 10 seedlings were pooled for each GFP extraction. The GFP fluorescence was determined relative to fresh weight of the seedlings. The GFP fluorescence was detected using a fluorometer; the fluorescence of wild-type C24 seedlings was subtracted. Relative GFP fluorescence of 12 d white light grown N9313 was set as 100 %. Results are mean values of 3 measurements (\pm SEM). One-way ANOVA was performed comparing all groups with Bonferroni's post-test. Statistical significance of difference is indicated as asterisks above bars (***) ($p < 0.001$)

The red light induction of GFP fluorescence of N9313 was diminished in plants with oxidized PQ pool due to DCMU treatment, according to far-red light acclimated plants. These data indicated that the red light induction of GFP fluorescence was influenced by the redox state of the PQ pool and therefore regulated by retrograde signals.

3.4.13.3 Effect of DCMU on proximal and distal *SIG5* promoter

The assumed influence of the redox state of the PQ pool of the GFP expression of N9313 indicated that *cis*-acting promoter elements, which responded to retrograde signals, were located in distal *SIG5* promoter regions. The *SIG5* promoter was previously shown to include several red light responsive areas in distal regions as well as in the proximal promoter (fig. 3-33, 3-35 A, 3-36). It was further analyzed, whether these red light responses were influenced by modulation of the redox state of the plastid PQ pool.

GFP was transiently expressed in tobacco leaves, driven by proximal and distal *SIG5* promoter fragments. It was analyzed whether the promoter fragments were able to induce the previously characterized red light response upon light independent oxidation of the PQ pool by DCMU treatment.

Determination of effectual DCMU concentration

Initially it was determined, which DCMU concentration sufficiently inhibited the photosynthetic electron transport in tobacco. Solutions with different DCMU concentrations were sprayed onto the leaves of 4-5 weeks old *Nicotiana benthamiana* plants. After 24 h incubation in continuous white light, the ΦPSII values were determined using a PAM fluorometer. The treatment with 1 mM DCMU reduced the ΦPSII value from 0.73 to about 0.36 (fig. 3-58), indicating an effective inhibition of the photosynthetic electron transport. Therefore solutions of the inhibitor with a concentration of 1 mM DCMU were applied in the subsequent experiment.

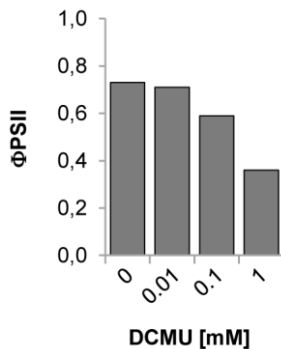


Figure 3-58. ΦPSII values upon treatment of tobacco leaves with DCMU. Leaves of 4-5 weeks old light grown tobacco plants were sprayed with different DCMU concentrations and incubated for 24 h in continuous white light of $100\text{-}120 \mu\text{mol photons m}^{-2} \text{s}^{-1}$. ΦPSII values were determined using a PAM fluorometer.

Determination of Chl fluorescence parameters

To test whether the DCMU treatments induced an LTR in the tobacco leaf cells, Chl fluorescence parameters were determined in more detail, according to 3.4.12.2. The F_s/F_m ratio was typically increasing after acclimation to far-red light. The F_s/F_m ratio of DCMU treated leaves increased significantly even upon red light illumination from 0.4 to 0.8 (fig. 3-59 A). The excitation pressure of PSII (1-qP) of DCMU treated plants increased (fig. 3-59 B), in contrast to the ΦPSII (effective quantum yield) values that were significantly reduced from 0.6 to 0.2 after 4 d (fig. 3-59 C).

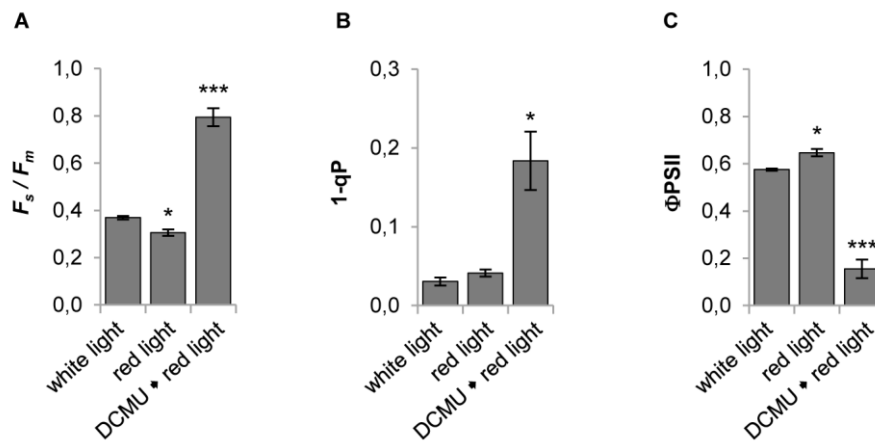


Figure 3-59. Chl fluorescence parameter after red light treatment with or without DCMU treatment. The leaves were incubated 4 d at 100-120 $\mu\text{mol photons m}^{-2} \text{s}^{-1}$ continuous monochromatic red light with or without treatment with 1 mM DCMU prior to the light treatment. As a reference, plants were illuminated with white light. F_s/F_m (A), 1-qP (B) and Φ_{PSII} values (C) were determined using a PAM fluorometer. All values were determined by 3 independent measurements (\pm SEM). * indicates significant differences from the white light reference plant values (Student *t*-test, * $p < 0.05$, *** $p < 0.001$).

The Chl fluorescence parameters showed that the DCMU treatment of the leaves oxidized the PQ pool and induced changes in the Chl antenna that responded to a LTR upon far-red light treatment. Hence the GFP fluorescence values of the infiltrated tobacco leaves were analyzed.

GFP fluorescence values

The 2 kb *SIG5* promoter, the distal 0.8 kb promoter and the proximal 1.2 kb *SIG5* promoter (for definition see fig. 3-27) were tested for their ability to induce red light responsive GFP fluorescence upon DCMU treatment. As previously described, the promoter fragments used in this study were fused to a $\Delta 35S$ promoter and a *GFP-GUS* reporter gene. The reporter gene was transiently expressed in tobacco leaves. After infiltration, the leaves were incubated 4 d at 100-120 $\mu\text{mol photons m}^{-2} \text{s}^{-1}$ continuous monochromatic red light or far-red light. Prior to the red light illumination, some leaves were sprayed with 1 mM DCMU to prevent the red light induced reduction of the plastid PQ pool. As a result, the 2 kb fragment as well as the distal and the proximal *SIG5* promoter fragment induced reporter gene expression upon red light illumination (fig. 3-60 A), whereas leaves treated with 1 mM DCMU showed diminished GFP fluorescence intensities (fig. 3-60 B). The far-red light illuminated leaves showed almost no detectable GFP fluorescence (fig. 3-60 C).

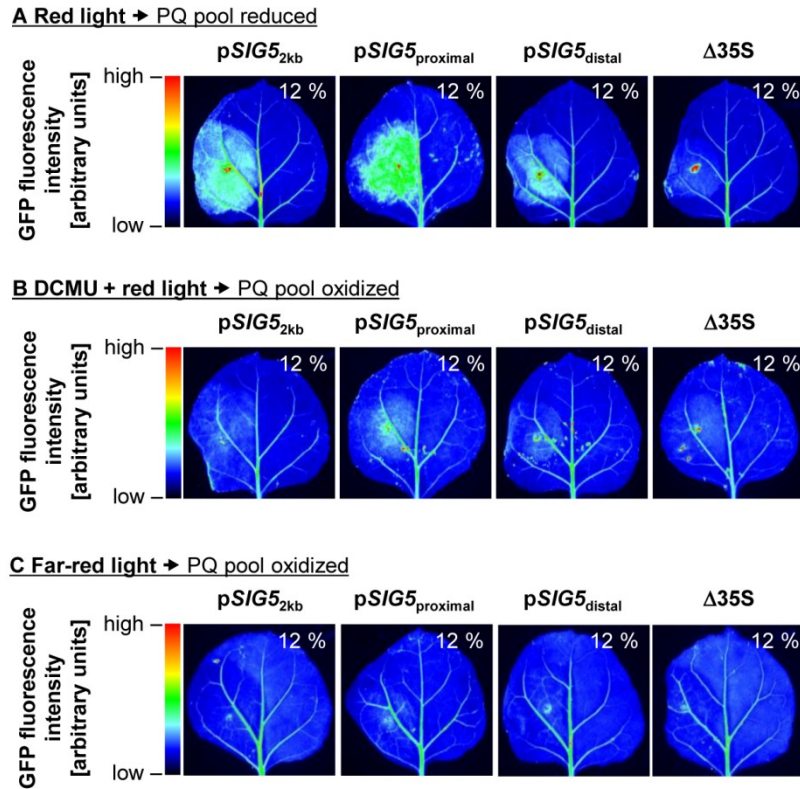


Figure 3-60. GFP expression mediated by *SIG5* promoter fragments upon modulation of the redox state of the PQ pool in tobacco. The total 2 kb, the proximal 1.2 kb and the distal 0.8 kb *SIG5* promoter fragments were fused to $\Delta 35S$ promoter and GFP. Only the left side of the leaves was infiltrated. **A:** Leaves were incubated 4 d at $100\text{--}120\ \mu\text{mol photons m}^{-2}\ \text{s}^{-1}$ continuous monochromatic red light. **B:** The leaves were sprayed with 1 mM DCMU after infiltration before the plants were transferred to red light. **C:** The leaves were incubated 4 d at $100\text{--}120\ \mu\text{mol photons m}^{-2}\ \text{s}^{-1}$ continuous monochromatic far-red light. The GFP was transiently expressed in tobacco leaves. The GFP fluorescence was observed under UV illumination with percentage representing the sensitivity of the detector. False color code depicts fluorescence intensity. The experiment was repeated once, the picture is representative.

These pictures showed that the red light induction of transcription was prevented by oxidation of the PQ pool due to the DCMU treatment. Far-red light illumination also oxidized the PQ pool and did not induce GFP expression. Taken together, the results indicated that the redox status of the plastid PQ pool regulated the reporter gene expression. As a conclusion, distal regions as well as the proximal *SIG5* promoter included *cis*-acting elements, which responded to retrograde signals.

3.4.13.4 The effect of DCMU on the red light sensitivity of the *SIG5* promoter

To test for the role of retrograde plastid signals regulating *SIG5* transcription in Arabidopsis, the organellar redox state of Arabidopsis seedlings was modified by DCMU and the effect of *GFP* and *SIG5* mRNA levels of N9313 and wild-type C24 was determined. 10 d old white light grown seedlings were dark adapted for 24 h to diminish transcript levels. The seedlings were transferred to monochromatic red or far-red light, with or without being sprayed with $10\ \mu\text{M}$ DCMU prior to the transfer. The transcript abundances were determined by qRT-PCR. The DCMU treatment prior to the red light illumination diminished the red light mediated accumulation of *GFP* transcripts in N9313 from a 14-fold to a 6-fold induction

(fig. 3-61 A). Similar to *GFP*, the red light induced accumulation of *SIG5* transcripts was diminished by the pretreatment with 10 μM DCMU prior to illumination, in N9313 (90-fold to 5-fold; fig. 3-61 C) as well as in the corresponding wild-type (25-fold to 6-fold; fig. 3-61 B).

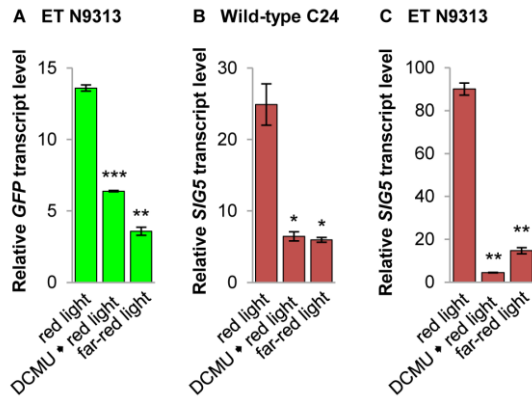


Figure 3-61. Relative transcript level in ET N9313 and C24 in response to monochromatic light and DCMU treatment. 10 d old seedlings were grown under short day conditions on MS medium supplemented with 0.5 % (w/v) sucrose at 120 $\mu\text{mol photons m}^{-2} \text{s}^{-1}$ white light. Seedlings were dark adapted for 24 h and then exposed to 100-120 $\mu\text{mol photons m}^{-2} \text{s}^{-1}$ monochromatic red or far-red light for 24 h with or without treatment with 10 μM DCMU before illumination. Relative *GFP* and *SIG5* transcript levels were determined by qRT-PCR relative to *ACT2* transcript level. Relative transcript level of dark adapted seedlings prior to the transfer to monochromatic light was set to 1.0. The data are means of 2 biological replicates (\pm SEM). * indicates significant differences from the red light treated sample (Student *t*-test, * $p < 0.05$, ** $p < 0.01$, *** $p < 0.001$).

The DCMU treatment inhibited the red light induction of *GFP* transcripts as well as the *SIG5* transcripts in N9313 seedlings. This indicated that the distal *SIG5* promoter, upstream of the ET T-DNA insertion site, as well as the proximal promoter included *cis*-acting elements that responded to retrograde signals originating in the redox state of the PQ pool. They validated the transient expression analysis in tobacco (fig. 3.60). Taken together, the red light induction of *SIG5* transcription was regulated by retrograde signals as well as by red/far-red light sensing photoreceptor phyB (fig. 3-41).

3.4.14 Modulation of *SIG5* transcription by exogenously applied sucrose

In addition to retrograde pathways, photosynthesis could modulate transcription of nuclear encoded genes by glucose or sucrose, its end-products. The accumulation of carbohydrates in plant cells decreased transcript abundances of photosynthetic genes (Krapp *et al.*, 1993; Sheen, 1994; Smeekens, 2000). As a result, via feedback inhibition of Calvin cycle enzymes (Edmondson *et al.*, 1990; Krapp *et al.*, 1993), the photosynthetic efficiency decreased (Goldschmidt and Huber, 1992).

It was analyzed whether the Arabidopsis *SIG5* promoter mediated transcription in a way that was influenced by the concentration of available carbohydrates in the cells.

3.4.14.1 The effect of exogenous sucrose feeding on the distal *SIG5* promoter

It was analyzed whether the GFP fluorescence of N9313 was influenced by the sucrose availability in the medium. N9313 seedlings were grown on MS medium supplemented with 0.5 % or with 2 % (w/v) sucrose for 10 d under short day conditions at $120 \mu\text{mol photons m}^{-2} \text{s}^{-1}$ white light. The GFP fluorescence was quantified. The GFP fluorescence of N9313 negatively correlated with the sucrose concentration in the medium ($r = -0.36$) (fig. 3-62).

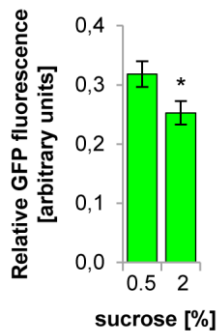


Figure 3-62. GFP fluorescence in N9313 upon sucrose application. The seedlings were grown on MS medium supplemented with 0.5 % or 2 % (w/v) sucrose for 10 d under short day conditions at $120 \mu\text{mol photons m}^{-2} \text{s}^{-1}$ white light. The GFP fluorescence was detected using a top reader fluorometer. The chlorophyll fluorescence of wild-type seedlings was subtracted. The data are mean values of 17-21 seedlings (\pm SEM). * indicates significant differences from the 0.5 % sucrose value. (Student *t*-test, $p < 0.05$)

The correlation between GFP fluorescence intensity in ET N9313 and sucrose availability in the media indicated that *SIG5* transcription in Arabidopsis was regulated by the intracellular sucrose concentration.

3.4.14.2 *SIG5* promoter-driven transient expression in tobacco upon sucrose feeding

The sucrose responsibilities of the distal and the proximal Arabidopsis *SIG5* promoter (for definition see fig. 3-27) were analyzed in more detail by promoter-reporter gene analyses. As previously described, the promoter fragments were fused to $\Delta 35S$ promoter and *GFP::GUS* reporter gene. Both promoter fragments were analyzed for their ability to mediate transcription of reporter genes when transiently expressed in tobacco leaves.

Analysis of osmotic control treatments

For carbohydrate treatment, the tobacco leaves were transferred to tap water supplemented with 2 % (w/v) sucrose. As osmotic control, tap water supplemented with 4 % (w/v) sorbitol was used. 4 % sorbitol mimicked the osmotic effect of 2 % sucrose in the cells, which is intracellularly cleaved into glucose and fructose (Copeland, 1990). In contrast to glucose and fructose, sugar alcohols like sorbitol and mannitol were usually not metabolized by plants (Thorne *et al.*, 2008). As a result, the leaves incubated with 4 % sorbitol started wilting immediately after treatment (data not shown). To test whether the treatment with 4 % sorbitol induced senescence, the Chl contents of the leaves were determined (Seltmann *et al.*, 2010). The total Chl content of leaves treated with 4 % sorbitol was significantly reduced (fig. 3-63). In contrast, the treatment with 2 % sucrose did not influence the Chl content of the leaves.

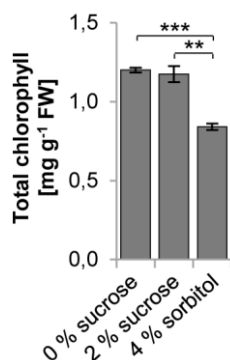


Figure 3-63. Total Chl content of tobacco leaves upon treatment with external carbohydrates. The plants were illuminated with 100-120 $\mu\text{mol photons m}^{-2} \text{s}^{-1}$ continuous white light. The leaves were removed from the plant under water using a razor blade and transferred to tap water without or supplemented with 2 % (w/v) sucrose or 4 % (w/v) sorbitol. After 2 d the chlorophyll content was quantified spectrophotometrically. The data are means of three replicates (\pm SEM). One-way ANOVA was performed comparing all groups with Bonferroni's post-test. Statistical significance of difference is indicated as asterisks above bars. (** $p < 0.01$, *** $p < 0.001$)

The reduced Chl levels demonstrated that treatment with 4 % sorbitol induced senescence of the leaves. Alternatively, the leaves were treated with 2 % (w/v) mannitol. Similar to the sorbitol treated leaves, also the leaves incubated with mannitol started wilting. Consequently, the tobacco leaves treated with the osmotic controls sorbitol or mannitol were not further analyzed. In the following the GFP fluorescence values of infiltrated tobacco leaves incubated with 2 % sucrose in tap water were compared with GFP fluorescence values of leaves incubated with tap water.

Transient expression in tobacco upon sucrose feeding

Tobacco leaves were infiltrated with the same volumes of *Agrobacterium* solutions with the same titer. 2 d after the infiltration, the leaves were cut under water with a razor blade and transferred to tap water. 4 d after the infiltration, the GFP fluorescence was observed under UV illumination. The GFP fluorescence of leaves incubated in tap water supplemented with 2 % sucrose were slightly diminished when driven by the distal *SIG5* promoter, compared with the GFP fluorescence levels of leaves incubated without sucrose (fig. 3-64). The GFP fluorescence intensity regulated by the proximal *SIG5* promoter fragment was slightly enhanced upon sucrose treatment.

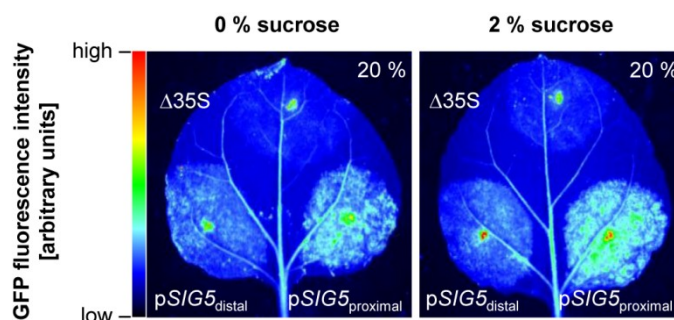


Figure 3-64. GFP expression driven by *SIG5* promoter fragments upon sucrose feeding in tobacco. Proximal or distal Arabidopsis *SIG5* promoter sequences were fused to $\Delta 35\text{S}$ promoter and GFP. The GFP was transiently expressed in tobacco leaves. The plants were illuminated with 100-120 $\mu\text{mol photons m}^{-2} \text{s}^{-1}$ continuous white light. 2 d after infiltration the leaves were cut under water with a razor blade and transferred to tap water. For sucrose treatment the tap water was supplemented with 2 % (w/v) sucrose. 4 d after infiltration the GFP fluorescence was observed under UV illumination with percentage representing the sensitivity of the detector. False color code depicts fluorescence intensity. The experiment was repeated once, the picture is representative.

The reduction of transcription initiation frequency was hard to detect with *GFP* as reporter gene, due to the relatively high stabilities of *GFP* mRNA as well as GFP proteins (Corish and Tyler-Smith, 1999; Sacchetti *et al.*, 2001). To further characterize the sucrose sensitivity of the distal and proximal *SIG5* promoter regions with special focus to the osmotic effect of sucrose treatment, transcript levels were quantified in a subsequent approach using Arabidopsis ET line N9313.

3.4.14.3 Impact of carbohydrates on *GFP* and *SIG5* transcript level

To determine the influence of carbohydrates on *GFP* and *SIG5* transcript level, N9313 and wild-type seedlings were treated with different sucrose concentrations and transcript levels were quantified. 10 d old seedlings, grown on MS medium without carbohydrates under 50 $\mu\text{mol photons m}^{-2} \text{s}^{-1}$ continuous white light, were transferred to MS medium supplemented with 2 % (w/v) sucrose, or as osmotic controls to MS medium supplemented with 2 % (w/v) or 4 % (w/v) sorbitol. 2 % and 4 % sorbitol mimicked the osmotic effect of the applied 2 % sucrose on the apoplast and the symplast, respectively. After 48 h incubation time the transcript levels were quantified by qRT-PCR.

The mRNA level of the nuclear encoded small subunit of RubisCO (*RBCS*) in Arabidopsis has been shown to decrease upon elevated sucrose levels (Cheng *et al.*, 1992; Oswald *et al.*, 2001). To verify that the chosen treatment conditions were effectively influencing mRNA abundances of nuclear encoded photosynthetic genes, the *RBCS* transcript levels of the seedlings were quantified. The *RBCS* transcript levels of the seedlings were diminished to 56 % upon 48 h sucrose feeding (fig. 3-65 A), indicating an inhibition of overall photosynthesis by diminished transcription of photosynthetic genes. The quantification of *SIG5* transcript level in C24 showed that the mRNA levels were significantly reduced to 28 % after treatment with 2 % sucrose (fig. 3-65 B), similar to the *GFP* mRNA levels of N9313 seedlings (53 %; fig. 3-65 D). In contrast, the *SIG5* mRNA level of N9313 was not reduced (fig. 3-65 C). Treatments with sorbitol as osmotic control did not decrease the transcript levels, demonstrating that the reduction of transcription was not due to osmotic effects.

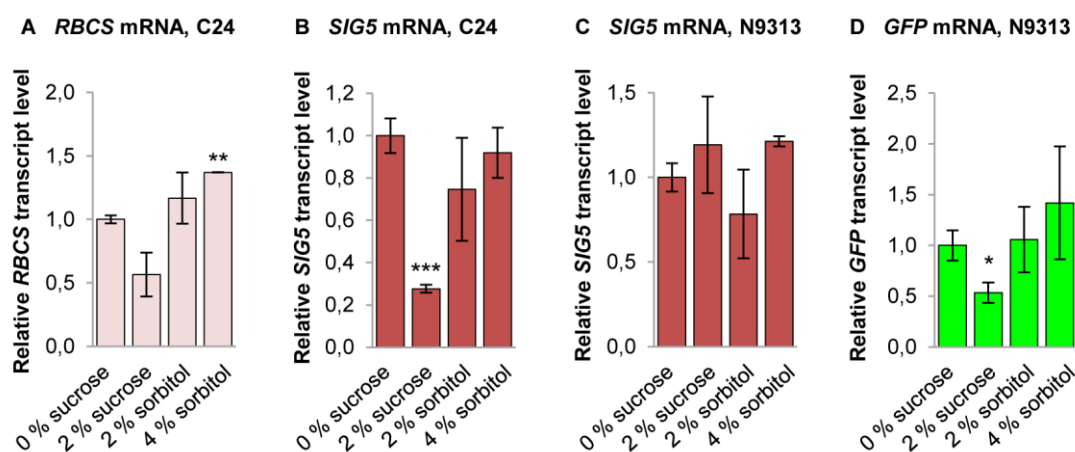


Figure 3-65. Relative transcript levels in response to exogenous carbohydrate application. 10 d old seedlings grown at $50 \mu\text{mol photons m}^{-2} \text{s}^{-1}$ constant white light on MS medium without carbohydrates were transferred to MS medium supplemented with 2 % (w/v) sucrose, 2 % (w/v) sorbitol or 4 % (w/v) sorbitol for 48 h. The relative transcript abundances were determined by qRT-PCR relative to *ACT2* transcript levels. The transcript level of 12 d old seedlings grown on MS medium without carbohydrates was set to 1.0. The data are means of 2 (*RBCS* values, 4 % sorbitol values), 3 (*SIG5*, C24) or 4 replicates (\pm SEM). ** indicates significant differences from the reference without carbohydrates (Student *t*-test, * $p < 0.05$, ** $p < 0.01$, *** $p < 0.001$).

The previous experiments demonstrated that the Arabidopsis *SIG5* promoter regulated transcription in response to exogenously applied sucrose. Analyses of C24 as well as N9313 seedlings showed that this regulation was mediated by distal regions of the *SIG5* promoter. The truncated *SIG5* promoter of N9313 did not respond to sucrose, whereas the activation mediated by the distal promoter, regulating *GFP* transcription, was inhibited.

These analyses demonstrated that Arabidopsis *SIG5* was regulated by photosynthesis on different levels. The redox state of the plastid PQ pool was assumed to modulate transcription initiation from the distal as well as from the proximal *SIG5* promoter (chapter 3.4.12). The inhibition of transcription by sucrose was connected with overall photosynthesis rate (reviewed in Rolland *et al.*, 2006).

As the regulatory elements mediating sucrose responses were located upstream of the T-DNA insertion site of N9313, the 0.8 kb distal *SIG5* promoter upstream of the T-DNA was analyzed *in silico* for the presence of sucrose-sensitive *cis*-acting elements. The analyses with PlantCARE (Rombauts *et al.*, 1999) and PLACE (Higo *et al.*, 1999) databases showed that no known sucrose or sugar-sensitive *cis*-acting element was located within this sequence. However, two ABRE-elements, involved in ABA responses, and an ethylene-responsive ERE-element were predicted (tab. 3-10).

Table 3-10. Phytohormone-responsive *cis*-acting elements identified in 0.8 kb upstream of the T-DNA insertion site of N9313 as predicted by PlantCARE and PLACE databases.

Motif	Sequence ^a	Position ^b	Description
ABRE	CACGTG (+) ACGTGGC (-)	-1800 to -1794 -1727 to -1720	<i>cis</i> -acting element involved in the ABA responsiveness
ERE	ATTTCAA (-)	-1757 to -1749	Ethylene responsive element

^a(+) and (-) indicates the sense and complementary strand, respectively

^bpositions are relative to the translation start site of *SIG5*

ABA as well as ethylene were stress hormones that interacted with sugar sensing (reviewed in Leon and Sheen, 2003) and photosynthetic redox sensing in plants (Oswald *et al.*, 2001). The identification of ABA and ethylene responsive motifs in the sucrose-sensitive distal *SIG5* promoter indicated, that these phytohormones connected the sucrose-mediated modulation of photosynthesis with the regulation of *SIG5* transcription.

3.4.15 Impact of general stress on *GFP* and *SIG5* transcription

In addition to the induction of *SIG5* transcription by light (Tsunoyama *et al.*, 2002; Mochizuki *et al.*, 2004; Onda *et al.*, 2008), *SIG5* transcripts also responded to various stress conditions, such as low temperature, high salt and high osmotic conditions (Nagashima *et al.*, 2004b). To further characterize the Arabidopsis *SIG5* promoter, the stress response of the *SIG5* promoter was analyzed.

According to Nagashima *et al.* (2004b) the effects of cold stress on illuminated plants was analyzed. Seedlings of N9313 and the wild-type C24 were grown for 10 d (on MS medium lacking sucrose, with 50 $\mu\text{mol photons m}^{-2} \text{s}^{-1}$ of continuous light at 23 °C) and then transferred to 4 °C for 1 h. The seedlings were still illuminated during the cold treatment. Samples taken prior to the temperature shift served as unstressed references. The cold treatment resulted in a 53-fold accumulation of *SIG5* transcripts in C24 (fig. 3-66 A) and an 80-fold accumulation in N9313 (fig. 3-66 B) in this 1 h treatment. According to the *SIG5* mRNA, the *GFP* transcripts of N9313 accumulated (8-fold; fig. 3-66 C).

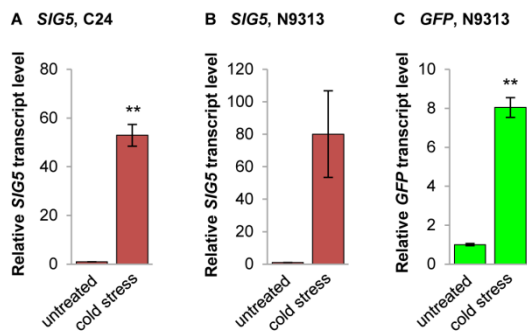


Figure 3-66. Relative *SIG5* transcript level in cold stressed C24 wild-type (A) and *SIG5* and *GFP* transcript levels in N9313 (B and C). The seedlings were grown on MS medium without sucrose at 23 °C illuminated with 50 $\mu\text{mol photons m}^{-2} \text{s}^{-1}$ continuous white light. 10 d old seedlings were shifted to 4 °C for 1 h. Relative transcript levels were determined by qRT-PCR relative to *ACT2* transcript level. The transcript levels of seedlings prior to the light shift were set to 1.0. Results are mean values of 2 biological replicates (\pm SEM). ** indicates significant differences (Student *t*-test, $p < 0.01$).

The best analyzed function of *SIG5* was controlling transcription of *psbD* (Christopher and Mullet, 1994; Hoffer and Christopher, 1997; Tsunoyama *et al.*, 2002, 2004; Nagashima *et al.*, 2004b). Various stress conditions like the combination of cold and light resulted in light-induced PSII inactivation (photoinhibition, Giardi *et al.*, 1997). It was assumed that environmental stress was linked to the repair of PSII damages via *SIG5* (Nagashima *et al.*, 2004b). The induction of *SIG5* and *GFP* transcription in N9313 demonstrated that in both, distal as well as proximal *SIG5* promoter regions, enhancer elements were located, which responded to such environmental stress conditions.

4

DISCUSSION

4.1 The identification of *cis*-elements by screening ET lines

A total collection of 401 *Arabidopsis thaliana* *GAL4-GFP* lines has been generated in the lab of Jim Haseloff (Laplaze *et al.*, 2005). 116 lines are available at the European Arabidopsis Stock Centre (NASC; <http://arabidopsis.info>). To identify light-regulated *cis*-acting promoter elements, 62 lines (Haseloff, 1999; Laplaze *et al.*, 2005) are screened for light dependent reporter gene expression. The GFP fluorescence of different ET lines is of different intensity (fig. 3-1) and in some lines undetectable. Additionally, the GFP fluorescence is located to different tissues in the different ET lines analyzed (fig. 3-2, 3-8 and 3-14). This demonstrates that the *GAL4-GFP* T-DNA itself is unable to induce reporter gene expression and the GFP fluorescence of the ET lines is under control of distinct *cis*-acting regulatory promoter elements.

The screen identifies seven lines whose GFP fluorescence intensity positively or negatively correlates with the light intensity during growth of the seedlings (fig. 3-1). These correlations between light intensity and GFP fluorescence indicate that light-sensitive *cis*-acting elements are located nearby the insertion sites of the ET T-DNAs. The three ET lines that show the highest GFP values (<0.2) are chosen for further analysis: N9249, N9266 and N9313. The high-level GFP fluorescence indicates a control by highly active light-responsive *cis*-acting promoter motifs.

4.2 Enhancer trap N9249

4.2.1 The genome of N9249 contains multiple ET T-DNA insertion sites

The GFP fluorescence values of ET line N9249 correlate with light intensity during growth, indicating that the reporter gene is under the control of a light-responsive enhancer element. The relative GFP fluorescence of N9249 is of medium intensity, compared with the other ET lines (fig. 3-1). The number of T-DNA insertion sites in ET N9249 is determined by Southern blot analysis and results in several fragments on the blot after hybridization (fig. 3-7). In general, multiple fragments on the blot indicate multiple T-DNA insertion sites in the

nuclear genome. As only a single T-DNA insertion site is identified in N9249 by TAIL-PCR, the different fragments on the Southern blot are analyzed in more detail to check whether other reasons than multiple insertion sites can explain the fragment pattern. The *GAL4* probe sequence is analyzed by BLASTN for unspecific binding to wild-type sequences. Unspecific binding is predicted to be implausible. Genomic DNA of wild-type C24 is used as control and does not lead to detectable DNA fragments. Therefore the observed hybridization signals on the Southern blot are due to specific hybridization of the probe with the ET T-DNA sequence.

Cleavage of the DNA with *ApoI* causes nine different fragment sizes on the blot. The different signal intensities on the blot indicate an even larger number of different DNA fragments, as fragments with similar length will overlap on the blot, what increases the hybridization signal strength compared to proximate fragments. Due to the possibility of star activity of *ApoI*, the restriction time is limited; therefore the multiple fragments are expected to be caused by incomplete cleavage. By contrast, the cleavage with *BglII* is completed (as demonstrated by the *BglII* restriction of N9313 DNA, fig. 3-19 A); therefore the three DNA fragments on the blot which appear after restriction of N9249 DNA with *BglII* indicate up to three different T-DNA insertion sites in the genome of N9249.

An *in silico* restriction analysis of the mapped T-DNA insertion site of N9249 allows the assigning of some fragments on the blot (fig. 3-7, black triangles). The *in silico* restriction analysis is performed with sequence information from reference accession Columbia (Col-0), available in The Arabidopsis Information Resource (TAIR) database of genetic and molecular data from *Arabidopsis thaliana* (TAIR10, www.arabidopsis.org; Huala *et al.*, 2001; Lamesch *et al.*, 2012). As the ET lines are produced in C24 background, the Col-0 reference nucleotide sequence is compared with the C24 nucleotide sequence. The 1001 Genomes project recently released the whole genome sequence of C24 (www.1001genomes.org; Cao *et al.*, 2011; Schneeberger *et al.*, 2011). As a result of comparison, polymorphisms between the accessions do not cause additional *ApoI* or *BglII* restriction sites adjacent to the identified T-DNA insertion of N9249. It is concluded, that two to three different ET T-DNAs are inserted in the genome of N9249.

4.2.2 Connections between GFP fluorescence pattern and the mapped T-DNA insertion site

Although the genome of N9249 contains multiple T-DNA insertion sites one can assume that there is a connection between the identified insertion site and the GFP fluorescence pattern of N9249. It is possible, that the unidentified T-DNAs are inserted far-away to enhancer elements. In that case, the identified T-DNA of N9249 is probably the only one that contributes to the GFP expression of N9249.

The identified ET T-DNA of N9249 is inserted between the genes At5g57560 and At5g57565 (fig. 3-5). At5g57560 or *TCH4* is annotated by TAIR database as xyloglucan

endotransglucosylase XTH22, a cell wall modifying enzyme with function in the process of cell expansion (Fry *et al.*, 1992). *TCH4* expression is rapidly regulated in response to environmental stimuli. *TCH4* expression is upregulated by darkness (Xu *et al.*, 1995; Xu *et al.*, 1996). *TCH4* is highly expressed in developing tissues like young expanding leaves, emerging lateral root primordia, root tips, elongating hypocotyls or developing siliques (Xu *et al.*, 1995). GFP fluorescence in 10 d old N9249 seedlings is mainly localized in the epidermis and with a weaker intensity also in the root (fig. 3-2), but it is not detectable in the leaf and hypocotyl mesophyll or root tips. Therefore there is no obvious connection between the *TCH4* expression pattern and the GFP fluorescence pattern of N9249. The same is true for the second gene adjacent to the identified T-DNA insertion site of N9249, At5g57565. At5g57565 is annotated to encode a protein kinase with putative serine/threonine kinase activity. There is no information available about regulation or expression pattern of this enzyme: At5g57565 has been discovered and added to the *Arabidopsis thaliana* genome in 2004, whereas DNA chips and microarrays are available from 1999 on. At5g57565 is not part of the commonly used Affymetrix ATH1 Whole Genome GeneChip that bases on information from the international Arabidopsis sequencing project that has been formally completed in the year 2000.

4.2.3 Conclusions on N9249

Southern blot analysis demonstrated that up to three different ET T-DNA insertions are located at different positions in the genome of N9249. Due to these divers T-DNA insertions, divers TAIL-PCR products are expected. However, the TAIL-PCR conditions chosen (appendix 6.1) amplify a single TR3.2-AD1 specific fragment. It has not been possible to adapt the TAIL-PCR protocol in a way that additional specific TR3.2-AD products have been amplified. Therefore it has not been possible to localize more than one T-DNA insertion site in the genome of N9249. The analysis of the two genes adjacent to the mapped ET T-DNA insertion site of N9249 does not reveal an evident connection to the GFP fluorescence pattern of N9249. Backcrossing with C24 will allow the separation of the multiple ET T-DNA insertions and therefore the identification of the *cis*-acting elements that are responsible for the observed light-dependent GFP fluorescence pattern on N9249.

4.3 Enhancer trap N9266

4.3.1 Two T-DNAs are inserted in the genome of N9266

The GFP fluorescence values of ET line N9266 positively correlate with light intensity during growth. The relative GFP fluorescence values reach medium to high levels of up to 0.35, with significant differences between the light intensities analyzed (fig. 3-1). According to ET N9249, several fragments are detected on the Southern blot after hybridization with a DIG-labeled *GAL4* probe (fig. 3-13). The cleavage with *Bgl*III restriction enzyme results in two fragments of different sizes, indicating two different T-DNA insertion sites. The number

of fragments after cleavage with *ApoI* is even higher, 14 different fragment sizes are detected. As discussed previously, *ApoI* restriction is supposed to be incomplete or unspecific, resulting in such a high number of DNA fragments. The identified T-DNA insertion site on chromosome 1 allowed the assignment of most of the DNA fragments on the blot (fig. 3-13, black triangles). However, *Bg/III* cleaved DNA shows an additional fragment of about 4 kb size that cannot be explained by the identified T-DNA insertion site nor by sequence polymorphisms between the Arabidopsis accessions Col-0 and C24 (tested with www.1001genomes.org). This fragment indicates a second T-DNA insertion site at unknown position in the genome of N9266.

4.3.2 Connections between the identified T-DNA insertion site and the GFP fluorescence

The mapped T-DNA of N9266 is not inserted in a promoter but in an intergenic region between At1g79110 and At1g79120 (fig. 3-11). As *cis*-elements are not restricted to the 5'-non-coding sequence but can be located downstream of the CDS (Wray, 2007), it is discussed whether the expression pattern of At1g79110 and At1g79120 reflect the GFP fluorescence pattern of N9266. At1g79110 is annotated as *BGR2*, one of the BOI-related genes (BRGs) involved in resistance to the plant pathogen *Botrytis cinerea*. *BGR2* transcript levels offer a diurnal rhythm but are not light inducible (Smith *et al.*, 2004; Bläsing *et al.*, 2005; Edwards *et al.*, 2006). Microarray experiments showed that *BGR2* is predominantly expressed in cauline leaves (Schmid *et al.*, 2005), but not in mesophyll and epidermis cells of the cotyledon where the GFP fluorescence of N9266 is expressed (fig. 3-8). The second gene adjacent to the mapped T-DNA insertion site, At1g79120, is annotated by TAIR database as an ubiquitin carboxyl-terminal hydrolase family protein, a predicted but not characterized protein. The expression profile of this gene is analyzed using the web-based software tool Genevestigator (www.genevestigator.com; Hruz *et al.*, 2008). Genevestigator is a gene expression search engine that processes data from public experiments. The analysis shows At1g79120 transcript level increases with the age of the plant. At1g79120 transcripts are most prominent in rosette leaves, but not light-dependent induced. As there is no obvious connection between the regulation of *BGR2* or At1g79120 expression and the GFP fluorescence pattern of N9266 it is concluded, that probably the second, not localized T-DNA in the genome of N9266 is under the control of light-regulated *cis*-acting elements.

4.3.3 Conclusions on N9266

There is no obvious correlation between the light-dependent expression of the N9266 reporter gene in the mesophyll cells of the seedlings and in the leaf and hypocotyl epidermis (fig. 3-8) and the expression pattern of the two genes adjacent to the identified T-DNA insertion, *BGR2* and At1g79120. Southern blot analysis demonstrates that an additional ET T-DNA is inserted in the genome of N9266. The localization of the second T-DNA insertion site failed as it has not been possible to adapt the TAIL-PCR protocol in a way that a second

TR3.2-AD primer specific TAIL-PCR product has been amplified for N9266, even in combination with different AD primers. Similar to N9249, backcrossing with C24 will enable the separation of the two ET T-DNA insertions. This will permit the identification of the *cis*-acting elements that probably are responsible for the observed light-dependent GFP fluorescence pattern on N9266.

4.4 Enhancer trap N9313

The ET line N9313 shows the most pronounced light-dependent GFP fluorescence of the ET lines analyzed, reaching the highest relative values of up to 0.4 (fig. 3-1). The differences between the light intensities analyzed are significant discriminative with *p* values of <0.001. A single ET T-DNA is inserted in the genome of N9313 (fig. 3-19), indicating that the GFP fluorescence is regulated by light-sensitive *cis*-acting elements adjacent to the mapped T-DNA. The T-DNA insertion site of ET N9313 is localized in the promoters of *SIG5* and *At5g24130* (fig. 3-17).

The inserted T-DNA is located about 2 kb downstream of the translation start site of *At5g24130* in reverse orientation (fig. 3-17). As the functionality of palindromic as well as most non-palindromic *cis*-acting promoter elements shows no effect based on orientation (Geisler *et al.*, 2006) the reverse orientation of the T-DNA cannot exclude the possibility that the observed GFP fluorescence pattern are due to promoter motifs regulating *At5g24130* expression. *At5g24130* is annotated in the TAIR database to encode a protein with unknown function (www.arabidopsis.org). The protein is predominantly expressed in developing seeds during embryogenesis and in petals during differentiation and expansion stage (Schmid *et al.*, 2005). It is predicted to be located in mitochondria (Haezlewood *et al.*, 2005, 2007). Microarray analyses do not detect any correlation between *At5g24130* transcription and light (Smith *et al.*, 2004; Blaesing *et al.*, 2005; Edwards *et al.*, 2006; Covington and Harmer, 2007; Michael *et al.*, 2008). In summary, a correlation between the regulation of *At5g24130* expression and the N9313 GFP expression is not detectable. Therefore the discussion of possible connections between N9313 GFP fluorescence and *At5g24130* is disregarded in the following.

4.4.1 The chloroplast gene expression system

Sigma factors are subunits of plastid RNA polymerases and required for recognition of promoter elements. Chloroplasts have their own gene expression system, and both transcriptional and post-transcriptional mechanisms participate in the regulation of organellar gene expression during development and in response to environmental cues (Mullet, 1993; Stern *et al.*, 1997; Maliga, 1998). In plastids transcription is performed by two different types of DNA-dependent RNA polymerases. One is the nuclear-encoded polymerase (NEP), a monomeric enzyme of the T7 bacteriophage-type (Hedtke *et al.*, 1997). Another enzyme is the multimeric eubacteria-type RNA polymerase,

called plastid-encoded polymerase (PEP) (Hu and Bogorad, 1990; Hedtke *et al.*, 1997; Liere and Maliga, 2001). PEP is mainly involved in transcribing genes engaged in photosynthesis and genes with housekeeping functions of chloroplasts (Hajdukiewicz *et al.*, 1997; Krause *et al.*, 2000; Legen *et al.*, 2002). PEP is a multi-subunit enzyme with plastid-encoded catalytic core subunits ($\alpha_2\beta\beta'\beta''$) (Hu and Bogorad, 1990; Allison *et al.*, 1996; Serino and Maliga, 1998) that perform the elongation step of RNA synthesis. This core polymerase is able to bind the promoter and to initiate transcription only when completed with a nuclear-encoded transcription initiation factor of the σ^{70} type (Sugiura, 1989). In Arabidopsis the activity of PEP is regulated by six different sigma factors, encoded by *SIG1* to *SIG6* (Isono *et al.*, 1997a; Tanaka *et al.*, 1997; Allison, 2000; Fujiwara *et al.*, 2000), also designated as *AtSig1* to *AtSig6* (Fujiwara *et al.*, 2000, Tsunoyama *et al.*, 2004), *AthSig1* to *AthSig6* (Liere *et al.*, 2011) or *SigA* to *SigE* (Tanaka *et al.*, 1997; Kanamura *et al.*, 1999). The heterogeneity of the sigma factors is responsible for transcriptional activation of different sets of genes in response to developmental and environmental signals (Liu and Troxler, 1996; Tan and Troxler, 1999).

4.4.2 SIG5 function in Arabidopsis

SIG5 encodes a mature protein of 517 amino acids (Fujiwara *et al.*, 2000). The best analyzed function of *SIG5* (also designated as sigma factor ϵ) is controlling plastid transcription of *psbD* (Nagashima *et al.*, 2004b; Tsunoyama *et al.*, 2004) and *psbA* (Tsunoyama *et al.*, 2004; Kubota *et al.*, 2007). These genes encode the PSII reaction center core proteins, D2 and D1. The D1 and D2 proteins are subject to photodamage under high-irradiance light, a process called photoinhibition. Photoinhibition is the light-driven damaging of the photosynthesis machinery, leading to degradation of the PSII reaction center core proteins and their *de novo* synthesis (reviewed in Tyystjärvi, 2008). The D1 protein is the main target of photoinhibition, and as a consequence the D1 protein turns over at a rate considerably faster than any other PSII subunit (Mattoo *et al.*, 1989), and proportional to light intensity (Baroli and Melis, 1996). The D2 protein also shows a light-induced turnover (Christopher and Mullet, 1994; Prasil *et al.*, 2012) and is degraded under UV light (Trebst and Depka, 1990; Jansen *et al.*, 1996; Turcsányi and Vass, 2000; Szilárd *et al.*, 2007). The *de novo* syntheses of the D1 but also the D2 protein are an essential process of the PSII photoinhibition-repair cycle (Schuster *et al.*, 1988; Stern *et al.*, 1997).

SIG5 function is not limited to regulate photosynthetic gene expression. During flowering, a longer *SIG5* protein is synthesized from an alternative translational start codon (Fujiwara *et al.*, 2000) by alternative splicing (Yao *et al.*, 2003). This longer *SIG5* protein is targeted to both mitochondria and plastids of flowers (Yao *et al.*, 2003). The shorter *SIG5* protein is exclusively targeted to chloroplasts, when transiently expressed in leaf cells (Yao *et al.*, 2003). In mitochondria, *SIG5* is interacting with ANK6, an ankyrin repeat protein essential for fertilization, specifically for gamete recognition (Yu *et al.*, 2010). It is suggested

that *SIG5*, like *ANK6*, has a central function in ovule development and fertilization (Yu *et al.*, 2010).

4.4.3 Blue light regulation of *SIG5* transcription

In contrast to most of the plastid-encoded photosynthesis genes, expression of *psbA* and *psbD* is activated at the level of transcription in response to light, and serves to maintain high rates of synthesis of D1 and D2 and PSII activity under high-light conditions (Greenberg *et al.*, 1989; Klein and Mullet, 1990). Higher plant *psbD* genes are located in an operon that includes *psbC* (encoding PSII component CP43) and is transcribed from multiple promoters (Hoffer and Christopher, 1997). In mature leaves, the *psbD* operon is predominantly transcribed from the *psbD* blue-light-responsive promoter (BLRP), which is selectively activated by illumination with high-fluence blue/UV-A light (Gamble and Mullet, 1989; Christopher and Mullet, 1994). *SIG5* specifically recognizes the *psbD*-BLRP (Nagashima *et al.*, 2004b; Tsunoyama *et al.*, 2004; Onda *et al.*, 2008). Blue light extensively induced *SIG5* transcript abundances in rosette leaves of 4 weeks old Arabidopsis plants (Tsunoyama *et al.*, 2002; Mochizuki *et al.*, 2004; Onda *et al.*, 2008). This blue light induction of *SIG5* is regulating *psbD* transcription via recognition and initiation of transcription from the *psbD*-BLRP (Nagashima *et al.*, 2004b; Tsunoyama *et al.*, 2004).

Whereas the structure of the *psbD* promoter has been subject of several analyses (Gamble and Mullet, 1989; Christopher and Mullet, 1994; Allison and Maliga, 1995; Hoffer and Christopher, 1997; Kim *et al.*, 1999a; Thum *et al.*, 2001b), the structure of the promoter of *SIG5* is not analyzed so far. The N9313 T-DNA insertion within the promoter of *SIG5* provides an opportunity to analyze the *SIG5* promoter structure in more detail. N9313 is used for promoter analysis with the aim to differentiate between distal and proximal sensed signals regulating light-dependent transcription of *SIG5*.

4.4.3.1 196 bp of the proximal *SIG5* promoter mediate the main blue light sensitivity of *SIG5*

The blue light induction of *GFP* and *SIG5* transcript levels of N9313 is used to locate the blue light sensitive *cis*-acting elements of the *SIG5* promoter. It is shown that the distal *SIG5* promoter is slightly blue light sensitive (fig. 3-22) whereas the 1.2 kb promoter region downstream of the T-DNA insertion site of N9313 mediates the accumulation of transcripts upon illumination with monochromatic blue light (fig. 3-23 B). With respect to the 5-fold shorter decay rate of *SIG5* transcripts compared to the decay rate of *GFP* transcripts (fig. 3-24), the blue light activation of the *SIG5* promoter largely contributes to the proximal promoter region. The quantification of *SIG5* transcripts of different SALK T-DNA insertion lines demonstrates, that the key blue light sensitive region of the *SIG5* promoter is located in the 196-bp sequence between the nucleotides -887 and -691 relative to the translation start site of *SIG5* (fig. 3-30). An *in silico* analysis of this 196-bp sequence by PlantCARE and PLACE predicts five different light-sensitive motifs: two GATA motifs, an ACE-motif, a

GA-motif and an I-box (tab. 3-3). It is assumed that the blue light induction of *SIG5* transcription is mediated by these *cis*-acting elements. Among these elements, GATA-motifs and I-boxes are particular common elements of light-regulated promoters (Argüello-Astorga and Herrero-Estrella, 1998; Martínez-Hernández *et al.*, 2002). Therefore the two GATA-motifs and the I-box most likely mediate the main blue light sensitivity of the Arabidopsis *SIG5* promoter. It is supposed that the predicted motifs act combinatorial, as solely elements fail in mediating light responses (Geisler *et al.*, 2006; López-Ochoa *et al.*, 2007).

4.4.3.2 *cry1* and *cry2* are the UV-A/blue light photoreceptors mediating the main blue light induction of *SIG5*

Higher plants display two types of chloroplast relocalization responses: A chloroplast accumulation response that maximizes light capture in low light, and a chloroplast avoidance response that minimizes chloroplast photodamage in high light (Wada *et al.*, 2003). *Phot2* is responsible for the chloroplast avoidance response, whereas *phot1* acts redundantly with *phot2* to achieve the accumulation response (Jarillo *et al.*, 2001; Kagawa *et al.*, 2001; Sakai *et al.*, 2001). The *phot2*-mediated chloroplast-avoidance response is of critical importance for plant survival in high light conditions (Kasahara *et al.*, 2002). Hence it is postulated that phototropins may act as regulators of light-dependent *SIG5* transcription in Arabidopsis seedlings. This study demonstrates that in cotyledons the phototropins *phot1* and *phot2* are not involved in regulating *SIG5* transcription. The GFP fluorescence values of N9313 in *phot1phot2* mutant background corresponds to N9313 values (fig. 3-37); similarly the *SIG5* transcript levels of *phot1* and *phot1phot2* mutants corresponds to wild-type levels after blue light illumination (fig. 3-38 A). The blue light induction of *SIG5* transcription in rosette leaves of Arabidopsis is also mediated by cryptochromes rather than by phototropins (Onda *et al.*, 2008).

In contrast to phototropins, the cryptochromes *cry1* and *cry2* influence *SIG5* transcription in seedlings. The full-length *SIG5* promoter is regulated by *cry1* rather than by *cry2*; the blue light induction of *SIG5* transcription is not reduced in *cry2* mutants, whereas *cry1* mutants accumulate only very reduced *SIG5* transcript level, similar to *cry1cry2* double mutants (fig. 3-38 B). The analysis of *SIG5* transcript level of N9313 in *cry1cry2* mutant background demonstrates that the blue light induction of transcription is predominantly mediated via the proximal *SIG5* promoter: The blue light induction of *SIG5* transcription controlled by the proximal promoter is impaired to similar levels in these seedlings (8 % in comparison with N9313; fig. 3-39 B) compared with *cry1cry2* mutants (9 % in comparison with *Ler*; fig. 3-38 B). This means that the full-length *SIG5* promoter, as present in the *cry1cry2* mutant, is similarly impaired by the *cry1cry2* mutation than the proximal *SIG5* promoter, defined by the T-DNA insertion of N9313. These data is consistent with the previous findings, that the blue light sensitivity of the *SIG5* promoter is mainly located in proximal regions downstream of the T-DNA insertion site of N9313. It is concluded, that the identified proximal blue light sensitive 196-bp sequence (4.4.3.1) is regulated by *cry1* under the high blue light intensities analyzed. This predominant role of *cry1* for regulation of *SIG5*

transcription in seedlings is consistent with the previous analyses of adult *Arabidopsis* plants: Both *cry1* and *cry2* function as photoreceptor for *SIG5* in rosette leaves (Mochizuki *et al.*, 2004; Nagashima *et al.*, 2004b), but *cry2* mediates transcription only at low fluence rates ($5 \mu\text{mol photons m}^{-2} \text{s}^{-1}$ blue light) (Onda *et al.*, 2008). In line with those findings, the blue light induction of the *psbD*-BLRP is mediated by *cry1* and *cry2* but not *phot1* (Thum *et al.*, 2001a).

The distal *SIG5* promoter is regulated differentially by blue light. The GFP fluorescence levels of N9313 in *cry1cry2* mutant background are significantly decreased. As the single *cry1* mutation has only little effect on GFP fluorescence (fig. 3-37), this indicates that *cry2* has a predominant role in regulating the blue light sensitivity of the distal *SIG5* promoter. The *cry2* photoreceptor is a light-labile protein (Mockler *et al.*, 2003), which is proteolytically degraded in the light (Shalitin *et al.*, 2002). The seedlings are grown at $120 \mu\text{mol photons m}^{-2} \text{s}^{-1}$ white light when the GFP fluorescence intensities are quantified. Under these conditions, the *cry2* photoreceptor is expected to be mostly degraded. Nevertheless the observed effect of the *cry2* mutation on the GFP fluorescence indicates that the function of *cry2* as additional regulator of the *SIG5* promoter is not limited to low light intensities.

In mature *Arabidopsis* leaves, the *cry2* mutation has no effect on accumulation of *SIG5* transcripts upon illumination with $50 \mu\text{mol photons m}^{-2} \text{s}^{-1}$ blue light for 90 min (Onda *et al.*, 2008). It must be taken into consideration, that the *cry2*-mediated regulation of *SIG5* transcription in *Arabidopsis* seedlings can exhibit kinetics different from those of the *cry1*-controlled pathway. Therefore it cannot be concluded, that the regulation of *SIG5* transcription by *cry2* under higher light intensities is absent in adult leaves.

4.4.3.3 *phyB* is essential for the blue light induction of *SIG5*

Although the red light photoreceptors are so named because they absorb red light, these pigments also absorb and respond to blue light via their so-called absorption bands (Schäfer and Haupt, 1983). Indeed, the blue light induced accumulation of *SIG5* transcription is impaired in *phyB*, but not *phyA*, mutants (fig. 3-41). This indicates a role for *phyB* but not the type I phytochrome *phyA* in regulating the blue light induction of *SIG5* transcription in seedlings. Though, primer extension analyses show that *phyA* is required for the blue light induced transcription from the *Arabidopsis psbD*-BLRP in rosette leaves (Thum *et al.*, 2001a). *PhyA* and to a minor extent *phyB* also mediate the blue light induction of *psbA* transcription (Chun *et al.*, 2001). However, these experiments do not allow conclusions according to the role of *SIG5* in regulating the expression of *psbD* or *psbA*.

In a previous work it has been mentioned that the light induced accumulation of *SIG5* transcripts is not affected in *phyA* and *phyB* mutant seedlings (Nagashima *et al.*, 2004b). Having a closer look on these data, the presented results are not in contrast to the results obtained by this study. Nagashima *et al.* (2004b) quantified transcript levels by Northern blot analysis, performed after 1.5 h to 6 h illumination of dark-adapted seedlings with

50 $\mu\text{mol photons m}^{-2} \text{s}^{-1}$ white light. Having a closer look onto the Northern blot, the accumulation of *SIG5* transcripts is attenuated after 6 h illumination in *phyB* mutants (fig. 4-1).

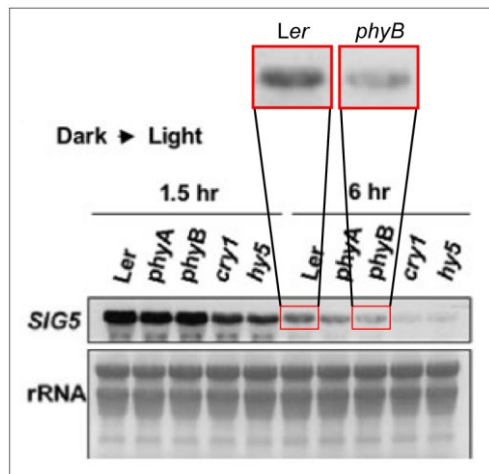


Figure 4-1. Northern blot analyses of the light induction of *SIG5* in light signal transduction mutants.

The wild-type (*Ler*) and mutant plants (*phyA*, *phyB*, *cry1* and *hy5*) were cultivated under 50 $\mu\text{mol photons m}^{-2} \text{s}^{-1}$ continuous white light for 10-11 d, dark-adapted for 30 h, and reilluminated for 1.5 or 6 h. The detail is taken from Nagashima *et al.* (2004b). The accumulation of *SIG5* transcripts is reduced after 6 h illumination in *phyB* mutants compared to the wild-type.

The accumulation of *SIG5* transcripts is impaired in *phyB* mutants upon illumination with blue, red and far-red light (fig. 3-41), and it is concluded also upon white light illumination. Therefore the qRT-PCR data of the present thesis correspond to the attenuated *SIG5* transcript level on the previously published Northern blot. This gives rise to the identification of *phyB* as photoreceptor that is involved in the blue light-mediated induction of *SIG5* transcription in Arabidopsis seedlings.

4.4.4 The modulation of *SIG5* transcription by red and far-red light

4.4.4.1 The transcription of *SIG5* is stimulated by red and far-red light

Seedlings grown under red/far-red light show increased GFP fluorescence levels compared with white light grown seedlings (fig. 3-21). Previously, the *SIG5* transcription in rosette leaves of Arabidopsis has been described as red light insensitive (Tsunoyama *et al.*, 2002, Mochizuki *et al.*, 2004; Onda *et al.*, 2008). The observed red/far-red light mediated induction of N9313 GFP fluorescence is characterized in more detail by quantification of transcript levels upon illumination with monochromatic red or monochromatic far-red light. Far-red light illumination slightly accumulates *GFP* transcript levels whereas red light induces a significant increase of *GFP* mRNA (fig. 3-22). Similarly the *SIG5* transcript levels are red- and also little far-red light induced (fig. 3-23). It is concluded that the induction of GFP fluorescence is due to transcriptional regulation of the *SIG5* promoter.

This raises the question why previous publications from the lab of Yoshinori Toyoshima do not show a red light induction of *SIG5* transcription. Thereupon the experimental procedures are modified and adapted to the conditions analyzed by Yoshinori Toyoshima (Tsunoyama *et al.*, 2002, Mochizuki *et al.*, 2004; Onda *et al.*, 2008). Growth conditions, and the durations of dark-adaptation and red light illumination are adjusted. As a

result, the red light induction of *SIG5* transcripts is not limited to seedlings but also occurs in rosette leaves of 4 weeks old plants after 24 h red light illumination (fig. 3-25). This demonstrates that the observed red light induction of *SIG5* transcripts and of *GFP* transcripts of N9313 is not limited to cotyledons or seedling development. Additionally the duration of red light illumination is reduced to 3 h, but also after 3 h illumination the red light induction of *SIG5* transcription is detectable (fig. 3-26). Therefore the mRNA accumulation occurs fast enough, that it is expected to be detectable at the time points analyzed by Toyoshimas group, ranging from 1.5 h to 5 h.

It is further analyzed whether the *Arabidopsis thaliana* accession Col-0, which is analyzed by Toyoshimas group, does not show the red light response that is observed in ET line N9313 and the corresponding genetic background, accession C24. The accessions Col-0 and *Ler* are analyzed as wild-type control of different T-DNA insertion lines and mutants, and both show a similar red light induction of *SIG5* transcription in seedlings (fig. 3-36, 3-41, 3-45). Thereupon it is assumed, that differences in the applied red light spectra cause the differences in the red light responses. However, comparison of the red light emission spectra of the LED used by Toyoshima (EYELA, LED-R) and the LED used in this study do not reveal distinct differences (fig. 4-2). The spectrum used by Toyoshima is rather broader than smaller compared with the LEDs used in the present study.

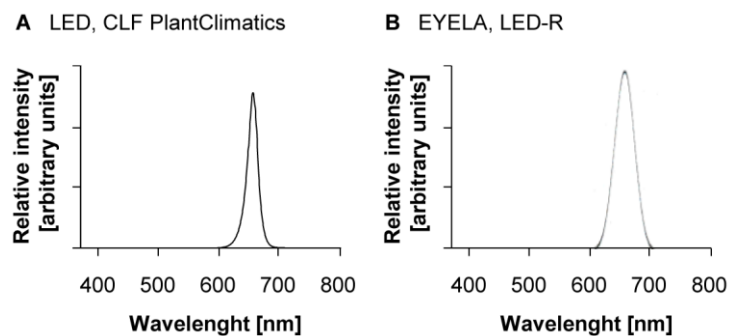


Figure 4-2. Spectra of LED panel used in FloraLED chambers (CLF PlantClimatics) and of EYELA LED-R (Tokyo Rikakikai Co. Ltd., Tokyo, Japan). Red light peaks at 673 nm and 670 nm, respectively.

The internal standards used for normalization in qRT-PCR analysis are also compared, but Mochizuki *et al.*, 2004 as well as Onda *et al.* (2008) use the same reference gene, *ACT2* (At3g18780) that is used in the present study (Tsunoyama *et al.* (2002) quantified transcript level by Northern blot analysis). In summary, it is not possible to fathom plausible reasons for the differences in the red light response of *Arabidopsis* between the analyses made in the framework of this thesis and the data previously published by the group of Yoshinori Toyoshima.

4.4.4.2 *phyA* and *phyB* mediate the red and far-red light induction of *SIG5*

The analysis of *phyA* and *phyB* mutants demonstrates that the red light induction of *SIG5* transcription is inhibited in *phyB* mutants (fig. 3-41). Although *phyA* controls Arabidopsis gene expression under continuous red light (Franklin *et al.*, 2007; Molas and Kiss, 2008), even at fluence rates higher than 50 $\mu\text{mol photons m}^{-2} \text{s}^{-1}$ (Franklin *et al.*, 2007), *phyA* is not involved in regulating *SIG5* transcription upon illumination with red light. The influence of *phyA* and *phyB* on *SIG5* transcription has previously been analyzed by Nagashima *et al.* (2004b). They do not show an influence of phytochromes on white light induced *SIG5* transcription. As discussed previously, their Northern blot analysis display attenuated *SIG5* mRNA level in *phyB* mutants (4.4.3.3), whereas *SIG5* mRNA level in *phyA* mutants correspond to wild-type levels (fig. 4-1). *PhyA* mediates the activation of photosynthetic genes like *psbA* upon far-red light illumination (Smith, 1995; Chun *et al.*, 2001; Tepperman *et al.*, 2001) and is the main photoreceptor under far-red light in Arabidopsis (Quail *et al.*, 1995; Wang *et al.*, 2002). *PhyA* is a light-labile photoreceptor (Canton and Quail, 1998; Sharrock and Clack, 2002), but continuous far-red light as applied within the frame of this thesis is known to establish a small fraction of the *phyA* population in the P_{fr} form over an extended period (Kendrick and Kronenberg, 1994). Consistent with this, the far-red light induction of *SIG5* transcription is attenuated in *phyA* mutants (fig. 3-41). Additionally, the far-red light induction of *SIG5* transcription is attenuated in *phyB* mutant seedlings (fig. 3-41). *PhyB* is described as the main red light photoreceptor (Chen *et al.*, 2004), but *phyB* is also affecting a number of responses that are mediated by far-red light (Nagatani *et al.*, 1991; Whitelam and Smith, 1991), such as developmental responses associated with the end-of-day far-red light signaling (Nagatani *et al.*, 1991).

Illumination with red light increases overall chloroplast transcription activity (Thompson *et al.*, 1983; Hoffer and Christopher, 1997) and transcription from the *psbD* light-responsive promoter (Hoffer and Christopher, 1997; Thum *et al.*, 2001a, b). During leaf-development of barley, the red light modulation of *psbD*-BLRP activity is partially reverted by far-red light (Christopher, 1996). Similarly, the blue light induction of *psbD* is partially attenuated if far-red light is given immediately following the blue light treatment (Gamble and Mullet, 1989). This implicates that phytochromes mediate the *psbD*-BLRP activity. Obviously *phyB* is expected to regulate the *psbD*-BLRP, but *phyA* is identified as regulator of the blue light-induction of *psbD*-BLRP (Thum *et al.*, 2001a); in *phyB* mutants the blue light induced transcription from the *psbD*-BLRP responds to wild-type levels (Thum *et al.*, 2001a). This indicates a unique role for *phyB* in regulating *SIG5* transcription but not *psbD* expression upon red light treatment. However, it must be mentioned that the analysis of the *psbD*-BLRP is performed with 21 d old Arabidopsis plants (Thum *et al.*, 2001a), whereas the present thesis analyzes *SIG5* expression of seedlings. Therefore it can be supposed, that the regulation of *SIG5* expression by *phyB* is limited to seedling stage of development, and consequently also the *psbD*-BLRP activity is expected to be attenuated in *phyB* mutant seedlings according to reduced *SIG5* protein levels. However, this hypothesis needs experimental evidence.

4.4.5 HY5 and COP1 are part of the network regulating *SIG5* in the light

The COP/DET/FUS complex and HY5 regulate many light-induced events in leaf and chloroplast development, and the activity of these genes is modulated by cryptochromes and phytochromes (Koornneef *et al.*, 1980; Oyama *et al.*, 1997; Whitelam and Devlin, 1998). The white light induced accumulation of *SIG5* transcription is attenuated in *hy5* deficient seedlings (Nagashima *et al.*, 2004b). Additionally, UV-B light stimulates *SIG5* transcription in a HY5/HYH dependent pathway (Brown and Jenkins, 2008; Jiang *et al.*, 2009) that is controlled by COP1 (Oravec *et al.*, 2006). In the present thesis it is shown that both the blue light and the red light induction of *SIG5* transcription are restricted in HY5 deficient seedlings (fig. 3-45).

HY5 protein stability is regulated by the COP/DET/FUS protein degradation machinery (Ang *et al.*, 1998; Holm *et al.*, 2002; Saijo *et al.*, 2003). The blue light induced transcription of the *SIG5* target gene *psbA* is also regulated by the COP1/DET/FUS complex (Ang and Deng, 1994; Kwok *et al.*, 1996; Schwechheimer *et al.*, 2002). It is shown that the *SIG5* transcript levels are considerably elevated in dark-treated *cop1* mutants compared with the wild-type (tab. 3-8). This confirms designating HY5 as regulator of *SIG5* transcription and demonstrates that COP1 is an upstream-regulator in red- and blue light regulation of *SIG5* expression.

HY5 recently is identified as regulator of cold-induced genes (Catala *et al.*, 2011). *SIG5* is regulated in response to oxidative stress, with mRNA levels being elevated upon cold treatment during illumination (fig. 3-66)⁶. *SIG5* transcription is inducible by various stress conditions, such as low temperature but also high salt and high osmotic conditions (Nagashima *et al.* 2004b). They show that salt stress-dependent *SIG5* induction is observed even in the absence of light, postulating that light and stress induction of *SIG5* are separate. About 10 % of the cold-inducible genes of Arabidopsis are regulated by HY5, with HY5 protein stability being regulated by COP1 (Catala *et al.*, 2011). In a genome-wide array with cold treated *hy5* mutants, *SIG5* transcription is not significantly reduced compared with the wild-type (Catala *et al.*, 2011). It can be assumed that HY5 is presumably not involved in the light-independent stress response of *SIG5*, supporting the findings of Nagashima *et al.* (2004b) that light and stress induction of *SIG5* are separate.

4.4.5.1 A G-box is a functional light-sensitive *cis*-acting element of the *SIG5* promoter

The red/far-red light sensitivity of the *SIG5* promoter is not restricted to a single region but is mediated by multiple light sensitive sequences with additive functions: The analyses of *GFP* and *SIG5* transcript levels of N9313, promoter-reporter gene fusions in tobacco and Arabidopsis, and the analyses of different truncations of the *SIG5* promoter by T-DNA insertions demonstrate that the elements are located in the proximal as well as in the distal *SIG5* promoter, covering at least 2 kb of the promoter (fig. 3-22, 3-23, 3-33, 3-35, 3-36). For

⁶ The role of *SIG5* under oxidative stress is discussed in more detail in chapter 4.4.6.2

red light sensing, at least three different regulatory sites are indicated (fig. 3-36 A): Enhancers are located between nucleotide position -691 and -877, as well as between position -877 and -1032, while the *SIG5* mRNA pattern indicates a suppressor elements between position -1032 and -1618. Light sensitive *cis*-acting elements are known to act combinatorial. The number, combination and spacing of different LREs determine the light-response of the respective promoter (Terzaghi and Cashmore, 1995; Puente *et al.*, 1996; Argüello-Astorga and Herrero-Estrella, 1998; Chattopadhyay *et al.*, 1998a; Geisler *et al.*, 2006). Far-red light-sensitivity of the *SIG5* promoter gradually decreases the shorter the promoter was (fig. 3-36 B), demonstrating the existence of further light responsive elements, such as the G-box located at position -1794.

The G-box binding TF HY5 is essential for the induction of *GFP* expression in N9313 (fig. 3-44). Therefore it is assumed, that the *cry2*, *phyA* and *phyB* mediated white light induction of the distal *SIG5* promoter (fig. 3-37, fig. 3-40) is controlled via HY5. Within the distal 0.8 kb sequence, 15 different light-sensitive motifs are predicted by *in silico* analysis performed with PlantCARE and PLACE (tab. 3-4). Among these are three potential HY5 binding sites, a G-box, a GC-box and a GATA-motif (tab. 3-7). Site-directed mutagenesis of these elements demonstrates that only the G-box at position -1794 is a functional motif when investigated by promoter-reporter gene analysis in tobacco (fig. 3-47). The G-box motif is involved in the red light mediated induction of transcription (fig. 3-48), indicating the regulation of G-box binding factors by *phyB*.

The HY5 binding site G-box is also a prominent hit in *phyA* regulated promoters (Hudson and Quail, 2002). The far-red light mediated induction of photosynthesis genes like *RBCS* is regulated by *phyA* and HY5 (Tepperman *et al.*, 2001). Two distinct flanking consensus sequences are identified adjacent to the G-box core sequence: one predominating in *phyA*-induced promoters (CCACGTGTCA), the other in *phyA*-repressed promoters (CCACGTGAAG) (Hudson and Quail, 2002). The nucleotides flanking the identified G-box in the *SIG5* promoter (CCACGTGTAT) do not match to these sequences. It is assumed, that the G-box is regulated by *phyB* under red light but not by *phyA* under far-red light.

The G-box is a known binding site for PIFs (reviewed in Chen and Chory, 2011). Among the PIFs, PIF3 is of special interest. Like other PIFs, PIF3 is interacting with *phyA* (Zhu *et al.*, 2000) and *phyB* (Zhu *et al.*, 2000; Leivar *et al.*, 2008) and is degraded in the light (Bauer *et al.*, 2004), but PIF3 also acts as a regulator of chloroplast development, modulating the expression of a subset of light-induced genes encoding chloroplast components (Monte *et al.*, 2004). PIF3 is interacting with ACGT-containing element (ACE-motifs) family of binding sequences, to which also G-boxes belong (Shin *et al.*, 2007). In addition to the distal G-box, three ACE-motifs are localized within the Arabidopsis *SIG5* promoter. Two ACE-motifs are located within the distal 0.8 kb *SIG5* promoter (tab. 3-3), and a third one is identified in the 196-bp blue light responsive region (tab. 3-4). These ACE-motifs are potential PIF3 binding sites that maybe are involved in regulating the light-dependent induction of *SIG5* transcription. The fact, that PIF3 is mainly involved in *phyB* signaling (Koornneef *et al.*, 1980; Ni *et al.*, 1999; Zhu *et al.*, 2000), which is identified as

key regulator of *SIG5* transcription (discussed in chapter 4.4.3.3 and 4.4.4.2), supports the hypothesis of PIF3 being a regulator of *SIG5* expression. However, this hypothesis lacks experimental confirmation.

4.4.5.2 The interaction of transcription factors with the *SIG5* promoter

The identification of a G-box as functional light-regulated *cis*-acting element enhances the assumption, that HY5 is regulating *SIG5* transcription by direct interaction with the *SIG5* promoter. Moreover, Lee *et al.* (2007) identify *SIG5* as one of about 3900 putative HY5 binding target genes by ChiP-chip analysis. However, in targeted yeast one-hybrid approach there is no direct interaction detectable between HY5 and the *SIG5* promoter (fig. 3-50). The reasons for this discrepancy between ChiP-chip and Y1H can be manifold. Possibly HY5 is not solely interacting with the *SIG5* promoter. As bZIP proteins extensively heterodimerize (Schindler *et al.*, 1992, Mallappa *et al.*, 2006), heterodimerization of HY5 with other bZIP proteins is a potential mechanism for regulating *SIG5* transcription. For example, GBF1/ZBF2 is a possible candidate for such an interaction with HY5. GBF1/ZBF2 is a G-box binding bZIP factor that differentially regulates the expression of blue light-inducible genes during photomorphogenesis, downstream of cry1 and cry2 photoreceptors (Mallappa *et al.*, 2006). In the yeast one-hybrid approach such a putative HY5 interaction partner might be missing.

Alternatively, HY5 is not physically interacting with the *SIG5* promoter but transcription factors like the HY5 regulated HYH (Holm *et al.*, 2002; Lee *et al.*, 2007) may regulate *SIG5 in vivo*. Y1H screen is performed to identify TFs that are directly interacting with the distal *SIG5* promoter. The screen is performed with peptides encoded by a cDNA library isolated from 3 d old etiolated seedlings (Kim *et al.*, 1997). As early light-responsive genes include a large proportion of TFs (Casal and Yanovsky, 2005; Jiao *et al.*, 2007) it is assumed, that TFs are already overrepresented in the mRNA pool of etiolated seedlings. However, it is not possible to detect interaction between a TF and the distal *SIG5* promoter. It is supposed that the distal promoter of *SIG5* is regulated by TFs, whose expression during germination needs to be initiated by illumination.

In addition to the postulated cross-talk of phytochrome and cryptochrome signaling via common TFs, a direct interaction between the photoreceptors can occur. Targeted yeast two-hybrid assays showed that cry1 can interact with phyA (Ahmad *et al.*, 1998a), and *in vivo* FRET assays showed interaction between cry2 and phyB (Más *et al.*, 2000). Furthermore, cry1 is phosphorylated by phyA *in vitro* (Ahmad *et al.*, 1998a). However, as *SIG5* transcripts in *hy5* mutants are almost abolished (fig. 3-45), it is concluded that phytochromes as well as cryptochromes use HY5 as integration point rather than direct interacting with each other for regulating *SIG5* expression.

In addition to HY5 and COP1, various components of plant light signaling networks are identified. For example, BBX22 is a newly identified positive regulator of photomorphogenesis (Chang *et al.*, 2008; Datta *et al.*, 2008). Recently, BBX22 is

denominated as positive regulator of *SIG5* expression, as *SIG5* mRNA abundance is elevated in *BBX22* overexpressing Arabidopsis lines (Chang *et al.*, 2011). *BBX22* is light-dependently expressed and regulated by HY5 and COP1 (Chang *et al.*, 2008, 2011; Datta *et al.*, 2008). As several of the known *BBX22*-regulated genes are enriched upon blue light treatment (Chang *et al.*, 2011), *BBX22* is a possible candidate for the signal transduction chain that mediates blue light dependent transcription of *SIG5* and subsequently *psbA* and *psbD*.

AtPP7 and HYH are also reported as downstream components in blue light signaling. The Ser/Thr protein phosphatase AtPP7 acts as positive regulator of blue light-mediated photomorphogenic growth (Guo *et al.*, 1998; Møller *et al.*, 2003) and mediates cryptochrome signaling (Møller *et al.*, 2003). As the blue light-dependent accumulation of *SIG5* transcripts is diminished in AtPP7-deficient mutants (Møller *et al.*, 2003), AtPP7 is positively regulating cryptochrome dependent *SIG5* function in Arabidopsis (Tsunoyama *et al.*, 2004). HYH, a transcription factor and a close homolog of HY5, also acts as a positive regulator in blue light signaling (Holm *et al.*, 2002). HYH is a HY5 target gene (Holm *et al.*, 2002; Lee *et al.*, 2007), and UV-B light has been shown to stimulate *SIG5* transcription in a HY5/HYH dependent pathway (Brown and Jenkins, 2008; Jiang *et al.*, 2009). Therefore HY5 is presumably regulating *SIG5* transcription mediated by HYH.

From this first study on the *SIG5* promoter it can be concluded, that the signal transduction is integratively controlled by cryptochromes and phytochromes, dependent on HY5 and controlled by COP1. The light signal is under the control of HY5, but additional TFs are mediating the blue light signal by direct interaction with the *SIG5* promoter. The proximal blue light-sensitive 196-bp sequence between nucleotides -887 and -691 relative to the translation start site of *SIG5* lacks HY5 binding sites. The distal *SIG5* promoter includes additional blue light sensitive elements that are regulated by cry2 and phyB. The identified signal transduction chain regulating *SIG5* transcription at high blue light intensities via HY5 is depicted in fig. 4-3.

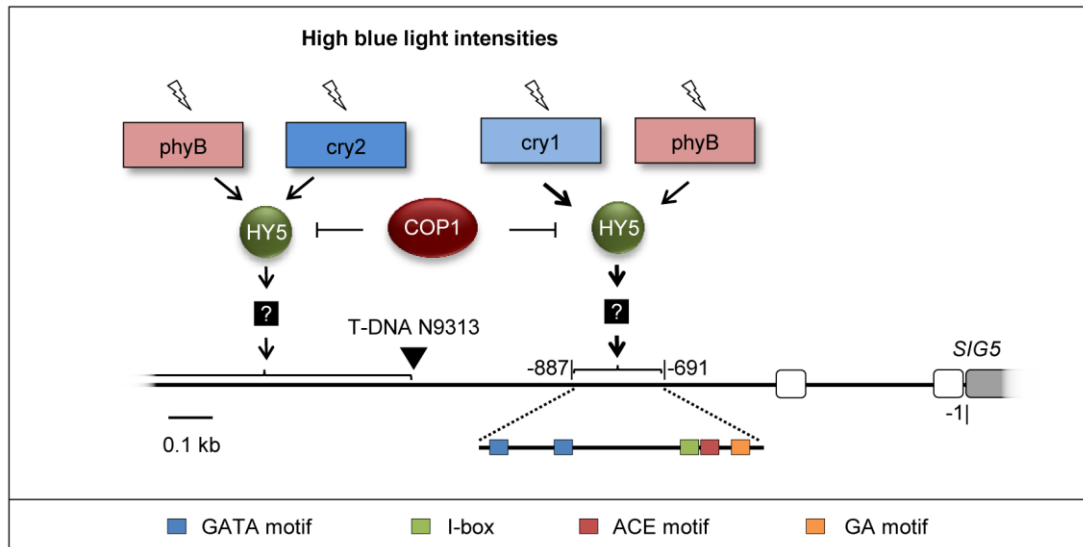


Figure 4-3. Transcriptional network regulating *SIG5* transcription upon blue light illumination. HY5 serves as integration point downstream of the photoreceptors cry1, cry2 and phyB. Yet unidentified TFs are interacting with the *SIG5* promoter. COP1 mediated degradation of HY5 is inhibited by light. High blue light is sensed in a cry1 and phyB dependent pathway within a 196-bp sequence that contains five light sensitive *cis*-acting promoter elements that probably mediate the blue light sensitivity of *SIG5* transcription. cry2 and phyB are involved in additional blue light sensing via the distal *SIG5* promoter, upstream of the T-DNA insertion site of N9313 at position -1198 relative to *SIG5* translational start site (marked by arrowhead).

HY5 is also an essential part of the signal transduction chain under red/far-red light, but again additional TFs are supposed to mediate the light signal by direct interaction with multiple light responsive *cis*-acting elements located over at least 2 kb of the *SIG5* promoter. A G-box in the distal *SIG5* promoter is involved in regulating the red light response of *SIG5*. The identified signal transduction chain regulating *SIG5* transcription at red/far-red light is depicted in fig. 4-4.

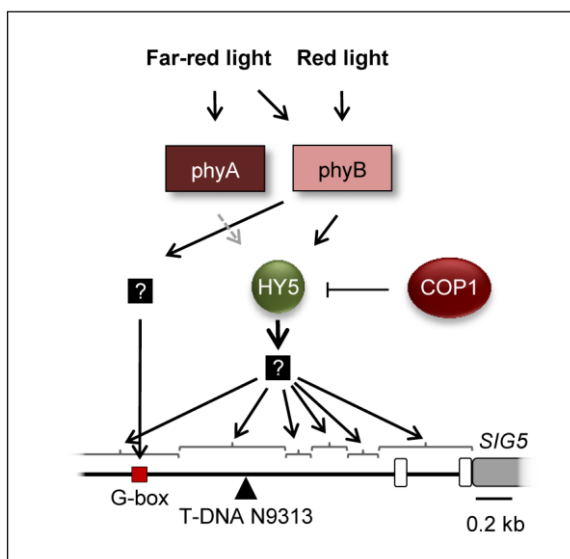


Figure 4-4. Transcriptional network regulating *SIG5* transcription upon red/far-red light illumination. HY5 serves as integration point downstream of the photoreceptors phyA and phyB. Yet unidentified TFs are interacting with the *SIG5* promoter. The COP1 mediated degradation of HY5 is inhibited by light. Red/far-red light is sensed by multiple *cis*-acting elements covering at least 2 kb of the *SIG5* promoter. In the distal promoter a G-box is mediating the red light-induction of transcription. The T-DNA insertion site of N9313 is marked by arrowhead.

4.4.6 Photosynthesis is regulating *SIG5* transcription by retrograde signals

The red light induced accumulation of *SIG5* transcripts is reduced but not completely avoided in *phyAphyB* mutants (fig. 3-41). This indicates that the red light response of *SIG5* is not solely regulated by phyA and phyB. All five Arabidopsis phytochromes act at least partially redundant (Poppe *et al.*, 1996; Robson and Smith, 1996; Devlin *et al.*, 1998, 1999; Hennig *et al.*, 2002; Franklin *et al.*, 2003b). The GFP fluorescence levels of white light grown N9313 are attenuated in *phyAphyB* mutant background similar to *hyl* mutant background (fig. 3-40); this demonstrates that phyC, phyD and phyE play only minor roles in regulating *SIG5* transcription. The GFP fluorescence of N9313 in *hylcry1cry2* background has been determined, and the lack of cry1 and cry2 further reduces the GFP fluorescence level compared to the *hyl* mutation, but only to about 33 % compared with N9313. This indicates that additional regulatory pathways, parallel to the photoreceptors, mediate the regulation of *SIG5* transcription in *Arabidopsis thaliana* seedlings. As *SIG5* is a regulator of transcription of the photosynthesis genes *psbA* and *psbD* it was assumed, that probably photosynthesis itself functions as light sensor that regulates *SIG5* transcription in Arabidopsis seedlings.

4.4.6.1 *SIG5* regulation by the redox status of the plastoquinone pool

In a highly variable light environment, light quality and light quantity gradients induce an imbalance in excitation energy distribution between the two photosystems that reduces photosynthetic efficiency. To counteract such imbalances, that typically appear in canopies of trees or forests, in dense plant populations, and aquatic environments, plants re-distribute light energy in a short term by state transitions (Allen and Forsberg, 2001; Haldrup *et al.*, 2001) and in a long term by re-adjustment of photosystem stoichiometry. While a short-term response acts via post-translational phosphorylation of existing antenna proteins, the long-term response (LTR) re-adjusts the photosystem stoichiometry (Chow *et al.*, 1990). The LTR requires the synthesis of new components and hence has to affect gene expression (Allen *et al.*, 1995; Fey *et al.*, 2005). Both processes are regulated by redox signals, generated in the thylakoid membrane of higher plants due to excitations imbalances (Allen *et al.*, 1981; Pfannschmidt *et al.*, 1999a, b; Allen and Pfannschmidt, 2000; Rintamäki *et al.*, 2000).

The correlation between *SIG5* function and photosynthesis indicate that the expression of the nuclear encoded *SIG5* can be regulated by retrograde signals, coupling *SIG5* transcription with the physiological state of the chloroplasts. The applied monochromatic red light is predominantly absorbed by the antenna of PSII (Duysens and Ames, 1962; Myers, 1971) and therefore leads to a reduction of the components of the PET chain. The red light induction of *SIG5* transcript accumulation is prevented by treatment with DCMU (fig. 3-61). DCMU inhibits the photosynthetic electron flow by blocking the Q_B binding site of the PSII reaction center protein D1, thus resulting in the oxidation of the PQ pool (Trebst, 1980; Sandmann and Bölgel, 1986). In contrast to DCMU, DBMIB, which leads to an overall reduction of the PQ pool (Trebst, 1980), does not alter the GFP fluorescence level of N9313

(fig. 3-53). It is concluded that the red/far-red light induction, according to the light intensity dependent induction, is also mediated by retrograde signaling, presumably originating in the redox status of the PQ pool. According to this, the transcription of the SIG5 target gene *psbA* is regulated by photosynthetic light via the redox state of the PQ pool (Pfannschmidt and Link, 1994; Pfannschmidt *et al.*, 1999a, b; Fey *et al.*, 2005).

The redox state of the PQ pool is also known to regulate gene expression in dependence of the light intensity. Genes that are induced by high light are also induced by DBMIB treatment in the absence of high light; in contrast, DCMU treatment inhibits high-light induced gene expression (Escoubas *et al.*, 1995; Karpinski *et al.*, 1999; Kimura *et al.*, 2003; Masuda *et al.*, 2003). Therefore not only the red/far-red light ratio but also the light intensity can be sensed by the redox state of the PQ pool which subsequently regulates SIG5 transcription. However, as a block of the PET has extensive effects on the photosynthetic apparatus, the supposed redox state of the PQ pool as origin for a retrograde signal regulating SIG5 transcription needs further experimental evidence. Nevertheless it must be mentioned, that the effects of red and far-red light illumination as well as high and low white light intensities during growth similarly alter SIG5 transcription, supporting this hypothesis.

Whereas the transcription of SIG5 is probably stimulated by a reduced PQ pool, the transcription of the SIG5 target gene *psbA* is stimulated under conditions leading to an oxidized PQ pool (Pfannschmidt *et al.*, 1999a, b; Allen and Pfannschmidt, 2000; Shimizu *et al.*, 2010). This difference in regulation of SIG5 and *psbA* transcription is explainable at different levels, but the simplest and most expansive explanation is the redundancy of some sigma factors under conditions of non-competition (Homann and Link, 2003; Privat *et al.*, 2003; Nagashima *et al.*, 2004a; Tsunoyama *et al.*, 2004). *psbA* is regulated not only by SIG5 but also by other sigma factors. As examples, *psbA* transcript levels are decreased in *sig6* mutant seedlings (Ishizaki *et al.*, 2005), and in an electrophoretic mobility shift assay binding of SIG6 to the *psbA* promoter is demonstrated (Türkeri *et al.*, 2011). The same study also detects binding of SIG1 to the *psbA* promoter (Türkeri *et al.*, 2011). *psbA* transcript levels are unaltered in *sig2* mutants (Shirano *et al.*, 2000; Kanamaru *et al.*, 2001), but another study demonstrates binding of SIG2 to the *psbA* promoter (Tsunoyama *et al.*, 2004). Also SIG3 is shown to recognize the *psbA* promoter in mustard (Homann and Link, 2003; Privat *et al.*, 2003). Therefore the complex sigma factor network regulating *psbA* transcription cause regulatory pattern distinct from the regulation of SIG5 (and *psbD* that is probably exclusively regulated by SIG5).

4.4.6.2 The role of SIG5 under oxidative stress

Photosynthesis as well as the redox state of the cell is closely connected with oxidative stress. Oxidative stress arises from an imbalance in the generation and removal of ROS. As SIG5 is able to recognize both, the *psbA* promoter as well as the *psbD* promoter, one can assume a relevant role in adaptation to light, and therefore also to oxidative stress,

accords to this sigma factor. The *psbA* and *psbD* encoded proteins, D1 and D2, are the Chl binding proteins of the reaction center core of PSII. They bind all the redox-active components involved in the light driven electron transfer of PSII. PSII is prone to light-induced inactivation upon oxidative damage due to the highly oxidative chemistry of water splitting, especially under high irradiance (Barber and Andersson, 1992; Asada, 1999). The D1 and the D2 proteins are the primary targets of such damage (Mattoo *et al.*, 1981, 1984, 1989; Ohad *et al.*, 1985; Christopher and Mullet, 1994). Plants are able to repair damaged PSII complexes through disassembly of PSII complexes, synthesis of new D1 and D2 subunits, and reassembly of the proteins and cofactors into functional complexes (Melis, 1989). To maintain high rates of their synthesis, transcription of *psbA* and *psbD* are elevated in response to light (Gamble *et al.*, 1988; Klein and Mullet, 1990). It is hypothesized that transcription of *SIG5* as regulator of D1 and D2 synthesis is controlled in response to oxidative stress to maintain functional PSII. Indeed, it is shown that cold treatment of Arabidopsis seedlings under continuous illumination induces accumulation of *SIG5* transcripts (fig. 3-66). As the light conditions are not altered, the induction of transcription is thought to be regulated in response to the oxidative stress that occurs due to the combination of light and cold treatment (Soitamo *et al.*, 2008). *SIG5* transcription in Arabidopsis seedlings responds to various abiotic stress conditions, such as high light, high salt and high osmotic conditions (Nagashima *et al.*, 2004b). The same study demonstrates that these stress conditions also activate the *psbD*-BLRP and that the recovery of PSII activity from a high-light induced damage is delayed in the *sig5-2* mutant.

Most *cis*-acting elements are not exclusively regulated by retrograde signals, and *cis*-acting elements required for retrograde regulation are either identical to or largely overlapping with light-responsive elements (Vorst *et al.*, 1993; Bolle *et al.*, 1996; Kusnetsov *et al.*, 1996). The attenuated red light induction of transcription upon DCMU treatment is mediated by proximal and distal promoter regions (fig. 3-60, 3-61). It is assumed that the red/far-red light sensitive *cis*-acting elements in the *SIG5* promoter may be the same that are regulated by red/far-red light sensing photoreceptors.

4.4.6.3 Redox-regulation of *SIG5* function by phosphorylation

This thesis shows that the expression of *SIG5* is redox-regulated at the level of transcription. Evidence for such mechanism is given by the analysis of the blue light intensities necessary to induce transcription from the *SIG5* and the *psbD*-BLRP promoters. The blue light-induced accumulation of *SIG5* transcripts requires blue light with a fluence threshold of about $5 \mu\text{mol photons m}^{-2} \text{s}^{-1}$, being consistent with the fluence threshold for the cryptochrome activation by phosphorylation (Shalitin *et al.*, 2002, 2003). For activation of the *psbD*-BLRP an additional light signal of about $50 \mu\text{mol photons m}^{-2} \text{s}^{-1}$ is required, which is not restricted to blue light (Mochizuki *et al.*, 2004).

Accordant findings, which link the redox state to the SIG5 function, are available for the SIG5 target promoter *psbD*-BLRP. Two different mechanisms by which higher light functions on the activation of the *psbD*-BLRP are currently discussed and both involve phosphorylation as regulatory event. First, the *psbD*-BLRP contains a well conserved *cis*-element, a PGT box, which is bound by the PGT box-binding factor (PGTF) (Kim and Mullet, 1995; Baba *et al.*, 2001). PGTF binding to the PGT box is regulated in a light dependent manner. ADP-dependent phosphorylation of PGTF results in loss of the affinity for the PFT box *in vitro* (Kim *et al.*, 1999b). The link between the redox state and the PGTF phosphorylation is the chloroplast ATP synthase, which catalyzes the light driven synthesis of ATP and acts as key regulatory component of photosynthesis. The ATP synthase is regulated at several levels (Ort and Oxborough, 1992), but already early the activity of the ATP synthase has been shown to be regulated by the redox state (Junesch and Gräber, 1987). In plants and green algae the ATPase is redox-regulated by thioredoxin (Junesch and Gräber, 1991; Schwarz *et al.*, 1997; Kohzuma *et al.*, 2012). In other words, the PET determines the rate of *psbD*-BLRP transcription via the intracellular ATP to ADP ratio.

The same can be assumed for the second mechanism which is suggested to activate *psbD*-BLRP in the light. A PEP-associated Ser/Thr protein kinase, termed plastid transcription kinase (PTK) (Baginsky *et al.*, 1999) of the CK2 family, which thus is named cpCK2 (Ogrzwalla *et al.*, 2002; Salinas *et al.*, 2006), is identified to catalyze phosphorylation of the PEP core enzymes and sigma factors, resulting in inactivation of PEP (Homann and Link, 2003; Shimizu *et al.*, 2010). This ATP-dependent phosphorylation results in changes of chloroplast transcription (Tiller and Link, 1993; Christopher *et al.*, 1997; Türkeri *et al.*, 2011). Moreover, the catalytic component of cpCK2 is antagonistically regulated by phosphorylation and redox state (Baginsky *et al.*, 1997, 1999). The protein kinase itself responds to SH-group regulation by glutathione and transmits the redox signal via its phosphorylation activity to the plastid transcription apparatus via phosphorylation sites of sigma factors (Baginsky *et al.*, 1997, 1999; Ogrzwalla *et al.*, 2002; Türkeri *et al.*, 2011). Light dependent reduction of glutathione (Baena-Gonzales *et al.*, 2001) inactivates cpCK2, while dephosphorylation of PEP under high light conditions further enhances PEP-dependent transcription. In its simplest form, the proposed mechanism is thought to involve enhanced promoter binding by the phosphorylated sigma factors, resulting in initiation arrest and inhibition of elongation (Tiller and Link, 1993).

The results of the present thesis support these previous findings that the *psbD*-BLRP expression is regulated by the redox state at several levels. The PET determines the *psbD*-BLRP transcription via the ADP to ATP ratio and via the reduction of glutathione at posttranslational level, and via redox signaling resulting in the modification of the SIG5 transcription initiation rate.

A similar mechanism has recently been identified to regulate the expression of *psaA*, encoding a PSI core protein, in dependence from the redox status. *psaA* transcription is regulated by SIG1 (Tozawa *et al.*, 2007), whose activity is regulated by phosphorylation. The phosphorylation of SIG1 is enhanced under conditions oxidizing the PQ pool, leading to

a selective inhibition of *psaA* transcription (Shimizu *et al.*, 2010). Some of the N-terminal phosphorylation sites are conserved in Arabidopsis SIG1, SIG3 and SIG5 (Shimizu *et al.*, 2010), and additional hypothetic phosphorylation sites are detected in the *SIG5* sequence (Lerbs-Mache, 2011). Therefore SIG1 and SIG5 function are both regulated by the redox state of the PQ pool, adjusting the amounts of PSI and PSII to the prevalent light intensities; however this mechanism cannot consider an adaptation to varying red/far-red ratios. Higher light intensities lead to an overall reduced PQ pool, conditions which inhibit phosphorylation of SIG1 and SIG5 and therefore stimulate transcription of *psaA* and *psbD*. Consequently, the post-translational phosphorylation of sigma factors under redox control may be involved in maintaining the photosynthetic efficiency under varying light intensities.

4.4.6.4 Integration of carbohydrate metabolism and redox signals

As photosynthesis is a process that produces soluble sugars, it must be balanced with processes utilizing soluble sugars. Therefore it is assumed, that *SIG5* transcription, which is shown to be regulated by retrograde signaling, may be also regulated by soluble sugars. So is the *psbA* mRNA level down-regulated by elevated carbohydrate contents in tomato leaves (Van Oosten and Besford, 1995). Indeed, the *SIG5* transcript levels correlate with the concentration of sucrose in the medium (fig. 3-65 B).

The analysis of ET line N9313 demonstrates that the intracellular sucrose concentration is sensed exclusively by the distal *SIG5* promoter (fig. 3-65 C, D). *In silico* analysis of the distal promoter with PlantCARE (Rombauts *et al.*, 1999) and PLACE (Higo *et al.*, 1999) databases reveal that none of the known sucrose- or sugar-responsive *cis*-acting elements are located within this region. However, the light-sensitive GC-box and the G-box are identified within this region (tab. 3-4); both motifs, together with a third element, the TATCCA element, mediate sugar response in rice (Lu *et al.*, 1998).

Two ABRE-elements, involved in ABA responses, and an ethylene-responsive ERE-element are identified within the distal *SIG5* promoter (tab. 3-10). In plants, individual signal transduction chains for photosynthetic redox sensing, light sensing, sugar sensing and stress hormones such as ethylene and ABA are tightly connected to adjust the metabolic imbalances which occur as a result of fluctuating environmental conditions (e.g. Dijkwel *et al.*, 1997; Oswald *et al.*, 2001; Brocard-Gifford *et al.*, 2003; Gibson, 2004). As example, ABA down-regulates *LHCB* genes in Arabidopsis like high light treatment (Staneloni *et al.*, 2008). ABA and ethylene are stress hormones that are known to interact with sugar sensing in plants (reviewed in Rolland *et al.*, 2006). Due to the identification of ABA- and ethylene-responsive motifs in the sucrose-sensitive distal *SIG5* promoter it is speculated, that these phytohormones directly connect sucrose-signaling with modulation of photosynthesis via the regulation of *SIG5* transcription. However, experimental evidence is needed to confirm this assumption.

Due to the supposed regulation of *SIG5* transcription by the redox state of the PQ pool, it is assumed, that the sucrose sensitivity of *SIG5* interacts with photosynthetic redox sensing

in Arabidopsis seedlings. In Arabidopsis cell culture, a block in photosynthetic electron flux by DCMU prevents the increase in transcript levels of photosynthetic genes like *RBCS* that typically occurs when intracellular sugar levels are depleted (Oswald *et al.*, 2001). Another known example for the connection between sucrose metabolism and redox sensing is the ADP-glucose pyrophosphorylase (AGPase). AGPase catalyzes the first step of starch synthesis and is the key regulatory enzyme of starch synthesis in plastids (Preiss, 1988; Martin and Smith, 1995). AGPase is regulated by sucrose and glucose levels and additionally posttranslational activated by redox-changes (Tiessen *et al.*, 2002; Hendriks *et al.*, 2003; Geigenberger *et al.*, 2005).

The TF ABI4 is a key regulator of nuclear gene expression upon retrograde signaling (Koussevitzky *et al.*, 2007). ABI4 as integrator of sugar signaling with retrograde signaling has been described by analysis of the Arabidopsis *sun6* (*sucrose uncoupled 6*) mutant. In *sun6* plants, plastocyanin transcription increases in response to exogenous sucrose rather than decreasing as in the wild-type (Oswald *et al.*, 2001). SUN6 is identical to ABI4 (Huijser *et al.*, 2000). ABI4 is a negatively acting TF that is assumed to competitively bind G-box motifs in response to plastid signals and therefore blocking the enhancers of PhANGs (Koussevitzky *et al.*, 2007). Furthermore, ABI4 is discussed as mediator of a ‘master switch’ that acts in a binary mode by either inducing or repressing the same large set of nuclear chloroplast genes, thus integrating diverse plastid signals (Richly *et al.*, 2003; Biehl *et al.*, 2005; Ruckle *et al.*, 2007). Therefore ABI4 reveals a linking between sucrose controlled gene expression and plastid redox signals and is a potential integration point of sucrose signaling and retrograde signaling regulating *SIG5* transcription. However, this hypothesis needs experimental evidence.

CMA5 is a minimal light-responsive unit that demonstrates the tight connections and interactions of photoreceptors, retrograde signals and sucrose. The *CMA5* sequence contains an I-box and a G-box element, both of which are essential for the activation of *CMA5* in a phytochrome-, cryptochrome-, and plastid signal-dependent manner (Martínez-Hernández *et al.*, 2002). Furthermore, it is shown that *CMA5* is able to respond not only to light and chloroplast signals, but also to sugar signals in a pathway involving ABA (Acevedo-Hernández *et al.*, 2005). The latter response is mediated by direct binding of the ABI4 transcription factor to the S-box, a conserved element found in close association with the G-box motif of *CMA5* (Martínez-Hernández *et al.*, 2002; Acevedo-Hernández *et al.*, 2005). G-boxes are found in several sucrose-related promoters (reviewed in Rolland *et al.*, 2002, Lu *et al.*, 1998, 2002) and therefore provide a link between sucrose-sensitivity and light-sensitivity of gene expression. Analysis of *GFP* and *SIG5* transcript levels of N9313 and C24 demonstrate that the sucrose sensitivity is mediated by distal but not the proximal *SIG5* promoter (fig. 3-65 B-D). Therefore the G-box that is located in this region (tab. 3-4) is potentially involved in the observed sugar induced drop of *SIG5* transcription.

ABI4 plays a key role in transmitting information concerning the abundance of ascorbate and hence the ability of cells to buffer oxidative challenges. Low redox buffering capacity is mediated through ABA and ABI4 (Foyer *et al.*, 2012). ABI4 is also involved in

the suppression of phyA dependent signaling pathways by sucrose (Dijkwel *et al.*, 1997). Recently Foyer *et al.* (2012) observe altered *SIG5* mRNA levels in *abi4* mutants. These results support the hypothesis, that ABI4 may be a regulator of *SIG5* transcription in Arabidopsis, with the potential to integrate plastid redox signals, sugar signaling, phytohormones and also photoreceptor signaling.

Another connection between carbohydrate signaling and photoreceptor signaling has been revealed by analysis of *cop1* mutants. Sucrose is involved in regulating the function of the central regulator of photomorphogenesis, COP1. At least the function of COP1 as repressor of flowering is released by sucrose (Nakagawa and Komeda, 2004). Furthermore Arabidopsis *cop1* mutants accumulate high levels of *CAB* and *RBCS* transcripts in the presence of high sucrose concentrations in the medium (Ang and Deng, 1994). As COP1 is identified as regulator of *SIG5* transcription (tab. 3-8), it is possible that COP1 function is not limited to regulate the photoreceptor-mediated pathways but also controls the sucrose-sensitivity of *SIG5*.

4.4.6.5 Regulation of *SIG5* by photosynthesis – concluding remarks

In summary there are several facts that indicate regulation of *SIG5* expression by retrograde signaling: (i) the nuclear encoded *SIG5* is a plastid protein; (ii) the main function of *SIG5* is the regulation of photosynthetic gene expression; (iii) the transcription of *SIG5* is light-dependent; (iv) *SIG5* transcription is stimulated by multiple abiotic stress conditions (Nagashima *et al.*, 2004b; the present thesis); (v) the transcription of *psbA*, a target of *SIG5*, is regulated by the redox status of the PQ pool (Pfannschmidt and Link, 1994; Allen and Pfannschmidt, 1999; Pfannschmidt *et al.*, 1999a, b); (vi) the regulation of PEP activity by phosphorylation is redox-dependent (discussed in chapter 4.4.6.3); (vii) *SIG5* transcription is regulated by sucrose availability, with carbohydrate metabolism being redox regulated (4.4.6.4). The present thesis demonstrates that the light-dependent regulation of *SIG5* function is not restricted to photoreceptors but also modulated by retrograde signaling (fig. 4-5). Furthermore, oxidative stress and the plant sucrose metabolism are shown to be integrated with plastid redox signals. This results in retrograde signals that adapt *SIG5* transcription to plastid metabolism and functional state. Multiple regulatory layers are identified, which in parts function separately on distinct regions of the *SIG5* promoter. It demonstrates that the regulation of *SIG5* transcription is a much more dynamic event than previously thought. It is concluded, that this high flexibility of *SIG5* expression is essential for maintaining suitable plastid function and photosynthesis in a highly variable environment.

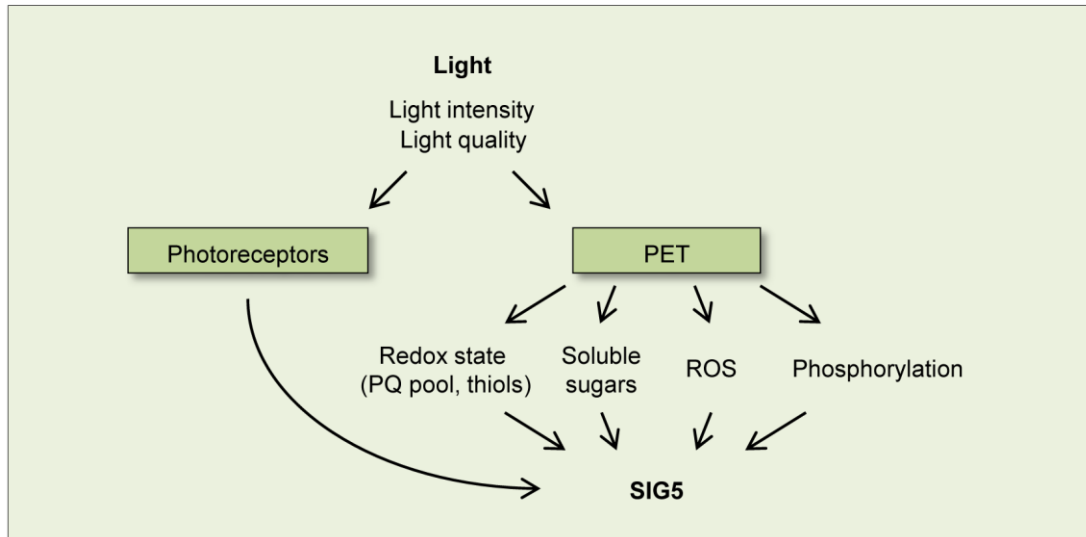


Figure 4-5. Regulation of *SIG5* activity by light. Changes in environmental conditions (e.g., light quality and light quantity) affect the rate of PET, which determines the redox state of the cell, the production of soluble sugars and the generation of ROS. These changes generate retrograde signals that modulate transcription of *SIG5*. Also the phosphorylation status of *SIG5* is affected by light. The different signals are tightly connected and integrated by phytohormones like ABA and ethylene and TFs like HY5, PIFs or ABI4. In addition to the retrograde signals, several blue light and red/far-red light sensing photoreceptors modulate the transcription of *SIG5*.

4.4.7 Conclusions

The focus of this study is the identification and characterization of light-regulated *cis*-elements of nuclear promoters in *Arabidopsis thaliana*. The ET line N9313 is identified as a tool that enables the distinct analyses of the promoter of *SIG5*, distinguishing between proximal and more distal regions. The distal promoter regions are excluded from common promoter analyses, mostly as the frequency of functional *cis*-acting elements decreases further away from the transcription start, with most motifs being inactive in more than 1 kb upstream of the translational start site (Geisler *et al.*, 2006; Ibraheem *et al.*, 2010). Consistent with this, promoter analyses are often restricted to 0.5 kb or, rarer, to 1 kb upstream of the CDS. The analysis of N9313 leads to the identification of light sensitive elements located in more than 1.2 kb upstream of the *SIG5* CDS. This demonstrates that enhancer trapping is a useful tool for identification and subsequent characterization of such additional regulatory promoter elements.

With the comparison of *GFP* and *SIG5* transcript level of N9313, the distinct blue light, red light and far-red light sensitive regions of the promoter are described. It is shown that *SIG5* can control plastid gene expression not only in blue light, but generally in a light quality and light intensity dependent manner. Furthermore, the red and far-red light sensitivity of *SIG5* transcription is demonstrated to be not only regulated by photoreceptors, but also influenced by retrograde signals, supposedly originating in the redox status of the PQ pool. The redox status of the PQ pool is tightly connected with the overall PET, the cellular redox status, oxidative stress, stress related phytohormones like ethylene and ABA, and also the end products of photosynthesis, ATP and NADPH on the one hand, and

different soluble sugars on the other hand. Regulation of *SIG5* transcription is embedded in this complex regulatory network. Subsequent analysis of N9313 will enable the combination of a detailed elucidation of regulation of *SIG5* transcription with the continuative analysis of structure and function of the *SIG5* promoter.

REFERENCES

- Acevedo-Hernandez GJ, Leon P, Herrera-Estrella LR** (2005) Sugar and ABA responsiveness of a minimal *RBCS* light-responsive unit is mediated by direct binding of ABI4. *Plant J* 43: 506-519
- Adams WW, Demmig-Adams B** (1992) Operation of the xanthophyll cycle in higher-plants in response to diurnal changes in incident sunlight. *Planta* 186: 390-398
- Ahmad M, Cashmore AR** (1993) HY4 gene of *A. thaliana* encodes a protein with characteristics of a blue-light photoreceptor. *Nature* 366: 162-166
- Ahmad M, Jarillo JA, Smirnova O, Cashmore AR** (1998a) The CRY1 blue light photoreceptor of Arabidopsis interacts with phytochrome A *in vitro*. *Mol Cell* 1: 939-948
- Ahmad M, Jarillo JA, Cashmore AR** (1998b) Chimeric proteins between cry1 and cry2 Arabidopsis blue light photoreceptors indicate overlapping functions and varying protein stability. *Plant Cell* 10: 197-207
- Aich S, Delbaere LTJ, Chen RD** (2001) Continuous spectrophotometric assay for beta-glucuronidase. *Biotechniques* 30: 846-850
- Al-Sady B, Ni W, Kircher S, Schäfer E, Quail PH** (2006) Photoactivated phytochrome induces rapid PIF3 phosphorylation prior to proteasome-mediated degradation. *Mol Cell* 23: 439-446
- Allen JF, Bennett J, Steinback KE, Arntzen CJ** (1981) Chloroplast protein-phosphorylation couples plastoquinone redox state to distribution of excitation-energy between photosystems. *Nature* 291: 25-29
- Allen JF** (1995) Thylakoid protein-phosphorylation, state 1- state 2 transitions, and photosystem stoichiometry adjustment – redox control at multiple levels of gene expression. *Physiol Plant* 93: 196-205
- Allen JF, Pfannschmidt T** (2000) Balancing the two photosystems: photosynthetic electron transfer governs transcription of reaction centre genes in chloroplasts. *Philos Trans R Soc Lond B Biol Sci* 355: 1351-1359
- Allen JF, Forsberg J** (2001) Molecular recognition in thylakoid structure and function. *Trends Plant Sci* 6: 317-326
- Allen JF** (2003) Cyclic, pseudocyclic and noncyclic photophosphorylation: new links in the chain. *Trends Plant Sci* 8: 15-19
- Allison LA, Simon LD, Maliga P** (1996) Deletion of *rpoB* reveals a second distinct transcription system in plastids of higher plants. *EMBO J* 15: 2802-2809
- Allison LA** (2000) The role of sigma factors in plastid transcription. *Biochimie* 82: 537-548
- Altschul SF, Gish W, Miller W, Myers EW, Lipman DJ** (1990) Basic local alignment search tool. *J Mol Biol* 215: 403-410
- Altschul SF, Madden TL, Schaffer AA, Zhang JH, Zhang Z, Miller W, Lipman DJ** (1997) Gapped BLAST and PSI-BLAST: a new generation of protein database search programs. *Nucl Acids Res* 25: 3389-3402

- An YQ, McDowell JM, Huang S, McKinney EC, Chambliss S, Meagher RB** (1996) Strong, constitutive expression of the Arabidopsis ACT2/ACT8 actin subclass in vegetative tissues. *Plant J* 10: 107-121
- Anderson SL, Teakle GR, Martinocatt SJ, Kay SA** (1994) Circadian clock-regulated and phytochrome-regulated transcription is conferred by a 78 bp *cis*-acting domain of the Arabidopsis *CAB2* promoter. *Plant J* 6: 457-470
- Ang LH, Deng XW** (1994) Regulatory hierarchy of photomorphogenic loci – allele-specific and light-dependent interaction between the HY5 and COP1 loci. *Plant Cell* 6: 613-628
- Ang LH, Chattopadhyay S, Wei N, Oyama T, Okada K, Batschauer A, Deng XW** (1998) Molecular interaction between COP1 and HY5 defines a regulatory switch for light control of Arabidopsis development. *Mol Cell* 1: 213-222
- Apel K, Hirt H** (2004) Reactive oxygen species: Metabolism, oxidative stress, and signal transduction. *Annu Rev Plant Biol* 55: 373-399
- Arenas-Huertero F, Arroyo A, Zhou L, Sheen J, Leon P** (2000) Analysis of Arabidopsis glucose insensitive mutants, *gin5* and *gin6*, reveals a central role of the plant hormone ABA in the regulation of plant vegetative development by sugar. *Genes & Dev* 14: 2085-2096
- Argüello-Astorga G, Herrera-Estrella L** (1998) Evolution of light-regulated plant promoters. *Annu Rev Plant Physiol Plant Mol Biol* 49: 525-555
- Arner ESJ, Holmgren A** (2000) Physiological functions of thioredoxin and thioredoxin reductase. *Eur J Biochem* 267: 6102-6109
- Arvidsson S, Kwasniewski M, Riano-Pachon DM, Mueller-Roeber B** (2008) QuantPrime – a flexible tool for reliable high-throughput primer design for quantitative PCR. *BMC Bioinformatics* 9: 465
- Asada K** (1999) The water-water cycle in chloroplasts: Scavenging of active oxygens and dissipation of excess photons. *Annu Rev Plant Physiol Plant Mol Biol* 50: 601-639
- Atanassova R, Leterrier M, Gaillard C, Agasse A, Sagot E, Coutos-Thevenot P, Delrot S** (2003) Sugar-regulated expression of a putative hexose transport gene in grape. *Plant Physiol* 131: 326-334
- Aukerman MJ, Hirschfeld M, Wester L, Weaver M, Clack T, Amasino RM, Sharrock RA** (1997) A deletion in the *PHYD* gene of the Arabidopsis Wassilewskija ecotype defines a role for phytochrome D in red/far-red light sensing. *Plant Cell* 9: 1317-1326
- Baba K, Nakano T, Yamagishi K, Yoshida S** (2001) Involvement of a nuclear-encoded basic helix-loop-helix protein in transcription of the light-responsive promoter of *psbD*. *Plant Physiol* 125: 595-603
- Baena-Gonzalez E, Baginsky S, Mulo P, Summer H, Aro EM, Link G** (2001) Chloroplast transcription at different light intensities. Glutathione-mediated phosphorylation of the major RNA polymerase involved in redox-regulated organellar gene expression. *Plant Physiol* 127: 1044-1052
- Baginsky S, Tiller K, Link G** (1997) Transcription factor phosphorylation by a protein kinase associated with chloroplast RNA polymerase from mustard (*Sinapis alba*). *Plant Mol Biol* 34: 181-189
- Baginsky S, Tiller K, Pfannschmidt T, Link G** (1999) PTK, the chloroplast RNA polymerase-associated protein kinase from mustard (*Sinapis alba*), mediates redox control of plastid *in vitro* transcription. *Plant Mol Biol* 39: 1013-1023
- Baier M, Ströher E, Dietz KJ** (2004) The acceptor availability at photosystem I and ABA control nuclear expression of 2-Cys peroxiredoxin-A in *Arabidopsis thaliana*. *Plant Cell Physiol* 45: 997-1006
- Banerjee R, Schleicher E, Meier S, Viana RM, Pokorný R, Ahmad M, Bittl R, Batschauer A** (2007) The signaling state of Arabidopsis cryptochrome 2 contains flavin semiquinone. *J Biol Chem* 282: 14916-14922
- Barber J, Andersson B** (1992) Too much of a good thing – light can be bad for photosynthesis. *Trends Biochem Sci* 17: 61-66
- Baroli I, Melis A** (1996) Photoinhibition and repair in *Dunaliella salina* acclimated to different growth irradiances. *Planta* 198: 640-646

- Bartels PG, Watson CW** (1978) Inhibition of carotenoid synthesis by fluridone and norflurazone. *Weed Sci* 26: 198-203
- Baruah A, Simkova K, Hinch DK, Apel K, Laloi C** (2009) Modulation of $^1\text{O}_2$ -mediated retrograde signaling by the PLEIOTROPIC RESPONSE LOCUS 1 (PRL1) protein, a central integrator of stress and energy signaling. *Plant J* 60: 22-32
- Baudry A, Ito S, Song YH, Strait AA, Kiba T, Lu S, Henriques R, Pruneda-Paz JL, Chua NH, Tobin EM, Kay SA, Imaizumi T** (2010) F-box proteins FKF1 and LKP2 act in concert with ZEITLUPE to control Arabidopsis clock progression. *Plant Cell* 22: 606-622
- Bauer J, Chen KH, Hiltbunner A, Wehrli E, Eugster M, Schnell D, Kessler F** (2000) The major protein import receptor of plastids is essential for chloroplast biogenesis. *Nature* 403: 203-207
- Bauer D, Viczian A, Kircher S, Nobis T, Nitschke R, Kunkel T, Panigrahi KCS, Adam E, Fejes E, Schäfer E, Nagy F** (2004) Constitutive photomorphogenesis 1 and multiple photoreceptors control degradation of phytochrome interacting factor 3, a transcription factor required for light signaling in Arabidopsis. *Plant Cell* 16: 1433-1445
- Baxter-Burell A, Chang R, Springer P, Bailey-Serres J** (2003) Gene and enhancer trap transposable elements reveal oxygen deprivation-regulated genes and their complex patterns of expression in Arabidopsis. *Ann Bot* 91: 129-141
- Bechtold N, Ellis J, Pelletier G** (1993) *In planta Agrobacterium*-mediated gene transfer by infiltration of adult *Arabidopsis thaliana* plants. *C R Acad Sci Paris Life Sci* 316: 1194-1199
- Beck C** (2005) Signaling pathways from the chloroplast to the nucleus. *Planta* 222: 743-756
- Bellafiore S, Bameche F, Peltier G, Rochaix JD** (2005) State transitions and light adaptation require chloroplast thylakoid protein kinase STN7. *Nature* 433: 892-895
- Biehl A, Richly E, Noutsos C, Salamini F, Leister D** (2005) Analysis of 101 nuclear transcriptomes reveals 23 distinct regulons and their relationship to metabolism, chromosomal gene distribution and co-ordination of nuclear and plastid gene expression. *Gene* 344: 33-41
- Blackwood EM, Kadonaga JT** (1998) Going the distance: a current view of enhancer action. *Science* 281: 60-63
- Bläsing OE, Gibon Y, Günther M, Höhne M, Morcuende R, Osuna D, Thimm O, Usadel B, Scheible WR, Stitt M** (2005) Sugars and circadian regulation make major contributions to the global regulation of diurnal gene expression in Arabidopsis. *Plant Cell* 17: 3257-3281
- Block A, Dangl JL, Hahlbrock K, Schulze-Lefert P** (1990) Functional borders, genetic fine-structure, and distance requirements of *cis* elements mediating light responsiveness of the parsley chalcone synthase promoter. *Proc Natl Acad Sci USA* 87: 5387-5391
- Bolle C, Kusnetsov VV, Herrmann RG, Oelmüller R** (1996) The spinach *AtpC* and *AtpD* genes contain elements for light-regulated, plastid-dependent and organ-specific expression in the vicinity of the transcription start sites. *Plant J* 9: 21-30
- Bolwell GP, Davies DR, Gerrish C, Auh CK, Murphy TM** (1998) Comparative biochemistry of the oxidative burst produced by rose and french bean cells reveals two distinct mechanisms. *Plant Physiol* 116: 1379-1385
- Bolwell GP, Bindschedler LV, Blee KA, Butt VS, Davies DR, Gardner SL, Gerrish C, Minibayeva F** (2002) The apoplastic oxidative burst in response to biotic stress in plants: a three-component system. *J Exp Bot* 53: 1367-1376
- Bonardi V, Pesaresi P, Becker T, Schleiff E, Wagner R, Pfannschmidt T, Jahns P, Leister D** (2005) Photosystem II core phosphorylation and photosynthetic acclimation require two different protein kinases. *Nature* 437: 1179-1182
- Borello U, Ceccarelli E, Giuliano G** (1993) Constitutive, light-responsive and circadian clock-responsive factors compete for the different L-box elements in plant light-regulated promoters. *Plant J* 4: 611-619
- Boter M, Ruiz-Rivero O, Abdeen A, Prat S** (2004) Conserved MYC transcription factors play a key role in jasmonate signaling both in tomato and Arabidopsis. *Genes & Dev* 18: 1577-1591

- Bouly JP, Giovani B, Djamei A, Mueller M, Zeugner A, Dudkin EA, Batschauer A, Ahmad M** (2003) Novel ATP-binding and autophosphorylation activity associated with Arabidopsis and human cryptochrome-1. *Eur J Biochem* 270: 2921-2928
- Bouly JP, Schleicher E, Dionisio-Sese M, Vandenbusche F, Van Der Straeten D, Bakrim N, Meier S, Batschauer A, Galland P, Bittl R, Ahmad M** (2007) Cryptochrome blue light photoreceptors are activated through interconversion of flavin redox states. *J Biol Chem* 282: 9383-9391
- Bowler C, Neuhaus G, Yamagata H, Chua NH** (1994) Cyclic GMP and calcium mediate phytochrome phototransduction. *Cell* 77: 73-81
- Brand AH, Perrimon N** (1993) Targeted gene expression as a means of altering cell fates and generating dominant phenotypes. *Development* 118: 401-415
- Bräutigam K, Dietzel L, Kleine T, Ströher E, Wormuth D, Dietz KJ, Radke D, Wirtz M, Hell R, Doermann P, Nunes-Nesi A, Schauer N, Fernie AR, Oliver SN, Geigenberger P, Leister D, Pfannschmidt T** (2009) Dynamic plastid redox signals integrate gene expression and metabolism to induce distinct metabolic states in photosynthetic acclimation in Arabidopsis. *Plant Cell* 21: 2715-2732
- Briggs WR, Christie JM** (2002) Phototropins 1 and 2: versatile plant blue-light receptors. *Trends Plant Sci* 7: 204-210
- Brocard-Gifford IM, Lynch TJ, Finkelstein RR** (2003) Regulatory networks in seeds integrating developmental, abscisic acid, sugar, and light signaling. *Plant Physiol* 131: 78-92
- Brown BA, Jenkins GI** (2008) UV-B signaling pathways with different fluence-rate response profiles are distinguished in mature Arabidopsis leaf tissue by requirement for UVR8, HY5, and HYH. *Plant Physiol* 146: 576-588
- Brudler R, Hitomi K, Daiyasu H, Toh H, Kucho K, Ishiura M, Kanehisa M, Roberts VA, Todo T, Tainer JA, Getzoff ED** (2003) Identification of a new cryptochrome class: Structure, function, and evolution. *Mol Cell* 11: 59-67
- Buchanan BB, Balmer Y** (2005) Redox regulation: a broadening horizon. *Ann Rev Plant Biol* 56: 187-220
- Burney S, Hoang N, Caruso M, Dudkin EA, Ahmad M, Bouly JP** (2009) Conformational change induced by ATP binding correlates with enhanced biological function of Arabidopsis cryptochrome. *FEBS Lett* 583: 1427-1433
- Campisi L, Yang Y, Yi Y, Heilig E, Herman B, Cassista AJ, Allen DW, Xiang H, Jack T** (1999) Generation of enhancer trap lines in Arabidopsis and characterization of expression patterns in the inflorescence. *Plant J* 17: 699-707
- Canton FR, Quail PH** (1999) Both phyA and phyB mediate light-imposed repression of *PHYA* gene expression in Arabidopsis. *Plant Physiol* 121: 1207-1215
- Cao J, Schneeberger K, Ossowski S, Guenther T, Bender S, Fitz J, Koenig D, Lanz C, Stegle O, Lippert C, Wang X, Ott F, Mueller J, Alonso-Blanco C, Borgwardt K, Schmid KJ, Weigel D** (2011) Whole-genome sequencing of multiple *Arabidopsis thaliana* populations. *Nat Genet* 43: 956-963
- Cary AJ, Che P, Howell SH** (2002) Developmental events and shoot apical meristem gene expression patterns during shoot development in *Arabidopsis thaliana*. *Plant J* 32: 867-877
- Casal JJ, Sanchez RA** (1998) Phytochromes and seed germination. *Seed Sci Res* 8: 317-329
- Casal JJ, Yanovsky MJ** (2005) Regulation of gene expression by light. *Int J Dev Biol* 49: 501-511
- Cashmore AR, Jarillo JA, Wu YJ, Liu DM** (1999) Cryptochromes: blue light receptors for plants and animals. *Science* 284: 760-765
- Castresana C, Garcialuque I, Alonso E, Malik VS, Cashmore AR** (1988) Both positive and negative regulatory elements mediate expression of a photoregulated *CAB* gene from *Nicotiana plumbaginifolia*. *EMBO J* 7: 1929-1936
- Catala R, Medina J, Salinas J** (2011) Integration of low temperature and light signaling during cold acclimation response in Arabidopsis. *Proc Natl Acad Sci USA* 108: 16475-16480

- Chandok MR, Sopory SK, Oelmüller R** (2001) Cytoplasmic kinase and phosphatase activities can induce *psaF* gene expression in the absence of functional plastids: evidence that phosphorylation/dephosphorylation events are involved in interorganellar crosstalk. *Mol Gen Genet* 264: 819-826
- Chang CSJ, Li YH, Chen LT, Chen WC, Hsieh WP, Shin J, Jane WN, Chou SJ, Choi G, Hu JM, Somerville S, Wu SH** (2008) LZFI, a HY5-regulated transcriptional factor, functions in Arabidopsis de-etiolation. *Plant J* 54: 205-219
- Chang CSJ, Maloof JN, Wu SH** (2011) COP1-mediated degradation of BBX22/LZFI optimizes seedling development in Arabidopsis. *Plant Physiol* 156: 228-239
- Chattopadhyay S, Puente P, Deng XW, Wei N** (1998a) Combinatorial interaction of light-responsive elements plays a critical role in determining the response characteristics of light-regulated promoters in Arabidopsis. *Plant J* 15: 69-77
- Chattopadhyay S, Ang LH, Puente P, Deng XW, Wei N** (1998b) Arabidopsis bZIP protein HY5 directly interacts with light-responsive promoters in mediating light-control of gene expression. *Plant Cell* 10: 673-684
- Chen M, Chory J, Fankhauser C** (2004) Light signal transduction in higher plants. *Annu Rev Genet* 38: 87-117
- Chen M, Chory J** (2011) Phytochrome signaling mechanisms and the control of plant development. *Trends Cell Biol* 21: 664-671
- Cheng CL, Acedo GN, Cristinsin M, Conkling MA** (1992) Sucrose mimics the light induction of Arabidopsis nitrate reductase gene transcription. *Proc Natl Acad Sci USA* 89: 1861-1864
- Cho YH, Yoo SD, Sheen J** (2006) Regulatory functions of nuclear hexokinase1 complex in glucose signaling. *Cell* 127: 579-589
- Choi G, Yi H, Lee J, Kwon YK, Soo Soh M, Shin B, Luka Z, Hahn TR, Song PS** (1999) Phytochrome signalling is mediated through nucleoside diphosphate kinase 2. *Nature* 401: 610-613
- Chow WS, Melis A, Anderson JM** (1990) Adjustments of photosystem stoichiometry in chloroplasts improve the quantum efficiency of photosynthesis. *Proc Natl Acad Sci USA* 87: 7502-7506
- Christie JM, Reymond P, Powell GK, Bernasconi P, Raibekas AA, Liscum E, Briggs WR** (1998) Arabidopsis NPH1: A flavoprotein with the properties of a photoreceptor for phototropism. *Science* 282: 1698-1701
- Christie JM, Salomon M, Nozue K, Wada M, Briggs WR** (1999) LOV (light, oxygen, or voltage) domains of the blue-light photoreceptor phototropin (*nph1*): Binding sites for the chromophore flavin mononucleotide. *Proc Natl Acad Sci USA* 96: 8779-8783
- Christie JM, Briggs WR** (2005) Blue light sensing and signaling by the phototropins. In WR Briggs, JL Spudich, eds, *Handbook of Photosensory Receptors*. Wiley-VCH, Weinheim, Germany, pp 277-303
- Christopher DA, Mullet JE** (1994) Separate photosensory pathways coregulate blue-light/ultraviolet-A-activated *psbD-psbC* transcription and light-induced D2 and CP43 degradation in barley (*Hordeum vulgare*) chloroplasts. *Plant Physiol* 104: 1119-1129
- Christopher DA** (1996) Leaf development and phytochrome modulate the activation of *psbD-psbC* transcription by high-fluence blue light in barley chloroplasts. *Photosynth Res* 47: 239-251
- Chun L, Kawakami A, Christopher DA** (2001) Phytochrome A mediates blue light and UV-A-dependent chloroplast gene transcription in green leaves. *Plant Physiol* 125: 1957-1966
- Clack T, Mathews S, Sharrock RA** (1994) The phytochrome apoprotein family in Arabidopsis is encoded by five genes – the sequences and expression of *PHYD* and *PHYE*. *Plant Mol Biol* 25: 413-427
- Clack T, Shokry A, Moffet M, Liu P, Faul M, Sharrock RA** (2009) Obligate heterodimerization of Arabidopsis phytochromes C and E and interaction with the PIF3 basic helix-loop-helix transcription factor. *Plant Cell* 21: 786-799
- Clough RC, Vierstra RD** (1997) Phytochrome degradation. *Plant Cell Env* 20: 713-721
- Clough SJ, Bent AF** (1998) Floral dip: A simplified method for *Agrobacterium*-mediated transformation of *Arabidopsis thaliana*. *Plant J* 16: 735-743

- Copeland L.** (1990) Enzymes of sucrose metabolism. *Methods Plant Biochem* 3: 73-85
- Corish P, Tyler-Smith C** (1999) Attenuation of green fluorescent protein half-life in mammalian cells. *Protein Eng* 12: 1035-1040
- Covington MF, Harmer SL** (2007) The circadian clock regulates auxin signaling and responses in *Arabidopsis*. *PLoS Biol* 5: 1773-1784
- Crosson S, Moffat K** (2001) Structure of a flavin-binding plant photoreceptor domain: Insights into light-mediated signal transduction. *Proc Natl Acad Sci USA* 98: 2995-3000
- Crosson S, Moffat K** (2002) Photoexcited structure of a plant photoreceptor domain reveals a light-driven molecular switch. *Plant Cell* 14: 1067-1075
- Datta S, Johansson H, Hettiarachchi C, Irigoyen ML, Desai M, Rubio V, Holm M** (2008) LZFI/SALT TOLERANCE HOMOLOG3, an *Arabidopsis* B-box protein involved in light-dependent development and gene expression, undergoes COP1-mediated ubiquitination. *Plant Cell* 20: 2324-2338
- De Boer GJ, Testerink C, Pielage G, Nijkamp HJJ, Stuitje AR** (1999) Sequences surrounding the transcription initiation site of the *Arabidopsis* enoyl-acyl carrier protein reductase gene control seed expression in transgenic tobacco. *Plant Mol Biol* 39: 1197-1207
- DeBlasio SL, Mullen JL, Luesse DR, Hangarter RP** (2003) Phytochrome modulation of blue light-induced chloroplast movements in *Arabidopsis*. *Plant Physiol* 133: 1471-1479
- Dehesh K, Franci C, Parks BM, Seeley KA, Short TW, Tepperman JM, Quail PH** (1993) *Arabidopsis* HY8 locus encodes phytochrome A. *Plant Cell* 5: 1081-1088
- Desikan R, Neill SJ, Hancock JT** (2000) Hydrogen peroxide-induced gene expression in *Arabidopsis thaliana*. *Free Radic Biol Med* 28: 773-778
- Desikan R, Mackerness SAH, Hancock JT, Neill SJ** (2001) Regulation of the *Arabidopsis* transcriptome by oxidative stress. *Plant Physiol* 127: 159-172
- Devlin PF, Patel SR, Whitelam GC** (1998) Phytochrome E influences internode elongation and flowering time in *Arabidopsis*. *Plant Cell* 10: 1479-1488
- Devlin PF, Robson PRH, Patel SR, Goosey L, Sharrock RA, Whitelam GC** (1999) Phytochrome D acts in the shade-avoidance syndrome in *Arabidopsis* by controlling elongation growth and flowering time. *Plant Physiol* 119: 909-915
- Dietz KJ, Schreiber U, Heber U** (1985) The relationship between the redox state of Q_A and photosynthesis in leaves at various carbon-dioxide, oxygen and light regimes. *Planta* 166: 219-226
- Dijkwel PP, Huijser C, Weisbeek PJ, Chua NH, Smeekens SCM** (1997) Sucrose control of phytochrome A signaling in *Arabidopsis*. *Plant Cell* 9: 583-595
- Doke N** (1985) NADPH-dependent O_2 -generation in membrane-fractions isolated from wounded potato-tubers inoculated with *Phytophthora infestans*. *Phys Plant Path* 27: 311-322
- Donald RGK, Cashmore AR** (1990) Mutation of either G-box or I-box sequences profoundly affects expression from the *Arabidopsis* *RBCS-1A* promoter. *EMBO J* 9: 1717-1726
- Duek PD, Elmer MV, van Oosten VR, Fankhauser C** (2004) The degradation of HFR1, a putative bHLH class transcription factor involved in light signaling, is regulated by phosphorylation and requires COP1. *Curr Biol* 14: 2296-2301
- Durfee T, Becherer K, Chen PL, Yeh SH, Yang Y, Kilburn AE, Lee WH, Elledge SJ** (1993) The retinoblastoma protein associates with the protein phosphatase type 1 catalytic subunit. *Genes & Dev* 7: 555-569
- Duysens LNM, Amesz J** (1962) Function and identification of two photochemical systems in photosynthesis. *Biochim Biophys Acta* 64: 243-260
- Edmondson DL, Badger MR, Andrews TJ** (1990) A kinetic characterization of slow inactivation of ribulosebiphosphate carboxylase during catalysis. *Plant Physiol* 93: 1376-1382

- Edwards KD, Anderson PE, Hall A, Salathia NS, Locke JCW, Lynn JR, Straume M, Smith JQ, Millar AJ** (2006) FLOWERING LOCUS C mediates natural variation in the high-temperature response of the *Arabidopsis* circadian clock. *Plant Cell* 18: 639-650
- English JJ, Davenport GF, Elmayan T, Vaucheret H, Baulcombe DC** (1997) Requirement of sense transcription for homology-dependent virus resistance and trans-inactivation. *Plant J* 12: 597-603
- Escoubas JM, Lomas M, LaRoche J, Falkowski PG** (1995) Light intensity regulation of *CAB* gene transcription is signaled by the redox state of the plastoquinone pool. *Proc Natl Acad Sci USA* 92: 10237-10241
- Estavillo GM, Crisp PA, Pornsiriwong W, Wirtz M, Collinge D, Carrie C, Giraud E, Whelan J, David P, Javot H, Brearley C, Hell R, Marin E, Pogson BJ** (2011) Evidence for a SAL1-PAP chloroplast retrograde pathway that functions in drought and high light signaling in *Arabidopsis*. *Plant Cell* 23: 3992-4012
- Evans L** (1971) Flower induction and the florigen concept. *Annu Rev Plant Physiol Plant Mol Biol* 22: 365-394
- Fankhauser C, Yeh KC, Lagarias JC, Zhang H, Elich TD, Chory J** (1999) PKS1, a substrate phosphorylated by phytochrome that modulates light signaling in *Arabidopsis*. *Science* 284: 1539-1541
- Fankhauser C** (2000) Phytochromes as light-modulated protein kinases. *Sem Cell Dev Biol* 11: 467-473
- Farineau J, Bottin H, Garab G** (1984) Effect of dibromothymoquinone (DBMIB) on reduction rates of photosystem I donors in intact chloroplasts. *Biochem Biophys Res Commun* 120: 721-725
- Fey V, Wagner R, Brautigam K, Wirtz M, Hell R, Dietzmann A, Leister D, Oelmüller R, Pfanschmidt T** (2005) Retrograde plastid redox signals in the expression of nuclear genes for chloroplast proteins of *Arabidopsis thaliana*. *J Biol Chem* 280: 5318-5328
- Fields S** (1993) The two-hybrid system to detect protein-protein interactions. *Methods: A Companion to Meth Enzymol* 5: 116-124
- Folta KM, Spalding EP** (2001) Unexpected roles for cryptochrome 2 and phototropin revealed by high-resolution analysis of blue light-mediated hypocotyl growth inhibition. *Plant J* 26: 471-478
- Folta KM, Kaufman LS** (2003) Phototropin 1 is required for high-fluence blue-light-mediated mRNA destabilization. *Plant Mol Biol* 51: 609-618
- Foyer CH, Lelandais M, Kunert KJ** (1994) Photooxidative stress in plants. *Physiol Plant* 92: 696-717
- Foyer CH, Kerchev PI, Hancock RD** (2012) The ABA-INSENSITIVE-4 (ABI4) transcription factor links redox-hormone and sugar signaling pathways. *Plant Signal Behav* 7: 276-281
- Franklin KA, Davis SJ, Stoddart WM, Vierstra RD, Whitelam GC** (2003a) Mutant analyses define multiple roles for phytochrome C in *Arabidopsis* photomorphogenesis. *Plant Cell* 15: 1981-1989
- Franklin KA, Prækel U, Stoddart WM, Billingham OE, Halliday KJ, Whitelam GC** (2003b) Phytochromes B, D, and E act redundantly to control multiple physiological responses in *Arabidopsis*. *Plant Physiol* 131: 1340-1346
- Franklin KA, Allen T, Whitelam GC** (2007) Phytochrome A is an irradiance-dependent red light sensor. *Plant J* 50: 108-117
- Franklin KA, Quail PH** (2010) Phytochrome functions in *Arabidopsis* development. *J Exp Bot* 61: 11-24
- Friedrich G, Soriano P** (1991) Promoter traps in embryonic stem-cells – a genetic screen to identify and mutate developmental genes in mice. *Genes & Dev* 5: 1513-1523
- Frohman MA, Dush MK, Martin GR** (1988) Rapid production of full-length cDNAs from rare transcripts – amplification using a single gene-specific oligonucleotide primer. *Proc Natl Acad Sci USA* 85: 8998-9002
- Fry SC, Smith RC, Renwick KF, Martin DJ, Hodge SK, Matthews KJ** (1992) Xyloglucan endotransglycosylase, a new wall-loosening enzyme activity from plants. *Biochem J* 282: 821-828
- Fujiwara M, Nagashima A, Kanamaru K, Tanaka K, Takahashi H** (2000) Three new nuclear genes, *sigD*, *sigE* and *sigF*, encoding putative plastid RNA polymerase σ factors in *Arabidopsis thaliana*. *FEBS Lett* 481: 47-52

- Furuya M** (1993) Phytochromes – their molecular-species, gene families, and functions. *Annu Rev Plant Physiol Plant Mol Biol* 44: 617-645
- Gallois JL, Nora FR, Mizukami Y, Sablowski R** (2004) WUSCHEL induces shoot stem cell activity and developmental plasticity in the root meristem. *Genes & Dev* 18: 375-380
- Gamble PE, Sexton TB, Mullet JE** (1988) Light-dependent changes in *psbD* and *psbC* transcripts of barley chloroplasts – accumulation of two transcripts maintains *psbD* and *psbC* translation capability in mature chloroplasts. *EMBO J* 7: 1289-1297
- Gamble PE, Mullet JE** (1989) Blue-light regulates the accumulation of two *psbD-psbC* transcripts in barley chloroplasts. *EMBO J* 8: 2785-2794
- Gao Y, Li JM, Strickland E, Hua SJ, Zhao HY, Chen ZL, Qu LJ, Deng XW** (2004) An Arabidopsis promoter microarray and its initial usage in the identification of HY5 binding targets *in vivo*. *Plant Mol Biol* 54: 683-699
- Gardner MJ, Baker AJ, Assie JM, Poethig RS, Haseloff JP, Webb AAR** (2009) *GAL4-GFP* enhancer trap lines for analysis of stomatal guard cell development and gene expression. *J Exp Bot* 60: 213-226
- Geigenberger P, Kolbe A, Tiessen A** (2005) Redox regulation of carbon storage and partitioning in response to light and sugars. *J Exp Bot* 56: 1469-1479
- Geisler M, Kleczkowski LA, Karpinski S** (2006) A universal algorithm for genome-wide *in silico* identification of biologically significant gene promoter putative *cis*-regulatory elements; identification of new elements for reactive oxygen species and sucrose signaling in Arabidopsis. *Plant J* 45: 384-398
- Ghezzi P, Bonetto V** (2003) Redox proteomics: Identification of oxidatively, modified proteins. *Proteomics* 3: 1145-1153
- Giardi MT, Masojidek J, Godde D** (1997) Effects of abiotic stresses on the turnover of the D1 reaction centre II protein. *Physiol Plant* 101: 635-642
- Gibson SI** (2004) Sugar and phytohormone response pathways: navigating a signalling network. *J Exp Bot* 55: 253-264
- Gibson SI** (2005) Control of plant development and gene expression by sugar signaling. *Curr Opin Plant Biol* 8: 93-102
- Gidoni D, Brosio P, Bondnutter D, Bedbrook J, Dunsmuir P** (1989) Novel *cis*-acting elements in Petunia *CAB* gene promoters. *Mol Gen Genet* 215: 337-344
- Gietz RD, Schiestl RH** (2007) High-efficiency yeast transformation using the LiAc/SS carrier DNA/PEG method. *Nat Protoc* 2: 31-34
- Gilmartin PM, Sarokin L, Memelink J, Chua NH** (1990) Molecular light switches for plant genes. *Plant Cell* 2: 369-378
- Giuliano G, Pichersky E, Malik VS, Timko MP, Scolnik PA, Cashmore AR** (1988) An evolutionarily conserved protein-binding sequence upstream of a plant light-regulated gene. *Proc Natl Acad Sci USA* 85: 7089-7093
- Goldschmidt EE, Huber SC** (1992) Regulation of photosynthesis by end-product accumulation in leaves of plants storing starch, sucrose, and hexose sugars. *Plant Physiol* 99: 1443-1448
- Gray JC, Sullivan JA, Wang JH, Jerome CA, MacLean D** (2003) Coordination of plastid and nuclear gene expression. *Philos Trans R Soc Lond B Biol Sci* 358: 135-145
- Greenberg BM, Gaba V, Canaani O, Malkin S, Mattoo AK, Edelman M** (1989) Separate photosensitizers mediate degradation of the 32-kDa photosystem II reaction center protein in the visible and UV spectral regions. *Proc Natl Acad Sci USA* 86: 6617-6620
- Grob U, Stuber K** (1987) Discrimination of phytochrome dependent light inducible from non-light inducible plant genes – prediction of a common light-responsive element (LRE) in phytochrome dependent light inducible plant genes. *Nucl Acids Res* 15: 9957-9973
- Guo H, Yang H, Mockler TC, Lin C** (1998) Regulation of flowering time by Arabidopsis photoreceptors. *Science* 279: 1360-1363

- Gustafson K, Boulianne GL** (1996) Distinct expression patterns detected within individual tissues by the GAL4 enhancer trap technique. *Genome* 39: 174-182
- Gutierrez RA, Ewing RM, Cherry JM, Green PJ** (2002) Identification of unstable transcripts in Arabidopsis by cDNA microarray analysis: Rapid decay is associated with a group of touch- and specific clock-controlled genes. *Proc Natl Acad Sci USA* 99: 11513-11518
- Ha SB, An GH** (1988) Identification of upstream regulatory elements involved in the developmental expression of the *Arabidopsis thaliana CAB1* gene. *Proc Natl Acad Sci USA* 85: 8017-8021
- Hajdukiewicz PTJ, Allison LA, Maliga P** (1997) The two RNA polymerases encoded by the nuclear and the plastid compartments transcribe distinct groups of genes in tobacco plastids. *EMBO J* 16: 4041-4048
- Haldrup A, Jensen PE, Lunde C, Scheller HV** (2001) Balance of power: a view of the mechanism of photosynthetic state transitions. *Trends Plant Sci* 6: 301-305
- Halford NG, Hey S, Jhurrea D, Laurie S, McKibbin RS, Paul M, Zhang YH** (2003) Metabolic signalling and carbon partitioning: role of Snf1-related (SnRK1) protein kinase. *J Exp Bot* 54: 467-475
- Halliwell B** (1987) Oxidative damage, lipid-peroxidation and antioxidant protection in chloroplasts. *Chem Phys Lipids* 44: 327-340
- Halliwell B, Gutteridge JMC** (1999) Free radicals in biology and medicine. 3rd ed. Oxford University Press Oxford
- Hardtke CS, Deng XW** (2000) The cell biology of the COP/DET/FUS proteins. Regulating proteolysis in photomorphogenesis and beyond? *Plant Physiol* 124: 1548-1557
- Harrington GN, Bush DR** (2003) The bifunctional role of hexokinase in metabolism and glucose signaling. *Plant Cell* 15: 2493-2496
- Harrison SJ, Mott EK, Parsley K, Aspinall S, Gray JC, Cottage A** (2006) A rapid and robust method of identifying transformed *Arabidopsis thaliana* seedlings following floral dip transformation. *Plant Methods* 2: 19
- Harter K, Kircher S, Frohnmeier H, Krenz M, Nagy F, Schäfer E** (1994) Light-regulated modification and nuclear translocation of cytosolic G-box binding-factors in parsley. *Plant Cell* 6: 545-559
- Haseloff J, Siemering KR, Prasher DC, Hodge S** (1997) Removal of a cryptic intron and subcellular localization of green fluorescent protein are required to mark transgenic Arabidopsis plants brightly. *Proc Natl Acad Sci USA* 94: 2122-2127
- Haseloff J** (1999) GFP variants for multispectral imaging of living cells. *Methods Cell Biol* 58: 139-151
- Haynes D, Ralph P, Prange J, Dennison B** (2000) The impact of the herbicide diuron on photosynthesis in three species of tropical seagrass. *Mar Pollut Bull* 41: 288-293
- He YH, Tang WN, Swain JD, Green AL, Jack TP, Gan SS** (2001) Networking senescence-regulating pathways by using Arabidopsis enhancer trap lines. *Plant Physiol* 126: 707-716
- Heazlewood JL, Tonti-Filippini J, Verboom RE, Millar AH** (2005) Combining experimental and predicted datasets for determination of the subcellular location of proteins in Arabidopsis. *Plant Physiol* 139: 598-609
- Heazlewood JL, Verboom RE, Tonti-Filippini J, Small I, Millar A** (2007) SUBA: The Arabidopsis subcellular database. *Nucl Acids Res* 35: D213-D218
- Hedtke B, Borner T, Weihe A** (1997) Mitochondrial and chloroplast phage-type RNA polymerases in Arabidopsis. *Science* 277: 809-811
- Heiber I, Ströher E, Raatz B, Busse I, Kahmann U, Bevan MW, Dietz KJ, Baier M** (2007) The redox imbalanced mutants of Arabidopsis differentiate signaling pathways for redox regulation of chloroplast antioxidant enzymes. *Plant Physiol* 143: 1774-1788
- Hendriks JHM, Kolbe A, Gibon Y, Stitt M, Geigenberger P** (2003) ADP-glucose pyrophosphorylase is activated by posttranslational redox-modification in response to light and to sugars in leaves of Arabidopsis and other plant species. *Plant Physiol* 133: 838-849

- Hennig L, Funk M, Whitelam GC, Schäfer E** (1999a) Functional interaction of cryptochrome 1 and phytochrome D. *Plant J* 20: 289-294
- Hennig L, Buche C, Eichenberg K, Schäfer E** (1999b) Dynamic properties of endogenous phytochrome A in *Arabidopsis* seedlings. *Plant Physiol* 121: 571-577
- Hennig L, Stoddart WM, Dieterle M, Whitelam GC, Schäfer E** (2002) Phytochrome E controls light-induced germination of *Arabidopsis*. *Plant Physiol* 128: 194-200
- Higo K, Ugawa Y, Iwamoto M, Korenaga T** (1999) Plant *cis*-acting regulatory DNA elements (PLACE) database: 1999. *Nucl Acids Res* 27: 297-300
- Hill SA** (1998) Carbohydrate metabolism in plants. *Trends Plant Sci* 3: 370-371
- Hirschfeld M, Tepperman JM, Clack T, Quail PH, Sharrock RA** (1998) Coordination of phytochrome levels in *phyB* mutants of *Arabidopsis* as revealed by apoprotein-specific monoclonal antibodies. *Genetics* 149: 523-535
- Hoecker U, Tepperman JM, Quail PH** (1999) SPA1, a WD-repeat protein specific to phytochrome A signal transduction. *Science* 284: 496-499
- Hoffer PH, Christopher DA** (1997) Structure and blue-light-responsive transcription of a chloroplast *psbD* promoter from *Arabidopsis thaliana*. *Plant Physiol* 115: 213-222
- Hoffman PD, Batschauer A, Hays JB** (1996) *PHH1*, a novel gene from *Arabidopsis thaliana* that encodes a protein similar to plant blue-light photoreceptors and microbial photolyases. *Mol Gen Genet* 253: 259-265
- Holm M, Ma LG, Qu LJ, Deng XW** (2002) Two interacting bZIP proteins are direct targets of COP1-mediated control of light-dependent gene expression in *Arabidopsis*. *Genes & Dev* 16: 1247-1259
- Holmgren A** (1989) Thioredoxin and glutaredoxin systems. *J Biol Chem* 264: 13963-13966
- Homann A, Link G** (2003) DNA-binding and transcription characteristics of three cloned sigma factors from mustard (*Sinapis alba* L.) suggest overlapping and distinct roles in plastid gene expression. *Eur J Biochem* 270: 1288-1300
- Hou CX, Pursiheimo S, Rintamaki E, Aro EM** (2002) Environmental and metabolic control of LHCII protein phosphorylation: revealing the mechanisms for dual regulation of the LHCII kinase. *Plant Cell Env* 25: 1515-1525
- Hruz T, Laule O, Szabo G, Wessendorp F, Bleuler S, Oertle L, Widmayer P, Gruissem W, Zimmermann P** (2008) Genevestigator v3: a reference expression database for the meta-analysis of transcriptomes. *Adv bioinformatics* 2008: 420747
- Hu J, Bogorad L** (1990) Maize chloroplast RNA-polymerase – the 180-kilodalton, 120-kilodalton, and 38-kilodalton polypeptides are encoded in chloroplast genes. *Proc Natl Acad Sci USA* 87: 1531-1535
- Huala E, Oeller PW, Liscum E, Han IS, Larsen E, Briggs WR** (1997) *Arabidopsis* NPH1: A protein kinase with a putative redox-sensing domain. *Science* 278: 2120-2123
- Hudson ME, Quail PH** (2003) Identification of promoter motifs involved in the network of phytochrome A-regulated gene expression by combined analysis of genomic sequence and microarray data. *Plant Physiol* 133: 1605-1616
- Huijser C, Kortstee A, Pego J, Weisbeek P, Wisman E, Smeekens S** (2000) The *Arabidopsis* SUCROSE UNCOUPLED-6 gene is identical to ABSCISIC ACID INSENSITIVE-4: involvement of abscisic acid in sugar responses. *Plant J* 23: 577-585
- Huner NPA, Oquist G, Sarhan F** (1998) Energy balance and acclimation to light and cold. *Trends Plant Sci* 3: 224-230
- Huq E, Al-Sady B, Hudson M, Kim CH, Apel M, Quail PH** (2004) PHYTOCHROME-INTERACTING FACTOR 1 is a critical bHLH regulator of chlorophyll biosynthesis. *Science* 305: 1937-1941
- Huq E, Quail PH** (2002) PIF4, a phytochrome-interacting bHLH factor, functions as a negative regulator of phytochrome B signaling in *Arabidopsis*. *EMBO J* 21: 2441-2450

- Ibraheem O, Botha CEJ, Bradley G** (2010) *In silico* analysis of *cis*-acting regulatory elements in 5' regulatory regions of sucrose transporter gene families in rice (*Oryza sativa* Japonica) and *Arabidopsis thaliana*. *Comput Biol Chem* 34: 268-283
- Ilag LL, Kumar AM, Soll D** (1994) Light regulation of chlorophyll biosynthesis at the level of 5-aminolevulinic acid formation in *Arabidopsis*. *Plant Cell* 6: 265-275
- Imaizumi T, Tran HG, Swartz TE, Briggs WR, Kay SA** (2003) FKF1 is essential for photoperiodic-specific light signalling in *Arabidopsis*. *Nature* 426: 302-306
- Isegawa Y, Sheng J, Sokawa Y, Yamanishi K, Nakagomi O, Ueda S** (1992) Selective amplification of cDNA sequence from total RNA by cassette-ligation mediated polymerase chain-reaction (PCR) – application to sequencing 6.5 kb genome segment of Hantavirus strain B-1. *Mol Cell Probes* 6: 467-475
- Ishizaki Y, Tsunoyama Y, Hatano K, Ando K, Kato K, Shinmyo A, Kobori M, Takeba G, Nakahira Y, Shiina T** (2005) A nuclear-encoded sigma factor, *Arabidopsis* SIG6, recognizes sigma-70 type chloroplast promoters and regulates early chloroplast development in cotyledons. *Plant J* 42: 133-144
- Isono K, Niwa Y, Satoh K, Kobayashi H** (1997) Evidence for transcriptional regulation of plastid photosynthesis genes in *Arabidopsis thaliana* roots. *Plant Physiol* 114: 623-630
- Jang JC, Leon P, Zhou L, Sheen J** (1997) Hexokinase as a sugar sensor in higher plants. *Plant Cell* 9: 5-19
- Jansen MAK, Babu TS, Heller D, Gaba V, Mattoo AK, Edelman M** (1996) Ultraviolet-B effects on *Spirodela oligorrhiza*: Induction of different protection mechanisms. *Plant Science* 115: 217-223
- Jarillo JA, Gabrys H, Capel J, Alonso JM, Ecker JR, Cashmore AR** (2001) Phototropin-related NPL1 controls chloroplast relocation induced by blue light. *Nature* 410: 952-954
- Jarvis P** (2008) Targeting of nucleus-encoded proteins to chloroplasts in plants. *New Phytol* 179: 257-285
- Jiang L, Wang Y, Bjorn LO, Li S** (2009) *Arabidopsis* *RADICAL-INDUCED CELL DEATH1* is involved in UV-B signaling. *Photochem Photobiol Sci* 8: 838-846
- Jiao YL, Ma LG, Strickland E, Deng XW** (2005) Conservation and divergence of light-regulated genome expression patterns during seedling development in rice and *Arabidopsis*. *Plant Cell* 17: 3239-3256
- Jiao Y, Lau OS, Deng XW** (2007) Light-regulated transcriptional networks in higher plants. *Nat Rev Genet* 8: 217-230
- Jones AM, Quail PH** (1986) Quaternary structure of 124-kilodalton phytochrome from *Avena sativa* L. *Biochem* 25: 2987-2995
- Junesch U, Gräber P** (1987) Influence of the redox state and the activation of the chloroplast ATP synthase on proton-transport-coupled ATP synthesis hydrolysis. *Biochim Biophys Acta* 893: 275-288
- Junesch U, Gräber P** (1991) The rate of ATP-synthesis as a function of ΔpH and $\Delta\psi$ catalyzed by the active, reduced H^+ -ATPase from chloroplasts. *FEBS Lett* 294: 275-278
- Kagawa T, Sakai T, Suetsugu N, Oikawa K, Ishiguro S, Kato T, Tabata S, Okada K, Wada M** (2001) *Arabidopsis* NPL1: A phototropin homolog controlling the chloroplast high-light avoidance response. *Science* 291: 2138-2141
- Kagawa T, Kasahara M, Abe T, Yoshida S, Wada M** (2004) Function analysis of phototropin 2 using fern mutants deficient in blue light-induced chloroplast avoidance movement. *Plant Cell Physiol* 45: 416-426
- Kakizaki T, Matsumura H, Nakayama K, Che FS, Terauchi R, Inaba T** (2009) Coordination of plastid protein import and nuclear gene expression by plastid-to-nucleus retrograde signaling. *Plant Physiol* 151: 1339-1353
- Kanamaru K, Nagashima A, Fujiwara M, Shimada H, Shirano Y, Nakabayashi K, Shibata D, Tanaka K, Takahashi H** (2001) An *Arabidopsis* sigma factor (SIG2)-dependent expression of plastid-encoded tRNAs in chloroplasts. *Plant Cell Physiol* 42: 1034-1043
- Karimi M, Inzé D, Depicker A** (2002) GATEWAY™ vectors for *Agrobacterium*-mediated plant transformation. *Trends Plant Sci* 7: 193-195

- Karpinska B, Wingsle G, Karpinski S** (2000) Antagonistic effects of hydrogen peroxide and glutathione on acclimation to excess excitation energy in *Arabidopsis*. *IUBMB Life* 50: 21-26
- Karpinski S, Escobar C, Karpinska B, Creissen G, Mullineaux PM** (1997) Photosynthetic electron transport regulates the expression of cytosolic ascorbate peroxidase genes in *Arabidopsis* during excess light stress. *Plant Cell* 9: 627-640
- Karpinski S, Reynolds H, Karpinska B, Wingsle G, Creissen G, Mullineaux P** (1999) Systemic signaling and acclimation in response to excess excitation energy in *Arabidopsis*. *Science* 284: 654-657
- Kasahara M, Kagawa T, Oikawa K, Suetsugu N, Miyao M, Wada M** (2002) Chloroplast avoidance movement reduces photodamage in plants. *Nature* 420: 829-832
- Keegan L, Gill G, Ptashne M** (1986) Separation of DNA-binding from the transcription-activating function of a eukaryotic regulatory protein. *Science* 231: 699-704
- Keller MM, Jaillais Y, Pedmale UV, Moreno JE, Chory J, Ballaré CL** (2011) Cryptochrome1 and phytochrome B control shade-avoidance responses in *Arabidopsis* via partially independent hormonal cascades. *Plant J* 67: 195-207
- Kendrick RE, Kronenberg G** (1994) Photomorphogenesis in plants. Kluwer Academic Publishers, Dordrecht, The Netherlands
- Kevei E, Schäfer E, Nagy F** (2007) Light-regulated nucleo-cytoplasmic partitioning of phytochromes. *J Exp Bot* 58: 3113-3124
- Kim MY, Mullet JE** (1995) Identification of a sequence-specific DNA-binding factor required for transcription of the barley chloroplast blue light-responsive *psbD-psbC* promoter. *Plant Cell* 7: 1445-1457
- Kim J, Harter K, Theologis A** (1997) Protein-protein interactions among the Aux/IAA-proteins. *Proc Natl Acad Sci USA* 94: 11786-11791
- Kim M, Thum KE, Morishige DT, Mullet JE** (1999a) Detailed architecture of the barley chloroplast *psbD-psbC* blue light-responsive promoter. *J Bact Chem* 274: 4684-4692
- Kim M, Christopher DA, Mullet JE** (1999b) ADP-dependent phosphorylation regulates association of a DNA-binding complex with the barley chloroplast *psbD* blue-light-responsive promoter. *Plant Physiol* 119: 663-670
- Kim WY, Fujiwara S, Suh SS, Kim J, Kim Y, Han L, Davin, K, Putterill J, Nam HG, Somers DE** (2007) ZEITLUPE is a circadian photoreceptor stabilized by GIGANTEA in blue light. *Nature* 449: 356-360
- Kimura M, Yamamoto YY, Seki M, Sakurai T, Sato M, Abe T, Yoshida S, Manabe K, Shinozaki K, Matsui M** (2003) Identification of *Arabidopsis* genes regulated by high light-stress using cDNA microarray. *Photochem Photobiol* 77: 226-233
- Kinoshita T, Doi M, Suetsugu N, Kagawa T, Wada M, Shimazaki K** (2001) Phot1 and phot2 mediate blue light regulation of stomatal opening. *Nature* 414: 656-660
- Kircher S, Gil P, Kozma-Bognar L, Fejes E, Speth V, Husselstein-Muller T, Bauer D, Adam E, Schäfer E, Nagy F** (2002) Nucleocytoplasmic partitioning of the plant photoreceptors phytochrome A, B, C, D, and E is regulated differentially by light and exhibits a diurnal rhythm. *Plant Cell* 14: 1541-1555
- Klein RR, Mullet JE** (1990) Light-induced transcription of chloroplast genes – *psbA* transcription is differentially enhanced in illuminated barley. *J Biol Chem* 265: 1895-1902
- Kleine T, Lockhart P, Batschauer A** (2003) An *Arabidopsis* protein closely related to *Synechocystis* cryptochrome is targeted to organelles. *Plant J* 35: 93-103
- Kleine T, Kindgren P, Benedict C, Hendrickson L, Strand Å** (2007) Genome-wide gene expression analysis reveals a critical role for CRYPTOCHROME1 in the response of *Arabidopsis* to high irradiance. *Plant Physiol* 144: 1391-1406
- Klimczak LJ, Schindler U, Cashmore AR** (1992) DNA-binding activity of the *Arabidopsis* G-box binding-factor GBF1 is stimulated by phosphorylation by casein kinase-II from broccoli. *Plant Cell* 4: 87-98

- Klimczak LJ, Collinge MA, Farini D, Giuliano G, Walker JC, Cashmore AR** (1995) Reconstitution of Arabidopsis casein kinase-II from recombinant subunits and phosphorylation of transcription factor GBF1. *Plant Cell* 7: 105-115
- Kohzuma K, Dal Bosco C, Kanazawa A, Dhingra A, Nitschke W, Meurer J, Kramer DM** (2012) Thioredoxin-insensitive plastid ATP synthase that performs moonlighting functions. *Proc Natl Acad Sci USA* 109: 3293-3298
- Koncz C, Schell J** (1986) The promoter of T_L-DNA gene 5 controls the tissue-specific expression of chimaeric genes carried by a novel type of *Agrobacterium* binary vector. *Mol Gen Genet* 204: 383-396
- Koorneef M, Rolff E, Spruit CJP** (1980) Genetic-control of light-inhibited hypocotyl elongation in *Arabidopsis thaliana* (L) Heynh. *Z Pflanzenphysiol* 100: 147-160
- Koussevitzky S, Nott A, Mockler TC, Hong F, Sachetto-Martins G, Surpin M, Lim J, Mittler R, Chory J** (2007) Signals from chloroplasts converge to regulate nuclear gene expression. *Science* 316: 715-719
- Krapp A, Hofmann B, Schäfer C, Stitt M** (1993) Regulation of the expression of *rbcS* and other photosynthetic genes by carbohydrates: a mechanism for the "sink regulation" of photosynthesis? *Plant J* 3: 817-828
- Krause K, Maier RM, Kofer W, Krupinska K, Herrmann RG** (2000) Disruption of plastid-encoded RNA polymerase genes in tobacco: expression of only a distinct set of genes is not based on selective transcription of the plastid chromosome. *Mol Gen Genet* 263: 1022-1030
- Kubota Y, Miyao A, Hirochika H, Tozawa Y, Yasuda H, Tsunoyama Y, Niwa Y, Imamura S, Shirai M, Asayama M** (2007) Two novel nuclear genes, *OsSIG5* and *OsSIG6*, encoding potential plastid sigma factors of RNA polymerase in rice: Tissue-specific and light-responsive gene expression. *Plant Cell Physiol* 48: 186-192
- Kuhlemeier C, Cuzzo M, Green PJ, Goyvaerts E, Ward K, Chua NH** (1988) Localization and conditional redundancy of regulatory elements in *RBCS-3A*, a pea gene encoding the small subunit of ribulose-bisphosphate carboxylase. *Proc Natl Acad Sci USA* 85: 4662-4666
- Kuhlemeier C** (1992) Transcriptional and posttranscriptional regulation of gene-expression in plants. *Plant Mol Biol* 19: 1-14
- Kusnetsov V, Bolle C, Lubberstedt T, Sopory S, Herrmann RG, Oelmüller R** (1996) Evidence that the plastid signal and light operate via the same *cis*-acting elements in the promoters of nuclear genes for plastid proteins. *Mol Gen Genet* 252: 631-639
- Kwok SF, Piekos B, Misera S, Deng XW** (1996) A complement of ten essential and pleiotropic Arabidopsis COP/DET/FUS genes is necessary for repression of photomorphogenesis in darkness. *Plant Physiol* 110: 731-742
- Lagarias JC, Rapoport H** (1980) Chromopeptides from phytochrome. The structure and linkage of the P_R form of the phytochrome chromophore. *J Am Chem Soc* 102: 4821-4828
- Lamesch P, Berardini TZ, Li D, Swarbreck D, Wilks C, Sasidharan R, Muller R, Dreher K, Alexander DL, Garcia-Hernandez M, Karthikeyan AS, Lee CH, Nelson WD, Ploetz L, Singh S, Wensel A, Huala E** (2012) The Arabidopsis Information Resource (TAIR): improved gene annotation and new tools. *Nucl Acids Res* 40: D1202-D1210
- Laplaze L, Parizot B, Baker A, Ricaud L, Martini-Łre A, Auguy F, Franche C, Nussaume L, Bogusz D, Haseloff J** (2005) *GAL4-GFP* enhancer trap lines for genetic manipulation of lateral root development in *Arabidopsis thaliana*. *J Exp Bot* 56: 2433-2442
- Larkin RM, Alonso JM, Ecker JR, Chory J** (2003) GUN4, a regulator of chlorophyll synthesis and intracellular signaling. *Science* 299: 902-906
- Lascève G, Leymarie J, Olney MA, Liscum E, Christie JM, Vavasseur A, Briggs WR** (1999) Arabidopsis contains at least four independent blue-light-activated signal transduction pathways. *Plant Physiol* 120: 605-614
- Lau OS, Deng XW** (2010) Plant hormone signaling lightens up: integrators of light and hormones. *Curr Opin Plant Biol* 13: 571-577

- Lee J, He K, Stolc V, Lee H, Figueroa P, Gao Y, Tongprasit W, Zhao H, Lee I, Deng XW** (2007) Analysis of transcription factor HY5 genomic binding sites revealed its hierarchical role in light regulation of development. *Plant Cell* 19: 731-749
- Legen J, Kemp S, Krause K, Profanter B, Herrmann RG, Maier RM** (2002) Comparative analysis of plastid transcription profiles of entire plastid chromosomes from tobacco attributed to wild-type and PEP-deficient transcription machineries. *Plant J* 31: 171-188
- Leivar P, Monte E, Al-Sady B, Carle C, Storer A, Alonso JM, Ecker JR, Quail PH** (2008) The Arabidopsis phytochrome-interacting factor PIF7, together with PIF3 and PIF4, regulates responses to prolonged red light by modulating phyB levels. *Plant Cell* 20: 337-352
- Leivar P, Quail PH** (2011) PIFs: pivotal components in a cellular signaling hub. *Trends Plant Sci* 16: 19-28
- Leon P, Sheen J** (2003) Sugar and hormone connections. *Trends Plant Sci* 8: 110-116
- Lerbs-Mache S** (2011) Function of plastid sigma factors in higher plants: regulation of gene expression or just preservation of constitutive transcription? *Plant Mol Biol* 76: 235-249
- Li Z, Wakao S, Fischer BB, Niyogi KK** (2009) Sensing and responding to excess light. *Annu Rev Plant Biol* 60: 239-260
- Lian HL, He SB, Zhang YC, Zhu DM, Zhang JY, Jia KP, Sun SX, Li L, Yang HQ** (2011) Blue-light-dependent interaction of cryptochrome 1 with SPA1 defines a dynamic signaling mechanism. *Genes & Dev* 25: 1023-1028
- Liere K, Maliga P** (2001) Plastid RNA polymerases in higher plants. In EM Aro, B Andersson, eds, *Regulation of Photosynthesis*. Kluwer, Rotterdam, Netherlands, pp 29-49
- Liere K, Weihe A, Boerner T** (2011) The transcription machineries of plant mitochondria and chloroplasts: Composition, function, and regulation. *J Plant Physiol* 168: 1345-1360
- Lin C, Ahmad M, Chan J, Cashmore AR** (1995a) CRY2, a second member of the Arabidopsis cryptochrome gene family. *Plant Phys* 110: 1047
- Lin CT, Robertson DE, Ahmad M, Raibekas AA, Jorns MS, Dutton PL, Cashmore AR** (1995b) Association of flavin adenine-dinucleotide with the *Arabidopsis* blue-light receptor CRY1. *Science* 269: 968-970
- Lin C, Yang H, Guo H, Mockler T, Chen J, Cashmore AR** (1998) Enhancement of blue-light sensitivity of Arabidopsis seedlings by a blue light receptor cryptochrome 2. *Proc Natl Acad Sci USA* 95: 2686-2690
- Lin C** (2002) Blue light receptors and signal transduction. *Plant Cell* 14: S207-S225
- Liscum E, Hodgson DW, Campbell TJ** (2003) Blue light signaling through the cryptochromes and phototropins. So that's what the blues is all about. *Plant Physiol* 133: 1429-1436
- Liu YG, Mitsukawa N, Oosumi T, Whittier RF** (1995) Efficient isolation and mapping of *Arabidopsis thaliana* T-DNA insert junctions by thermal asymmetric interlaced PCR. *Plant J* 8: 457-463
- Liu B, Troxler RF** (1996) Molecular characterization of a positively photoregulated nuclear gene for a chloroplast RNA polymerase sigma factor in *Cyanidium caldarium*. *Proc Natl Acad Sci USA* 93: 3313-3318
- Liu H, Yu X, Li K, Klejnot J, Yang H, Lisiero D, Lin C** (2008) Photoexcited CRY2 interacts with CIB1 to regulate transcription and floral initiation in Arabidopsis. *Science* 322: 1535-1539
- Liu H, Liu B, Zhao C, Pepper M, Lin C** (2011) The action mechanisms of plant cryptochromes. *Trends Plant Sci* 16: 684-691
- Loh EY, Elliott JF, Cwirla S, Lanier LL, Davis MM** (1989) Polymerase chain-reaction with single-sided specificity – analysis of T-cell receptor delta-chain. *Science* 243: 217-220
- López-Juez E, Dillon E, Magyar Z, Khan S, Hazeldine S, de Jager SM, Murray JAH, Beechster GTS, Bogre L, Shanahan H** (2008) Distinct light-initiated gene expression and cell cycle programs in the shoot apex and cotyledons of Arabidopsis. *Plant Cell* 20: 947-968

- López-Ochoa L, Acevedo-Hernández G, Martínez-Hernández A, Argüello-Astorga G, Herrera-Estrella L** (2007) Structural relationships between diverse *cis*-acting elements are critical for the functional properties of a *rbcS* minimal light regulatory unit. *J Exp Bot* 58: 4397-4406
- Lorenzo O, Chico JM, Sánchez-Serrano JJ, Solano R** (2004) Jasmonate-insensitive1 encodes a MYC transcription factor essential to discriminate between different jasmonate-regulated defense responses in *Arabidopsis*. *Plant Cell* 16: 1938-1950
- Loreti E, Alpi A, Perata P** (2000) Glucose and disaccharide-sensing mechanisms modulate the expression of alpha-amylase in barley embryos. *Plant Physiol* 123: 939-948
- Lorrain S, Genould T, Fankhauser C** (2006) Let there be light in the nucleus! *Curr Opin Plant Biol* 9: 509-514
- Lorrain S, Allen T, Duek PD, Whitelam GC, Fankhauser C** (2008) Phytochrome-mediated inhibition of shade avoidance involves degradation of growth-promoting bHLH transcription factors. *Plant J* 53: 312-323
- Lu YT, Feldman LJ** (1997) Light-regulated root gravitropism: a role for, and characterization of, a calcium/calmodulin-dependent protein kinase homolog. *Planta* 203: S91-S97
- Lu CA, Lim EK, Yu SM** (1998) Sugar response sequence in the promoter of a rice α -amylase gene serves as a transcriptional enhancer. *J Biol Chem* 273: 10120-10131
- Lu CA, Ho THD, Ho SL, Yu SM** (2002) Three novel MYB proteins with one DNA binding repeat mediate sugar and hormone regulation of alpha-amylase gene expression. *Plant Cell* 14: 1963-1980
- Lübberstedt T, Oelmüller R, Wanner G, Herrmann RG** (1994) Interacting *cis*-elements in the plastocyanin promoter from spinach ensure regulated high-level expression. *Mol Gen Genet* 242: 602-613
- Ma LG, Li JM, Qu LJ, Hager J, Chen ZL, Zhao HY, Deng XW** (2001) Light control of *Arabidopsis* development entails coordinated regulation of genome expression and cellular pathways. *Plant Cell* 13: 2589-2607
- Mahalingam R, Fedoroff N** (2003) Stress response, cell death and signalling: the many faces of reactive oxygen species. *Physiol Plant* 119: 56-68
- Maliga P** (1998) Two plastid RNA polymerases of higher plants: an evolving story. *Trends Plant Sci* 3: 4-6
- Mallappa C, Yadav V, Negi P, Chattopadhyay S** (2006) A basic leucine zipper transcription factor, G-box-binding factor 1, regulates blue light-mediated photomorphogenic growth in *Arabidopsis*. *J Biol Chem* 281: 22190-22199
- Martin C, Smith AM** (1995) Starch biosynthesis. *Plant Cell* 7: 971-985
- Martin W, Herrmann RG** (1998) Gene transfer from organelles to the nucleus: How much, what happens, and why? *Plant Physiol* 118: 9-17
- Martínez-García JF, Huq E, Quail PH** (2000) Direct targeting of light signals to a promoter element-bound transcription factor. *Science* 288: 859-863
- Martínez-García JF, Galstyan A, Salla-Martret M, Cifuentes-Esquivel N, Gallemi M, Bou-Torrent J** (2010) Regulatory components of shade avoidance syndrome. *Adv Bot Res* 52: 65-116
- Martínez-Hernández A, López-Ochoa L, Argüello-Astorga G, Herrera-Estrella L** (2002) Functional properties and regulatory complexity of a minimal *RBCS* light-responsive unit activated by phytochrome, cryptochrome, and plastid signals. *Plant Physiol* 128: 1223-1233
- Martínez-Noël G, Tognetti J, Nagaraj V, Wiemken A, Pontis H** (2006) Calcium is essential for fructan synthesis induction mediated by sucrose in wheat. *Planta* 225: 183-191
- Más P, Devlin PF, Panda S, Kay SA** (2000) Functional interaction of phytochrome B and cryptochrome 2. *Nature* 408: 207-211
- Masuda T, Tanaka A, Melis A** (2003) Chlorophyll antenna size adjustments by irradiance in *Dunaliella salina* involve coordinate regulation of chlorophyll a oxygenase (*CAO*) and *LHCB* gene expression. *Plant Mol Biol* 51: 757-771
- Mattoo AK, Pick U, Hoffmanfalk H, Edelman M** (1981) The rapidly metabolized 32,000-dalton polypeptide of the chloroplast is the proteinaceous shield regulating photosystem II electron-transport and mediating diuron herbicide sensitivity. *Proc Natl Acad Sci USA* 78: 1572-1576

- Mattoo AK, Hoffmanfalk H, Marder JB, Edelman M** (1984) Regulation of protein-metabolism – coupling of photosynthetic electron-transport to *in vivo* degradation of the rapidly metabolized 32-kilodalton protein of the chloroplast membranes. *Proc Natl Acad Sci USA* 81: 1380-1384
- Mattoo AK, Marder JB, Edelman M** (1989) Dynamics of the photosystem II reaction center. *Cell* 56: 241-246
- Maxwell DP, Laudenbach DE, Huner NPA** (1995) Redox regulation of light-harvesting complex-II and *CAB* messenger-RNA abundance in *Dunaliella salina*. *Plant Physiol* 109: 787-795
- McClung CR** (2001) Circadian rhythms in plants. *Annu Rev Plant Physiol Plant Mol Biol* 52: 139-162
- McCormac AC, Fischer A, Kumar AM, Soll D, Terry MJ** (2001) Regulation of *HEMA1* expression by phytochrome and a plastid signal during de-etiolation in *Arabidopsis thaliana*. *Plant J* 25: 549-561
- McKendree WL, Ferl RJ** (1992) Functional elements of the *Arabidopsis ADH* promoter include the G-box. *Plant Mol Biol* 19: 859-862
- McNellis TW, von Arnim AG, Araki T, Komeda Y, Misera S, Deng XW** (1994) Genetic and molecular analysis of an allelic series of *cop1* mutants suggests functional roles for the multiple protein domains. *Plant Cell* 6: 487-500
- Melis A** (1989) Spectroscopic methods in photosynthesis: Photosystem stoichiometry and chlorophyll antenna size. *Philos Trans R Soc Lond B Biol Sci* 323: 397-409
- Menkens AE, Cashmore AR** (1994) Isolation and characterization of a fourth *Arabidopsis thaliana* G-box-binding factor, which has similarities to Fos oncoprotein. *Proc Natl Acad Sci USA* 91: 2522-2526
- Menkens AE, Schindler U, Cashmore AR** (1995) The G-box – a ubiquitous regulatory DNA element in plants bound by the GBF family of bZIP proteins. *Trends Biochem Sci* 20: 506-510
- Michael TP, McClung CR** (2003) Enhancer trapping reveals widespread circadian clock transcriptional control in *Arabidopsis*. *Plant Physiol* 132: 629-639
- Michael TP, Mockler TC, Breton G, McEntee C, Byer A, Trout JD, Hazen SP, Shen R, Priest HD, Sullivan CM, Givan SA, Yanovsky M, Hong Fangxin, Kay SA, Chory J** (2008) Network discovery pipeline elucidates conserved time-of-day-specific *cis*-regulatory modules. *PLoS Genet* 4: e14
- Mitra A, Choi HK, An GH** (1989) Structural and functional analyses of *Arabidopsis thaliana* chlorophyll a/b-binding protein (*CAB*) promoters. *Plant Mol Biol* 12: 169-179
- Mittler R, Vanderauwera S, Gollery M, Van Breusegem F** (2004) Reactive oxygen gene network of plants. *Trends Plant Sci* 9: 490-498
- Mochizuki N, Brusslan JA, Larkin R, Nagatani A, Chory J** (2001) *Arabidopsis genomes uncoupled 5 (GUN5)* mutant reveals the involvement of Mg-chelatase H subunit in plastid-to-nucleus signal transduction. *Proc Natl Acad Sci USA* 98: 2053-2058
- Mochizuki T, Onda Y, Fujiwara E, Wada M, Toyoshima Y** (2004) Two independent light signals cooperate in the activation of the plastid *psbD* blue light-responsive promoter in *Arabidopsis*. *FEBS Lett* 571: 26-30
- Mochizuki N, Tanaka R, Tanaka A, Masuda T, Nagatani A** (2008) The steady-state level of Mg-protoporphyrin IX is not a determinant of plastid-to-nucleus signaling in *Arabidopsis*. *Proc Natl Acad Sci USA* 105: 15184-15189
- Mochizuki N, Tanaka R, Grimm B, Masuda T, Moulin M, Smith AG, Tanaka A, Terry MJ** (2010) The cell biology of tetrapyrroles: a life and death struggle. *Trends Plant Sci* 15: 488-498
- Mockler T, Yang HY, Yu XH, Parikh D, Cheng YC, Dolan S, Lin CT** (2003) Regulation of photoperiodic flowering by *Arabidopsis* photoreceptors. *Proc Natl Acad Sci USA* 100: 2140-2145
- Møller SG, Kim YS, Kunkel T, Chua NH** (2003) PP7 is a positive regulator of blue light signaling in *Arabidopsis*. *Plant Cell* 15: 1111-1119
- Møller IM, Jensen PE, Hansson A** (2007) Oxidative modifications to cellular components in plants. *Annu Rev Plant Biol* 58: 459-481

- Monte E, Alonso JM, Ecker JR, Zhang YL, Li X, Young J, Austin-Phillips S, Quail PH (2003) Isolation and characterization of *phyC* mutants in Arabidopsis reveals complex crosstalk between phytochrome signaling pathways. *Plant Cell* 15: 1962-1980
- Monte E, Tepperman JM, Al-Sady B, Kaczorowski KA, Alonso JM, Ecker JR, Li X, Zhang YL, Quail PH (2004) The phytochrome-interacting transcription factor, PIF3, acts early, selectively, and positively in light-induced chloroplast development. *Proc Natl Acad Sci USA* 101: 16091-16098
- Montemartini M, Kalisz HM, Hecht HJ, Steinert P, Flohe L (1999) Activation of active-site cysteine residues in the peroxiredoxin-type trypanedoxin peroxidase of *Crithidia fasciculata*. *Eur J Biochem* 264: 516-524
- Montrichard F, Alkhalifoui F, Yano H, Vensel WH, Hurkman WJ, Buchanan BB (2009) Thioredoxin targets in plants: The first 30 years. *J Proteomics* 72: 452-474
- Moore B, Zhou L, Rolland F, Hall Q, Cheng WH, Liu YX, Hwang I, Jones T, Sheen J (2003) Role of the Arabidopsis glucose sensor HXK1 in nutrient, light, and hormonal signaling. *Science* 300: 332-336
- Moseyko N, Zhu T, Chang HS, Wang X, Feldman LJ (2002) Transcription profiling of the early gravitropic response in Arabidopsis using high-density oligonucleotide probe microarrays. *Plant Physiol* 130: 720-728
- Moulin M, McCormac AC, Terry MJ, Smith AG (2008) Tetrapyrrole profiling in Arabidopsis seedlings reveals that retrograde plastid nuclear signaling is not due to Mg-protoporphyrin IX accumulation. *Proc Natl Acad Sci USA* 105: 15178-15183
- Mueller PR, Wold B (1989) *In vivo* footprinting of a muscle specific enhancer by ligation mediated PCR. *Science* 246: 780-786
- Müller P, Ahmad M (2011) Light-activated cryptochrome reacts with molecular oxygen to form a flavin-superoxide radical pair consistent with magnetoreception. *J Biol Chem* 286: 21033-21040
- Mullet JE (1993) Dynamic regulation of chloroplast transcription. *Plant Physiol* 103: 309-313
- Mullineaux P, Rausch T (2005) Glutathione, photosynthesis and the redox regulation of stress-responsive gene expression. *Photosynth Res* 86: 459-474
- Mundy J, Yamaguchishinozaki K, Chua NH (1990) Nuclear proteins bind conserved elements in the abscisic acid-responsive promoter of a rice *rab* gene. *Proc Natl Acad Sci USA* 87: 1406-1410
- Muramoto T, Kohchi T, Yokota A, Hwang I, Goodman HM (1999) The Arabidopsis photomorphogenic mutant *hyl* is deficient in phytochrome chromophore biosynthesis as a result of a mutation in a plastid heme oxygenase. *Plant Cell* 11: 335-348
- Myers J (1971) Enhancement studies in photosynthesis. *Ann Rev Plant Physiol* 22: 289-312
- Nagashima A, Hanaoka M, Motohashi R, Seki M, Shinozaki K, Kanamaru K, Takahashi H, Tanaka K (2004a) DNA microarray analysis of plastid gene expression in an Arabidopsis mutant deficient in a plastid transcription factor sigma, SIG2. *Biosci Biotechnol Biochem* 68: 694-704
- Nagashima A, Hanaoka M, Shikanai T, Fujiwara M, Kanamaru K, Takahashi H, Tanaka K (2004b) The multiple-stress responsive plastid sigma factor, SIG5, directs activation of the *psbD* blue light-responsive promoter (BLRP) in *Arabidopsis thaliana*. *Plant Cell Physiol* 45: 357-368
- Nagatani A, Chory J, Furuya M (1991) Phytochrome B is not detectable in the *hy3* mutant of Arabidopsis, which is deficient in responding to end-of-day far-red light treatments. *Plant Cell* 3: 1119-1122
- Nagatani A, Reed JW, Chory J (1993) Isolation and initial characterization of Arabidopsis mutants that are deficient in phytochrome A. *Plant Physiol* 102: 269-277
- Nagy F, Schäfer E (2002) Phytochromes control photomorphogenesis by differentially regulated, interacting signaling pathways in higher plants. *Annu Rev Plant Biol* 53: 329-355
- Nakagawa M, Komeda Y (2004) Flowering of Arabidopsis *cop1* mutants in darkness. *Plant Cell Physiol* 45: 398-406
- Narsai R, Howell KA, Millar AH, O'Toole N, Small I, Whelan J (2007) Genome-wide analysis of mRNA decay rates and their determinants in *Arabidopsis thaliana*. *Plant Cell* 19: 3418-3436

- Neff MM, Chory J (1998) Genetic interactions between phytochrome A, phytochrome B, and cryptochrome 1 during Arabidopsis development. *Plant Physiol* 118: 27-35
- Neuhaus G, Bowler C, Kern R, Chua NH (1993) Calcium/calmodulin-dependent and calcium/calmodulin-independent phytochrome signal-transduction pathways. *Cell* 73: 937-952
- Ni M, Tepperman JM, Quail PH (1999) Binding of phytochrome B to its nuclear signalling partner PIF3 is reversibly induced by light. *Nature* 400: 781-784
- O'Kane CJ, Gehring WJ (1987) Detection *in situ* of genomic regulatory elements in *Drosophila*. *Proc Natl Acad Sci USA* 84: 9123-9127
- Oelmuller R, Levitan I, Bergfeld R, Rajasekhar VK, Mohr H (1986) Expression of nuclear genes as affected by treatments acting on the plastids. *Planta* 168: 482-492
- Ogrzewalla K, Piotrowski M, Reinbothe S, Link G (2002) The plastid transcription kinase from mustard (*Sinapis alba* L.) – a nuclear-encoded CK2-type chloroplast enzyme with redox-sensitive function. *Eur J Biochem* 269: 3329-3337
- Ohad I, Kyle DJ, Hirschberg J (1985) Light-dependent degradation of the Q_B-protein in isolated pea thylakoids. *EMBO J* 4: 1655-1659
- Ohgishi M, Saji K, Okada K, Sakai T (2004) Functional analysis of each blue light receptor, cry1, cry2, phot1, and phot2, by using combinatorial multiple mutants in Arabidopsis. *Proc Natl Acad Sci USA* 101: 5696
- Ohto MA, Nakamura K (1995) Sugar-induced increase of calcium-dependent protein-kinases associated with the plasma-membrane in leaf tissues of tobacco. *Plant Physiol* 109: 973-981
- Okamoto H, Matsui M, Deng XW (2001) Overexpression of the heterotrimeric G-protein α -subunit enhances phytochrome-mediated inhibition of hypocotyl elongation in Arabidopsis. *Plant Cell* 13: 1639-1652
- Onda Y, Yagi Y, Saito Y, Takenaka N, Toyoshima Y (2008) Light induction of Arabidopsis *SIG1* and *SIG5* transcripts in mature leaves: differential roles of cryptochrome 1 and cryptochrome 2 and dual function of SIG5 in the recognition of plastid promoters. *Plant J* 55: 968-978
- O'Neill SD (1992) The photoperiodic control of flowering – progress toward understanding the mechanism of induction. *Photochem Photobiol* 56: 789-801
- Oravec A, Baumann A, Mate Z, Brzezinska A, Molinier J, Oakeley EJ, Adam E, Schäfer E, Nagy F, Ulm R (2006) CONSTITUTIVELY PHOTOMORPHOGENIC 1 is required for the UV-B response in *Arabidopsis*. *Plant Cell* 18: 1975-1990
- Ort DR, Oxborough K (1992) *In situ* regulation of chloroplast coupling factor activity. *Annu Rev Plant Physiol Plant Mol Biol* 43: 269-291
- Osterlund MT, Ang LH, Deng XW (1999) The role of COP1 in repression of Arabidopsis photomorphogenic development. *Trends Cell Biol* 9: 113-118
- Osterlund MT, Wei N, Deng XW (2000) The roles of photoreceptor systems and the COP1-targeted destabilization of HY5 in light control of Arabidopsis seedling development. *Plant Physiol* 124: 1520-1524
- Oswald O, Martin T, Dominy PJ, Graham IA (2001) Plastid redox state and sugars: interactive regulators of nuclear-encoded photosynthetic gene expression. *Proc Natl Acad Sci USA* 98: 2047-2052
- Oyama T, Shimura Y, Okada K (1997) The Arabidopsis HY5 gene encodes a bZIP protein that regulates stimulus-induced development of root and hypocotyl. *Genes & Dev* 11: 2983-2995
- Park SC, Kwon HB, Shih MC (1996) *Cis*-acting elements essential for light regulation of the nuclear gene encoding the A subunit of chloroplast glyceraldehyde 3-phosphate dehydrogenase in *Arabidopsis thaliana*. *Plant Physiol* 112: 1563-1571
- Park E, Kim J, Lee Y, Shin J, Oh E, Chung WI, Liu JR, Choi G (2004) Degradation of phytochrome interacting factor 3 in phytochrome-mediated light signaling. *Plant Cell Physiol* 45: 968-975
- Parks BM, Quail PH (1993) *hy8*, a new class of Arabidopsis long hypocotyl mutants deficient in functional phytochrome A. *Plant Cell* 5: 39-48

- Pego JV, Smeekens SCM** (2000) Plant fructokinases: a sweet family get-together. *Trends Plant Sci* 5: 531-536
- Pesaresi P, Schneider A, Kleine T, Leister D** (2007) Interorganellar communication. *Curr Opin Plant Biol* 10: 600-606
- Pfaffl MW, Tichopad A, Prgomet C, Neuvians TP** (2004) Determination of stable housekeeping genes, differentially regulated target genes and sample integrity: BestKeeper – Excel-based tool using pairwise correlations. *Biotechnol Lett* 26: 509-515
- Pfannschmidt T, Link G** (1994) Separation of two classes of plastid DNA-dependent RNA-polymerases that are differentially expressed in Mustard (*Sinapis alba* L) seedlings. *Plant Mol Biol* 25: 69-81
- Pfannschmidt T, Nilsson A, Tullberg A, Link G, Allen JF** (1999a) Direct transcriptional control of the chloroplast genes *psbA* and *psaAB* adjusts photosynthesis to light energy distribution in plants. *IUBMB Life* 48: 271-276
- Pfannschmidt T, Nilsson A, Allen JF** (1999b) Photosynthetic control of chloroplast gene expression. *Nature* 397: 625-628
- Pfannschmidt T, Schütze K, Brost M, Oelmüller R** (2001) A novel mechanism of nuclear photosynthesis gene regulation by redox signals from the chloroplast during photosystem stoichiometry adjustment. *J Biol Chem* 276: 36125-36130
- Pfannschmidt T** (2003) Chloroplast redox signals: how photosynthesis controls its own genes. *Trends Plant Sci* 8: 33-41
- Pfannschmidt T** (2010) Plastidial retrograde signalling – a true "plastid factor" or just metabolite signatures? *Trends Plant Sci* 15: 427-435
- Pogson BJ, Woo NS, Foerster B, Small ID** (2008) Plastid signalling to the nucleus and beyond. *Trends Plant Sci* 13: 602-609
- Pokorny R, Klar T, Hennecke U, Carell T, Batschauer A, Essen LO** (2008) Recognition and repair of UV lesions in loop structures of duplex DNA by DASH-type cryptochrome. *Proc Natl Acad Sci USA* 105: 21023-21027
- Poppe C, Hangarter RP, Sharrock RA, Nagy F, Schäfer E** (1996) The light-induced reduction of the gravitropic growth-orientation of seedlings of *Arabidopsis thaliana* (L) Heynh is a photomorphogenic response mediated synergistically by the far-red-absorbing forms of phytochromes A and B. *Planta* 199: 511-514
- Porra RJ** (2002) The chequered history of the development and use of simultaneous equations for the accurate determination of chlorophylls *a* and *b*. *Photosynth Res* 73, 149-156
- Prasil O, Adir N, Ohad I** (1992) Dynamics of photosystem II: mechanism of photoinhibition and recovery processes. In J Barber, ed, *The Photosystems: Structure, Function and Molecular Biology*. Elsevier Publishers, Amsterdam, Netherlands, pp. 295-348
- Privat I, Hakimi MA, Buhot L, Favory JJ, Lerbs-Mache S** (2003) Characterization of Arabidopsis plastid sigma-like transcription factors SIG1, SIG2 and SIG3. *Plant Mol Biol* 51: 385-399
- Puente P, Wei N, Deng XW** (1996) Combinatorial interplay of promoter elements constitutes the minimal determinants for light and developmental control of gene expression in Arabidopsis. *EMBO J* 15: 3732-3743
- Quail PH, Boylan MT, Parks BM, Short TW, Xu Y, Wagner D** (1995) Phytochromes: photosensory perception and signal transduction. *Science* 268: 675-680
- Quail PH** (1997) An emerging molecular map of the phytochromes. *Plant Cell Env* 20: 657-665
- Quail PH** (1998) The phytochrome family: dissection of functional roles and signalling pathways among family members. *Philos Trans R Soc Lond B Biol Sci* 353: 1399-1403
- Quail PH** (2002) Phytochrome photosensory signalling networks. *Nat Rev Mol Cell Biol* 3: 85-93
- Raghavan V, Demaggio AE** (1971) Enhancement of protein synthesis in isolated chloroplasts by irradiation of fern gametophytes with blue light. *Plant Physiol* 48: 82-85

- Rai VK, Laloraya MM** (1967) Correlative studies on plant growth and metabolism II. Effect of light and of gibberellic acid on changes in protein and soluble nitrogen in Lettuce seedlings. *Plant Physiol* 42: 440-444
- Rani V** (2007) Computational methods to dissect *cis*-regulatory transcriptional networks. *J Biosci* 32: 1325-1330
- Ransom-Hodgkins WD, Vaughn MW, Bush DR** (2003) Protein phosphorylation plays a key role in sucrose-mediated transcriptional regulation of a phloem-specific proton-sucrose symporter. *Planta* 217: 483-489
- Reed JW, Nagpal P, Poole DS, Furuya M, Chory J** (1993) Mutations in the gene for the red/far-red light receptor phytochrome B alter cell elongation and physiological responses throughout Arabidopsis development. *Plant Cell* 5: 147-157
- Reinbothe S, Reinbothe C, Lebedev N, Apel K** (1996) PORA and PORB, two light-dependent protochlorophyllide-reducing enzymes of angiosperm chlorophyll biosynthesis. *Plant Cell* 8: 763-769
- Richly E, Dietzmann A, Biehl A, Kurth J, Laloi C, Apel K, Salamini F, Leister D** (2003) Covariations in the nuclear chloroplast transcriptome reveal a regulatory master-switch. *EMBO Rep* 4: 491-498
- Rintamaki E, Martinsuo P, Pursiheimo S, Aro EM** (2000) Cooperative regulation of light-harvesting complex II phosphorylation via the plastoquinol and ferredoxin-thioredoxin system in chloroplasts. *Proc Natl Acad Sci USA* 97: 11644-11649
- Rizzini L, Favory JJ, Cloix C, Faggionato D, O'Hara A, Kaiserli E, Baumeister R, Schäfer E, Nagy F, Jenkins GI, Ulm R** (2011) Perception of UV-B by the Arabidopsis UVR8 protein. *Science* 332: 103-106
- Robson PRH, Smith H** (1996) Genetic and transgenic evidence that phytochromes A and B act to modulate the gravitropic orientation of *Arabidopsis thaliana* hypocotyls. *Plant Physiol* 110: 211-216
- Roitsch T** (1999) Source-sink regulation by sugar and stress. *Curr Opin Plant Biol* 2: 198-206
- Rolland F, Baena-Gonzalez E, Sheen J** (2006) Sugar sensing and signaling in plants: conserved and novel mechanisms. *Annu Rev Plant Biol* 57: 675-709
- Rombauts S, Déhais P, Van Montagu M, Rouzé P** (1999) PlantCARE, a plant *cis*-acting regulatory element database. *Nucl Acids Res* 27: 295-296
- Ross J** (1995) Messenger-RNA stability in mammalian-cells. *Microbiol Rev* 59: 423-450
- Rossel JB, Walter PB, Hendrickson L, Chow WS, Poole A, Mullineaux PM, Pogson BJ** (2006) A mutation affecting *ASCORBATE PEROXIDASE 2* gene expression reveals a link between responses to high light and drought tolerance. *Plant Cell Env* 29: 269-281
- Rouhier N, Lemaire SD, Jacquot JP** (2008) The role of glutathione in photosynthetic organisms: emerging functions for glutaredoxins and glutathionylation. *Annu Rev Plant Biol* 59: 143-166
- Ruckle ME, DeMarco SM, Larkin RM** (2007) Plastid signals remodel light signaling networks and are essential for efficient chloroplast biogenesis in Arabidopsis. *Plant Cell* 19: 3944-3960
- Sabatini S, Heidstra R, Wildwater M, Scheres B** (2003) SCARECROW is involved in positioning the stem cell niche in the *Arabidopsis* root meristem. *Genes & Dev* 17: 354-358
- Sacchetti A, El Sewedy T, Nasr AF, Alberti S** (2001) Efficient GFP mutations profoundly affect mRNA transcription and translation rates. *FEBS Lett* 492: 151-155
- Saijo Y, Sullivan JA, Wang HY, Yang JP, Shen YP, Rubio V, Ma LG, Hoecker U, Deng XW** (2003) The COP1-SPA1 interaction defines a critical step in phytochrome A-mediated regulation of HY5 activity. *Genes & Dev* 17: 2642-2647
- Sakai T, Kagawa T, Kasahara M, Swartz TE, Christie JM, Briggs WR, Wada M, Okada K** (2001) Arabidopsis *nph1* and *npl1*: Blue light receptors that mediate both phototropism and chloroplast relocation. *Proc Natl Acad Sci USA* 98: 6969-6974
- Salinas P, Fuentes D, Vidal E, Jordana X, Echeverria M, Holuigue L** (2006) An extensive survey of CK2 alpha and beta subunits in Arabidopsis: Multiple isoforms exhibit differential subcellular localization. *Plant Cell Physiol* 47: 1295-1308

- Salomon M, Christie JM, Knieb E, Lempert U, Briggs WR** (2000) Photochemical and mutational analysis of the FMN-binding domains of the plant blue light receptor, phototropin. *Biochemistry* 39: 9401-9410
- Sandmann G, Bölger P** (1986) Sites of herbicide action at the photosynthetic apparatus. In LA Staehelin, JC Arntzen, eds, *Encyclopedia of Plant Physiology*. Springer-Verlag, Berlin, Germany, pp. 595-602
- Schäfer E, Haupt W** (1983) Blue light effects in phytochrome-mediated responses. In W Shropshire Jr., H Mors, eds, *Encyclopedia of Plant Physiology, New Series, Vol. 16B, Photomorphogenesis*. Springer-Verlag, Berlin, Germany, pp. 723-744
- Schindler U, Cashmore AR** (1990) Photoregulated gene-expression may involve ubiquitous DNA-binding proteins. *EMBO J* 9: 3415-3427
- Schindler U, Menkens AE, Beckmann H, Ecker JR, Cashmore AR** (1992) Heterodimerization between light-regulated and ubiquitously expressed Arabidopsis GBF bZIP proteins. *EMBO J* 11: 1261-1273
- Schmid M, Davison TS, Henz SR, Pape UJ, Demar M, Vingron M, Scholkopf B, Weigel D, Lohmann JU** (2005) A gene expression map of *Arabidopsis thaliana* development. *Nat Genet* 37: 501-506
- Schneeberger K, Ossowski S, Ott F, Klein JD, Wang X, Lanz C, Smith LM, Cao J, Fitz J, Warthmann N, Henz SR, Huson DH, Weigel D** (2011) Reference-guided assembly of four diverse *Arabidopsis thaliana* genomes. *Proc Natl Acad Sci USA* 108: 10249-10254
- Schopfer P, Plachy C, Frahry G** (2001) Release of reactive oxygen intermediates (superoxide radicals, hydrogen peroxide, and hydroxyl radicals) and peroxidase in germinating radish seeds controlled by light, gibberellin, and abscisic acid. *Plant Physiol* 125: 1591-1602
- Schreiber U, Schliwa U, Bilger W** (1986) Continuous recording of photochemical and non-photochemical chlorophyll fluorescence quenching with a new type of modulation fluorometer. *Photosynth Res* 10: 51-62
- Schultz TF** (2005) The ZEITLUPE family of putative photoreceptors. In WR Briggs, JL Spudich, eds, *Handbook of Photosensory Receptors*. Wiley-VCH, Weinheim, Germany, pp 337-347
- Schulze-Lefert P, Dangl JL, Beckerandre M, Hahlbrock K, Schulz W** (1989) Inducible *in vivo* DNA footprints define sequences necessary for UV-light activation of the parsley chalcone synthase gene. *EMBO J* 8: 651-656
- Schurmann P** (2003) Redox signaling in the chloroplast: the ferredoxin/thioredoxin system. *Antioxid Redox Signal* 5: 69-78
- Schuster G, Timberg R, Ohad I** (1988) Turnover of thylakoid photosystem II proteins during photoinhibition of *Chlamydomonas reinhardtii*. *Eur J Biochem* 177: 403-410
- Schwarz O, Schurmann P, Strotmann H** (1997) Kinetics and thioredoxin specificity of thiol modulation of the chloroplast H⁺-ATPase. *J Biol Chem* 272: 16924-16927
- Schwechheimer C, Serino G, Deng XW** (2002) Multiple ubiquitin ligase-mediated processes require COP9 signalosome and AXR1 function. *Plant Cell* 14: 2553-2563
- Scott EK, Mason L, Arrenberg AB, Ziv L, Gosse NJ, Xiao T, Chi NC, Asakawa K, Kawakami K, Baier H** (2007) Targeting neural circuitry in zebrafish using GAL4 enhancer trapping. *Nat Methods* 4: 323-326
- Selby CP, Sancar A** (2006) A cryptochrome/photolyase class of enzymes with single-stranded DNA-specific photolyase activity. *Proc Natl Acad Sci USA* 103: 17696-17700
- Sellaro R, Yanovsky MJ, Casal JJ** (2011) Repression of shade-avoidance reactions by sunfleck induction of *HY5* expression in Arabidopsis. *Plant J* 68: 919-928
- Seltmann MA, Stingl NE, Lautenschlaeger JK, Krischke M, Mueller MJ, Berger S** (2010) Differential impact of lipoxygenase 2 and jasmonates on natural and stress-induced senescence in Arabidopsis. *Plant Physiol* 152: 1940-1950
- Seo HS, Yang JY, Ishikawa M, Bolle C, Ballesteros ML, Chua NH** (2003) LAF1 ubiquitination by COP1 controls photomorphogenesis and is stimulated by SPA1. *Nature* 423: 995-999
- Seo HS, Watanabe E, Tokutomi S, Nagatani A, Chua NH** (2004) Photoreceptor ubiquitination by COP1 E3 ligase desensitizes phytochrome A signaling. *Genes & Dev* 18: 617-622

- Serino G, Maliga P** (1998) RNA polymerase subunits encoded by the plastid *rpo* genes are not shared with the nucleus-encoded plastid enzyme. *Plant Physiol* 117: 1165-1170
- Sessa G, Meller Y, Fluhr R** (1995) A GCC element and a G-box motif participate in ethylene-induced expression of the *PRB-1B* gene. *Plant Mol Biol* 28: 145-153
- Shaikhali J, Heiber I, Seidel T, Stroher E, Hiltcher H, Birkmann S, Dietz KJ, Baier M** (2008) The redox-sensitive transcription factor Rap2.4a controls nuclear expression of 2-Cys peroxiredoxin A and other chloroplast antioxidant enzymes. *BMC Plant Biol* 8: 48
- Shalitin D, Yang HY, Mockler TC, Maymon M, Guo HW, Whitelam GC, Lin CT** (2002) Regulation of *Arabidopsis* cryptochrome 2 by blue-light-dependent phosphorylation. *Nature* 418: 447
- Shalitin D, Yu XH, Maymon M, Mockler T, Lin CT** (2003) Blue light-dependent *in vivo* and *in vitro* phosphorylation of *Arabidopsis* cryptochrome 1. *Plant Cell* 15: 2421-2429
- Sharrock RA, Quail PH** (1989) Novel phytochrome sequences in *Arabidopsis thaliana* – Structure, evolution, and differential expression of a plant regulatory photoreceptor family. *Genes & Dev* 3: 1745-1757
- Sharrock RA, Clack T** (2002) Patterns of expression and normalized levels of the five *Arabidopsis* phytochromes. *Plant Physiol* 130: 442-456
- Sharrock RA, Clack T** (2004) Heterodimerization of type II phytochromes in *Arabidopsis*. *Proc Natl Acad Sci USA* 101: 11500-11505
- Sheen J** (1994) Feedback-control of gene-expression. *Photosynth Res* 39: 427-438
- Shikata H, Shibata M, Ushijima T, Nakashima M, Kong SG, Matsuoka K, Lin C, Matsushita T** (2012) The RS domain of *Arabidopsis* splicing factor RRC1 is required for phytochrome B signal transduction. *Plant J* Feb 10. doi: 10.1111/j.1365-313X.2012.04937.x. [Epub ahead of print]
- Shimizu M, Kato H, Ogawa T, Kurachi A, Nakagawa Y, Kobayashi H** (2010) Sigma factor phosphorylation in the photosynthetic control of photosystem stoichiometry. *Proc Natl Acad Sci USA* 107: 10760-10764
- Shin J, Park E, Choi G** (2007) PIF3 regulates anthocyanin biosynthesis in an HY5-dependent manner with both factors directly binding anthocyanin biosynthetic gene promoters in *Arabidopsis*. *Plant J* 49: 981-994
- Shinomura T, Nagatani A, Hanzawa H, Kubota M, Watanabe M, Furuya M** (1996) Action spectra for phytochrome A- and B-specific photoinduction of seed germination in *Arabidopsis thaliana*. *Proc Natl Acad Sci USA* 93: 8129-8133
- Shirano Y, Shimada H, Kanamaru K, Fujiwara M, Tanaka K, Takahashi H, Unno K, Sato S, Tabata S, Hayashi H, Miyake C, Yokota A, Shibata D** (2000) Chloroplast development in *Arabidopsis thaliana* requires the nuclear-encoded transcription factor Sigma B. *FEBS Lett* 485: 178-182
- Smeekens S** (2000) Sugar-induced signal transduction in plants. *Annu Rev Plant Physiol Plant Mol Biol* 51: 49-81
- Smith H** (1995) Physiological and ecological function within the phytochrome family. *Annu Rev Plant Physiol Plant Mol Biol* 46: 289-315
- Smith H** (2000) Phytochromes and light signal perception by plants – an emerging synthesis. *Nature* 407: 585-591
- Smith SM, Fulton DC, Chia T, Thorneycroft D, Chapple A, Dunstan H, Hylton C, Zeeman SC, Smith AM** (2004) Diurnal changes in the transcriptome encoding enzymes of starch metabolism provide evidence for both transcriptional and posttranscriptional regulation of starch metabolism in *Arabidopsis* leaves. *Plant Physiol* 136: 2687-2699
- Smith AM, Zeeman SC, Smith SM** (2005) Starch degradation. *Annu Rev Plant Biol* 56: 73-98
- Sobell HM** (1985) Actinomycin and DNA transcription. *Proc Natl Acad Sci USA* 82: 5328-5331
- Söderman EM, Brocard IM, Lynch TJ, Finkelstein RR** (2000) Regulation and function of the *Arabidopsis ABA-insensitive4* gene in seed and abscisic acid response signaling networks. *Plant Physiol* 124: 1752-1765

- Soitamo AJ, Piippo M, Allahverdiyeva Y, Battchikova N, Aro EM** (2008) Light has a specific role in modulating Arabidopsis gene expression at low temperature. *BMC Plant Biol* 8:
- Somers DE, Sharrock RA, Tepperman JM, Quail PH** (1991) The *hy3* long hypocotyl mutant of Arabidopsis is deficient in phytochrome B. *Plant Cell* 3: 1263-1274
- Somers DE, Devlin PF, Kay SA** (1998) Phytochromes and cryptochromes in the entrainment of the Arabidopsis circadian clock. *Science* 282: 1488-1490
- Song YH, Yoo CM, Hong AP, Kim SH, Jeong HJ, Shin SY, Kim HJ, Yun DJ, Lim CO, Bahk JD, Lee SY, Nagao RT, Key JL, Hong JC** (2008) DNA-binding study identifies C-box and hybrid C/G-box or C/A-box motifs as high-affinity binding sites for STF1 and LONG HYPOCOTYL 5 proteins. *Plant Physiol* 146: 1862-1877
- Springer PS** (2000) Gene traps: Tools for plant development and genomics. *Plant Cell* 12: 1007-1020
- Staneloni RJ, Rodriguez-Batiller MaJ, Casal JJ** (2008) Abscisic acid, high-light, and oxidative stress down-regulate a photosynthetic gene via a promoter motif not involved in phytochrome-mediated transcriptional regulation. *Mol Plant* 1: 75-83
- Steiner S, Dietzel L, Schroeter Y, Fey V, Wagner R, Pfanschmidt T** (2009) The role of phosphorylation in redox regulation of photosynthesis genes *psaA* and *psbA* during photosynthetic acclimation of mustard. *Mol Plant* 2: 416-429
- Stephenson PG, Fankhauser C, Terry MJ** (2009) PIF3 is a repressor of chloroplast development. *Proc Natl Acad Sci USA* 106: 7654-7659
- Stern DB, Higgs DC, Yang JJ** (1997) Transcription and translation in chloroplasts. *Trends Plant Sci* 2: 308-315
- Stower H** (2012) Gene regulation: Resolving transcription factor binding. *Nat Rev Genet* 13: 71
- Struhl K** (2001) Gene regulation – a paradigm for precision. *Science* 293: 1054-1055
- Sugiura M** (1989) The chloroplast chromosomes in land plants. *Annu Rev Cell Biol* 5: 51-70
- Sullivan JA, Gray JC** (1999) Plastid translation is required for the expression of nuclear photosynthesis genes in the dark and in roots of the pea *lip1* mutant. *Plant Cell* 11: 901-910
- Sullivan JA, Shirasu K, Deng XW** (2003) The diverse roles of ubiquitin and the 26S proteasome in the life of plants. *Nat Rev Genet* 4: 948-958
- Sundaresan V, Springer P, Volpe T, Haward S, Jones JD, Dean C, Ma H, Martienssen R** (1995) Patterns of gene action in plant development revealed by enhancer trap and gene trap transposable elements. *Genes & Dev* 9: 1797-1810
- Susek RE, Ausubel FM, Chory J** (1993) Signal transduction mutants of Arabidopsis uncouple nuclear *CAB* and *RBCS* gene expression from chloroplast development. *Cell* 74: 787-799
- Swaminathan K, Yang YZ, Grotz N, Campisi L, Jack T** (2000) An enhancer trap line associated with a D-class cyclin gene in Arabidopsis. *Plant Physiol* 124: 1658-1667
- Szilárd A, Sass L, Deak Z, Vass I** (2007) The sensitivity of photosystem II to damage by UV-B radiation depends on the oxidation state of the water-splitting complex. *Biochim Biophys Acta* 1767: 876-882
- Takano M, Inagaki N, Xie XZ, Yuzurihara N, Hihara F, Ishizuka T, Yano M, Nishimura M, Miyao A, Hirochika H, Shinomura T** (2005) Distinct and cooperative functions of phytochromes A, B, and C in the control of deetiolation and flowering in rice. *Plant Cell* 17: 3311-3325
- Tan S, Troxler RF** (1999) Characterization of two chloroplast RNA polymerase sigma factors from *Zea mays*: Photoregulation and differential expression. *Proc Natl Acad Sci USA* 96: 5316-5321
- Tanaka K, Tozawa Y, Mochizuki N, Shinozaki K, Nagatani A, Wakasa K, Takahashi H** (1997) Characterization of three cDNA species encoding plastid RNA polymerase sigma factors in *Arabidopsis thaliana*: Evidence for the sigma factor heterogeneity in higher plant plastids. *FEBS Lett* 413: 309-313
- Tepperman JM, Zhu T, Chang HS, Wang X, Quail PH** (2001) Multiple transcription-factor genes are early targets of phytochrome A signaling. *Proc Natl Acad Sci USA* 98: 9437-9442

- Tepperman JM, Hudson ME, Khanna R, Zhu T, Chang SH, Wang X, Quail PH** (2004) Expression profiling of *phyB* mutant demonstrates substantial contribution of other phytochromes to red-light-regulated gene expression during seedling de-etiolation. *Plant J* 38: 725-739
- Tepperman JM, Hwang YS, Quail PH** (2006) PhyA dominates in transduction of red-light signals to rapidly responding genes at the initiation of Arabidopsis seedling de-etiolation. *Plant J* 48: 728-742
- Terzaghi WB, Cashmore AR** (1995) Light-regulated transcription. *Annu Rev Plant Physiol Plant Mol Biol* 46: 445-474
- Thompson WF, Everett M, Polans NO, Jorgensen RA, Palmer JD** (1983) Phytochrome control of RNA levels in developing pea and mung-bean leaves. *Planta* 158: 487-500
- Thorne T, Stasolla C, Yeung EC, de Klerk G-J, R.George, George EF** (2008) The components of plant tissue culture media II: organic additions, osmotic and pH effects, and support systems. In EF George, MA Hall, GJ de Klerk, eds, *Plant Propagation by Tissue Culture*. 3rd ed. Springer-Verlag, Berlin, Germany 115-174
- Thum KE, Kim M, Christopher DA, Mullet JE** (2001a) Cryptochrome 1, cryptochrome 2, and phytochrome A co-activate the chloroplast *psbD* blue light-responsive promoter. *Plant Cell* 13: 2747-2760
- Thum KE, Kim M, Morishige DT, Eibl C, Koop HU, Mullet JE** (2001b) Analysis of barley chloroplast *psbD* light-responsive promoter elements in transplastomic tobacco. *Plant Mol Biol* 47: 353-366
- Tiessen A, Hendriks JHM, Stitt M, Branscheid A, Gibon Y, Farre EM, Geigenberger P** (2002) Starch synthesis in potato tubers is regulated by post-translational redox modification of ADP-glucose pyrophosphorylase: A novel regulatory mechanism linking starch synthesis to the sucrose supply. *Plant Cell* 14: 2191-2213
- Tiessen A, Prescha K, Branscheid A, Palacios N, McKibbin R, Halford NG, Geigenberger P** (2003) Evidence that SNF1-related kinase and hexokinase are involved in separate sugar-signalling pathways modulating post-translational redox activation of ADP-glucose pyrophosphorylase in potato tubers. *Plant J* 35: 490-500
- Tiller K, Link G** (1993) Phosphorylation and dephosphorylation affect functional-characteristics of chloroplast and etioplast transcription systems from mustard (*Sinapis alba* L). *EMBO J* 12: 1745-1753
- Topping JF, Agyeman F, Henricot B, Lindsey K** (1994) Identification of molecular markers of embryogenesis in *Arabidopsis thaliana* by promoter trapping. *Plant J* 5: 895-903
- Tozawa Y, Teraishi M, Sasaki T, Sonoike K, Nishiyama Y, Itaya M, Miyao A, Hirochika H** (2007) The plastid sigma factor SIG1 maintains photosystem I activity via regulated expression of the *psaA* operon in rice chloroplasts. *Plant J* 52: 124-132
- Trebst A** (1980) Inhibitors in electron flow: Tools for the functional and structural localization of carriers and energy conservation sites. *Methods Enzymol* 69: 675-715
- Trebst A, Depka B** (1990) Degradation of the D1 protein subunit of photosystem II in isolated thylakoids by UV-light. *Z Naturforsch Sect C Biosci* 45: 765-771
- Tsugeki R, Fedoroff NV** (1999) Genetic ablation of root cap cells in Arabidopsis. *Proc Natl Acad Sci USA* 96: 12941-12946
- Tsunoyama Y, Ishizaki Y, Morikawa K, Kobori M, Nakahira Y, Takeba G, Toyoshima Y, Shiina T** (2004) Blue light-induced transcription of plastid-encoded *psbD* gene is mediated by a nuclear-encoded transcription initiation factor, AtSig5. *Proc Natl Acad Sci USA* 101: 3304-3309
- Tsunoyama Y, Kazuya M, Takashi S, Yoshinori T** (2002) Blue light specific and differential expression of a plastid σ factor, Sig5 in *Arabidopsis thaliana*. *FEBS Lett* 516: S-225-228
- Turcsányi E, Vass I** (2000) Inhibition of photosynthetic electron transport by UV-A radiation targets the photosystem II complex. *Photochem Photobiol* 72: 513-520
- Türkeri H, Schweer J, Link G** (2012) Phylogenetic and functional features of the plastid transcription kinase cpCK2 from Arabidopsis signify a role of cysteinyl SH-groups in regulatory phosphorylation of plastid sigma factors. *FEBS J* 279: 395-409

- Tyystjärvi E** (2008) Photoinhibition of photosystem II and photodamage of the oxygen evolving manganese cluster. *Coord Chem Rev* 252: 361-376
- Van Oosten JJ, Besford RT** (1995) Some relationships between the gas exchange, biochemistry and molecular biology of photosynthesis during leaf development of tomato plants after transfer to different carbon dioxide concentrations. *Plant Cell Env* 18: 1253-1266
- Van Kooten O, Snel JFH** (1990) The use of chlorophyll fluorescence nomenclature in plant stress physiology. *Photosynth Res* 25: 147-150
- Vidal M, Legrain P** (1999) Yeast forward and reverse 'n'-hybrid systems. *Nucl Acids Res* 27: 919-929
- Vincze T, Posfai J, Roberts RJ** (2003) NEBcutter: a program to cleave DNA with restriction enzymes. *Nucl Acids Res* 31: 3688-3691
- Voinnet O, Rivas S, Mestre P, Baulcombe D** (2003) An enhanced transient expression system in plants based on suppression of gene silencing by the p19 protein of tomato bushy stunt virus. *Plant J* 33: 949-956
- Vonarnim AG, Deng XW** (1994) Light inactivation of *Arabidopsis* photomorphogenic repressor COP1 involves a cell-specific regulation of its nucleocytoplasmic partitioning. *Cell* 79: 1035-1045
- Vorst O, Kock P, Lever A, Weterings B, Weisbeek P, Smeekens S** (1993) The promoter of the *Arabidopsis thaliana* plastocyanin gene contains a far upstream enhancer-like element involved in chloroplast-dependent expression. *Plant J* 4: 933-945
- Wada M, Kagawa T, Sato Y** (2003) Chloroplast movement. *Annu Rev Plant Biol* 54: 455-468
- Wagner D, Koloszvari M, Quail PH** (1996) Two small spatially distinct regions of phytochrome B are required for efficient signaling rates. *Plant Cell* 8: 859-871
- Wang HY, Ma LG, Li JM, Zhao HY, Deng XW** (2001) Direct interaction of *Arabidopsis* cryptochromes with COP1 in light control development. *Science* 294: 154-158
- Wang H, Ma L, Habashi J, Li J, Zhao H, Deng XW** (2002) Analysis of far-red light-regulated genome expression profiles of phytochrome A pathway mutants in *Arabidopsis*. *Plant J* 32: 723-733
- Wang H, Deng XW** (2004) Phytochrome signaling mechanisms. In CR Somerville, EM Meyerowitz, eds, *The Arabidopsis Book*. American Society of Plant Physiologists, Rockville, USA
- Waters MT, Wang P, Korkaric M, Capper RG, Saunders NJ, Langdale JA** (2009) GLK transcription factors coordinate expression of the photosynthetic apparatus in *Arabidopsis*. *Plant Cell* 21: 1109-1128
- Wei N, Deng XW** (2003) The COP9 signalosome. *Annu Rev Cell Dev Biol* 19: 261-286
- Weigel D, Glazebrook J** (2002) *Arabidopsis: A laboratory manual*. Cold Spring Harbor Laboratory Press, Cold Spring Harbor, NY, USA
- Weijers D, van Hamburg JP, van Rijn E, Hooykaas PJJ, Offringa R** (2003) Diphtheria toxin-mediated cell ablation reveals interregional communication during *Arabidopsis* seed development. *Plant Physiol* 133: 1882-1892
- Weisshaar B, Armstrong GA, Block A, Silva ODE, Hahlbrock K** (1991) Light-inducible and constitutively expressed DNA-binding proteins recognizing a plant promoter element with functional relevance in light responsiveness. *EMBO J* 10: 1777-1786
- Weller JL, Nagatani A, Kendrick RE, Murfet IC, Reid JB** (1995) New *lv* mutants of pea are deficient in phytochrome B. *Plant Phys* 108: 525-532
- Wellmer F, Kircher S, Rugner A, Frohnmeyer R, Schäfer E, Harter A** (1999) Phosphorylation of the parsley bZIP transcription factor CPRF2 is regulated by light. *J Biol Chem* 274: 29476-29482
- Weston E, Thorogood K, Vinti G, López-Juez E** (2000) Light quantity controls leaf-cell and chloroplast development in *Arabidopsis thaliana* wild type and blue-light perception mutants. *Planta* 211: 807-815
- Whitelam GC, Smith H** (1991) Retention of phytochrome-mediated shade avoidance responses in phytochrome-deficient mutants of *Arabidopsis*, cucumber and tomato. *J Plant Physiol* 139: 119-125
- Whitelam GC, Johnson E, Peng JR, Carol P, Anderson ML, Cowl JS, Harberd NP** (1993) Phytochrome A null mutants of *Arabidopsis* display a wild-type phenotype in white light. *Plant Cell* 5: 757-768

- Whitelam GC, Devlin PF** (1997) Roles of different phytochromes in Arabidopsis photomorphogenesis. *Plant Cell Env* 20: 752-758
- Whitelam GC, Devlin PF** (1998) Light signalling in Arabidopsis. *Plant Physiol Biochem* 36: 125-133
- Woodson JD, Chory J** (2008) Coordination of gene expression between organellar and nuclear genomes. *Nat Rev Genet* 9: 383-395
- Wray GA** (2007) The evolutionary significance of *cis*-regulatory mutations. *Nat Rev Genet* 8: 206-216
- Wysocka-Diller JW, Helariutta Y, Fukaki H, Malamy JE, Benfey PN** (2000) Molecular analysis of SCARECROW function reveals a radial patterning mechanism common to root and shoot. *Development* 127: 595-603
- Xiao W, Sheen J, Jang JC** (2000) The role of hexokinase in plant sugar signal transduction and growth and development. *Plant Mol Biol* 44: 451-461
- Xu W, Purugganan MM, Polisensky DH, Antosiewicz DM, Fry SC, Braam J** (1995) Arabidopsis *TCH4*, regulated by hormones and the environment, encodes a xyloglucan endotransglycosylase. *Plant Cell* 7: 1555-1567
- Xu W, Campbell P, Vargheese AK, Braam J** (1996) The Arabidopsis XET-related gene family: environmental and hormonal regulation of expression. *Plant J* 9: 879-889
- Xu P, Xiang Y, Zhu H, Xu H, Zhang Z, Zhang C, Zhang L, Ma Z** (2009) Wheat cryptochromes: subcellular localization and involvement in photomorphogenesis and osmotic stress responses. *Plant Physiol* 149: 760-774
- Yadav V, Kundu S, Chattopadhyay D, Negi P, Wei N, Deng XW, Chattopadhyay S** (2002) Light regulated modulation of Z-box containing promoters by photoreceptors and downstream regulatory components, COP1 and HY5, in Arabidopsis. *Plant J* 31: 741-753
- Yadav V, Mallappa C, Gangappa SN, Bhatia S, Chattopadhyay S** (2005) A basic helix-loop-helix transcription factor in Arabidopsis, MYC2, acts as a repressor of blue light-mediated photomorphogenic growth. *Plant Cell* 17: 1953-1966
- Yanagawa Y, Sullivan JA, Komatsu S, Gusmaroli G, Suzuki G, Yin J, Ishibashi T, Saijo Y, Rubio V, Kimura S, Wang J, Deng XW** (2004) Arabidopsis COP10 forms a complex with DDB1 and DET1 *in vivo* and enhances the activity of ubiquitin conjugating enzymes. *Genes & Dev* 18: 2172-2181
- Yang HQ, Tang RH, Cashmore AR** (2001) The signaling mechanism of Arabidopsis CRY1 involves direct interaction with COP1. *Plant Cell* 13: 2573-2587
- Yang JP, Lin RC, James S, Hoecker U, Liu BL, Xu L, Deng XW, Wang HY** (2005) Light regulates COP1-mediated degradation of HFR1, a transcription factor essential for light signaling in Arabidopsis. *Plant Cell* 17: 804-821
- Yanovsky MJ, Mazzella MA, Whitelam GC, Casal JJ** (2001) Resetting of the circadian clock by phytochromes and cryptochromes in Arabidopsis. *J Biol Rhythms* 16: 523-530
- Yanovsky MJ, Kay SA** (2002) Molecular basis of seasonal time measurement in Arabidopsis. *Nature* 419: 308-312
- Yao J, Roy-Chowdhury S, Allison LA** (2003) AtSig5 is an essential nucleus-encoded Arabidopsis σ -like factor. *Plant Physiol* 132: 739-747
- Yu F, Shi J, Zhou J, Gu J, Chen Q, Li J, Cheng W, Mao D, Tian L, Buchanan BB, Li L, Chen L, Li D, Luan S** (2010) ANK6, a mitochondrial ankyrin repeat protein, is required for male-female gamete recognition in *Arabidopsis thaliana*. *Proc Natl Acad Sci USA* 107: 22332-22337
- Zhang YH, Shewry PR, Jones H, Barcelo P, Lazzeri PA, Halford NG** (2001) Expression of antisense SnRK1 protein kinase sequence causes abnormal pollen development and male sterility in transgenic barley. *Plant J* 28: 431-441
- Zhang H, He H, Wang X, Wang X, Yang X, Li L, Deng XW** (2011) Genome-wide mapping of the HY5-mediated gene networks in Arabidopsis that involve both transcriptional and post-transcriptional regulation. *Plant J* 65: 346-358

- Zhu YX, Tepperman JM, Fairchild CD, Quail PH** (2000) Phytochrome B binds with greater apparent affinity than phytochrome A to the basic helix-loop-helix factor PIF3 in a reaction requiring the PAS domain of PIF3. *Proc Natl Acad Sci USA* 97: 13419-13424
- Zuo Z, Liu H, Liu B, Liu X, Lin C** (2011) Blue light-dependent interaction of CRY2 with SPA1 regulates COP1 activity and floral initiation in Arabidopsis. *Curr Biol* 21: 841-847

6

APPENDIX

6.1 TAIL-PCR settings

Table A1. Cycle setting used for TAIL-PCR.

Reaction	Cycles	Temperature [°C]	Time [s]
Primary	1	94	120
	5	94	60
		58	60
		72	150
	1	94	60
		25	180
		ramp to 72°C, 0.2°C min ⁻¹	
	15 ^a	72	150
		94	30
		60 ^{c,d} / 64 ^b	60
		72	150
		94	30
		60 ^{c,d} / 64 ^b	60
		72	150
	1	94	30
40 ^{c,d} / 44 ^b		60	
72		150	
72		300	
72		300	
Secondary	12 ^a	94	30
		60 ^{c,d} / 64 ^b	60
		72	150
		94	30
		60 ^{c,d} / 64 ^b	60
		72	150
		94	30
	1	40 ^{c,d} / 44 ^b	60
		72	150
		72	5
Tertiary	35 ^{b,c} / 40 ^d	94	60
		44 ^{b,c} / 46 ^d	60
		72	150
	1	72	5

^a super cycles each consisting of two high-stringency and one reduced-stringency

^b N9249

^c N9266

^d N9313

6.2 PCR primers

Table A2. Primers and annealing temperatures used for PCR to verify T-DNA insertion sites of ET lines.

Enhancer trap line	TA [°C]	Gene code	Forward primer / reverse primer (5' → 3')
N9249	55	At5g57565	GGTCTTTGTCCTCGCCG ACCGAGCATCGTTTACTC ^a
N9266	58	At1g79110	CGTATCACGCGGCGC ^a AGTATATCCTCTTTAATGTTGGCATG
N9313	54	At5g24120	CTCCGACTCTTGCATAT ^a CATCACAATCTTAAGGCTCA

^a leading to amplification of a PCR product in combination with primer TR3.2 if enhancer trap T-DNA is inserted in the mapped genomic sequence

Table A3. Primers and annealing temperatures used for identification of homozygous T-DNA insertions in the *SIG5* promoter.

SALK line	TA [°C]	Forward primer / reverse primer (5' → 3')
015625	50	CAATCATGGTTTAATTCGT ^a GATCCACAACCACAAGCC
077048, 072457	45	GTTATTGATCTGTACCTAGC ^a AAATACGATAGATGTGTTG
019261	45	ATCACAATCTTAAGGCTCAAAA AAATACGATAGATGTGTTG ^a
133729	45	ATCACAATCTTAAGGCTCAAAA ^a AAATACGATAGATGTGTTG

^a Leading to amplification of a T-DNA specific PCR product when combined with primer LBb1.3 annealing with the left border of the SALK T-DNA

Table A4. Primers and annealing temperatures used for site-directed mutagenesis of *cis*-acting elements.

Mutated <i>cis</i> -element	TA [°C]	Forward primer / reverse primer (5' → 3') ^{a, b}
First PCR – part I		
GATA-motif	60	GGTGGCGACCGGTACC CATCTTTTACTG AATAC TTTGAGTTATTTGCACATATAG ^c
G-box	60	GGTGGCGACCGGTACC CTGAGAAGACCATCCA ATT GATAATTCCTGATC ^d
GC-box	60	GGTGGCGACCGGTACC CTATAAATTGGCCA ATT CGTCTCTCTCTC
First PCR – part II		
GATA-motif	55	CTATATGTGCAAATAACTCAAAG TATTC AGTAAAAGATG ^c GTAACCTCCGACTCTTGCGAT
G-box	55	GATCAGGAATTATACA ATT GGATGGTCTTCTCAG ^d GTAACCTCCGACTCTTGCGAT
GC-box	55	GAGAGAGAGACGA ATT GGCCAATTTATAG GTAACCTCCGACTCTTGCGAT
Second PCR		
GATA-motif, G-box and GC-box	63	GGTGGCGACCGGTACC GTAACCTCCGACTCTTGCGAT

^a *cis*-acting regulatory promoter elements are underlined

^b Mutated nucleotides are highlighted in bold

^c Mutations according to Donald and Cashmore, 1990

^d Mutations according to McKendree and Ferl, 1992

Table A5. Primers and annealing temperatures used for construction of promoter-reporter gene fusions.

Promoter fragment	TA [°C]	Forward primer / reverse primer (5' → 3') ^a
pSIG5 _{-2002/-1}	55	<u>GAGCTCTTTTTCTGCAGCACAATCTTAAGGCTCAAAAATTG</u> GTAACCTCCGACTCTTGCG
pSIG5 _{-1197/-1}	58	<u>GAGCTCTTTTTCTGCAGCACAATCTTAAGGCTCAAAAATTG</u> TCGGATGCTTTACATGGTG
pSIG5 _{-2002/-1198}	45	<u>ACTAGTTTTTTCTGCAGGTAACCTCCGACTCTTGCG</u> GCTTGAGAGATTACATTATT
pSIG5 _{-2002/-1798}	48	<u>ACTAGTTTTTTCTGCAGGTAACCTCCGACTCTTGCG</u> GCTTGAGAGATTACATTATT
pSIG5 _{-1834/-1627}	50	<u>ACTAGTTTTTTCTGCAGGTTTGAATCTCAGGAAG</u> TGTTTTGGGTCCGACTG
pSIG5 _{-1784/-1501}	50	<u>ACTAGTTTTTTCTGCAGCAATCATGGTTAATTCGT</u> GATCCACAACCACAAGCC
pSIG5 _{-1548/-1314}	44	<u>ACTAGTTTTTTCTGCAGGGTTGCATGATGTTATT</u> CTCTTACATTACGTAAAC
pSIG5 _{-1453/-1198}	46	<u>ACTAGTTTTTTCTGCAGGTAACCTCCGACTCTTGCG</u> AAATACGATAGATGTGTTG

^a Restriction sites are underlined**Table A6. Primers and annealing temperatures used for amplification of del35S and 35S.**

PCR fragment	TA [°C]	Forward primer / reverse primer (5' → 3')
del35S	62	TTCGCAAGACCCTTCTCTATATAAGG GGGTACCGGTCGCCACC
35S	55	CCATGGAGTCAAAGATTCAA GGTGGCGACCGGTACC

Table A7. Primers used for RNA quantification by real-time PCR.

Gene	Gene code	Forward primer / reverse primer (5' → 3')	Length PCR product [bp]
ACT2 ^a	At3g18780	TCTCCGCTCTTTCTTTCCAAGC ACCATTGTCACACACGATTGGTTG	77
SIG5 ^a	At5g24120	TGGAGCTAATAACAGCAGACAGC TCGGCTTCAATGAATCGAGCAC	74
GFP	-	CCATTACCTGTCCACACAATC GTTTCATCCATGCCATGTG	113
HY5 ^a	At5g11260	AGAACAAGCGGCTGAAGAGGTTG TCCTCTCTTGTGCTGAGCTG	63
RBCS1A ^a	At1g67090	ACCTTCTGACCTTACCGATTCCG GTTGGAGCACGGATTTGTGTACC	108

^a one primer spans exon border to avoid amplification of genomic DNA**Table A8. Primers and annealing temperatures used for identification of Arabidopsis transformants.**

Primer binding site	TA [°C]	Primer nucleotide sequence (5' → 3')
pHGWF5.0 backbone	55	TTCGCAAGACCCTTCC
del35S minimal promoter	55	GTGGTGCAGATGAACTTCAGG

Table A9. Primers and annealing temperatures used for identification of mutant genotypes and homozygous T-DNA insertions.

Allele	TA [°C]	Forward primer / reverse primer (5' → 3')
<i>cry2-1</i>	58	CAGTTTTATCCTGGAAGAGCCTC CTTCTCCTTTACGGTATGGTCC
<i>hy1-1</i>	56	GGAATTAGCAGAGAAGGATCC TATCCGCTCTGCCACCTG
<i>phyA-201</i>	55	CCTTAAATGAAGTGTGACTGC GCAAGATGCACAGAACG
<i>phyB-5</i>	55	GTTGTGGAGTGGTTGCTTG CATAGCCGCCTCAGATTC
<i>phot1-5</i>	58	CCACTTGCAACCTATGCG CTCTTCACTGCGGTTTCTTC
<i>phot2-1</i>	54	CTCTGCCTCACAATAAGGAG CTGCCAGTATCACCAGAGC
SALK_056405C	58	GCGGTAGCCAGAGTAATCTATTCC TCCTCTCTTTGCTTGCTGAGCTG ATTTTGCCGATTTCCGAAC ^a

^a Lb1.3, annealing with the left border of the SALK T-DNA. Lb1.3 leads to a PCR product in SALK_056405C if combined with the reverse primer annealing the HY5 coding sequence.

Table A10. Primers and annealing temperatures used for construction of bait vector for Y1H.

Promoter fragment	TA [°C]	Forward primer / reverse primer (5' → 3') ^a
pSIG5-1197/-1	57	TTTTT <u>GAGCTCCACAATC</u> TTAAGGCTCAAAAATTG TTTTTGGGCCCTCGGATGCTTTACATGGTG
pSIG5-2002/-1198	60	TTTTTGAATTCGTAACCTCCGACTCTTGCG TTTTT <u>GAGCTCGCTTGAGAGATTACATTATT</u>
pSIG5-2002/-1798	62	TTTTTGAATTCGTAACCTCCGACTCTTGCG TTTTT <u>GAGCTCGTGGATGGTCTTCTCAG</u>
pSIG5-1834/-1627	50	TTTTTGAATTCGTTTTGGGTCCGACTG TTTTT <u>GAGCTCGTTTTGGAATCTCAGGAAG</u>
pSIG5-1784/-1501	55	TTTTTGAATTCGATCCACAACCACAAGCC TTTTT <u>GAGCTCCAATCATGGTTTAATTCGT</u>
pSIG5-1548/-1314	64	TTTTTGAATTCCTTACATTTACGTAAAC TTTTT <u>GAGCTCGGGTTGCATGATGTTATT</u>
pSIG5-1453/-1198	49	TTTTTGAATTCAAATACGATAGATGTGTTG TTTTT <u>GAGCTCGCTTGAGAGATTACATTATT</u>

^a Restriction sites are underlined

Table A11. Primers and annealing temperatures used for amplification of HY5 CDS and 196 bp RBCS1A promoter fragment to test for interaction in yeast.

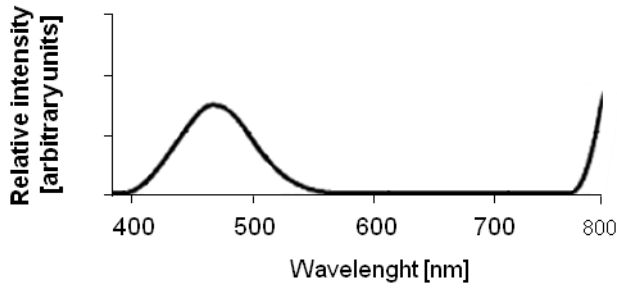
Gene / promoter of interest	TA [°C]	Forward primer / reverse primer (5' → 3') ^a
HY5 CDS	58	TTTTTGGATCCTACAGGAACAAGCGACTAGCTC ^b TTTTTCTCGAGTCAAAGGCTTGCATCAGC
RBCS1A promoter	55	TTTTT <u>GAGCTCGATTTT</u> GAGTGTGGATATGTGT TTTTTGAATTCAGGCAAGTAAATGAGCAAG

^a Restriction sites are underlined

^b two nucleotides added to HY5 CDS are marked in bold

6.3 Plexiglas transmission spectra and emission spectra of LEDs

A Blue light filter



B Red light filter

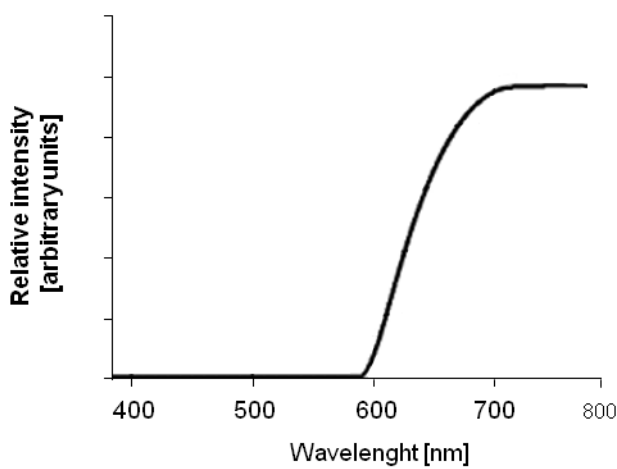


Figure A1. Transmission spectra of blue and red plexiglass used to filter distinct wavelength out of white light. **A:** Blue light filter. The transmitted blue light peaks at about 470 nm **B:** Red light filter, transmitting $\lambda > 600$ nm.

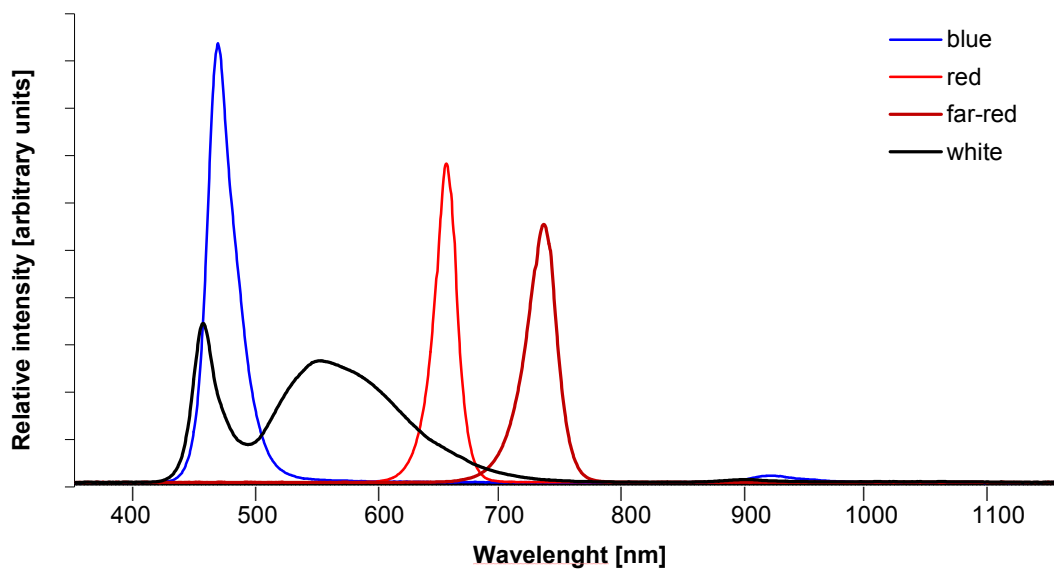


Figure A2. Spectra of blue, red, far-red and white light LED panels used in FloraLED chambers (CLF PlantClimatics, Emersacker, Germany). Blue light peaks at 471 nm, red light at 673 nm and far-red light at 745 nm.

6.4 Maps of plasmids

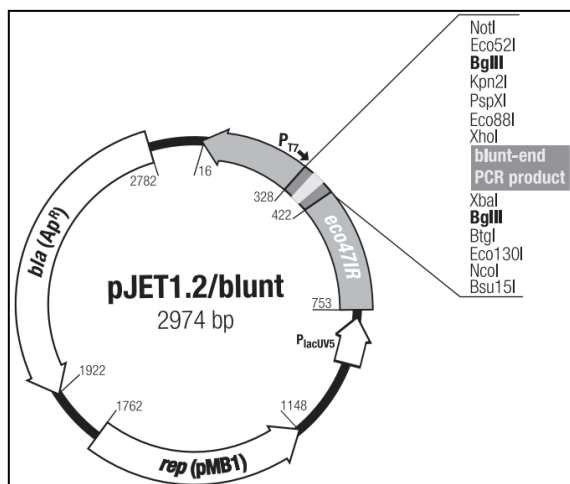


Figure A3. Map of pJET1.2/blunt vector. *bla* (Ap^R): β -lactamase gene conferring *E. coli* resistance to Ampicillin; *rep* (pMB1): replicon from the pMB1 plasmid; *eco471R*: lethal gene, enables positive selection of recombinant plasmid (Fermentas, St. Leon-Rot, Germany).

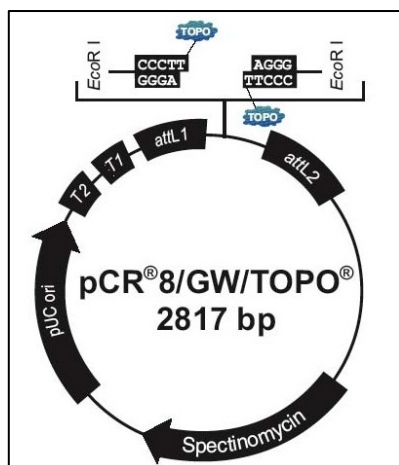


Figure A4. Map of pCR[®]8/GW/TOPO[®] vector. Spectinomycin: Spectinomycin resistance gene (Spn^R); pUC ori: pUC origin of replication; T2 / T1: *rrnB* T2 and T1 transcription termination sequences to prevent basal transcription of the PCR product of interest in *E. coli*; *attL1* / *attL2*: sites for recombination-based transfer of the gene of interest into a Gateway[®] destination vector (Invitrogen, Carlsbad, USA).

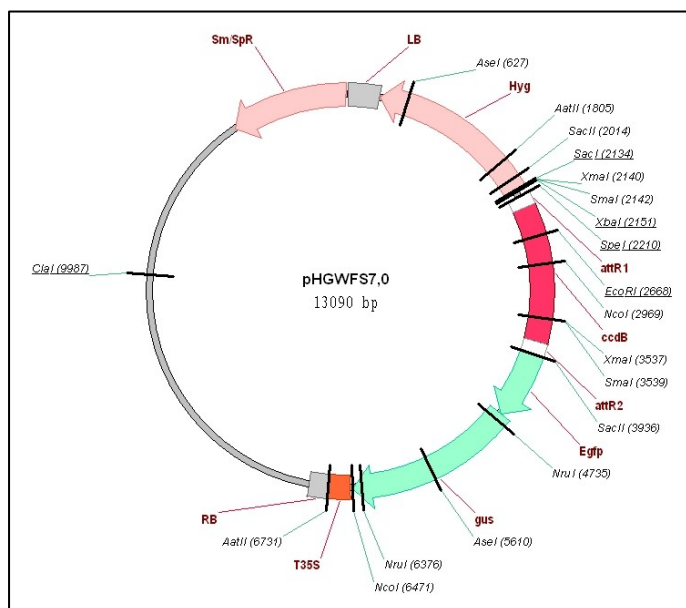


Figure A5. Map of pHGWFS7.0 vector. Sm/Sp^R: mediating streptomycin-spectinomycin resistance to *E. coli* and *Agrobacteria*; LB: T-DNA left border; Hyg: plant selectable marker gene mediating hygromycin B resistance under transcriptional regulation of the nopaline synthase (*nos*) promoter and *nos* terminator; *attR1* / *attR2*: sites for recombination-based transfer of the gene of interest from any Gateway[®] entry vector containing *attL1* / *attL2* sites generating *attB1* / *attB2* sites; *ccdB*: F plasmid-encoded gene that inhibits growth of *E. coli* without insert; *Egfp*: enhancer green fluorescent protein reporter gene linked to the endoplasmatic reticulum-targeting signal; *gus*: β -glucuronidase reporter gene, frame fusion with *Egfp* coding region; T35S: 35S terminator; RB: T-DNA right border (Karimi *et al.*, 2002).

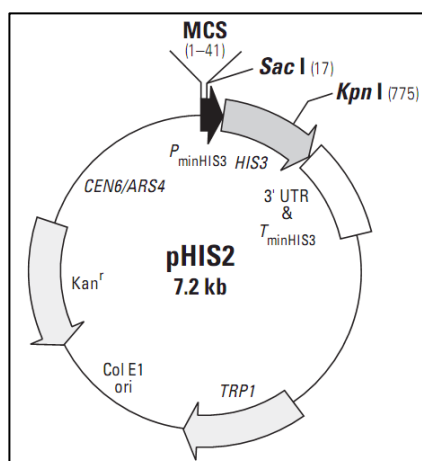


Figure A6. Map of pHIS2 vector. pHIS2 was used to generate DNA bait constructs for Y1H screen. MCS: Multiple cloning site; $P_{\min HIS3}$: Minimal promoter of the *HIS3* locus; *HIS3*: Yeast nutritional reporter gene; 3' UTR & $T_{\min HIS3}$: 3' UTR and terminator of the *HIS3* locus; *TRP1*: Yeast nutritional marker; ColE1 ori: ColE1 origin of replication for propagation in *E. coli*; Kan^r : Kanamycin resistance gene for selection in *E. coli*; *CEN6*: Centromeric sequence, ensures proper segregation of the plasmid during cell division in yeast; *ARS4*: Yeast autonomous replication sequence (Clontech Laboratories, Inc., Mountain View, USA).

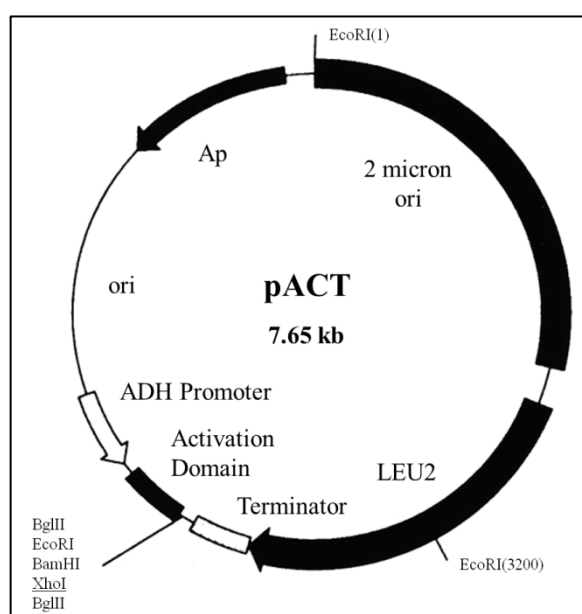


Figure A7. Map of pACT vector. pACT generates a fusion of the GAL4 AD and a protein encoded by a cDNA in a fusion library. Ap^r : *bla* gene, encoding ampicillin resistance for selection in *E. coli*; 2 micron ori: Origin of replication for replication in yeast; LEU2: Yeast nutritional marker; Terminator: ADH1 transcription termination signal, terminating transcription of the fusion protein; Activation Domain: GAL4 activation domain polypeptide containing an SV40 T-antigen nuclear localization signal; ADH Promoter: Constitutive promoter, driving expression of the fusion protein at high levels in yeast cells; ori: pBR322 plasmid replication origin (Durfee *et al.*, 1993).

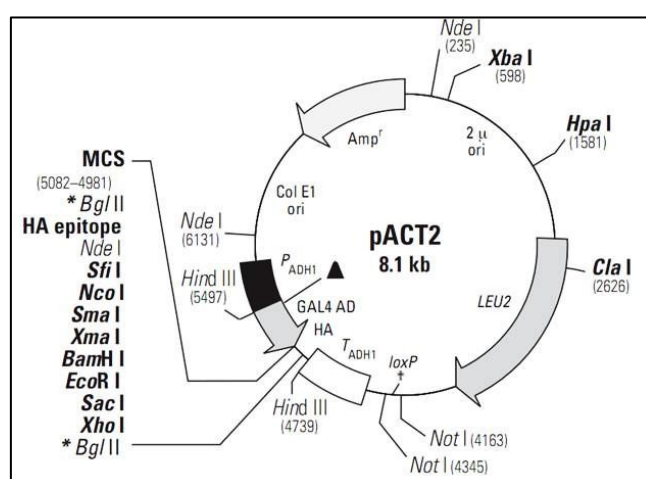


Figure A8. Map of pACT2 vector. pACT2 generates a fusion of the GAL4 AD and a protein whose coding sequence is ligated with the vector. Amp^r : *bla* gene, encoding ampicillin resistance for selection in *E. coli*; 2μ ori: Origin of replication for replication in yeast; LEU2: Yeast nutritional marker; *loxP*: Sites for specific recombination events; T_{ADH1} : ADH1 transcription termination signal, terminating transcription of the fusion protein; HA: Hemagglutinin epitope; GAL4 AD: GAL4 activation domain polypeptide containing an SV40 T-antigen nuclear localization signal; P_{ADH1} : Constitutive promoter, driving expression of the fusion protein at high levels in yeast cells; Col E1 ori: pBR322 plasmid replication origin (Clontech Laboratories, Inc., Mountain View, USA).

6.5 List of enhancer trap lines analyzed

Table A12. 62 *GAL4-GFP* enhancer trap lines, screened for light-dependent GFP fluorescence.

Number	Number	Number	Number
N906	N9265	N9292	N9322
N9090	N9266	N9294	N9323
N9094	N9270	N9296	N9324
N9102	N9271	N9299	N9325
N9118	N9272	N9303	N9327
N9128	N9274	N9305	N9328
N9201	N9276	N9306	N9330
N9208	N9277	N9310	N9331
N9212	N9278	N9311	N9332
N9216	N9280	N9312	N9333
N9231	N9282	N9313	N9334
N9240	N9285	N9314	N9335
N9242	N9287	N9317	N9336
N9249	N9288	N9318	N9339
N9258	N9289	N9320	
N9262	N9291	N9321	

6.6 List of tables

Chapter 2 – Material and methods

Table 2-1.	Mutants and SALK T-DNA insertion lines used for analysis of the influence of their gene products on light-dependent <i>SIG5</i> and <i>GFP</i> transcription	21
Table 2-2.	General PCR reaction protocol.....	25
Table 2-3.	TAIL-PCR primers.....	26
Table 2-4.	<i>cis</i> -acting elements, modified by site-directed mutagenesis.....	28
Table 2-5.	PCR protocol for DIG labeling of <i>GAL4</i> probe	34
Table 2-6.	General real-time PCR reaction protocol.....	37
Table 2-7.	Identification of mutant alleles by CAPS or SSLP markers	42

Chapter 3 - Results

Table 3-1.	Light responsive motifs identified in the 5' UTR of At5g57565 as predicted by PlantCARE and PLACE database.....	51
Table 3-2.	Light responsive motifs identified in about 1.1 kb upstream of the mapped T-DNA insertion site of ET N9266 as predicted by PlantCARE and PLACE databases.....	55
Table 3-3.	Light responsive motifs identified in the 196-bp blue light sensitive promoter region of <i>SIG5</i> as predicted by PlantCARE and PLACE databases	70
Table 3-4.	Light responsive motifs identified in 0.8 kb upstream of the mapped T-DNA insertion site of N9313 as predicted by PlantCARE and PLACE databases	76
Table 3-5.	Chl <i>a</i> content and total protein content of N9313 and N9313 crossed with <i>hy1cry1cry2</i> mutant.....	82
Table 3-6.	Relative <i>HY5</i> transcript abundances in two different <i>hy5</i> mutants.....	83
Table 3-7.	<i>HY5</i> binding sites of the 2 kb <i>SIG5</i> promoter and introduced mutations	85
Table 3-8.	cDNA insert sizes in λ -ACT library	91
Table 3-9.	Characterization of bait cDNAs, identified by Y1H screen	92
Table 3-10.	Phytohormone-responsive <i>cis</i> -acting elements identified in 0.8 kb upstream of the T-DNA insertion site of N9313 as predicted by PlantCARE and PLACE databases.....	105

6.7 List of figures

Chapter 1 – Introduction

Figure 1-1.	Photoconversion and dark reversion between the P _r (inactive) and the P _{fr} (active) form of phytochromes	5
Figure 1-2.	Phytochrome signaling pathways to turn on photomorphogenesis.....	10
Figure 1-3.	Mechanism of <i>HY5</i> regulation by light	11
Figure 1-4.	Possible signal transduction pathway of photosynthetic redox signals	14
Figure 1-5.	Simplified model of interactions between sugar and ABA signaling	17
Figure 1-6.	Arabidopsis <i>GAL4-GFP</i> ET lines	19

Chapter 2 – Material and methods

Figure 2-1.	Specific primers used for TAIL-PCR.....	26
Figure 2-2.	TAIL-PCR procedure for specific amplification or genomic sequence flanking a T-DNA insertion.....	27
Figure 2-3.	Schematic view of PCR-based site-directed mutagenesis.....	29
Figure 2-4.	Hypocotyl phototropism in etiolated wild-type and <i>phot1</i> mutant seedlings of <i>Arabidopsis thaliana</i> ..	42
Figure 2-5.	Schematic diagram of the yeast one-hybrid system	43

Chapter 3 - Results

Figure 3-1.	GFP fluorescence of <i>GAL4-GFP</i> ET lines, modulated by light intensity.....	48
Figure 3-2.	Spatial GFP expression in ET N9249 seedlings, analyzed by CLSM.....	49
Figure 3-3.	TAE agarose gel electrophoresis of tertiary TAIL-PCR products of N9249	49
Figure 3-4.	Attribution of components of tertiary TAIL-PCR product of N9249	50
Figure 3-5.	Diagram of the identified ET T-DNA insertion site in N9249	50
Figure 3-6.	TAE agarose gel electrophoresis of PCR amplicon, confirming the T-DNA insertion site of N9249 ..	51
Figure 3-7.	Molecular characterization of ET N9249 by Southern blot	52
Figure 3-8.	Spatial GFP expression in ET N9266 seedlings, analyzed by CLSM.....	53
Figure 3-9.	TAE agarose gel electrophoresis of tertiary TAIL-PCR products of ET N9266.....	53
Figure 3-10.	Attribution of components of tertiary TAIL-PCR product of N9266.....	54
Figure 3-11.	Diagram of the identified ET T-DNA insertion site in N9266	54
Figure 3-12.	TAE gel electrophoresis of PCR amplicon, confirming the T-DNA insertion site of N9266	55
Figure 3-13.	Molecular characterization of ET N9266 by Southern blot	56
Figure 3-14.	Spatial GFP expression in 10 d old seedlings of ET N9313, analyzed by CLSM	57
Figure 3-15.	TAE agarose gel electrophoresis of tertiary TAIL-PCR products of ET N9313.....	57
Figure 3-16.	Attribution of components of the type I tertiary TAIL-PCR product of N9313.....	58
Figure 3-17.	Diagram of the identified ET T-DNA insertion site in N9313	58
Figure 3-18.	TAE gel electrophoresis of PCR amplicon, confirming the T-DNA insertion site of N9313	59
Figure 3-19.	Molecular characterization of ET N9313 by Southern blot.....	59
Figure 3-20.	Relative <i>SIG5</i> transcript level in etiolated C24 wild-type and <i>SIG5</i> and <i>GFP</i> transcript levels in N9313	60
Figure 3-21.	GFP fluorescence in N9313 upon monochromatic light treatment	61
Figure 3-22.	Relative <i>GFP</i> transcript level in ET N9313 in response to monochromatic light.....	62
Figure 3-23.	Relative <i>SIG5</i> transcript level in C24 wild-type and ET N9313 in response to monochromatic light..	63
Figure 3-24.	Stability of <i>SIG5</i> and <i>GFP</i> transcripts in N9313	64
Figure 3-25.	Relative transcript levels in 4 weeks old N9313 plants	65
Figure 3-26.	Relative transcript levels in 4 weeks old N9313 plants upon 3 h red light illumination.....	66
Figure 3-27.	Diagram of three different <i>SIG5</i> promoter fragments, used for promoter-reporter gene analyses	67
Figure 3-28.	2 kb <i>SIG5</i> promoter mediated light response in tobacco and the proximal <i>SIG5</i> promoter was blue light sensitive	68
Figure 3-29.	Diagram of the localization of T-DNA insertions in the promoter of <i>SIG5</i>	69
Figure 3-30.	Relative <i>SIG5</i> transcript level in Col-0 wild-type and SALK T-DNA insertion lines in response to monochromatic blue light	69
Figure 3-31.	White light induced GFP expression, mediated by distal 0.8 kb <i>SIG5</i> promoter region in tobacco....	71
Figure 3-32.	Light-dependent reporter gene expression, mediated by distal 0.8 kb <i>SIG5</i> promoter in transgenic <i>Arabidopsis</i> seedlings	72
Figure 3-33.	Red light induced GFP expression mediated by proximal and distal <i>SIG5</i> promoter regions in tobacco	72
Figure 3-34.	Map of different distal <i>SIG5</i> promoter fragments used in promoter reporter gene analysis	73
Figure 3-35.	Red and blue light induced GFP expression mediated by several distal <i>SIG5</i> promoter fragments in tobacco	74
Figure 3-36.	Relative <i>SIG5</i> transcript level in Col-0 wild-type and SALK T-DNA insertion lines in response to monochromatic red and far-red light.....	75
Figure 3-37.	GFP fluorescence of N9313 and N9313 crossed with cryptochrome and phototropin mutants	77
Figure 3-38.	Relative <i>SIG5</i> transcript level in phototropin mutants and cryptochrome mutants in response to monochromatic blue light	78
Figure 3-39.	Relative transcript level in ET N9313 and N9313 x <i>cry1cry2</i> in response to blue light	79
Figure 3-40.	GFP fluorescence of N9313 and N9313 crossed with phytochrome and <i>hy1</i> mutants	80
Figure 3-41.	Relative <i>SIG5</i> transcript level in phytochrome mutants in response to monochromatic light	81
Figure 3-42.	GFP fluorescence of N9313 and N9313 crossed with <i>hy1cry1cry2</i> mutant.....	82
Figure 3-43.	Diagram illustrating the localization of mutations and T-DNA insertions in the <i>HY5</i> gene	83
Figure 3-44.	GFP fluorescence of N9313 in <i>hy5</i> background	84
Figure 3-45.	Relative <i>SIG5</i> transcript level in <i>hy5</i> mutants in response to monochromatic light.....	84
Figure 3-46.	Diagram of the localization of potential HY5 binding sites in the promoter of <i>SIG5</i>	85
Figure 3-47.	Transient GUS expression regulated by distal 0.8 kb <i>SIG5</i> promoter fragments with different mutated <i>cis</i> -elements	86
Figure 3-48.	GUS expression regulated by distal 0.8 kb <i>SIG5</i> promoter fragment with mutated G-box upon red light illumination	87
Figure 3-49.	Map of different <i>SIG5</i> promoter fragments tested for interaction with HY5 in yeast	88

Figure 3-50.	HY5 CDS is interacting with <i>RBCS1A</i> promoter fragment but not with <i>SIG5</i> promoter fragments	89
Figure 3-51.	Setting 3-AT concentration for Y187-pHIS2-p <i>SIG5</i>	91
Figure 3-52.	Growth of cDNA clones on media with different 3-AT concentrations	92
Figure 3-53.	GFP fluorescence in N9313 upon 4 h treatment with DCMU or DBMIB	94
Figure 3-54.	Φ PSII of N9313 seedlings with or without DCMU treatment	94
Figure 3-55.	Chl fluorescence parameter after light shift with or without DCMU pretreatment.....	95
Figure 3-56.	Chl <i>a/b</i> ratio after LTR.....	96
Figure 3-57.	GFP fluorescence after LTR.....	97
Figure 3-58.	Φ PSII values upon treatment of tobacco leaves with DCMU	98
Figure 3-59.	Chl fluorescence parameter after red light treatment with or without DCMU treatment	99
Figure 3-60.	GFP expression mediated by <i>SIG5</i> promoter fragments upon modulation of the redox state of the PQ pool in tobacco.....	100
Figure 3-61.	Relative transcript level in ET N9313 and C24 in response to monochromatic light and DCMU treatment.....	101
Figure 3-62.	GFP fluorescence in N9313 upon sucrose application.....	102
Figure 3-63.	Total Chl content of tobacco leaves upon treatment with external carbohydrates	103
Figure 3-64.	GFP expression driven by <i>SIG5</i> promoter fragments upon sucrose feeding in tobacco	103
Figure 3-65.	Relative transcript level in response to exogenous carbohydrate application	105
Figure 3-66.	Relative <i>SIG5</i> transcript level in cold stressed C24 wild-type and <i>SIG5</i> and <i>GFP</i> transcript levels in N9313	106
<u>Chapter 4 - Discussion</u>		
Figure 4-1.	Northern blot analyses of the light induction of <i>SIG5</i> in light signal transduction mutants	116
Figure 4-2.	Spectra of LED panel used in FloraLED chambers and of EYELA LED-R	117
Figure 4-3.	Transcriptional network regulating <i>SIG5</i> transcription upon blue light illumination	123
Figure 4-4.	Transcriptional network regulating <i>SIG5</i> transcription upon red/far-red light illumination.....	123
Figure 4-5.	Regulation of <i>SIG5</i> activity by light	131

CURRICULUM VITAE

Name: Marina Mellenthin

Geburtsdatum: 17.01.1982

Geburtsort: Otterndorf

Schulbildung: 08/1994 – 07/2001
Gymnasium Otterndorf

Studium: 10/2001 – 03/2007
Universität Bremen,
Biologiestudium, Abschluss Diplom

Seit 12/2007
Heinrich-Heine Universität, Düsseldorf
Promotionsstudium am Institut für Botanik

Düsseldorf, Mai 2012

DANKSAGUNG

Mein Dank gilt meiner Doktormutter Prof. Dr. Margarete Baier, die es mir ermöglicht hat an diesem spannenden und abwechslungsreichen Projekt zu arbeiten. Danke für die ständige Diskussionsbereitschaft und dass Du mich nie hast warten lassen.

Bedanken möchte ich mich auch bei Prof. Dr. Rüdiger Simon, insbesondere für die Betreuung meiner Arbeit nach dem Wechsel der AG nach Berlin.

Mein ganz besonderer Dank gilt Ulrike und Heiko. Danke für die tolle Zeit im Labor... für die ständige Hilfsbereitschaft, fürs Zuhören und Diskutieren und die schöne Atmosphäre... dank Euch waren die vergangenen Jahre für mich eine wunderbare Zeit!

Ein herzliches Dankeschön auch an Nicki und Wei, mit denen ich viele schöne Momente teilen durfte. Vielen Dank für die freundschaftliche Zusammenarbeit und die gute Stimmung im Labor.

Danke an alle anderen Ex-Düsseldorfer der Arbeitsgruppe, die es nach Berlin verschlagen hat, für die Bereitschaft zur Diskussion und Kritik.

Ich bedanke mich ausdrücklich bei Dr. Andrea Bräutigam für die fortwährende Hilfs- und Gesprächsbereitschaft während meiner gesamten Promotionszeit. Danke auch für das Korrekturlesen dieser Arbeit.

Danke an die vielen Düsseldorfer Forscher, die mir mit diesem und jenem ausgeholfen haben, und mir immer mit Rat zur Seite standen, insbesondere „unserem Gang“, der AG Ott und der AG Jahns, sowie der AG Simon. Nadine danke ich insbesondere für ihre Hilfe bei der letzten, sehr widerspenstigen Hefetrafo. Am Ende hat es dann ja doch geklappt ☺!

Ein riesiges Dankeschön geht an Rolf, meinen treuen Begleiter. Danke für das Gefühl, dass der eingeschlagene Weg der richtige sein wird und dass Du mir hilfst wo Du nur kannst.

Zuletzt und doch zuerst bedanke ich mich bei meinen Eltern. Ohne Euch wäre die Doktorarbeit nicht möglich gewesen. Danke für jedwede Unterstützung, und dass Ihr immer und ohne jeden Zweifel an mich geglaubt habt.

EIDESSTATTLICHE ERKLÄRUNG

Ich versichere an Eides Statt, dass die Dissertation von mir selbständig und ohne unzulässige fremde Hilfe unter Beachtung der „Grundsätze zur Sicherung guter wissenschaftlicher Praxis an der Heinrich-Heine-Universität Düsseldorf“ erstellt worden ist.

Ich versichere außerdem, dass ich die beigefügte Dissertation nur in diesem und in keinem anderen Promotionsverfahren eingereicht habe und dass diesem Promotionsverfahren keine gescheiterten Promotionsverfahren vorausgegangen sind.

Ort, Datum

Unterschrift